



UNIVERSIDAD DE JAÉN

**FACULTAD DE CIENCIAS DE LA
SALUD
DEPARTAMENTO DE FÍSICA**

TESIS DOCTORAL

**PROBABILISTIC SEISMIC HAZARD ASSESSMENT OF
EGYPT**

**PRESENTADA POR:
RASHAD FERIZ ZAKY SAWIRES**

**DIRIGIDA POR:
DR. D. JOSÉ ANTONIO PELÁEZ MONTILLA**

JAÉN, 24 DE OCTUBRE DE 2017

ISBN 978-84-9159-138-2

Probabilistic Seismic Hazard Assessment of Egypt

Ph.D. THESIS

to obtain the degree of

Doctor by the University of Jaén

Ciencia y Tecnología de la Tierra y del Medio Ambiente Ph.D. Program

Defended by

Rashad Feriz Zaky Sawires

Seismic Hazard and Active Tectonics Research Group,

Department of Physics,

University of Jaén

Thesis Advisor:

José A. Peláez, Ph.D.

July 2017

José A. Peláez, Ph.D.

Associate Professor in Geophysics, Physics Department,
University of Jaén, Spain

Certifies:

that the present memory, entitled “**Probabilistic Seismic Hazard Assessment of Egypt**”, has been developed under my supervision. Moreover, I must inform favorably to the examination of this Thesis in order to obtain the Ph.D. degree at the University of Jaén.

Assoc. Prof. José A. Peláez

Department of Physics

University of Jaén

A dissertation submitted in partial satisfaction of the requirements for the
Ph.D. degree at the University of Jaén, Spain

Rashad Feriz Zaky Sawires

B.Sc. in Geophysics, Assiut University (2005)

M.Sc. in Applied Geophysics, Assiut University (2011)

Jaén, July 2017

**THOSE WHO JOYFULLY LEAVE EVERYTHING IN
GOD'S HAND**

WILL EVENTUALLY SEE GOD'S HAND IN EVERYTHING.

DEDICATION

To my parents,

The reason of what I become today. Thanks for your great support and continuous care.

To my wife,

Her tender-loving care, patience, and dedication to me and our children, have been a constant source for inspiration for me while doing this thesis.

ACKNOWLEDGEMENTS

First of all, I would like to thank GOD, for having made everything possible by giving me strength and courage to do this thesis. Moreover, I would like to extend my gratefulness to the following research centers and individuals for their help during this work.

This research work is supported by the Egyptian Ministry of the Higher Education (Cultural Affairs and Missions Sector, Cairo). It has been conducted as a *Joint-Supervision Mission* between the Department of Geology, Assiut University (Egypt), and the Department of Physics, University of Jaén (Spain). I would like to express my sincere thanks, appreciation and gratitude to the Egyptian Government for giving me the opportunity to do this work attending different research teams in these scientific institutions.

I would like to express my special appreciation and thanks to Prof. **José A. Peláez** (Department of Physics, University of Jaén), for his valuable supervision and discussion. You have been a tremendous mentor for me. I would like to thank you for encouraging my research and for allowing me to grow as a research scientist. The suggestions and ideas you provided helped to improve the thesis considerably. Moreover, I thank you for inviting me to carry out my research work among your research group (*Spanish Seismic Hazard and Active Tectonics Research Group*) and providing me with all facilities I need during my stay in Spain.

My gratitude also goes to Prof. **Hamza A. Ibrahim** (Geology Department, Assiut University). He has done a lot of effort with me during the completion of the administrative requirements which were necessary for my travel to Spain. His advice on my research work as well as on my career have been priceless. I wish to express my deepest gratitude to Prof. **Raafat E. Fat-Helbary** (Manager of Aswan Regional Earthquake Research Centre, Aswan, Egypt) for his close guidance, comments, advice and for providing me with all possible data during this research project.

I am deeply grateful to Prof. **Mario Ordaz** (Instituto de Ingenieria, UNAM, Mexico) for providing me the most recent software (CRISIS, 2014) to do our assessment. Also, appreciation goes to Dr. **Mohamed Hamdache** (Département Etudes et Surveillance Sismique, CRAAG, Algiers, Algeria) for his valuable suggestions during his visits to the University of Jaén. Moreover, to Dr. **Francesco Panzera** (Università degli studi di Catania, Italy) for giving me some valuable comments about the seismic hazard deaggregation. Thanks also goes to Dr. **Jesús Henares** (University of Jaén) for helping me process the focal mechanism solutions data and interpret the stress inversion results. Also, I would like to thank Prof. **Samir Riad** (Geology Department, Assiut University), and Prof. **Ahmed Deif** (NRIAG, Helwan, Cairo) for providing me some important research papers during this work. Finally, thanks also are go to Prof. **Amin Saleh Aly** (Faculty of Engineering, Ain Shams University), who provides me some critical information about the Egyptian building codes.

A special thanks to **my family**. Words cannot express how grateful I am to my parents, my wife, and my children for all of the sacrifices that you have been made on my behalf.

Rashad Sawires

July, 2017

CONTENTS

	<u>Page</u>
• Resumen	1
• Abstract	5
• Chapter 1: Introduction	8
• Chapter 2: A Review of Seismic Hazard Assessment Studies and Hazard Description in the Building Codes for Egypt	15
• Chapter 3: An Earthquake Catalogue (2200 B.C. to 2013) for Seismotectonic and Seismic Hazard Assessment Studies in Egypt ...	46
• Chapter 4: Delineation and Characterization of a New Seismic Source Model for Seismic Hazard Studies in Egypt	83
• Chapter 5: Updated Probabilistic Seismic Hazard Values for Egypt	127
• Chapter 6: Probabilistic Seismic Hazard Deaggregation for Selected Egyptian Cities	150
• Summary, Conclusions and Recommendations	170
• Bibliography	178

LIST OF ABBREVIATIONS

A.D.	“Anno Domini” translated as “In the year of the Lord”
B.C.	Before Christ
BSSC	Building Seismic Safety Council
CMT	Centroid Moment Tensor
DSHA	Deterministic Seismic Hazard Assessment/Analysis
DST	Gulf of Aqaba-Dead Sea Transform Fault
ECLF	Egyptian Code for the Calculation of Loads and Forces
ECP	Egyptian Code of Practice
EDRDC	Earthquake Disaster Reduction Data Centre
EHB	Engdahl, E.R., van der Hilst, R., and Buland, R. (1998) Bulletin
EMR	Eastern Mediterranean Region
EMSC	European Mediterranean Seismological Centre
ENSN	Egyptian National Seismic Network
EGS	Egyptian Geological Survey
EGSMA	Egyptian Geological Survey and Mining Authority
ESEE	Egyptian Society of Earthquake Engineering
ETH	Eidgenössische Technische Hochschule/ Institute of Technology
Eurocode 8	European Building Code
FMS	Focal Mechanism Solution/ Fault Plane Solution
GEM	Global Earthquake Model
GIS	Geographic Information System
GMPE	Ground-Motion Prediction Equation/ Ground-Motion Attenuation Model/ Ground-Motion Scaling Relationship
GMT	Generic Mapping Tools Software
GPS	Global Positioning System
GSHAP	Global Seismic Hazard Assessment Project/Program
HRD	High Resolution Digitizer
ICC-IBC	International Building Code
IISEE	International Institute of Seismology and Earthquake Engineering
I_{\max}	Maximum Intensity
IPRG	Institute of Petroleum Research and Geophysics/ Seismological Bulletin of Israel
ISC	International Seismological Centre

List of Abbreviations

ISS	International Seismological Summary
<i>m_b</i>	Body-wave Magnitude
<i>m_D</i>	Duration Magnitude
<i>M_L</i>	Local Magnitude
<i>M_{max}</i>	Maximum Expected Magnitude
<i>M_{max}^{obs}</i>	Largest Observed Magnitude
<i>M_{min}</i>	Minimum Magnitude
<i>M_S</i>	Surface-wave Magnitude
<i>M_W</i>	Moment Magnitude
<i>M_W[*]</i>	Equivalent Moment Magnitude
NEHRP	National Earthquake Hazards Reduction Program
NEIC	National Earthquake Information Centre
NOAA	National Oceanic and Atmospheric Administration
NRIAG	National Research Institute of Astronomy and Geophysics
PDE	Preliminary Determination of Epicenters
PGA	Peak Ground Acceleration
PSHA	Probabilistic Seismic Hazard Assessment
<i>R</i>	Stress Ratio
<i>R'</i>	Stress Index
RCMT	Regional Centroid Moment Tensor
SA	Spectral Acceleration
<i>SA_{max}</i>	Maximum Spectral Acceleration
SHARE	Seismic Hazard Harmonization in Europe
<i>SH_{max}</i>	Maximum Horizontal Stress Axis
<i>SH_{min}</i>	Minimum Horizontal Stress Axis
UBC	The Uniform Building Code
UHS	Uniform Hazard Spectra
USGS	United States Geological Survey
<i>V_S³⁰</i>	Average Shear-wave Velocity in the Upper 30 m of the Soil Profile
WCC	Woodward-Clyde Consultants
WWSSN	World-Wide Standardized Seismograph Network
ZUR-RMT	Zurich Moment Tensor, Swiss Seismological Service

RESUMEN

En este estudio se ha llevado a cabo una evaluación de la peligrosidad sísmica probabilista para Egipto en términos de los valores de la aceleración pico del suelo (PGA) y la aceleración espectral (SA). También se presentan curvas de peligrosidad, espectros uniformes de diseño, y resultados de desagregación para las ciudades más importantes, enfocado a la mejora del conocimiento sobre ingeniería de terremotos en la región.

Inicialmente, se ha realizado una revisión de todas las evaluaciones de peligrosidad sísmica publicadas y disponibles, además de las acciones sísmicas incluidas en los códigos de construcción, a la hora de mostrar el estado de la cuestión de los estudios de evaluación de peligrosidad sísmica para el país. Esta revisión incluye la historia y desarrollo de las evaluaciones de peligrosidad sísmica y de la adopción de códigos sismorresistentes en Egipto. La mayor parte de los estudios previos de peligrosidad han sido analizados, y se ha llegado a la conclusión de que es deseable una nueva evaluación de peligrosidad de acuerdo con el estado de la cuestión, además de un cambio en la descripción de la peligrosidad del código de construcción egipcio actual.

Para hacer esta evaluación, se ha compilado un catálogo de terremotos incluyendo eventos en Egipto y su entorno (21° - 38° N, 22° - 38° E) en el periodo 2200 a.C. - 2013. Este catálogo se ha compilado a partir de diferentes fuentes, locales, regionales e internacionales (por ejemplo, el catálogo regional de Ambraseys *et al.*, 1994, el boletín del International Seismological Center, o los boletines anuales de la National Seismic Network egipcia). El catálogo inicial compilado contiene un total de 64613 terremotos (históricos e instrumentales), incluyendo todos los eventos con magnitud igual o superior a 3.0 de fuentes internacionales, en cualquier escala de magnitud, y de cualquier magnitud de fuentes locales. Las magnitudes estaban en diferentes escalas y provenían de diferentes fuentes. Además, se compiló una base de datos de soluciones de mecanismos focales. Esta base de datos contiene 688 soluciones de planos focales provenientes de diferentes fuentes publicadas e inéditas, cubriendo el periodo de tiempo desde 1940 hasta finales de 2013.

A la hora de establecer una magnitud unificada, la magnitud momento equivalente (M_W^*), se han desarrollado dos relaciones correlacionando la magnitud de ondas superficiales (M_S) y la magnitud de ondas internas (m_b) con la magnitud

momento. El catálogo sísmico ha sido desagrupado para eliminar todos los eventos dependientes del tiempo (réplicas, premonitorios y enjambres). Se ha obtenido un catálogo final Poissoniano con 16642 eventos, incluyendo terremotos principales con magnitud igual o superior a 3.0 M_w . Finalmente, se ha verificado el grado de completitud del catálogo completo. Los resultados de dicho análisis se han interpretado en el marco del establecimiento y desarrollo de las redes sísmicas nacionales e internacionales (por ejemplo, la World-Wide Standardized Seismograph Network y la National Seismic Network de Egipto).

Por otro lado, se ha propuesto un nuevo modelo de fuentes sísmicas para Egipto y su entorno próximo. Se ha tenido en cuenta la sismicidad, las soluciones de mecanismos focales y toda la información geológica y tectónica disponible. De esta forma, se han definido zonas que no sólo poseen una sismicidad homogénea, sino que también exhiben características sismotectónicas comunes. El modelo de fuentes sísmicas propuesto comprende un total de 88 fuentes sísmicas, 28 de las cuales incluyen la sismicidad superficial ($h \leq 35$ km) del territorio egipcio. Además de éstas, se han considerado fuentes sísmicas superficiales ($h \leq 20$ km) utilizadas en el proyecto Seismic Hazard Harmonization in Europe (SHARE) para la región Mediterránea oriental. A la hora de considerar la sismicidad intermedia ($20 < h \leq 100$ km), también se delimitaron específicamente siete fuentes sísmicas en esta región.

A partir del establecimiento del modelo de fuentes sísmicas, se crearon sub-catálogos de terremotos y soluciones de mecanismos focales. Se utilizó la relación de recurrencia de Gutenberg-Richter para determinar los parámetros sísmicos (parámetros a, actividad, y b) de cada una de las fuentes sísmicas delineadas. La máxima magnitud esperada en cada fuente sísmica fue también determinada, estadísticamente o geológicamente, a partir de la información de que se disponía. Además, la solución de mecanismo focal que prevalece en cada fuente sísmica fue calculada utilizando el método de la inversión del campo de esfuerzos. Esta caracterización de las fuentes sísmicas es una información esencial en peligrosidad sísmica y análisis de predicción.

Se han elegido seis conocidos modelos de atenuación del movimiento del suelo para modelizar la atenuación para las fuentes sísmicas consideradas. Además, se desarrolló un marco tipo árbol-lógico con 36 ramas para considerar la incertidumbre

epistémica en el valor de b , la máxima magnitud y el modelo de atenuación de movimiento del suelo.

Se han realizado cálculos en términos de valores de PGA y SA, para condiciones de roca y suelo, para una probabilidad de superación del 39.3%, 10% y 5% en 50 años (periodos de retorno de 100, 475 y 975 años, respectivamente). Se calcularon también las curvas de peligrosidad y los espectros uniformes de respuesta y diseño para 31 ciudades en Egipto, las cuales se han dibujado y comparado con los valores contemplados en el más reciente código de construcción sismorresistente en Egipto (ECP-201, 2011).

Es interesante destacar que los valores máximos de peligrosidad han sido observados en Nuweiba, específicamente en el entorno de la localización del llamado terremoto del Golfo de Aqaba ($7.2 M_w$), de 22 de Noviembre de 1995. Los máximos valores de SA obtenidos para roca y un amortiguamiento del 5% se observan para un periodo de 0.1 s, y son 0.38, 0.74 y 0.98 g, para periodos de retorno de 100, 475 y 975 años, respectivamente.

Finalmente se ha calculado la desagregación de la peligrosidad sísmica en términos de distancia y magnitud para las ciudades egipcias más importantes. Esto permite entender la contribución relativa de las diferentes fuentes sísmicas a la peligrosidad sísmica en una determinada localización. Específicamente se ha calculado la desagregación de la peligrosidad sísmica para los valores de PGA y SA para 0.2, 1.0 y 2.0 s, para un período de retorno de 475 años, considerando intervalos de 0.5 unidades en magnitud y 25 km en distancia. Se evaluaron los valores medio y modal de la magnitud y distancia para identificar la distribución de los terremotos de control, los que más contribuyen a la superación de un nivel dado de movimiento del suelo.

Los resultados de desagregación en la mayoría de las ciudades muestran que el escenario que más contribuye a la peligrosidad sísmica está controlado mayoritariamente por las fuentes sísmicas cercanas, especialmente para los valores de PGA. Sin embargo, los terremotos más distantes contribuyen más a la peligrosidad para grandes periodos espectrales (para 1.0 y 2.0 s). De hecho, el terremoto de control para El Cairo está comprendido en el rango de magnitudes entre 5.0-5.5 M_w y distancias entre 0-25 km para la PGA y la SA para periodos espectrales de 0.2 y 1.0 s, mientras que para un periodo espectral de 2.0 s, aunque el rango de distancias

permanece idéntico, el rango de magnitudes aumenta hasta 6.0-6.5 M_W . Sin embargo, para Puerto Saíd, al nordeste de Egipto, se obtienen terremotos de control en el rango de magnitudes 7.0-7.5 M_W y distancias 375-400 km para todos los periodos espectrales calculados.

Un importante resultado que se obtiene en este tipo de estudios es que la desagregación de la peligrosidad sísmica proporciona información útil sobre la distancia y magnitud de las fuentes sísmicas que contribuyen a la peligrosidad en una cierta localización, lo que puede aplicarse en la generación de escenarios de terremotos y seleccionar registros de aceleración para el diseño sísmico.

ABSTRACT

In the present study, a probabilistic seismic hazard assessment for Egypt is carried out in terms of peak ground acceleration (PGA) and spectral acceleration (SA) values. Hazard curves, uniform and design hazard spectra, and deaggregation results for the most important cities, are also presented, focused on improving the current earthquake engineering knowledge in the region.

In the beginning, a review of all available published seismic hazard assessments for Egypt, as well as the seismic actions included in the building codes have been done in order to show the state-of-the-art of the seismic hazard assessment studies for the country. This review include the history and development of seismic hazard assessments and the adoption of seismic building codes in Egypt. Mostly of the previous hazard studies have been analyzed in order to ensure that a new seismic hazard assessment according to the state-of-the-art is desirable, as well as a change in the hazard description of the actual Egyptian building code.

For doing this assessment, an earthquake catalogue for events occurred in Egypt and its vicinity (from 21° to 38°N, and from 22° to 38°E) during the period 2200 B.C. - 2013 was compiled from different sources, local, regional and international ones (e.g., the regional catalogue of Ambraseys *et al.*, 1994; the bulletin of the International Seismological Centre and the annual bulletin of the Egyptian National Seismic Network). The initial compiled catalogue comprised a total of 64613 earthquakes (historical and instrumental events) including all the events having an assigned magnitude over 3.0 for international sources and any magnitude for local sources on any magnitude scale. Earthquake magnitudes were reported in different scales and come from a variety of sources. In addition, a focal mechanism solutions database was collected. This database contains 688 fault plane solutions gathered from different published and unpublished sources, covering the time period from 1940 until the end of 2013.

For establishing a common magnitude, namely an equivalent moment magnitude (M_W^*), two new relationships correlating surface-waves (M_S) and body-waves (m_b) magnitudes with moment magnitude (M_W) were derived. The catalogue has been declustered to remove all time-dependent events (aftershocks, foreshocks and seismic swarms). A total of 16642 events represent the final Poissonian catalogue including main shocks with a magnitude above or equal to M_W 3.0. Finally, the degree

of completeness for the entire catalogue was checked for the different magnitude values. The results of the completeness analysis have been interpreted in the framework of the establishment and development of the international and national networks (e.g., the World-Wide Standardized Seismograph Network and the Egyptian National Seismic Network)

On the other hand, a new seismic source model for the Egyptian territory and its surroundings has been proposed. Seismicity data, focal mechanism solutions, as well as all available geological and tectonic information were taken into account during the definition of this model, in an attempt to define zones which do not show only a rather homogeneous seismicity release, but also exhibit similar seismotectonic characteristics. The proposed seismic source model comprises in total of eighty-eight seismic sources, twenty-eight of them including the shallow seismicity ($h \leq 35$ km) for the Egyptian territory. In addition, for the Eastern Mediterranean region, it has been considered the shallow seismic source zones ($h \leq 20$ km) used in the Seismic Hazard Harmonization in Europe (SHARE) project. Furthermore, to cover the intermediate-depth seismicity ($20 \leq h \leq 100$ km), seven seismic sources were delineated in the Eastern Mediterranean region.

Following the determination of zone boundaries, a separate earthquake and focal mechanism solution sub-catalogue for each seismic zone was created. The Gutenberg-Richter recurrence relationship was used to determine the seismicity parameters (b -value, activity “ a -value”) for the delineated seismic sources. The maximum expected magnitude in each source was determined statistically or geologically, from the available earthquake data. In addition, the prevailing focal mechanism solution was assigned using a stress field inversion approach in each source zone. This characterization of the seismic sources is an essential input for seismic hazard and forecasting analyses.

Six well-known ground-motion attenuation models have been chosen to model the attenuation in the considered seismic sources. A logic-tree framework consisting of 36 branches was setup, to consider the epistemic uncertainty in the Gutenberg-Richter b -values, maximum possible magnitudes and the selected ground-motion attenuation models.

Seismic hazard computations in terms of PGA and SA values, for both rock and stiff-soil site conditions, with 39.3%, 10% and 5% probability of exceedance in 50

years (return periods of 100, 475 and 975 years, respectively) were performed. Hazard curves and uniform hazard spectra for thirty-one cities in Egypt were computed and plotted against the PGA values considered in the most recent Egyptian building codes (e.g., ECP-201, 2011).

It is interesting to show that the maximum hazard values were observed at Nuweiba, specifically around the epicentral location of the M_W 7.2, November 22, 1995 Gulf of Aqaba earthquake. The maximum SA values (for a 5% damping) for Nuweiba, for rock-site conditions, are observed at 0.1 s, and are equal to 0.38, 0.74 and 0.98 g for return periods of 100, 475 and 975 years, respectively.

Finally, the seismic hazard deaggregation in terms of distance and magnitude was computed for the most important cities in Egypt, to help understanding the relative contributions of the different seismic sources. Seismic hazard deaggregation for PGA and SA of 0.2, 1.0 and 2.0 s, for a return period of 475 years, and considering bins of 0.5 for magnitude and 25 km for distance, was computed. The mean and modal values of magnitude and distance, to identify the distribution of control earthquakes that mostly contribute to the exceedance of the considered SA level, were also assessed.

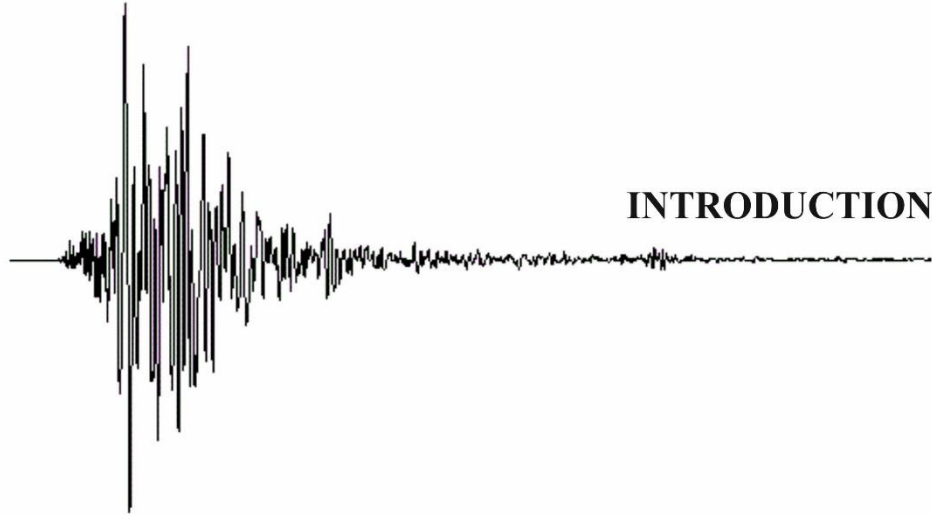
The deaggregation results at mostly cities indicate that the scenario which usually contributes to the seismic hazard is mainly controlled by the nearby seismic sources (especially for PGA). However, more distant events contribute more to the hazard for larger spectral periods (for 1.0 and 2.0 s). For instance, the control earthquake for Cairo has M_W values in the range 5.0-5.5 and focal distance between 0 and 25 km for PGA and SA at 0.2 and 1.0 s, whereas for 2.0 s the distance remains the same but the magnitude range become M_W 6.0-6.5. However, for Port Said, values of 7.0-7.5 M_W and 375-400 km for the control earthquake has been obtained for all computed spectral periods. A significant result of this type of work is that seismic hazard deaggregation provides useful data on the distance and magnitude of the contributing seismic sources to the hazard in a certain place, which can be applied to generate scenario earthquakes and select acceleration records for seismic design.



Chapter **1**

INTRODUCTION

HEADINGS:	Page
1.1 Motivation of the Study	9
1.2 Purpose and Scope.....	11
1.3 Thesis Outlines.....	13



INTRODUCTION

Earthquakes are sudden shuddering or trembling of the Earth produced by shock waves or vibrations passing through it. They generated in rocks by the sudden release of a strain that has been accumulating over a certain interval of time, sometimes for months, years or even for centuries. They are the expression of a continuous evolution of the Earth Planet and reshaping of the Earth's surface.

Of all natural hazards, earthquakes are those which historically have caused the most extensive impact and disruption in terms of damage to infrastructure, human-casualties and economic losses. Every year more than one million earthquakes shake different regions of the world. Some of them are so feeling and gentle that only the most sensitive instruments can detect the motion, and others so violent (e.g., M_w 9.0, December 26, 2004 Sumatra; M_w 7.6, October 8, 2005 Pakistan; M_w 7.9, May 12, 2008 China; M_w 7.0, January 21, 2010 Haiti; M_w 9.0, March 11, 2011 Japan; M_w 7.8, April 25, 2015 Nepal) that whole communities are shattering, and large sections of terrain are shifting in this process that can start landslides, block rivers, cause floods and set massive sea waves surging across the oceans.

The amount of damage and number of fatalities at a certain place caused by an earthquake depends on various factors: the size of the earthquake, distance from the epicenter, terrain, density of population, structural design of buildings, infrastructures, the ground-hydrogeologic conditions, seismogeological effects (rock falls, landslides, subsidence, liquefaction, etc.), etc. These known facts are primary sources for the large number of victims in recent earthquakes, especially in the developing countries.

Global seismic hazard and vulnerability to earthquakes are increasing steadily as urbanization and development occupy more areas prone to significant earthquakes.

The uncontrolled growth of cities is often associated with construction of seismically unsafe buildings and infrastructures, mostly due to the insufficient knowledge of the seismic hazard in the area. Moderate- or even small-size earthquakes, may turn catastrophic in areas with poor building and construction practice. The most effective way to decrease disasters and fatalities caused by earthquakes is to estimate the seismic hazard that could serve improving the seismic building codes.

1.1 MOTIVATION OF THE STUDY

The Arab Republic of Egypt is situated in the northeastern corner of the African Continent (Fig. 1-1). It is bordered from the north by the Mediterranean Sea, from the south by Sudan, from the west by Libya, and from the east by Palestine, Gulf of Aqaba and Red Sea. Its width is about 1225 km and its length, from the Mediterranean to the Sudanese border, is about 1075 km. The total area of Egypt is more than one million square kilometers (1019600 km²) which represents nearly one-thirtieth of the total area of the African Continent.

Tectonically, Egypt is situated in the northeastern corner of the African Plate, along the southeastern edge of the Eastern Mediterranean region (EMR). It is interacting with the Arabian and Eurasian Plates through divergent and convergent plate boundaries, respectively (see Fig. 2-1). Egypt is bounded by three active tectonic plate margins: the African-Eurasian plate margin, the Red Sea-Gulf of Suez plate margin and the Gulf of Aqaba-Dead Sea Transform Fault (DST).

The seismic activity of Egypt is mainly due to the interaction and the relative motion between the plates of Eurasia, Africa and Arabia (see Fig. 2-2). Within the last decades, some areas in Egypt have been struck by significant earthquakes (e.g., M_w 7.2, November 22, 1995 Gulf of Aqaba earthquake) causing much damage. Such events were interpreted as the result of this interaction.

Generally, the seismic risk is related to the occurrence of moderate-size earthquakes at near distances (e.g., M_s 5.9, October 12, 1992 Cairo earthquake) instead of big earthquakes that are known to occur at far distances along the Northern Red Sea, Gulf of Suez and Gulf of Aqaba (e.g., M_s 6.9, March 31, 1969 Shedwan, and M_w 7.2, November 22, 1995 Gulf of Aqaba earthquakes), as well as the Mediterranean offshore (e.g., M_s 6.8, September 12, 1955 Alexandria earthquake) (Ambraseys *et al.*, 1994; El-Sayed and Wahlström, 1996; Abou Elenean *et al.*, 2010).

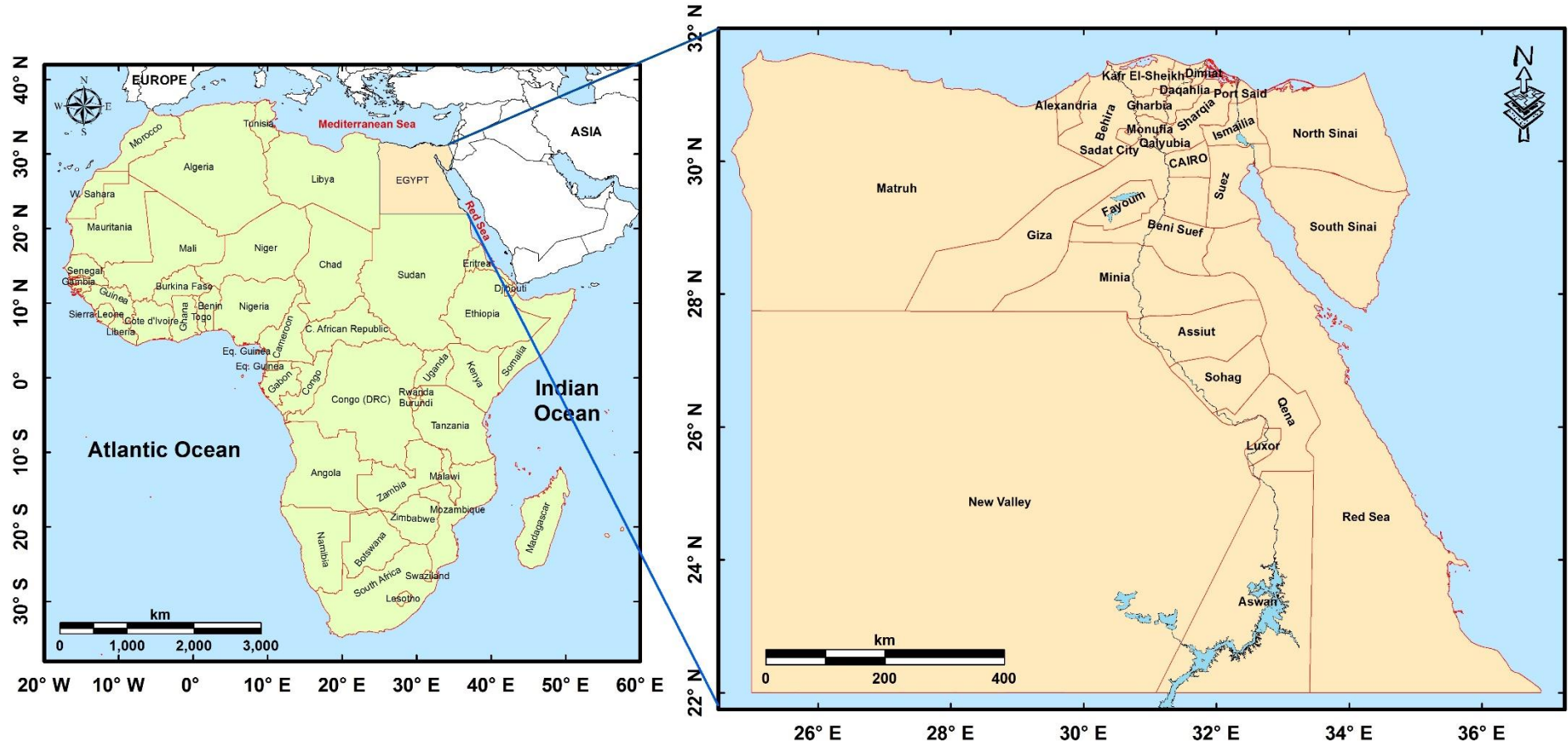


Figure (1-1): Map of Egypt showing its political and administrative boundaries in relation to the African Continent.

Although Egypt is affected by a moderate seismic activity compared to other countries, it is exposed to high seismic risk (Riad *et al.*, 2000). This is due to some factors: 1) the population in Egypt, as well as all important and archaeological sites, are concentrated within a narrow belt along the Nile Valley and Delta, 2) most of the overpopulated cities and villages are located near moderate to high active seismic foci, 3) the methods of construction vary between old (e.g., in the villages) and new buildings with poor construction practice, and finally, 4) the soil characteristics in different localities have a clear impact on seismic wave attenuation and amplification.

In Egyptian cities with a vibrant economy like Cairo, Alexandria, Aswan and Assiut, the occurrence of a significant earthquake could cause an economic downturn that may last for decades. Many of earthquake effects could be avoided by development of better construction methods, safety systems, early warning systems, and effective evacuation planning and event preparedness.

Until the beginning of the last decade, consideration of seismic action was nearly absent from the Egyptian building codes. Several seismic hazard assessment studies were conducted upon different regions in Egypt by many authors. Among these studies, only the seismic hazard map, based on the Peak Ground Acceleration (PGA), performed by Riad *et al.* (2000) was included in the Egyptian building codes for the years 2004, 2008 and 2011 (ECP-201: 2004, 2008, 2011).

In the same time, the Egyptian government has proposed a national plan aiming at construction of some new cities (e.g., New Capital) and strategic projects (e.g., New Suez Canal) all over the country, which in turn will solve the dense population problems in the Nile Valley and Delta regions, and will create new communities in these arid regions. A damaging earthquake is a real, as well as a current, threat to the safety, social integrity, and economic wellbeing of the population in the region. Thus, there is an urgent need to estimate the seismic hazard in Egypt and to supply this information for application and use in improving seismic zoning maps and building design and construction. They will serve for future risk studies, building codes and land-use planning.

1.2 PURPOSE AND SCOPE

Occurrences of earthquakes in different parts of the world and the resulting losses, especially human lives, have highlighted the structural inadequacy of many

buildings to support seismic loads. Today, scientists, technicians and engineers know a lot of details and information about earthquakes, where they are most likely to occur, how deep they originate and how they affect the ground. Researchers are applying this knowledge to future programs for predicting when and where the next earthquake might occur, and for constructing buildings and installations that might be better able to withstand earthquake violence. Man may never be able to control or even predict earthquakes with satisfactory accuracy, but he can learn to live with them in a relative safety.

Short and mid-term earthquake forecasting may one day be able to reduce significantly casualties associated with catastrophic earthquakes. However, a long-term preventive policy is the only possible way for the reduction of life losses and socioeconomic impact associated with them (Riad *et al.*, 2000). Such preventive policy should be based on: i) the assessment of seismic hazard and risk, ii) the implementation of safe building and construction codes, iii) the increased public awareness on natural disasters, and iv) a strategy of land-use planning taking into consideration the seismic hazard and other natural disasters.

In the present work, the overall purpose is to carry out a probabilistic seismic hazard analysis (PSHA) for Egypt, in terms of PGA, spectral acceleration (SA) values, uniform and design hazard spectra, and deaggregation. The output values and results could be used to modify and update the seismic action in the upcoming building codes.

This purpose will be reached throughout the following steps:

- Reviewing, comparing and analyzing the previous seismic hazard assessment studies available for different regions in Egypt, as well as the evolution of the representation of the seismic action in the successive Egyptian building codes.
- Gathering and analyzing the most interesting previous geological (e.g., active faults), geophysical (gravity and aeromagnetic), and main seismological (e.g., seismicity and seismotectonics) studies carried out by different authors and organizations in and around Egypt.
- Acquisition and collection of earthquake data (from different local and international sources) to compile a new unified earthquake catalogue representing the up-to-date seismicity of Egypt (until the end of 2013).

- Compilation and description of several focal mechanism solutions (FMSs) plots for Egypt as a general and for selected regions (e.g., Cairo, Aswan and Sinai Peninsula) in particular.
- Delimitation and characterization of a new seismic source model, for seismic active regions in and around Egypt, based on the known geological, seismological and geophysical information. Defining the earthquake recurrence characteristics of each defined seismic zone separately is also included. Moreover, reinterpretation of FMSs data, using stress inversion approach (Delvaux and Sperner, 2003; Delvaux and Barth, 2010), for each delineated seismic source in Egypt is taken place, which declared the relationship between the spatial distribution of earthquakes and the prevailing geological structures, are also included.
- Selection of the most appropriate worldwide and well-known ground-motion attenuation equations (GMPEs) taking into account the prevailing tectonic setting in and around Egypt.
- Computation of the seismic hazard values for Egypt, using a logic-tree approach, and following one of the standard methodologies to assess a PSHA.
- Proposing of seismic hazard values (e.g., PGA for a return period of 475 years, uniform hazard spectra (UHS) and a proposed design spectra) for some selected cities to be recommended and included in the upcoming Egyptian building codes.
- Appraisal of seismic hazard deaggregation results in order to determine the seismic sources that mostly contribute to the seismic hazard in significant locations, at certain hazard levels.


1.3 THESIS OUTLINES

The present dissertation is subdivided into the following chapters:

- **Chapter one (Introduction):** It is an overview about the main objectives of this work, motivation of the study, general background on the problem and the necessary steps doing this scientific research.
- **Chapter two (A review of seismic hazard assessment studies and hazard description in the building codes for Egypt):** This chapter reviews and compares critically the previous hazard assessments available for Egypt as well as the representation of the seismic action in the successive Egyptian building codes. All

previous assessments have been analyzed and compared in terms of the used earthquake catalogues, seismic source models, GMPEs, software code and main seismic hazard results.

- ***Chapter three (An earthquake catalogue for seismotectonic and seismic hazard assessment studies in Egypt):*** This chapter deals with earthquake data compilation, preparation and unifying of the different earthquake sizes using the well-known moment magnitude (M_W) scale. The declustering process and the completeness analysis of the unified catalogue are also included. Moreover, FMSs data compilation and interpretation are presented. Furthermore, a discussion about the seismicity of Egypt as well as important seismic active regions in Egypt is also included.
- ***Chapter four (Delineation and characterization of a new seismic source model for seismic hazard studies in Egypt):*** It includes the delineation and consideration of a new seismic source model for Egypt and its surroundings. The computed seismicity parameters, as well as the prevailed FMSs (using the stress inversion approach) for the delineated seismic sources will be displayed.
- ***Chapter five (Updated probabilistic seismic hazard values for Egypt):*** In this chapter, the selection and justification of the GMPEs, used in the current study, will be discussed. The considered logic-tree framework, after a detailed sensitivity analysis for different important input parameters, will be presented. It includes also the representation and the interpretation of the different hazard results of the assessment. Seismic hazard maps, for different soil conditions and return periods (for the whole territory), as well as hazard curves, UHS, and design spectra (for specific cities) are also included. Finally, a comparison between the obtained results with those of the current building code was performed.
- ***Chapter six (Probabilistic seismic hazard deaggregation for selected Egyptian cities):*** In this last chapter, the seismic hazard deaggregation results, in terms of distance and magnitude, for the most important cities in Egypt will be represented. The contribution to the seismic hazard from the nearby and distant seismic sources will be discussed in details for each city.
- ***Summary, conclusions and recommendations:*** It visualizes and presents the summary and main conclusions of the dissertation. Suggested recommendations are also presented.



Chapter **2**

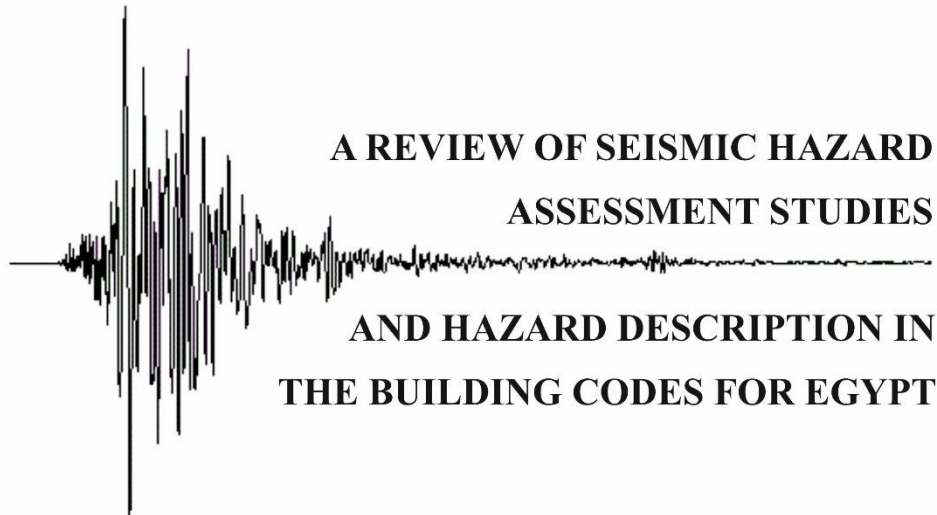
A Review of Seismic Hazard Assessment Studies and Hazard Description in the Building Codes for Egypt

Sawires, R., Peláez, J.A., Fat-Helbary, R.E., and Ibrahim, H.A. (2016). A review of seismic hazard assessment studies and hazard description in the building codes for Egypt. *Acta Geodaetica et Geophysica* 51, 151-180.

ABSTRACT

Reduction of damage in earthquake-prone areas requires modern building codes that should be continuously updated to reflect the improvement in our understanding of the physical effects of earthquake ground shaking on buildings and the increase in the quality and amount of seismological and tectonic studies, among other factors. This work reviews the published seismic hazard assessments available for Egypt as well as the seismic actions included in the building codes, in order to show the state-of-the-art of the seismic hazard assessment studies for the country. The review includes the history and development of seismic hazard assessments and the adoption of seismic building codes in Egypt. All the previous studies were analysed in order to conclude that a new seismic hazard assessment according to the state-of-the-art is desirable, as well as a change in the hazard description for the actual Egyptian building code.

HEADINGS:		Page
2.1	Introduction.....	15
2.2	Tectonic Setting of Egypt.....	16
2.2.1	Africa-Eurasia Plate Margin.....	17
2.2.2	Gulf of Suez-Red Sea Plate Margin.....	18
2.2.3	Gulf of Aqaba-Dead Sea Transform Fault.....	18
2.3	Seismicity of Egypt.....	18
2.4	Earthquake Risk.....	20
2.5	Previous Seismic Hazard Assessments Studies.....	23
2.5.1	Riad <i>et al.</i> (2000) Study.....	29
2.5.2	El-Hadidy (2012) and Mohamed <i>et al.</i> (2012) Studies.....	30
2.6	Seismic Design Codes.....	32
2.6.1	Regulations of the Egyptian Society of Earthquake Engineering.....	34
2.6.2	Egyptian Code for the Calculation of Loads and Forces.....	35
2.6.3	The Uniform Building Code.....	38
2.6.4	Egyptian Codes for the Calculation of Loads and Forces.....	39
2.7	Review and Remarks.....	43
2.8	Summary and Conclusion.....	44
2.9	Acknowledgments.....	45



Reduction of damage in earthquake-prone areas requires modern building codes that should be continuously updated to reflect the improvement in our understanding of the physical effects of earthquake ground shaking on buildings and the increase in the quality and amount of seismological and tectonic studies, among other factors. This chapter reviews the published seismic hazard assessments available for Egypt as well as the seismic actions included in the building codes, in order to show the state-of-the-art of the seismic hazard assessment studies for the country. The review includes the history and development of seismic hazard assessments and the adoption of seismic building codes in Egypt. All the previous studies were analyzed in order to conclude that a new seismic hazard assessment according to the state-of-the-art is desirable, as well as a change in the hazard description for the actual Egyptian building code.

2.1 INTRODUCTION

Of all natural hazards, earthquakes are those which historically have caused the most extensive impact and disruption in terms of damage to infrastructure, human-casualties and economic losses. Earthquakes, which happen within few seconds, can destroy people, the whole cities and villages, cultural and material assets created by the people for centuries, as well as changes in the ecological balance of environment. They have the power to trigger landslides, avalanches, flooding and tsunamis. Every year, more than one million earthquakes shake different regions of the world, some so feeling and gentle that only the most sensitive instruments can detect the motion, and others so violent that whole communities are shattered, and large sections of terrain

are shifted in this process that can start landslides, block rivers, cause floods, and set massive sea waves surging across the oceans.

The amount of damage and number of fatalities at a certain location caused by an earthquake, depends on various factors: the magnitude and characteristics of the earthquake focus, distance from the epicenter, soil characteristics, density of buildings and population, and structural design of buildings and infrastructures, among others. These facts are playing an important role in decreasing or increasing the number of victims in recent earthquakes, especially in the developing countries.

Today scientists, technicians and engineers know a lot of details and information about earthquakes, where they are most likely to occur, how deep they originate, and how they affect land. Researchers are applying this knowledge to future programs for predicting when and where the next earthquake might occur and for constructing buildings and installations that should be better able to withstand earthquake violence. Man may never be able to control or even predict earthquakes with satisfactory accuracy, but he can learn to live with them in relative safety. Occurrences of earthquakes in different parts of the world and the resulting losses, especially human lives, have highlighted the structural inadequacy of many buildings to support seismic loads.

The current chapter reviews and compares the main published work regarding the seismic hazard studies that have been done in Egypt. In addition, the seismic actions in the previous and current Egyptian buildings codes were reviewed and analyzed in relation to the different seismic hazard assessments.

2.2 TECTONIC SETTING OF EGYPT

Egypt is situated in the northeastern corner of the African Plate, along the southeastern edge of the EMR (Fig. 2-1). It is interacting with the Arabian and Eurasian Plates through divergent and convergent plate boundaries, respectively. Egypt is bounded by three active tectonic plate margins: the African-Eurasian plate margin, the Red Sea plate margin, and the Gulf of Aqaba-Dead Sea Transform Fault (DST). The seismic activity of Egypt is due to the interaction and the relative motion between the plates of Eurasia, Africa and Arabia. Within the last decade, some areas in Egypt have been struck by significant earthquakes causing considerable damage. Such events were interpreted as the result of this interaction.

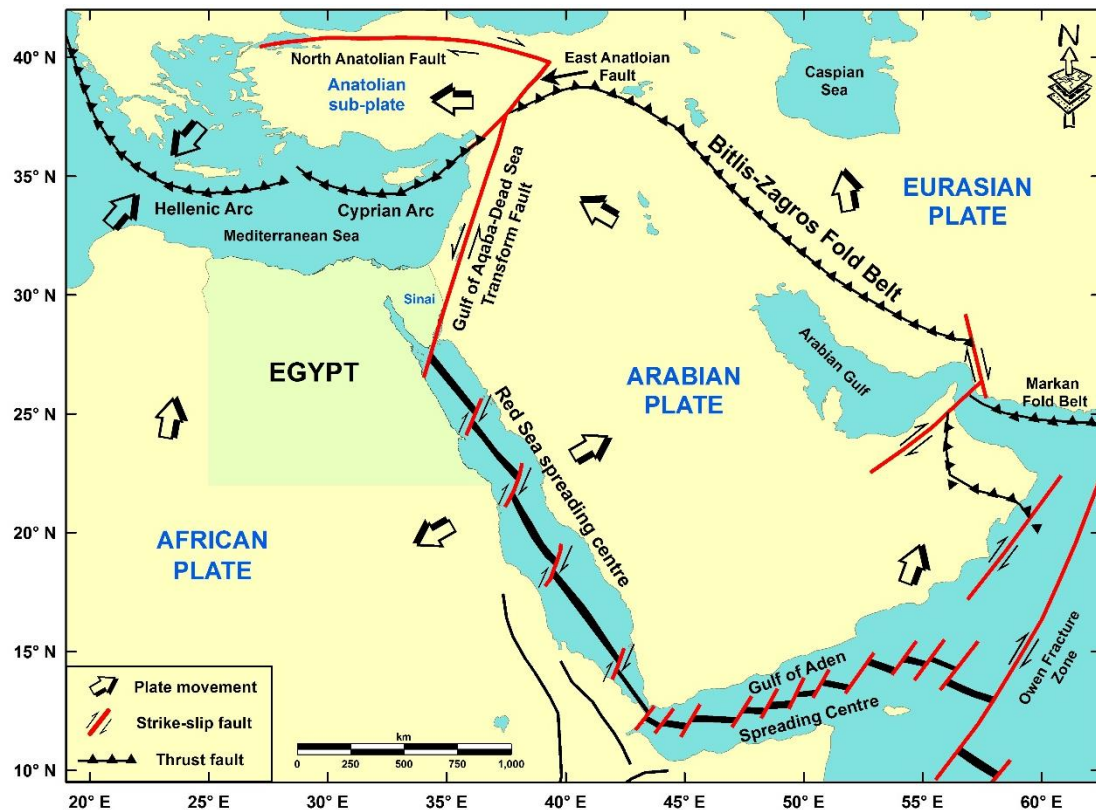


Figure (2-1): Global tectonic sketch for Egypt and its vicinity (compiled after Ziegler, 2001 and Pollastro, 2003).

The primary features of active plate boundaries in the vicinity of Egypt have been discussed in detail by many authors (e.g., McKenzie, 1972; Neev, 1975; Ben-Avraham *et al.*, 1987; WCC, 1985; Mesharf, 1990; Kebeasy, 1990). A summary of the three most important tectonic features in the vicinity of Egypt (Fig. 2-1), in relation to the known shallow seismicity, is given in the following paragraphs.

2.2.1 AFRICA-EURASIA PLATE MARGIN

The African and Eurasian Plates are converging across a wide zone in the Mediterranean Sea (Fig. 2-1). The effects of the plate interaction are mainly north and remote from the Egyptian coastal margin. Some of the largest events located to the south of Crete and Cyprus Islands were felt and caused few damage in the northern part of Egypt (e.g., August 8, 1303, intensity VIII offshore Mediterranean, June 26, 1926, M_S 7.4 Hellenic Arc, October 9, 1996, M_W 6.8 Cyprus, and October 12, 2013, M_S 6.4 Crete earthquakes).

2.2.2 GULF OF SUEZ-RED SEA PLATE MARGIN

The Arabian Plate is continuing to rotate away from the African Plate along the Red Sea spreading center (Fig. 2-1). The earthquake activity along that boundary is

related to the Red Sea rifting, plutonic activity and the intersection points of the NW (Gulf of Suez-Red Sea Faults) with the NE DST Faults (Abou Elenean 2007). Active sea-floor spreading has been identified as far as about 20° to 22° north latitudes (Cochran, 1983). The extension of this deformation zone toward the north (Suez-Cairo shear zone) is considered as the most active part of Northern Egypt. The largest earthquakes along this zone caused little damage in Northern Egypt (e.g., March 6, 1900, M_S 6.2 Gulf of Suez, and March 31, 1969, M_W 6.8 Shedwan Island earthquakes).

2.2.3 GULF OF AQABA-DEAD SEA TRANSFORM FAULT

It is a major left-lateral strike-slip fault, trending N-S to NNE-SSW, that accommodates the relative motion between Africa and Arabia (Salamon *et al.*, 2003). It connects a region of extension in the Northern Red Sea with the Taurus collision zone to the north (Fig. 2-1). The seismic activity of this shear boundary is relatively high and appeared to be clustered in some places where there is an intersection of two or more faults (NNE-SSW and WNW-ESE) or attributed to upwelling of magma (Abou Elenean 2007). Some larger earthquake events were reported along this fault trend and caused damage in Northern Egypt (e.g., March 18, 1068, intensity VIII Elat, May 20, 1202, intensity VIII Lebanon, and November 22, 1995, M_S 7.2 Gulf of Aqaba earthquakes).

2.3 SEISMICITY OF EGYPT

Egypt has a very long historical record of earthquakes going back four millennia. Moreover, detailed and reliable information is available for several destructive earthquakes in both historical and recent times (Badawy 2005). The seismicity of Egypt (Fig. 2-2) has been also studied by many authors (e.g., Maamoun *et al.*, 1984; Kebeasy, 1990; Ambraseys *et al.*, 1994, Abou Elenean, 1997, 2007; Badawy, 1999 and 2005) as well as the relationship between the surrounding plate boundaries and shallow seismicity (e.g., Abou Elenean, 1997).

With the establishment of the Egyptian National Seismic Network (ENSN) in 1997, much activity with more accurate parameters was revealed. The recorded earthquake activity shows a clustering and trending of the activity at specific tectonic structures and faults (Fig. 2-2). The highest seismicity rates were found at the eastern boundaries of Egypt, via the Gulf of Aqaba, which forms the southern end of the DST

fault, and the northern part of the Red Sea, which is a young oceanic spreading center (Abou Elenean 2007).

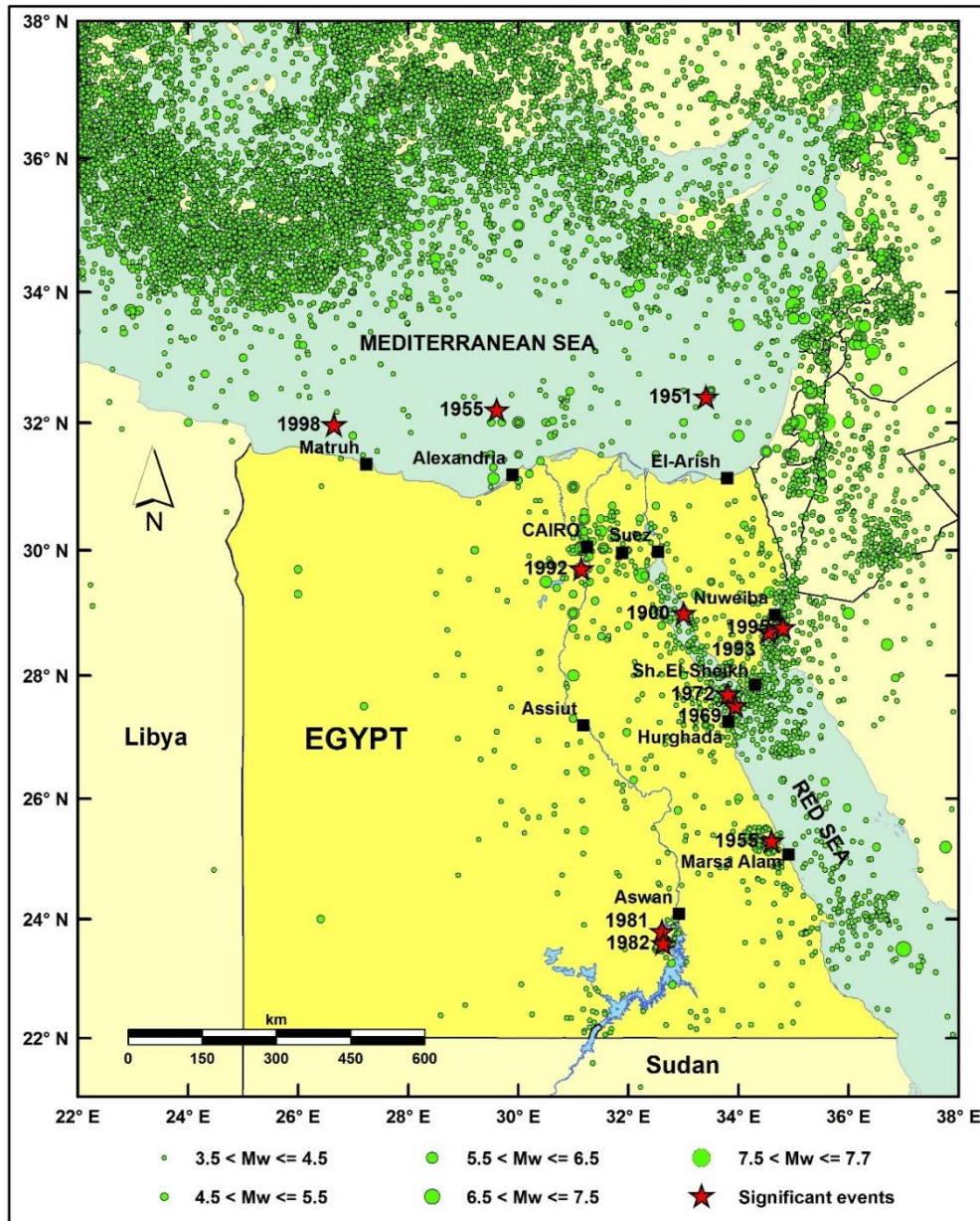


Figure (2-2): Declustered shallow seismicity and significant earthquakes for the time period (2200 B.C. - 2013).

However, significant seismic activity is also found along the entire Gulf of Suez and its extension on the northern part of the Egyptian Eastern Desert towards the Nile Delta along the E-W and WNW faults. This activity trend does not continue further towards the Mediterranean Sea and ceased closer to the west of the Nile Valley. The activity along the Northern Red Sea lies along the axial part of the rift. Furthermore, some clusters around supposed transform faults were clearly observed (Abou Elenean 2007). Away from this relatively active seismic zone, inland seismic activity (e.g. in Dahshour, Aswan, Abu-Dabbab and Abu-Simbel) has also occurred (Badawy 2005).

Badawy (2005) mentioned that, with the improvement of the ENSN, new seismically active zones have been discovered across and around Egypt (e.g., Southeast Beni Suef, west of Sohag, and along what used to be considered a seismic gap between the Southern Red Sea and Northernmost Red Sea). More recently, Abou Elenean (2007) described two seismicity clusters which were located in the southern part of the Western Desert (Southwest Aswan and Northeast Abu Simbel) (Fig. 2-2). He attributed these activities to some tectonically E-W active faults and reservoir-induced seismicity around Nasser's Lake. In addition, he identified some clusters along the Nile River, trending NW-SE to WNW-ESE, which were observed along the Nile Valley to the north of Idfu, west of Assiut and Southwest Beni Suef (Fig. 2-2).

2.4 EARTHQUAKE RISK

Egypt is affected by moderate seismic activity compared to other countries, nevertheless it is exposed to a relatively high seismic risk. This is due to number of factors: a) the population in Egypt, as well as all important and archaeological sites, are concentrated within a narrow belt along the Nile Valley and Delta, b) most of the moderate and significant earthquakes occurred near densely-populated cities and villages, c) the methods of construction vary between old and new buildings with poor construction practice, and finally, d) the soil characteristics in different localities in Egypt have a clear influence on seismic waves amplification. A damaging earthquake is a real, as well as a current, threat to the safety, social integrity, and economic well-being of the population in the region.

Earthquake damages in Egypt are generally related to the occurrence of moderate-size earthquakes at short distances (e.g., 1992, M_S 5.9 Cairo earthquake), rather than bigger earthquakes that are known to occur at far distances along the Northern Red Sea, Gulf of Suez, and Gulf of Aqaba (e.g., 1969, M_S 6.9 Shedwan, and 1995, M_W 7.2 Gulf of Aqaba earthquakes), as well as the Mediterranean offshore (e.g., 1955, M_S 6.8 Alexandria earthquake) (Abou Elenean *et al.*, 2010). Although the 1995, M_W 7.2 Gulf of Aqaba earthquake was the strongest one, it was the 1992, M_S 5.9 Cairo event that left the deepest imprints on everyone, not only because it resulted in hundreds killed and injured people, but also because it incurred a huge economic loss in damages, making it one of the costliest natural disasters in Egypt. The most significant local earthquakes ($M_W \geq 5.5$) which have been located in Egypt since the

year 1900 until the end of year 2013, were listed in Table (2-1) and depicted in Figure (2-2). Among those earthquakes, some details about the most terrifying and damaging events were described in the following.

Table (2-1): Instrumental earthquakes above M_w 5.5 that affected Egypt since 1900.

Date (yyyymmdd)	Time (hhmmss)	Longitude (°E)	Latitude (°N)	Depth (km)	M_w	Epicentral Region
19000306	175800	33.000	29.000	-	6.2	Gulf of Suez
19510130	230723	33.410	32.400	30	5.7	Offshore Sinai Peninsula
19550912	060924	29.610	32.200	20	6.4	Offshore Alexandria
19551112	053214	34.600	25.300	33	5.5	Abu Dabbab, Eastern Desert
19690331	071551	33.938	27.513	06	6.8	Shedwan Island, Red Sea
19720628	094935	33.810	27.700	07	5.5	Shedwan Island, Red Sea
19811114	090523	32.610	23.800	19	5.8	Aswan, Southern Egypt
19820423	144257	32.629	23.598	11	5.5	Aswan, Southern Egypt
19921012	130957	31.142	29.712	22	5.8	Dahshour, Southwest Cairo
19930803	124308	34.548	28.708	18	6.1	Gulf of Aqaba
19951122	041515	34.809	28.769	19	7.2	Gulf of Aqaba
19980528	183332	26.650	31.970	10	5.5	Offshore, Ras El-Hikma

- March 6, 1900 Gulf of Suez earthquake (M_S 6.2, M_w 6.2):** It was located in an unpopulated area in the Gulf of Suez between Zafarana and Gharib to the west of the gulf, and Maghara, in Sinai (Fig. 2-2). It caused rock falls. In Cairo, the earthquake consisted of three consecutive shocks lasting in all about 30 seconds. They were felt by everyone and some people gone out from their houses.
- September 12, 1955 offshore Alexandria earthquake (M_S 6.8, M_w 6.4):** This earthquake was felt in the entire Eastern Mediterranean Basin (Fig. 2-2). In Egypt, it was felt strongly, and led to the loss of 22 lives and damage in the Nile Delta between Alexandria and Cairo. Destruction of more than 300 buildings of old brick construction was reported. A maximum intensity of VII was assigned to a limited area in the Bihira province, where five people died and 41 were injured. In addition, intensities between V to VII were reported in 15 other localities (Kebeasy, 1990).
- November 12, 1955 Abu-Dabbab (Eastern Desert) earthquake (M_S 5.3, M_w 5.5):** This event was felt in Upper Egypt in Aswan, Qena and as far as Cairo, but no damage was reported.

- **March 31, 1969 Shedwan Island earthquake (M_S 6.9, M_W 6.8):** This event occurred to the northwest of Shedwan Island, in the surroundings of the Gulf of Suez (Fig. 2-2). On the island, fissures and cracks in the soil were found. Ten kilometers to the west from the fractured area in the sea, a submerged coral reef was raised above sea level after the event. This event was also felt in Saudi Arabia (Kebeasy, 1990; El-Sayed *et al.*, 1994).
- **November 14, 1981 Aswan (Kalabsha) earthquake (m_b 5.3, M_S 5.6, M_W 5.8):** This earthquake occurred in the Nubian Desert of Aswan (Fig. 2-2). It is of great significance because of its possible association with Nasser's Lake. Its effects were strongly felt to the north of its epicenter (Kalabsha) up to Assiut, and to the south up to Khartoum. The epicentral intensity was VII-VIII. Surface faulting was reported in the epicentral area. Several cracks on the western bank of the Nasser's Lake, and several rock-falls and minor cracks on the eastern bank were reported. This event caused a great alarm due to its proximity to the Aswan High Dam (Kebeasy, 1990, and El-Sayed *et al.*, 1994).
- **October 12, 1992 Cairo (Dahshour) earthquake (m_b 5.8, M_S 5.9, M_W 5.8):** It produced a disproportional amount of damage (estimated at more than 500 million of Egyptian pounds) and the loss of many lives. The shock was strongly felt and caused occasional damage and life loss in the Nile Delta, around Zagazig (Fig. 2-2). The mostly affected area was Cairo, Bulaq and the region to the south, along the western bank of the Nile to Gerza (Jirza) and El-Rouda. In all, 350 buildings collapsed completely and 9000 were irreparably damaged, 545 people died and 6512 people were injured. About 350 schools and 216 mosques were ruined, and about 50000 people were left homeless. It is considered one of the most significant earthquakes in Egypt during the last century (El-Sayed *et al.*, 1994; Abou Elenean *et al.*, 2000).
- **November 22, 1995 Gulf of Aqaba earthquake (M_W 7.2):** It was a strong earthquake located in the southern part of the Gulf of Aqaba (Fig. 2-2). Most of the reported damage was concentrated in the Sinai Peninsula, leading to loss of three lives. Damage was also reported in the platforms of the port facilities in Nuweiba (Abdel-Fattah *et al.*, 2006).
- **May 28, 1998 Ras El-Hikma earthquake (m_b 5.5, M_W 5.5):** It was located offshore, on the northwestern part of Egypt, and it was widely felt in Northern

Egypt (Fig. 2-2). The maximum intensity of VII was assigned at Ras El- Hikma village (~300 km west of Alexandria), and an intensity equal to V–VI at Alexandria. Ground fissures were observed along the beach, and also some cracks in the concrete buildings (Hassoup and Tealeb, 2000).

2.5 PREVIOUS SEISMIC HAZARD ASSESSMENT STUDIES

In the last decades, some seismic hazard assessments for the whole territory of Egypt and several studies for specific localities (e.g., Aswan and Sinai) have been done (Tables 2-2 and 2-3). Early assessments were done by Kebeasy *et al.* (1981), Albert (1986 and 1987), Sobaih *et al.* (1992), El-Sayed *et al.* (1994), Fat-Helbary and Ohta (1996), and Badawy (1998). Some of these studies evaluated the earthquake hazard regardless of seismic source zones, and others estimated the seismic hazard upon the delineation of seismic sources depending on the major tectonic trends prevailing in Egypt. Recently, several seismic hazard studies were carried out for both specific regions and the whole territory of Egypt. Among these studies are the following: Riad *et al.* (2000), El-Sayed *et al.* (2001), Fat-Helbary (2003), El-Hefnawy *et al.* (2006), Deif *et al.* (2009, 2011), Hamouda (2011a,b), and Mohamed *et al.* (2012).

Among these studies, the study carried out by Riad *et al.* (2000) computed the PGA values that were considered in the Egyptian building codes for the years 2004, 2008 and 2011, and also in the Global Seismic Hazard Assessment Project (GSHAP, 1999).

The GSHAP was launched in 1992 by the International Lithosphere Program (ILP) with the support of the International Council of Scientific Unions (ICSU), and was endorsed as a demonstration program in the framework of the United Nations International Decade for Natural Disaster Reduction (UN/IDNDR). This project was finished in 1999. The primary goal of GSHAP was to create a seismic hazard map in a harmonized and regionally coordinated fashion, using a PSHA. As a result of this project, a worldwide and four regional seismic hazard maps were created through a compilation of independent studies conducted for various parts of the Globe. Egypt is included in the map for Europe, Africa and the Middle East (Grünthal *et al.*, 1999). The probabilistic ground shaking map for the EMR was assembled at ETH Zurich, on the basis of contributions of different authors (for Egypt, S. Riad, E. Ibrahim and M. Sobaih). The resulting regional map is not a computed map, but rather a smoothed

composite map based on the existing ground shaking hazard maps of individual EMR countries (Grünthal *et al.*, 1999). All maps were computed for PGA values corresponding to a 10% probability of exceedance in 50 years.

Tables (2-2 and 2-3) describe, in some details, the main differences between the available mentioned seismic hazard assessments which carried out upon Egypt. Table (2-2) gives information, for each study, about the studied area, the approach used in the analysis, the spatial and temporal spanning of the used earthquake catalogue, the seismic source model, the considered attenuation relationship, the software code, and a brief description about the results obtained from each study. It is clear that the majority of these seismic hazard studies are preferred to use the probabilistic than the deterministic approach in their assessments. Both the probabilistic and deterministic approaches have an important role in the seismic hazard assessments. The two approaches have differences, advantages and disadvantages, which in turn can complement each other. The analyzer would prefer one approach over the other depending on several factors: a) how quantitative are the decisions to be made, b) the seismic environment, and finally c) the main scope of the project.

On the other hand, Table (2-3) compares the PGA values (for a return period of 475 years) for the available studies, for some of the most populated and important cities in Egypt. The observed differences might be attributed to several reasons; a) the use of different seismic hazard approaches, b) the consideration of distinct earthquake catalogues spanning different time periods, c) the considered seismic source model, or d) the used GMPE.

Below, we are describing in details two of the most significant studies carried out until now. The first study was performed by Riad *et al.* (2000) which, as mentioned before, is the work considered in the Egyptian building codes (ECP-201: 2004, 2008 and 2011). The other one, is the most recent study until now, performed by El-Hadidy (2012) and published by Mohamed *et al.* (2012), which includes the most updated earthquake data.

Table (2-2): Description of the seismic hazard assessments done upon different regions in Egypt.

The Study	Study Region	Analysis	Earthquake Catalogue	Seismic Source Model	Attenuation Relationship	Software Code	Results
Sobaih <i>et al.</i> (1992)	Whole Egypt	Probabilistic	Helwan station catalogue (1908-1984), Maamoun <i>et al.</i> (1984), ISC bulletin (1910-1984) and USGS bulletin (1903-1984).	10 shallow (area) seismic sources.	Maamoun <i>et al.</i> (1984)	Modified after McGuire (1976)	PGA values with a probability of exceedance of 10, 15 and 20% in 50, 100 and 500 years. Hazard curves for 4 cities were provided.
El-Sayed and Wahlström (1996)	Whole Egypt	Probabilistic	Historical events compiled from Ambraseys (1961, 1978, 1983) and Poirier and Taher (1980). Instrumental events (1900-1993) compiled from ISC bulletin, NEIC, IPRG, Maamoun <i>et al.</i> (1984) and ENSN.	7 shallow (area) seismic sources.	Maamoun <i>et al.</i> (1984)	EQRISK (McGuire 1976)	Intensity values to occur in a time period of 94 years with a probability of exceedance of 10% and 80%.
Fat-Helbary and Ohta (1996)	Aswan area	Probabilistic	Compiled from Maamoun <i>et al.</i> (1984) and Aswan bulletin.	6 shallow area sources and 5 line sources.	Fat-Helbary (1994)	Modified after McGuire (1976) and FRISK code.	PGA values with a 10% probability of exceedance in 100 years.
Badawy (1998)	Northern Egypt	Probabilistic	Historical events compiled from Kebeasy (1990), Maamoun and El-Khashab (1978) and El-Gamal <i>et al.</i> (1993). Instrumental events (until 1995) compiled from ISC bulletin and ENSN.	3 shallow (area) seismic sources.	Maamoun (1979) and Badawy (1998)	EQRISK software (McGuire 1976, 1994)	Expected intensity maps with a 10, 15 and 20% probability of exceedance in one year.
Fat-Helbary (1999)	Whole Egypt	Probabilistic	Historical events compiled from Ambraseys <i>et al.</i> (1994). Instrumental events (1900-1998) obtained by Maamoun <i>et al.</i> (1984), ISC bulletin, NEIC/PDE, Helwan and Aswan bulletins.	12 shallow (area) seismic sources.	Makropolis and Burton (1985)	Modified after McGuire (1976)	Expected intensity maps for return periods of 50 and 100 years, PGA values with a 10% probability of exceedance in 50 and 100 years, and hazard curves for 13 cities.

Table (2-2): Continued.

The Study	Study Region	Analysis	Earthquake Catalogue	Seismic Source Model	Attenuation Relationship	Software Code	Results
Riad <i>et al.</i> (2000)	Whole Egypt	Probabilistic	Historical events compiled from Maamoun (1979), Maamoun <i>et al.</i> (1984), Ben-Menahem (1979) and WCC (1985). Instrumental data (1900-1996) obtained by Makropoulos and Burton (1981), Maamoun <i>et al.</i> (1984), Ben-Menahem (1979), WCC (1985), Riad and Meyers (1985), IPRG and NEIC.	70 (area) shallow and intermediate-depth seismic sources modified after Papazachos (1990) and Shapira and Shamir (1994).	Campbell (1981) for shallow earthquakes and Crouse (1991) for intermediate activity.	EQRISK (McGuire, 1976)	PGA values with a 10% probability of exceedance in 10, 25, 50, 100 and 250 years.
El-Sayed <i>et al.</i> (2001)	Whole Egypt	Deterministic	Historical data compiled from Ambraseys <i>et al.</i> (1994) and Poirier and Taher (1980). Instrumental data (1900-1998) obtained by EMSC, ISC, IPRG, PDE/NEIC, Maamoun <i>et al.</i> (1984), CMT and Abou Elenean (1993).	5 major (area) source zones.	Computation of synthetic seismograms at a set of grid points.	Not mentioned.	Peak displacement, peak velocity and design ground acceleration values.
Fat-Helbary and Tealeb (2002)	Kalabsha (Aswan)	Probabilistic	Aswan annual bulletin.	6 individual regions using both area and line source models.	Fat-Helbary and Ohta (1996)	EQRISK (McGuire, 1976)	Hazard curves for 6 sites.
Fat-Helbary (2003)	Upper Egypt	Probabilistic	ENSN and Aswan annual bulletins (1900-2001).	12 shallow (area) seismic sources.	Makropoulos and Burton (1985)	EQRISK (McGuire, 1976)	Hazard curves for 8 cities in Upper Egypt.
El-Hefnawy <i>et al.</i> (2006)	Sinai Peninsula	Probabilistic	Historical events taken from Ambraseys <i>et al.</i> (1994). Instrumental data (until 2003) compiled from ISC bulletin, Papazachos and Papazachos (1997), ENSN and IPRG.	25 shallow (area) seismic sources.	Joyner and Boore (1981)	SEISRISK III (Bender and Perkins, 1987)	PGA values with a 10% probability of exceedance in 50 and 100 years.

Table (2-2): Continued.

The Study	Study Region	Analysis	Earthquake Catalogue	Seismic Source Model	Attenuation Relationship	Software Code	Results
El-Adham and El-Hemamy (2006)	El-Dabaa (Northern Western Desert)	Probabilistic	Data compiled from NEIC, EMSC (1902-1985), ISC (1964-1996), Maamoun <i>et al.</i> (1984) and ENSN.	8 shallow (area) seismic sources.	Joyner and Boore (1981)	SEISRISK III (Bender and Perkins, 1987)	PGA values with a 10% probability of exceedance in 50, 100 and 450 years.
Fat-Helbary <i>et al.</i> (2008)	Tushka (West of Aswan)	Probabilistic	Data taken from Maamoun <i>et al.</i> (1984), ISC, NEIC, PDE and Aswan bulletin (1982-2008).	9 shallow (area) seismic sources.	Makropoulos and Burton (1985)	HAZ81 (Petrovski <i>et al.</i> , 1983)	PGA values for a return period of 475 years, and a hazard curve for New-Tushka city.
Deif <i>et al.</i> (2009)	Sinai Peninsula	Probabilistic	Historical data taken from Ambraseys <i>et al.</i> (1994). Instrumental data (1900-2006) compiled from IPRG, Abou Elenean (1997), ENSN, Ambraseys and Adams (1993) and ISC.	28 shallow (area) seismic sources (after Abdel Rahman <i>et al.</i> , 2008).	Ambraseys <i>et al.</i> (1996)	SEISRISK III (Bender and Perkins, 1987)	PGA and SA (for 0.2, 0.5, 0.5, 1.0 and 2.0 s) values for a return period of 475 years, and UHS for 4 cities.
Deif <i>et al.</i> (2011)	Aswan area	Probabilistic	Data (1900-2009) compiled from Ambraseys <i>et al.</i> (1994), EHB, ISC, NEIC, CMT, Abou Elenean (1997), ENSN and Aswan bulletin.	24 shallow (area) seismic sources.	Ambraseys <i>et al.</i> (1996), Abrahamson and Silva (1997) and Boore <i>et al.</i> (1997) in a logic-tree approach.	Crisis 2007 (Ordaz <i>et al.</i> , 2007)	PGA and SA (for 0.1, 0.2, 0.3, 0.5, 0.8, 1.0 and 2.0 s) values for a return period of 475 years, UHS for return periods of 475 and 2475 years, deaggregation plots (for 0.1, 0.2, 1.0 and 2.0 s) for return periods of 475 and 2475 years.

Table (2-2): Continued.

The Study	Study Region	Analysis	Earthquake Catalogue	Seismic Source Model	Attenuation Relationship	Software Code	Results
Hamouda (2011a)	Nuweiba (Gulf of Aqaba)	Probabilistic	Historical data compiled from Ambraseys <i>et al.</i> (1994) and Ambraseys (2001). Instrumental data (1900-2006) compiled from ISC (2011), NEIC, NOAA and ENSN bulletins.	4 shallow (area) seismic sources.	Atkinson and Boore (1995, 1997)	Code provided by Kijko (Personal communication).	Expected magnitude curves and PGA values for different probability levels of exceedance.
Hamouda (2011b)	Hurghada (Red Sea)	Probabilistic	Historical data compiled from Maamoun <i>et al.</i> (1984), Ambraseys <i>et al.</i> (1994), Ambraseys (2001) and Badawy (2005a). Instrumental data (1900-2005) compiled from ISC (2011), NEIC, NOAA and ENSN bulletins.	4 shallow (area) seismic sources.	Atkinson and Boore (1995, 1997)	Code provided by Kijko (Personal communication).	Expected magnitude curves and PGA values for different probability levels of exceedance.
Mohamed <i>et al.</i> (2012)	Whole Egypt	Probabilistic	Historical data compiled from Ambraseys <i>et al.</i> (1994), Poirier and Taher (1980), Maamoun <i>et al.</i> (1984), Badawy (1998) and Badawy <i>et al.</i> (2010). Instrumental data (1900-2009) compiled from PDE, NEIC, ISC, EHB, CMT, Papazachos and Papazachou (2003), Abou Elenean (1997) and ENSN (1998-2010).	77 (area) shallow and intermediate sources modified after Papaioannou and Papazachos (2000), Abdel Rahman <i>et al.</i> (2008), Abou Elenean (2010) and Deif <i>et al.</i> (2011).	Abrahmson and Silva (1997), Boore <i>et al.</i> (1997), Campbell and Bozorgnia (2003), and Campbell and Bozorgnia (2008) for shallow sources, and Youngs <i>et al.</i> (1997) and Zhao <i>et al.</i> (2006) for intermediate sources, both in a logic-tree approach.	Crisis 2007 (Ordaz <i>et al.</i> , 2007)	PGA and SA (for 0.1, 0.2, 0.3 and 1.0 s) values for 475 and 2475 years return periods, and UHS (72, 475, 975 and 2475 return periods) for 7 cities.

2.5.1 RIAD *ET AL.* (2000) STUDY

This work included the following steps: compilation and creation of a database for seismic events spanning the time period (2800 B.C.–1996), definition of a seismic source model, and a probabilistic study based on an area source model. As a result, different PGA maps were obtained for all the Egyptian territory, for a probability of exceedance of 10 % in 10, 25, 50, 100 and 250 years. An explanation of the different aspects considered in the development of this study follows.

2.5.1.1 Earthquake Catalogue

A modified and updated earthquake catalogue for Egypt and surrounding areas affecting Egypt was prepared. The earthquake data were compiled from the following catalogues. For the period 2800 B.C. to 1899: Maamoun (1979), Ben-Menahem (1979), Maamoun *et al.* (1984) and WCC (1985). For the period 1900 to 1996: Ben-Menahem (1979), Makropoulos and Burton (1981), Maamoun *et al.* (1984), WCC (1985), Riad and Meyers (1985), Shapira (1994) and NEIC (1995, 1996).

Table (2-3): Computed PGA values (g) with a 10% probability of being exceeded in 50 years (return period of 475 years) for some selected cities in Egypt.

Study	Cairo	Alexandria	Suez	Assiut	Hurghada	Aswan
Fat-Helbary (1999)	0.15	0.07-0.10	0.17	0.05-0.07	0.17	0.25
Riad <i>et al.</i> (2000)	0.13	0.10-0.13	0.13	0.08-0.10	0.20-0.23	0.10-0.13
Fat-Helbary (2003)	-----	-----	-----	0.05	0.21	0.26
El-Hefnawy <i>et al.</i> (2006)	-----	-----	0.05	-----	0.09-0.10	-----
Fat-Helbary <i>et al.</i> (2008)	-----	-----	-----	0.05-0.06	0.14-0.15	0.11-0.14
Deif <i>et al.</i> (2009)	-----	-----	0.06-0.08	-----	0.06-0.08	-----
Deif <i>et al.</i> (2011)	-----	-----	-----	-----	-----	0.07
Mohamed <i>et al.</i> (2012)	0.10	0.05	0.10	0.05	0.13	0.07-0.10

2.5.1.2 Seismic Source Model

The delineation of the seismic source zones developed in this study was mainly based on the generally accepted concepts of the regional tectonics, available geological maps and seismicity. In this respect, observed seismic activity at or near a main fault, or in a faulted area, was a dominant parameter in identifying seismic source zones. The authors defined 56 seismic source zones of “shallow” ($h \leq 70$ km) seismic activity and six zones of “intermediate-depth” ($h \geq 70$ km) seismic activity. The regional delineation consisted of five basic trends: the Greek trend, based on the seismic zone regionalization of Papazachos (1990), the Dead Sea trend, mainly based

on the earthquake catalogue of Israel and its vicinity after Shapira and Shamir (1994), the Pelusium and Qattara trends, the Eastern Mediterranean trend and the Aswan area.

2.5.1.3 Ground-Motion Attenuation Equations

Since Egypt did not have an adequate strong-motion network, there isn't an attenuation relationship for PGA developed specifically for the country. Therefore, attenuation relationships developed for other regions were used. Furthermore, most active regions surrounding Egypt having shallow seismicity associated with surface ruptures, thus the authors used the regional attenuation relationship of Campbell (1981) for Central United States. In addition, they applied the attenuation model of Crouse (1991) for the subduction zones of Greece.

2.5.1.4 Approach, Software Code and Results

A PSHA procedure was followed in this work (using EQRISK software code, developed by McGuire, 1976). Iso-acceleration contour maps were computed with a 90% probability of non-exceedance for exposure times of 10, 25, 50, 100 and 250 years. PGA values with a 90% probability of not being exceeded in 50 years (return period of 475 years) will be shown in Section 2.6.4. In this study, the authors obtained the highest PGA levels at the Southern Gulf of Suez (range of 110-220 cm/s^2). In addition, the populated areas of Egypt (e.g., the Nile Delta, Cairo and Fayoum) are threatened by PGA values of the order of 110 cm/s^2 . Furthermore, they obtained seismic hazard values along the northern coast of Egypt of about 100 cm/s^2 .

2.5.2 EL-HADIDY (2012) AND MOHAMED *ET AL.* (2012) STUDIES

As part of the doctoral work of El-Hadidy (2012), a recent evaluation of the seismic hazard for all the Egyptian territory was carried out. This work included the following steps: compilation of an earthquake database for the time period 112 B.C. to 2011, consideration of a new seismic source model, and a probabilistic study within a logic-tree framework. As a result, PGA and SA values, and UHS for different locations were obtained. The seismic hazard values for rock were calculated for four spectral periods (0.1, 0.2, 0.3 and 1.0 s) and for four different return periods (72, 475, 950 and 2475 years). A brief explanation of the different aspects considered in the development of this study follows.

2.5.2.1 Earthquake Catalogue

An updated earthquake catalogue for Egypt and surrounding areas was used in this study. The historical seismicity data of Egypt (112 B.C. to 1899) was compiled from Maamoun *et al.* (1984), Poirier and Taher (1980), Ambraseys *et al.* (1994), Badawy (1998), Riad *et al.* (2000) and Badawy *et al.* (2010), while the instrumental data (1900 to 2011) were collected from the Preliminary Determination of Epicenters (PDE) bulletin, International Seismological Centre (ISC) bulletin, EHB (Engdahl *et al.*, 1998) catalogue, Centroid Moment Tensor (CMT) catalogue, Maamoun *et al.* (1984), Ambraseys *et al.* (1994), Papazachos and Papazachou (2003), Abou Elenean (1997) and the annual bulletin of the ENSN.

2.5.2.2 Seismic Source Model

Two alternative seismic source models were used in this work, which characterize earthquakes in three tectonic environments: subduction zones (Cyprian and Hellenic Arcs), strike-slip environments (DST), and normal faults (Red Sea-Gulf of Suez-Cairo trend), as well as five background seismicity zones.

The first model is the one proposed by Abou Elenean (2010). The authors established a detailed zonation map for whole Egypt and its surroundings, considering the seismicity distribution and FMSs data. Forty-one seismic source zones of “shallow” earthquakes ($h \leq 60$ km) in and around Egypt were considered. In addition, 7 seismic sources were considered for “intermediate-depth” ($60 \leq h \leq 200$ km) events within the Hellenic Arc (after Papazachos and Papaioannou, 1993). The second used model, which consisting of 72 sources, is the one proposed by El-Hadidy (2012). He compiled and integrated a new seismic zoning map for Egypt and its surroundings, which was mainly based on seismic sources from previous studies (Abdel-Rahman *et al.*, 2008; Deif *et al.*, 2011; and Papaioannou and Papazachos, 2000).

2.5.2.3 Ground-Motion Attenuation Equations

The authors of this study applied the GMPEs of Youngs *et al.* (1997) and Zaho *et al.* (2006) for subduction seismic sources, and the models of Abrahamson and Silva (1997), Boore *et al.* (1997), Campbell and Bozorgnia (2003) and Campbell and Bozorgnia (2008), in a logic-tree framework, for shallow seismic zones.

2.5.2.4 Approach, Software Code and Results

El-Hadidy (2012) and Mohamed *et al.* (2012) followed in their assessments a probabilistic approach. The seismic hazard analysis was computed using the CRISIS (2007) software code (Ordaz *et al.*, 2007). This study led to the generation of a number of seismic hazard maps at rock sites for different return periods and spectral accelerations. They obtained the highest PGA values close to the Gulf of Aqaba (220 cm/s² for a return period of 475 years). In addition, UHS for rock sites for 7 cities (Cairo, Alexandria, Aswan, Assiut, Sharm El-Sheikh, El-Arish and Matruh) were specifically computed.

From Table (2-3), an overall decrease in the hazard values in the second study by El-Hadidy (2012) and Mohamed *et al.* (2012) was observed, with the exception of the Gulf of Aqaba region (Fig. 2-3). In addition, a significant difference in the PGA values for the different cities was observed among these two studies. As mentioned before, these differences are clearly related to the distinct input parameters into both analyses. The authors in the second assessment used a combination of GMPEs in a logic-tree approach, which gives different ground-motion values than those used in the study conducted by Riad *et al.* (2000). Moreover, authors used a different seismic source model with different seismicity parameters.

2.6 SEISMIC DESIGN CODES

The first version of the Egyptian Concrete Code started in 1930, then it was updated in 1962, 1969 and 1988. Before 1989, consideration of seismic input was absent from national codes in Egypt. Buildings were typically designed to resist gravity loads, and the only means of lateral load resistance was provided through the consideration of wind loads in some cases. The first official code of practice to consider seismic actions was published by the Ministry of Housing, Utilities and New Communities in 1988, the Reinforced Concrete Code (ESEE, 1988). However, the code overlooked a number of basic seismic considerations, including the influence of soil conditions and the dynamic characteristics of buildings (Fouad, 1994).

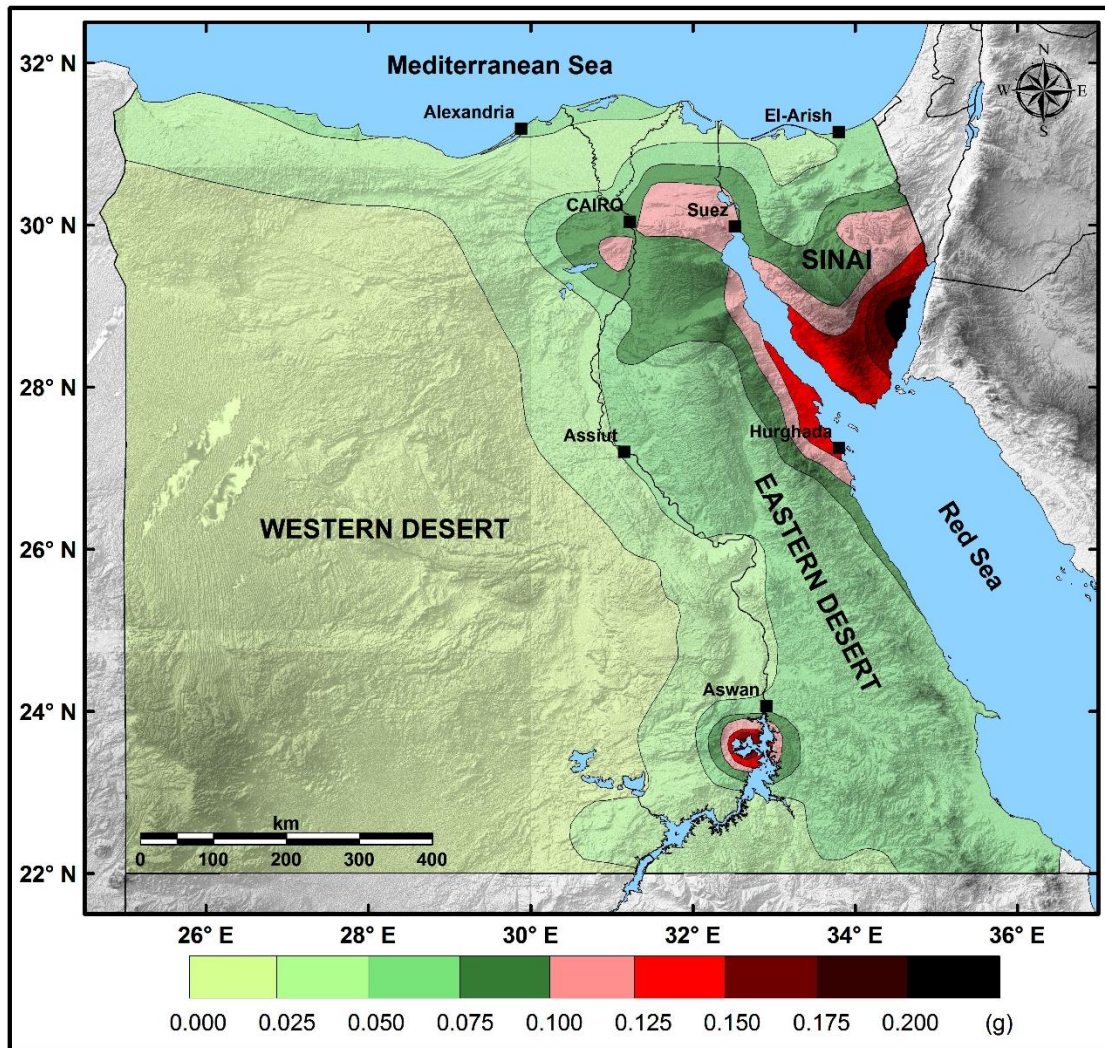


Figure (2-3): Peak ground horizontal acceleration (g) for rock sites, with a 90% probability of not being exceeded in 50 years (return period of 475 years) (replotted after El-Hadidy, 2012).

Following the M_s 5.9, October 12, 1992 Cairo earthquake, the Egyptian Code for Loads and Forces issued on December 1993 (ECP-201, 1993) provided an approach for determining seismic loads for different types of structures. Although this code represented an improvement in comparison with previous regulations (ESEE, 1988), it still adopted significantly simplified assumptions in terms of loading considerations and design procedures. In 2004, a new code (ECP-201, 2004) was issued and dealt with most of the shortcomings present in preceding standards, particularly on the earthquake loading side. This code largely follows the same framework adopted in Eurocode 8 (2004). It introduces the concept of design response spectra and codified force reduction factors for the design of structures, and includes safety verifications relevant to ultimate and serviceability limit states.

Most recently, the Egyptian building code gradually introduced ductility concepts and detailing procedures through its successive versions (ECP-201: 2004, 2008, 2011), although these aspects of the code still need considerable improvement and development (Abdel Raheem, 2013).

2.6.1 REGULATIONS OF THE EGYPTIAN SOCIETY OF EARTHQUAKE ENGINEERING (ESEE, 1988)

The Regulations for Earthquake-resistant Design of Buildings in Egypt were published by the Egyptian Society of Earthquake Engineering (ESEE) in 1988 (Sobaih, 1988). A basic consideration in earthquake-resistant design is to forecast the ground motion for the site of a proposed structure. The 1988 Egyptian regulations require that buildings subjected to seismic action could be analyzed under the action of an equivalent system of static forces applied horizontally at each floor or roof level.

2.6.1.1 Total Horizontal Seismic Force (Base Shear)

The ESEE (1988) states that every building shall be designed and constructed to withstand a total horizontal seismic base shear force V given by the following formula:

$$V = C_S \cdot W_t \quad (2-1)$$

where C_S is the seismic design coefficient and W_t is the total weight. In all mentioned equations, the original abbreviations that already have been used in the quoted building codes, were used for the different parameters.

The seismic design coefficient C_S must be determined from the following formula:

$$C_S = Z \cdot I \cdot S \cdot M \cdot R \cdot Q \quad (2-2)$$

where Z is the seismic zoning factor, I is the importance factor, depending on the building use and occupancy, S is the structural system type factor, that depends on the capacity of the structure to resist lateral forces, M is the material factor, that depends on the construction material, R is the risk factor, depending on the presence of flammable or toxic materials, and finally Q is the construction quality factor.

2.6.1.2 Seismic Action

The seismic zoning factor Z is determined from the equation:

$$Z = A \cdot C \cdot F \quad (2-3)$$

where A is the ground horizontal acceleration (Fig. 2-4), C is the standardized response spectrum for an average damping of 5 % (Fig. 2-5), and F is the foundation soil factor.

According to the ESEE (1988) regulations, Egypt was divided into four seismic zones (Z-0, Z-1, Z-2 and Z-3) according to the level of seismic activity and hazard (Fig. 2-4). The seismic hazard was described in terms of PGA (A factor in Eq. 2-3), which is equal to zero for areas in zone Z-0. These regions were considered of very low seismicity and do not need any special seismic design considerations. For zones Z-1, Z-2 and Z-3, the A values are equal to 0.02, 0.04 and 0.08 g, respectively. Regions of high seismic activity (Z-3 in Fig. 2-4) mainly include counties that are adjacent to the Red Sea and Mediterranean Sea shores and Southern Sinai Peninsula, and around Nasser's Lake. Also, as a measure of the seismic intensity, the regulations provide seismic intensity grades for each seismic zone. For zone Z-0, the intensity grade is considered $\leq V$, while for zones Z-1, Z-2 and Z-3, the intensity grades are VI, VII and VIII, respectively.

2.6.1.3 Soil Conditions

According to these regulations, the nature of the supporting soil at the construction site was classified into three subsoil types. This classification system was used to account for the influence of local ground conditions on the seismic action in terms of the foundation soil factor. $F = 1.0$ for rock, dense and very dense soils, $F = 1.3$ for compact soils, and $F = 1.5$ for very loose and loose soils.

2.6.2 EGYPTIAN CODE FOR THE CALCULATION OF LOADS AND FORCES (ECP-201: 1993)

The great economic and human losses due to the M_S 5.9, October 12, 1992 Cairo earthquake, were mainly related to the fact that buildings were designed to resist only vertical loads and had insufficient lateral resistance (Abdel Raheem, 2013). After that, it becomes a necessity to develop a new building code taking into account the shortcomings of the previous regulations. Hence, the Egyptian Code for the Calculation of Loads and Forces-ECLF (1993) was proposed.

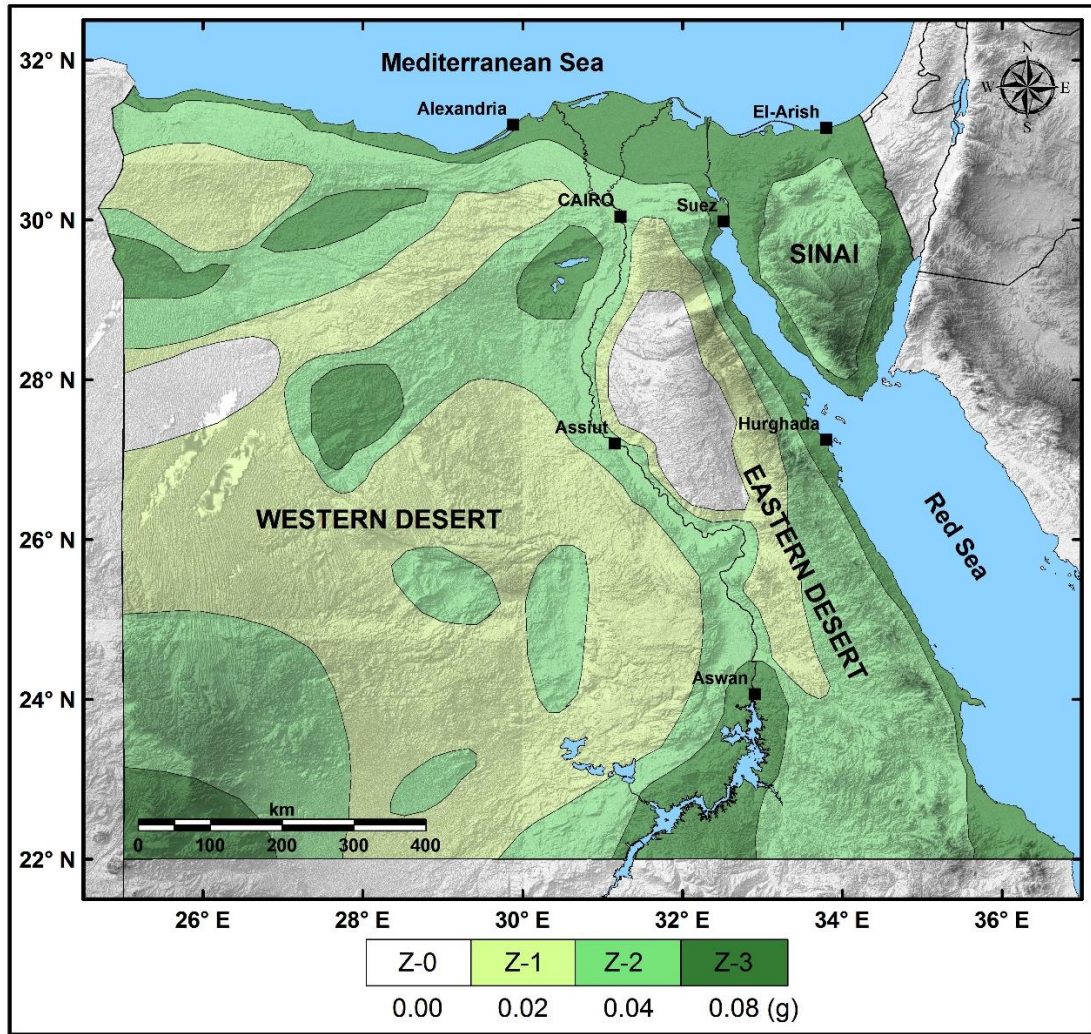


Figure (2-4): Seismic activity zoning map for Egypt (replotted after ESEE, 1988).

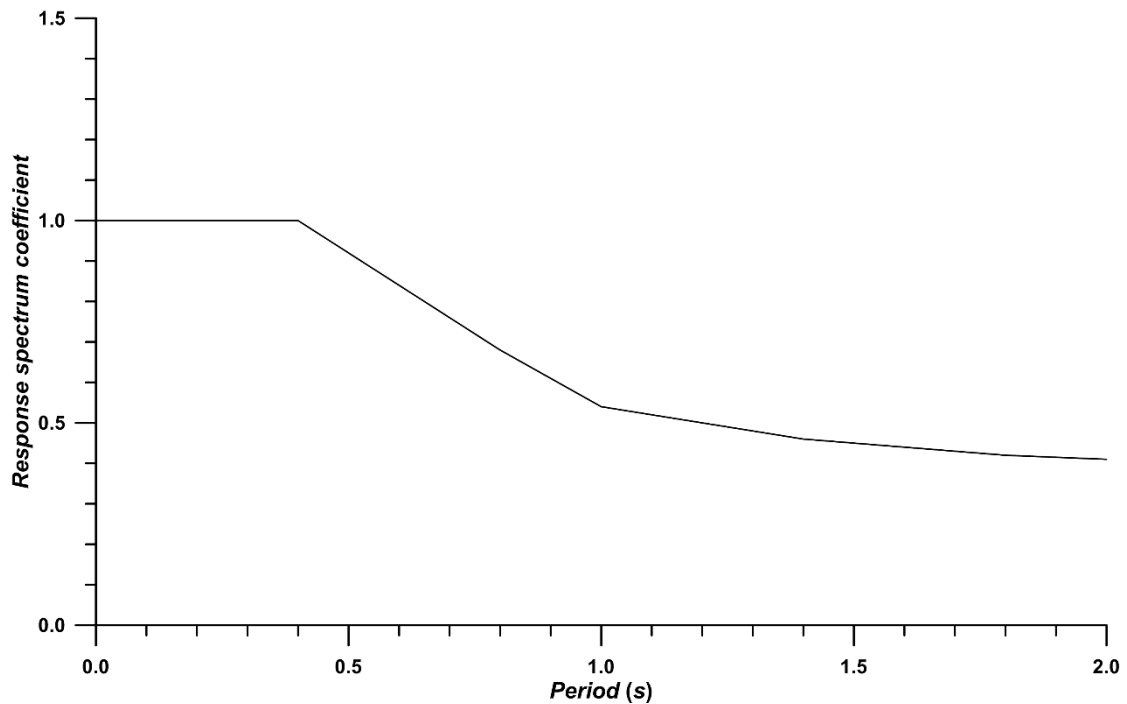


Figure (2-5): Standardized response spectrum coefficient for an average damping of 5% (replotted after Fouad, 1994).

2.6.2.1 Total Horizontal Seismic Force (Base Shear)

The ECP-201 (1993) allows to calculate the seismic design loads (lateral shear forces and torsional moments) for buildings which their height not exceed 100 m, with height to width (in the direction of the seismic force) ratio not exceeding 5, and provided that the structural system must be uniform in plan and all through the height of the building. The structures are to be designed to resist a total horizontal seismic force V acting above the foundation level in a direction parallel to each one of the two main axes of the structure separately. This force must be computed according to the equation.

$$V = Z \cdot I \cdot K \cdot C \cdot S \cdot W \quad (2-4)$$

where Z is the seismic zoning factor, I is the importance factor, depending on the building use and occupancy, K is the structural system coefficient, that depends on the capacity of the structure to resist lateral forces, C is the structural coefficient, that depends on the fundamental period of the building, S is the soil coefficient, and W is the total weight of the building.

The structural coefficient, C , must be computed from the equation:

$$C = \frac{1}{15\sqrt{T}} \quad (2-5)$$

where T is the fundamental period of vibration of the building in seconds, which depends on the total number of stories above the base of the building. C shall not be greater than 0.12.

Moreover different values for the common parameters and considered seismic hazard (seismic zoning factor), the ECP-201 (1993) code does not take into account coefficients concerning construction materials, risk factor nor construction quality factor like the previous ESEE (1988) regulations.

2.6.2.2 Seismic Action

No explicit value of the design PGA is given in this code. Instead, the seismic hazard is described in terms of a seismic zoning factor, Z , which represents a measure of the seismic intensity of the region. The factor is dependent on the site location within the seismic activity zoning map (Fig. 2-6).

In this code, Egypt is divided into three main zones (Z-1, Z-2 and Z-3) according to the level of seismic activity. Zone Z-1 includes all the regions which

affected by low-magnitude earthquakes. This zone nearly has the same distribution as ESEE (1988) map, but it extends to other areas in the Southern Eastern Desert. Zone Z-2 includes regions of low to moderate seismic activity, which located at some parts of Sinai Peninsula, Nile Delta, Nile Valley, Eastern Desert and Western Desert. It has more extension to the southwestern direction from Cairo than in the ESEE (1988) regulations. Zone Z-3 includes areas located along the Red Sea and Mediterranean Sea coasts, and some parts from Aswan, Fayoum and Ismailia. This last zone includes areas with moderate seismic activity. It covers the same geographical distribution as the ESEE (1988) code, except the area of Siwa at the Egyptian-Libyan borders. The seismic zoning factors for the three zones, in this building code, are equal to 0.1, 0.2 and 0.3 g, respectively, which completely show an increase in the acceleration values rather than the seismic zoning factor considered in the previous regulations.

2.6.2.3 Soil Conditions

The influence of the soil on the seismic action is included in the S factor. $S = 1.0$ for rock, dense or very dense soils, $S = 1.15$ for medium density soils or cohesive soils, and $S = 1.3$ for loose or weak cohesive soils. For medium and loose soil, this factor is less than the one considered in the previous ESEE (1988) regulations (F factor in Eq. 2-3).

2.6.3 THE UNIFORM BUILDING CODE (UBC-97)

Although this is not properly an Egyptian code, this regulation has been considered because it presents seismic zonation factors for many cities around the world (including Egypt) corresponding to locations of US embassies and consulates. The procedures and limitations for the design of structures shall be determined considering seismic zoning, site characteristics occupancy configuration, structural system and building height.

The UBC (1997) provided a seismic zonation map for the US, dividing it into six zones, from 0 (no seismic design is required) up to 4, for sites near active seismic sources, with zone 2 being subdivided into two, 2A and 2B. A seismic zone factor was provided for each one of these zones, which corresponds to the PGA value for rock-site conditions and for a 10% probability of exceedance in 50 years. The seismic zone factors for zones 1, 2A, 2B, 3 and 4 are 0.075, 0.15, 0.2, 0.3 and 0.4 g, respectively. Three Egyptian cities were included in the second zone 2A, they are Alexandria, Cairo and Port Said.

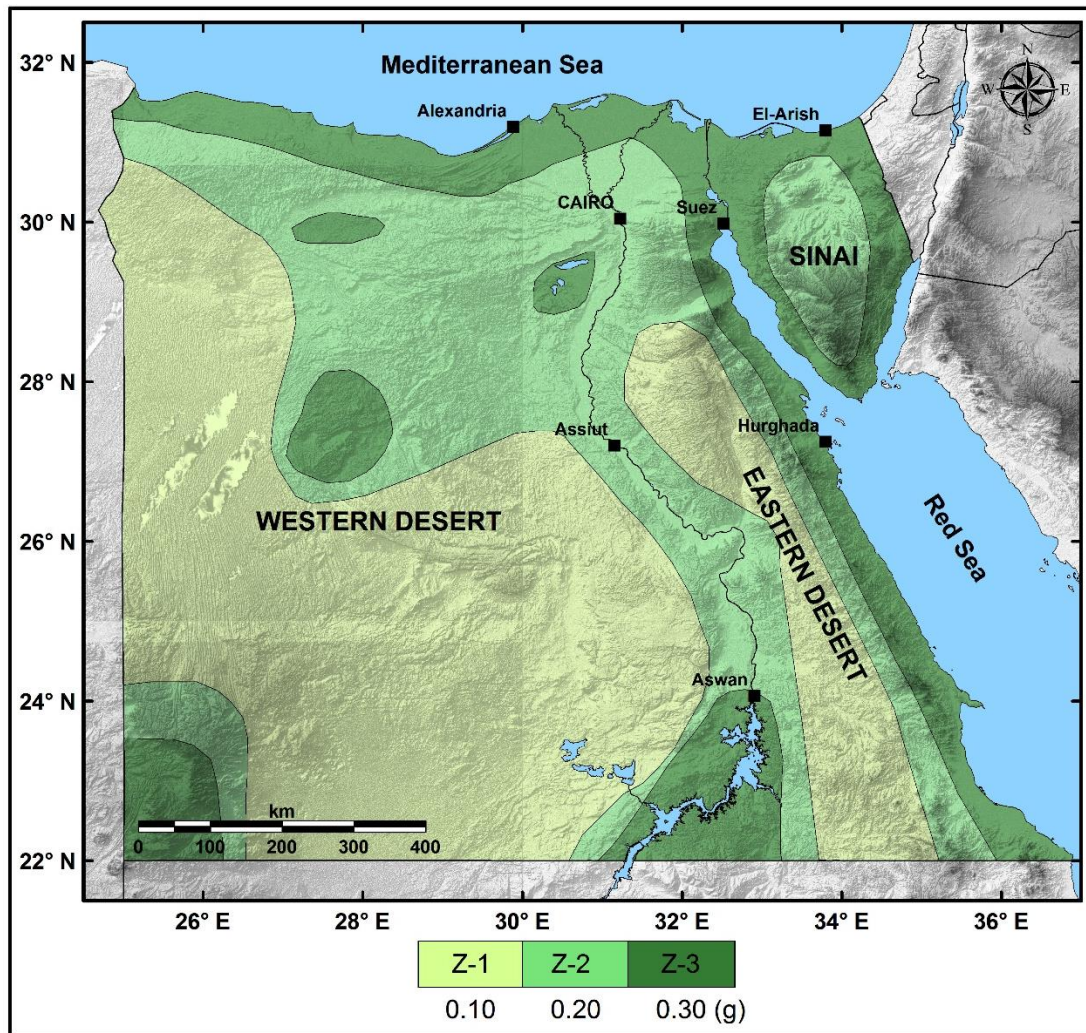


Figure (2-6): Seismic activity zoning map for Egypt (replotted after ECP-201, 1993).

2.6.4 EGYPTIAN CODES FOR THE CALCULATION OF LOADS AND FORCES (ECP-201: 2004, 2008, 2011)

After the occurrence of the M_S 5.9, October 12, 1992 Cairo earthquake, the scientists and engineers gave a great attention to revising code for seismic loads, and it was modified several times. Since October 1992, a set of Egyptian codes have been released to prevent buildings collapse and/or control major damages of structural elements. Furthermore, the Egyptian Government takes into their account generating several periodical building codes which consider more up-to-date aspects than the previous codes. Three codes were elaborated since 2004 until now. They are the ECP-201 (2004, 2008 and 2011). Concerning the seismic action in the three codes, there is a great similarity between them, thus the following discussion will be for all these regulations together.

2.6.4.1 Seismic Action

In these codes, Egypt is divided into five seismic zones (Fig. 2-7), depending on the seismic hazard values. By definition, the hazard within each zone is assumed to be constant. The seismic hazard is described in terms of a single parameter, a_g , which represents the design PGA for rock. For zones 1, 2, 3 and 4, the a_g values are 0.10, 0.125, 0.15 and 0.20 g, respectively. Zone 5 is subdivided into two sub-zones, 5a and 5b, with a_g values of 0.25 and 0.30 g, respectively.

These codes provide the seismic zoning map, which depicts the seismic hazard in terms of PGA with a 10% probability of exceedance in 50 years, corresponding to a return period of 475 years. The map was based on the work done by Riad *et al.* (2000), discussed before, and considered in the GSHAP (1999). In addition, the code was supplied with a complementary table that shall be used jointly with the seismic zoning map to determine the seismic zone for several cities and regions in Egypt.

2.6.4.2 Soil Conditions

According to the ECP-201 (2004, 2008) codes, the nature of the supporting soil at the construction site shall be classified into four subsoil types, from A to D (Table 2-4). In ECP-201 (2011), an additional soil type was also included that is named as E (Table 2-4). The classification is based upon the value of the average shear-wave velocity in the upper 30 m of the soil profile (V_s^{30}). For sites with ground conditions not matching any of the four subsoil classes defined by the code, special studies for the definition of the seismic action are required.

2.6.4.3 Basic Representation of the Seismic Action

Within the scope of ECP-201 (2004, 2008 and 2011) codes, the earthquake motion at a given point was represented by an elastic response spectra. The code provides two types of spectrum shapes, Type 1 and Type 2 (Fig. 2-8). The Type-2 response spectrum must be used for coastal areas lying on the Mediterranean Sea up to a distance of 40 km away from the coast, while Type-1 spectrum must be applied for all other regions. The selection of the appropriate acceleration values for a specific site must be determined according to the seismic zoning map (Fig. 2-7) and its companion table attached to the code itself.

The seismic action is represented by a horizontal elastic response spectrum, in the same way as Eurocode 8 (2004), defined by the following expression (Fig. 2-7):

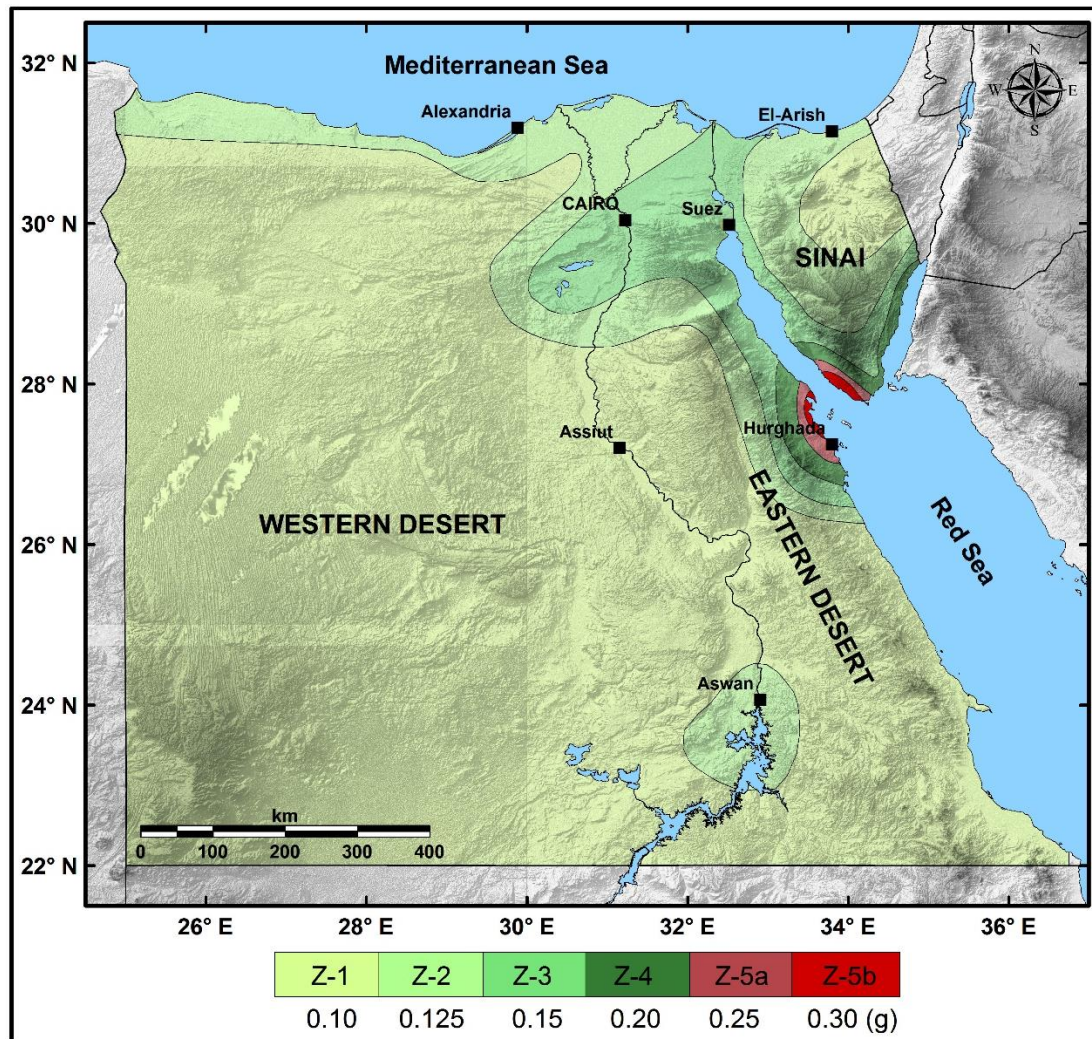


Figure (2-7): Seismic hazard zoning map for Egypt (replotted after ECP-201: 2004 and Riad *et al.*, 2000).

Table (2-4): Classification of subsoil conditions according to ECP-201 (2004, 2008 and 2011).

Soil Class	Description	Shear Wave Velocity
<i>ECP-201 (2004, 2008 and 2011) Codes</i>		
A	Rock layer (weak to medium weathering) extends to at least 15 m thick, and probably including at most 3 m of weaker material at the surface.	> 800 m/s
B	Cohesionless soil (gravel, sand) – very dense soil, or cohesive soil (silt, clay) – very stiff soil. Layers extend to at least 15 m thick.	360-800 m/s
C	Cohesionless soil (gravel, sand) - dense or medium-dense soil, or cohesive soil (silt, clay) – stiff to medium-stiff soil. Layers extend to at least 15 m thick.	180-360 m/s
D	Cohesionless soil (gravel, sand) – loose soil, or cohesive soil (silt, clay) – soft or collapsing soil. Layers extend to at least 15 m thick.	< 180 m/s
<i>Only considered in ECP-201 (2011) Code</i>		
E	Surface layer composed from alluvium deposits overlain more compatible material.	-----

$$S_e(T) = \begin{cases} a_g \cdot S \cdot \left[1 + \frac{T}{T_B} \cdot (2.5\eta - 1.0) \right] \gamma_I & 0 \leq T \leq T_B \\ 2.5a_g \cdot S \cdot \eta \gamma_I & T_B \leq T \leq T_C \\ 2.5a_g \cdot S \cdot \eta \cdot \left[\frac{T_C}{T} \right] \gamma_I & T_C \leq T \leq T_D \\ 2.5a_g \cdot S \cdot \eta \cdot \left[\frac{T_C \cdot T_D}{T^2} \right] \gamma_I & T_D \leq T \leq 4s \end{cases} \quad (2-6)$$

where T is the vibration period of a linear single-degree-of-freedom system, a_g is the design ground acceleration for the reference return period (475 years for a building with importance factor equals to 1.0), T_B and T_C are the lower and upper limits of the constant SA branch, T_D is the period value defining the beginning of the constant displacement response change of the spectrum, η is the design damping correction factor for the horizontal elastic response spectrum, where a reference value of $\eta = 1$ corresponds to a 5% viscous damping ratio, S is the soil factor, and γ_I is the importance factor of the building [considered only in the ECP-201 (2008 and 2011) codes]. S , T_B , T_C , and T_D are only functions of the ground type category (A to D) assigned to the site (Table 2-5).

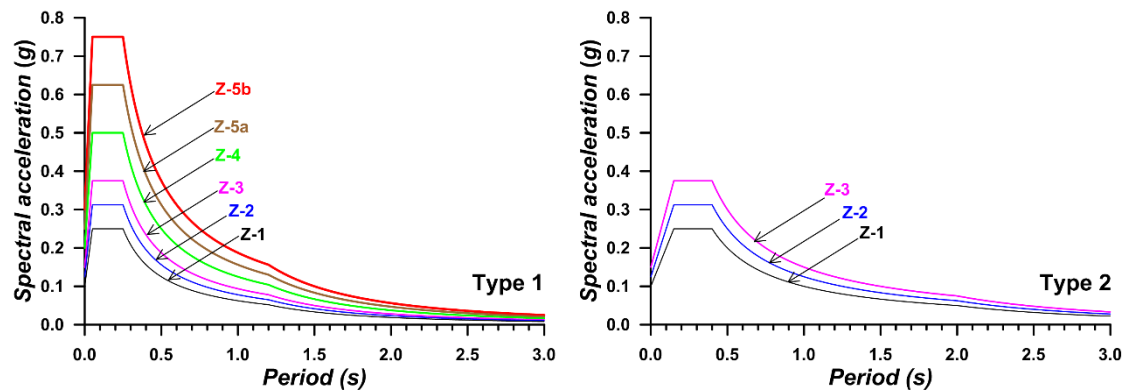


Figure (2-8): Type-1 elastic response spectra for all considered seismic zones (from 1 to 5) and Type-2 spectra for the zones (from 1 to 3) located along the Mediterranean Sea coast. Spectra plotted for rock and 5% damping.

Table (2-5): Parameters for the different soil classes for both Type-1 and Type-2 elastic response spectra in ECP-201 (2004, 2008 and 2011).

ECP-201 (2004 and 2008) Codes	Type-1 Spectrum				Type-2 Spectrum			
	S	T_B	T_C	T_D	S	T_B	T_C	T_D
A (rock)	1.00	0.05	0.25	1.20	1.00	0.15	0.40	2.00
B (stiff soil)	1.35	0.05	0.25	1.20	1.20	0.15	0.50	2.00
C (soft soil)	1.50	0.10	0.25	1.20	1.25	0.20	0.60	2.00
D (very soft soil)	1.80	0.10	0.30	1.20	1.35	0.20	0.80	2.00
ECP-201 (2011) Code								
E (alluvium deposits)	1.60	0.05	0.25	1.20	1.40	0.15	0.50	2.00

2.7 REVIEW AND REMARKS

One important and major difference between the ECP-201 (1993) and the subsequent codes is the fact of the adoption of a response spectrum. El-Arab (2011) proclaim that the newest provisions, ECP-201 (2004, 2008, 2011) have a similar formulation, with the exception of the importance factor both in response spectrum (γ_1) and in the base shear equation (J), which yields final identical base shear.

Table (2-6) is an attempt to show the similarities and differences between the Egyptian building codes from a point of view of the seismic action values. It displays the considered seismic action for a 2-stories residential building in rock site in some of the most populated cities, some of them were located within the highest seismic hazard area in Egypt. We noticed that the seismic zoning factor (A) for some cities (e.g., Cairo and Assiut) in the ECP-201 (1993) is approximately ten times those values (Z) considered in the ESEE (1988). This does not mean that the resultant seismic action is also ten times, because there is another factor that in turn decreasing the final result. This factor is the structural coefficient factor (C in Eqs. 2-3, 2-4) which behaves in the contrary, and reduces ten times in the ECP-201 (1993) than in previous regulations. Moreover, there is a significant increase (e.g., 19 times for Cairo city and 12 times for Assiut city) in the final seismic action values when comparing the most recent ECP-201 (2004, 2008, 2011) codes with the previous regulations (ESEE 1988; ECP-201 1993).

Table (2-6): Seismic action for rock, for a typical 2-stories residential building ($T = 0.2$ s).

City/ Seismic Action	ESEE (1988)	ECP-201 (1993)	ECP-201 (2004, 2008, 2011)
	$A \cdot C \cdot F$ Eq. (2-3)	$Z \cdot C \cdot S$ in Eq. (2-4)	$S_e(T)$ Eq. (2-6)
Cairo	$0.02 \cdot 1.00 \cdot 1.00 = 0.02$ g	$0.20 \cdot 0.12 \cdot 1.00 = 0.02$ g	Type-1 0.38 g
Alexandria	$0.08 \cdot 1.00 \cdot 1.00 = 0.08$ g	$0.30 \cdot 0.12 \cdot 1.00 = 0.04$ g	Type-2 0.33 g
Suez	$0.08 \cdot 1.00 \cdot 1.00 = 0.08$ g	$0.30 \cdot 0.12 \cdot 1.00 = 0.04$ g	Type-1 0.38 g
Assiut	$0.02 \cdot 1.00 \cdot 1.00 = 0.02$ g	$0.20 \cdot 0.12 \cdot 1.00 = 0.02$ g	Type-1 0.25 g
Hurghada	$0.08 \cdot 1.00 \cdot 1.00 = 0.08$ g	$0.30 \cdot 0.12 \cdot 1.00 = 0.04$ g	Type-1 0.63 g
Aswan	$0.08 \cdot 1.00 \cdot 1.00 = 0.08$ g	$0.30 \cdot 0.12 \cdot 1.00 = 0.04$ g	Type-1 0.31 g

All in all, these major changes among the successive Egyptian building codes, will in turn affect not only the values of the seismic action in each code, but will affect the building design itself. El-Arab (2011) noticed that the base shear value obtained from ECP-201 (2004, 2008) is greater than the values obtained using ECP-201 (1993).

2.8 SUMMARY AND CONCLUSION

This chapter aimed at reviewing and evaluating the previous seismic hazard assessment studies and their representation in the Egyptian building codes. We found that, many seismic hazard studies have been done in the last decades upon the whole Egyptian territory as well as for specific regions. We compared and described these studies in terms of the study region, the analysis approach, the used earthquake catalogue, the seismic source model, the considered attenuation relationship, the software code and the representation of the results (Table 2-2). In addition, we compared the obtained values between these studies by choosing six cities in Egypt and studying PGA values or the PGA range in which it is included each city in each study (Table 2-3). Moreover, a detailed review for the seismic action in the successive Egyptian building codes was outlined, showing the seismic action for specific cities considered in the different codes (Table 2-6).

Several seismic hazard assessments using different approaches have been done in Egypt. Each one of these assessments had used different earthquake catalogues, seismic source models, and attenuation relationships. Hence, it is expected to get different results among them. All the more, from Table (2-6) it is clear that successive building codes gives different seismic action values for each city. Other question is the fact that the current building code (ECP-201, 2011), which based on Riad *et al.* (2000) study, does not give a certain PGA value for each city in Egypt, and it just divides the whole territory of Egypt into six broad zones, assigning to each zone only one seismic action value. Moreover, the current building code uses two types of an elastic response spectra, one of them is for the sites which are located along the Mediterranean coast and the other is for all other sites in Egypt.

We are encouraging to use only one elastic response spectrum, including some parameters in order to consider the potential Eastern Mediterranean subduction zone effects. In conclusion, we are recommending the following. The establishment of a scientific committee which its main goal could be establishing a new building code that represents the seismic action for each city correctly and precisely. This committee should include geologists, seismologists and engineers. Geologists should be concerned to assess the current knowledge on active faults throughout Egypt. Seismologists should be established a new assessment of the seismic hazard for the Egyptian territory. This assessment should be based on the compilation of an updated

earthquake catalogue, and a consensual seismic source model based on all available geological, geophysical and seismological data.

Moreover, seismologists should be interested in establishing an attenuation relationship for Egypt if there are enough acceleration data to do it. If not, they have the choice to employ either a theoretical stochastic model or apply some worldwide widely-used attenuation models in a “consensus decision-making”. After that, engineers must start in designing and implementing a new building code which could represent the most updated and consensually knowledge on the seismic action for each city.

2.9 ACKNOWLEDGMENTS

We would like to thank the two anonymous reviewers for their valuable comments and suggestions. This research work is supported by the Egyptian Ministry of the Higher Education (Cultural Affairs and Missions Sector, Cairo) and the Spanish Seismic Hazard and Active Tectonics research group. In addition, appreciation is necessary goes to Prof. Amin Saleh Aly, Faculty of Engineering, Ain Shams University, who provides us some critical information about the Egyptian building codes.



Chapter **3**

An Earthquake Catalogue (2200 B.C. to 2013) for Seismotectonic and Seismic Hazard Assessment Studies in Egypt

Sawires, R., Peláez, J.A., Fat-Helbary, R.E., and Ibrahim, H.A. (2016). An earthquake catalogue (2200 B.C. to 2013) for seismotectonic and seismic hazard assessment studies in Egypt. In: D'Amico, S. (ed.) *Earthquakes and Their Impact on Society*, Springer, 97-136.

ABSTRACT

The instrumental earthquake catalogues show the overall seismicity of the Earth. However, examining and inspecting the historical records plus the instrumental recorded events is necessary to understand long-term seismicity. Moreover, regional seismic and focal mechanism catalogues provide critical information for different seismological investigations, including seismic hazard assessments and seismotectonic studies. The present work aims at preparing new and up-to-date unified and Poissonian earthquake catalogue for Egypt including the focal mechanism solutions data, so that the earthquake information can be reached from a single source.

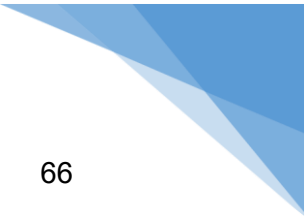
A catalogue for earthquakes that occurred in Egypt and its vicinity during the period 2200 B.C. - 2013 was compiled for achieving a unified magnitude scale. Data were obtained from different sources, local, regional and international (e.g., the regional catalogue of Ambraseys *et al.*, 1994; the International Seismological Centre (ISC) and the Annual Bulletin of the Egyptian National Seismological Network). The initial

compilation spanning a region from 21° to 38°N and from 22° to 38°E, and includes all the events having an assigned magnitude of 3.0 and above for international sources and any magnitude for local sources on any magnitude scale. Earthquake magnitudes are reported in different scales and come from a variety of sources. The initial compiled catalogue comprised a total of 64613 earthquakes (historical and instrumental events). In addition, a focal mechanism solution database was collected. This database contains 688 fault plane solutions gathered from different published and unpublished sources, covering the time period from 1940 until the end of 2013.

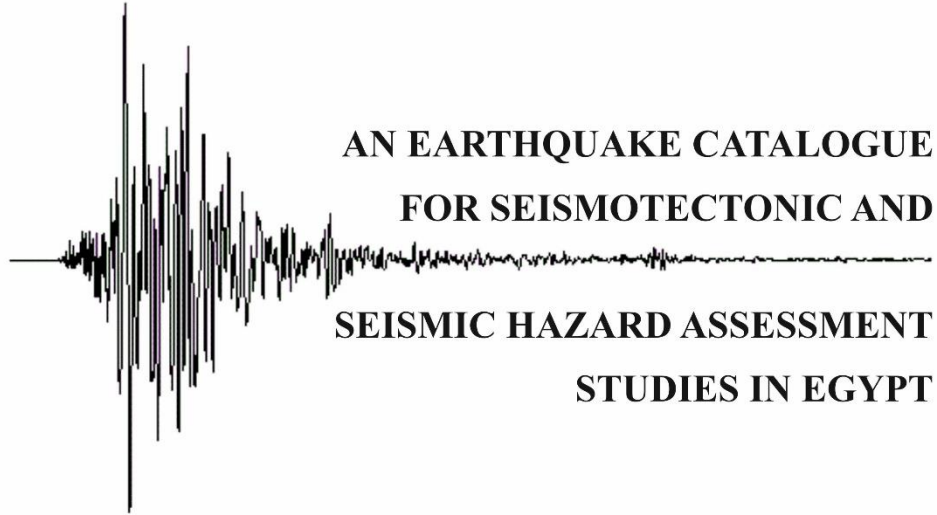
For establishing a common magnitude, namely an equivalent moment magnitude M_w , two new relationships correlating M_s and m_b with M_w were derived. After this process, the catalogue was cut off below magnitude M_w 3.0, because these magnitudes are not significant for seismic hazard studies. All non-Poissonian (dependent) events were removed using the approach proposed by Gardner and Knopoff (1974). A total of 16642 events represent the final Poissonian catalogue including main shocks with a magnitude above or equal to M_w 3.0.

Finally, the degree of completeness for the entire catalogue was checked for the different magnitude values. In addition, separately from the Mediterranean region, the completeness for the Egyptian territory sub-catalogue was also checked. The results derived in each case have been interpreted in the framework of the establishment and development of the international and national networks.

HEADINGS:		Page
3.1	Introduction.....	46
3.2	Tectonic Setting of Egypt.....	49
3.3	Seismicity of Egypt.....	51
3.4	Seismic Record in Egypt.....	54
	3.4.1 The Pre-instrumental Era (Pre-1900).....	54
	3.4.2 The Instrumental Period (Post-1900).....	57
3.5	Earthquake Catalogue Compilation.....	61
3.6	Catalogue Analysis.....	64
	3.6.1 Converting Intensities and Reported Magnitudes to Moment Magnitude.....	64



3.6.2	Catalogue Declustering.....	66
3.6.3	Catalogue Completeness.....	67
3.6.4	Magnitude-Frequency Relationship.....	72
3.7	Focal Mechanism Solutions Database (1940–2013).....	74
3.8	Discussion.....	75
3.9	Conclusions.....	79
3.10	Acknowledgments.....	82



Of all natural hazards, earthquakes are those which historically have caused the most extensive impact and disruption in terms of damage to infrastructure, human-casualties and economic losses. They are the expression of a continuing evolution of the Earth Planet and a reshaping of the Earth's surface. They are the deadliest of all natural disasters affecting the human environment. Every year more than one million earthquakes shake different regions of the world, some so feeling and gentle that only the most sensitive instruments can detect the motion, and others so violent that whole communities are shattered and large sections of terrain are shifted in this process that can start landslides, block rivers, cause floods, and set massive sea waves surging across the oceans.

The amount of damage and number of fatalities at a certain location caused by an earthquake depends on various factors: the magnitude and characteristics of the earthquake focus, distance from the epicenter, soil characteristics, density of buildings and population, and structural design of buildings and infrastructures, among others. These facts are playing an important role in decreasing or increasing the number of victims in recent earthquakes, especially in the developing countries. The increasing population in the earthquake-prone cities, poor construction quality and lack of building code enforcement are major reasons why the vulnerability due to earthquake is also increasing.

3.1 INTRODUCTION

Today scientists, technicians and engineers know a lot of details and information about earthquakes, where they are most likely to occur, how deep they originate, and how they affect land. Researchers are applying this knowledge to future programs for

predicting when and where the next earthquake might occur and for constructing buildings and installations that might be better able to withstand earthquake violence. Man may never be able to control or even predict earthquakes with satisfactory accuracy, but he can learn to live with them in relative safety. Occurrences of earthquakes in different parts of the world and the resulting losses, especially human lives, have highlighted the structural inadequacy of many buildings to support seismic loads.

Short and mid-term earthquake forecasting may one day be able to reduce significantly casualties associated with catastrophic earthquakes. However, a long-term preventive policy is the only possible way for the reduction of life losses and socioeconomic impact associated with them. Such preventive policy should be based on: i) the assessment of seismic hazard and risk, ii) the implementation of safe building construction codes, iii) the increased public awareness on natural disasters, and iv) a strategy of land-use planning taking into consideration the seismic hazard and other natural disasters (Riad *et al.*, 2000).

Seismic hazard estimation is an essential component for earthquake-resistant design, and for the preparation of seismic zoning maps which provide the necessary input information for the design of ordinary structures. The preparation of basic data for the seismic hazard assessment starts immediately after evaluating the seismic record (a complete, reliable, and processed earthquake catalogue).

Earthquake catalogues are the starting point for a seismic hazard assessment. Catalogues consist of estimates of past earthquake locations, described by three spatial and one temporal coordinates, and the magnitudes of events that have occurred in or near the region of interest. The quality, consistency and homogeneity of these data are directly reflected in the accuracy of the results of a seismic hazard assessment. Earthquake catalogues, along with a good understanding of the geology and seismotectonic environment are the fundamental bases for constructing the seismicity model, which is the first element needed to carry out the assessment.

A reliable knowledge of the earthquakes that occurred at a site of interest is the key stone for seismic hazard estimates and seismotectonic studies. The seismic history available is the result of a collection of quite heterogeneous pieces of information spanning from recent instrumental records to macroseismic observations obtained from old documentary sources. In general, this collection is characterized by different

levels of reliability due to heterogeneity in sampling procedures, data processing, and availability of relevant information. As concerns the instrumental part of the catalogue, changes in the monitoring networks (both in terms of geometry and density of stations), and the procedures for earthquake parameterization, could result in seismic compilations characterized by different levels of completeness and reliability.

A complete and consistent catalogue of earthquakes can provide good data for studying the distribution of earthquakes in a region as a function of space, time, and magnitude. However, most catalogues do not report the magnitude of earthquakes consistently over time, in addition to varying uncertainties in hypocenter locations. This may pose as an obstacle for delineating seismicity patterns or for assessing seismic hazards. Because earthquake magnitude has become an indispensable source parameter of earthquakes since its inception, it is important to convert the original magnitudes based on various scales in different time periods to a common magnitude scale throughout the whole period.

A unified catalogue is crucial for statistical analysis of earthquakes, even more for seismic hazard studies. A reliable earthquake catalogue is containing accurate information (e.g., epicentre locations, focal depths, and earthquake magnitudes) which is of utmost importance in order to determine various parameters needed for the seismic hazard assessments. A complete and consistent catalogue of earthquakes provides a key element for studying the distribution of earthquakes in a region as a function of space, time, and magnitude.

Although Egypt is affected by moderate seismic activity compared to other countries, it is exposed to high seismic risk. This is due to many factors: 1) the population in Egypt, as well as all important and archaeological sites, are concentrated within a narrow belt along the Nile Valley and Delta, 2) most of earthquakes occurred near overpopulated cities and villages, 3) the methods of construction vary between old (as those still being used in the villages) and new buildings with poor construction practice, and finally, 4) the soil characteristics in different localities in Egypt and their influence on seismic amplification. A damaging earthquake is a real, as well as a current, threat to the safety, social integrity, and economic wellbeing of the population in the region. Thus, earthquake hazard assessment studies in Egypt are greatly needed to identify areas with different degrees of vulnerability. They will serve for further risk studies, construction codes, and also for land-use planning.

The published seismic databases covering Egypt until now are inadequate to study the long-term seismicity and recurrence interval for large earthquakes in the region. Thus, the primary goal of this chapter was to catalogue all known events from every available published or unpublished source for the area between 21° to 38° N and 22° to 38° E. A unified earthquake catalogue was obtained (includes all the historical, instrumental and FMSs data), using for this purpose several empirical relationships among reported magnitudes, macroseismic intensity, and moment magnitude. Finally, all dependent events were removed as well as earthquakes with magnitudes smaller than M_w 3.0. The final catalogue covers the period from 2200 B.C. to 2013 and includes 16642 mainshocks. Its development and main characteristics are discussed below.

3.2 TECTONIC SETTING OF EGYPT

Egypt is situated in the northeastern corner of the African Plate, along the southeastern edge of the EMR. It is interacting with the Arabian and Eurasian Plates through divergent and convergent plate boundaries, respectively (Fig. 3-1). Egypt is bounded by three active tectonic plate margins: the African-Eurasian plate margin, the Gulf of Suez-Red Sea plate margin, and the DST. The seismic activity of Egypt is due to the interaction and the relative motion between the plates of Eurasia, Africa and Arabia. Within the last decade, some areas in Egypt have been struck by significant earthquakes causing considerable damage. Such events were interpreted as the result of this interaction.

The primary features of active plate boundaries in the vicinity of Egypt have been discussed in details by many authors (e.g., McKenzie, 1970 and 1972; Neev, 1975; Ben-Menahem *et al.*, 1976; Garfunkel and Bartov, 1977; Ben-Avraham *et al.*, 1987; WCC, 1985; Mesharf, 1990; Kebeasy, 1990). Also, the relation between those plate boundaries and shallow seismicity was studied by different authors (e.g., Sofratome Group, 1984; Abou Elenean, 1997; Abou Elenean and Hussein, 2007). A summary of the most important tectonic features in the vicinity of Egypt (Fig. 3-1) is given in the following paragraphs.

a. Africa-Eurasia Plate Margin: The African and Eurasian plates are converging across a wide zone in the Mediterranean Sea. The effects of the plate interaction are mainly north and remote from the Egyptian coastal margin. The zone is characterized by folding within the Mediterranean Sea floor and subduction of the northeastern

African plate beneath Cyprus and Crete (Maamoun *et al.*, 1980). Some evidences of secondary deformation appear to be occurring along the northern Egyptian coast as represented by moderate earthquake activity. The earthquake activities constitute a belt parallel to the Hellenic and Cyprian Arcs (Abou Elenean, 2007). Some of the largest events located to the south of Crete and Cyprus Islands were felt and caused few damage on the northern part of Egypt (e.g., August 8, 1303, intensity VIII offshore Mediterranean earthquake, February 13, 1756, intensity VI and June 26, 1926, M_S 7.4 Hellenic Arc earthquakes, October 9, 1996, M_W 6.8 Cyprus earthquake, and October 12, 2013, M_S 6.4 Crete earthquake).

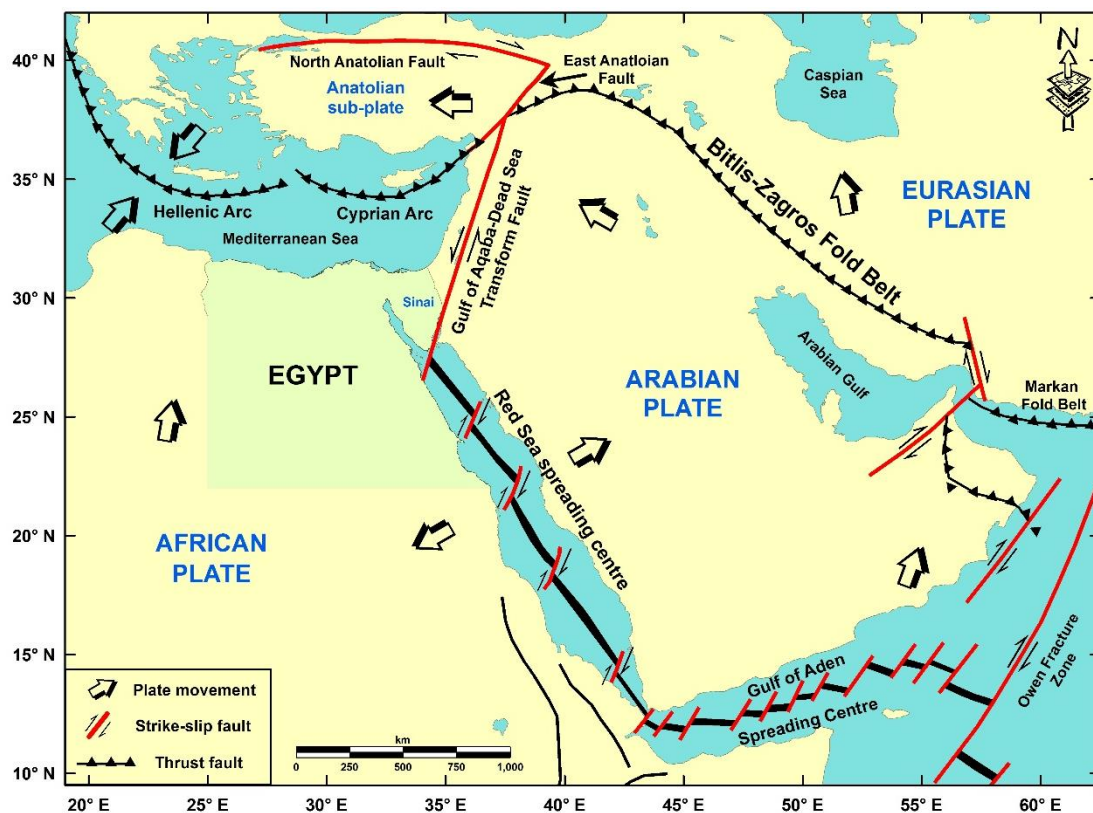


Figure (3-1): Global tectonic sketch for Egypt and its vicinity (compiled after Ziegler, 1988; Meulenkamp *et al.*, 1988; Dewey *et al.*, 1989; Guiraud and Bosworth, 1999).

b. Gulf of Suez-Red Sea Plate Margin: The Arabian Plate is continuing to rotate away from the African Plate along the Red Sea spreading center. The earthquake activity along that boundary is related to the Red Sea rifting, plutonic activity and the intersection points of the NW (Gulf of Suez-Red Sea Faults) with the NE DST (Abou Elenean, 2007). Active sea-floor spreading has been identified as far as about 20° to 22°N latitudes, from the continuous presence of basaltic crust in the axial rift of the Red Sea and the geophysical signatures of newly emplaced oceanic crust (Cochran, 1983). The extension of this deformation zone toward the north (Suez-Cairo shear

zone) is considered as the most active part of northern Egypt. Some evidences of an extension of the Suez-Cairo-Alexandria shear zone to the north, towards the Mediterranean Sea, were described (Kebeasy *et al.*, 1981; Ben-Avraham *et al.*, 1987). The largest earthquakes along this zone caused some damage in northern Egypt (e.g., July 11, 1879, intensity VI and March 6, 1900, M_S 6.2 Gulf of Suez earthquakes, and March 31, 1969, M_W 6.8 Shedwan Island earthquake).

c. Gulf of Aqaba-Dead Sea Transform Fault: It is a major left-lateral strike-slip fault that accommodates the relative motion between Africa and Arabia (Salamon *et al.*, 2003). It connects a region of extension in the Northern Red Sea with the Taurus collision zone to the north. This fault zone consists of *en echelon* faults with extensional jogs, with the largest such step over being the Dead Sea pull-apart basin. The main faults of this zone are trending N-S to NNE-SSW. They are found on the Sinai and Arabian deformed coastal areas, as well as within the Gulf of Aqaba (Ben-Avraham, 1985). The seismic activity of this shear boundary is relatively high and appeared to be clustered in some places where there is intersection of two or more faults (NNE-SSW and WNW-ESE) or attributed to upwelling of magma (Abou Elenean, 2007). Some larger events were reported along this fault trend and caused damage in Northern Egypt (e.g., March 18, 1068, intensity VIII Elat earthquake, May 20, 1202, intensity VIII Lebanon earthquake, and November 22, 1995, M_S 7.2 Gulf of Aqaba earthquake).

Based on the geophysical studies in the territory of Egypt, Youssef (1968) classified the main structural elements of Egypt into the following fault categories: a) Gulf of Suez-Red Sea, b) Gulf of Aqaba, c) E-W, d) N-S, and e) $N45^\circ W$ trends. However, Meshref (1990), from the magnetic tectonic trend analysis, showed the tectonic trends which influenced Egypt throughout its geologic history as: a) NW (Red Sea-Gulf of Suez), b) NNE (Aqaba), c) E-W (Tethyan or Mediterranean Sea), d) N-S (Nubian or East African), e) WNW (Drag), f) ENE (Syrian Arc), and g) NE (Aualitic or Tibesti) trends.

3.3 SEISMICITY OF EGYPT

The seismicity of Egypt was also studied by many authors (e.g., Sieberg, 1932 a,b; Ismail, 1960; Gergawi and El-Khashab, 1968; Maamoun *et al.*, 1984; Kebeasy, 1990; Ambraseys *et al.*, 1994; Abou Elenean, 1997, 2007; Badawy, 1999, 2005). Although Egypt is an area of relatively low to moderate seismicity, it has experienced

some damaging local shocks throughout its history, as well as the effects of larger earthquakes in the Hellenic Arc and EMR. It has also been affected by earthquakes in Southern Palestine and the Northern Red Sea (Ambraseys *et al.*, 1994).

Some of the most significant earthquakes in the last decades that took place in Egypt are discussed in some details in the following:

- **September 12, 1955 offshore Alexandria earthquake (M_S 6.8):** This earthquake was felt in the entire Eastern Mediterranean Basin. In Egypt, it was felt strongly and led to the loss of 22 lives and damage in the Nile Delta, between Alexandria and Cairo. Destruction of more than 300 buildings of old brick construction was reported in Rosetta, Idku, Damanhour, Mohmoudya and Abu-Hommos. A maximum intensity of VII was assigned to a limited area in the Bihira province, where five people died and 41 were injured. In addition, intensity between V to VII was reported in 15 other localities (Kebeasy, 1990).
- **March 31, 1969 Shedwan earthquake (M_S 6.9):** This event occurred to the northwest of Shedwan Island, in the surroundings of the Gulf of Suez. In this island, fissures and cracks in the soil were found. Ten kilometers west of the fractured area in the sea, a submerged coral reef was raised above sea level after the event. This earthquake was preceded by 35 large foreshocks during the last fifteen days of March 1969. This event was also felt in Saudi Arabia (Kebeasy, 1990; El-Sayed *et al.*, 1994).
- **December 9, 1978 Gilf El-Kebeir earthquake (m_b 5.3):** It is the largest instrumental earthquake in the southwestern region of Egypt. Its epicenter was located in the Gulf El-Kebir area. The southern part of Egypt was an unpopulated desert and the intensity distribution of this earthquake was not estimated. The nearest station to the epicenter was Helwan, 850 km away. Neither foreshocks nor aftershocks were recorded for this earthquake (Riad and Hosney, 1992).
- **November 14, 1981 Aswan (Kalabsha) earthquake (m_b 5.3, M_S 5.6):** This earthquake occurred in the Nubian Desert of Aswan. It is of great significance because of its possible association with Nasser's Lake. Its effects was strongly felt to the north of its epicenter (Kalabsha, about 60 km southeast of Aswan) up to Assiut (440 km to the north) and to the south up to Khartoum (870 km to the south). The epicentral intensity was VII-VIII. Eleven buildings were damaged and surface faulting was reported in the epicentral area. Several cracks on the western bank of the Nasser's

Lake, and several rock-falls and minor cracks on the eastern bank were reported. The largest crack was about 1 meter in width and 20 km in length. This earthquake was preceded by three foreshocks and followed by a large number of aftershocks. This event caused a great alarm due to its proximity to the Aswan High Dam (Kebeasy, 1990, and El-Sayed *et al.*, 1994).

- **July 2, 1984 Abu-Dabbab earthquake (m_b 5.1):** It was felt strongly in Aswan, Qena and Quseir. Large numbers of foreshocks and a large sequence of aftershocks were recorded (Kebeasy, 1990).
- **October 12, 1992 Cairo (Dahshour) earthquake (m_b 5.8, M_S 5.9):** Its epicenter was about 40 km south of Cairo, in Dahshour, causing a disproportional amount of damage (estimated at more than 500 million of Egyptian pounds) and the loss of many lives. The shock was strongly felt and caused occasional damage and life loss in the Nile Delta, around Zagazig. Damage extended throughout Fayoum and as far as south Beni-Suef and El-Minya. The area mostly affected was Cairo, in particular the old suburbs of Cairo, Bulaq and the region to the south, along the western bank of the Nile to Gerza (Jirza) and El-Rouda. In all, 350 buildings collapsed completely and 9000 were irreparably damaged, 545 people died and 6512 people were injured. Many of the casualties in Cairo were victims of panic-stricken stampedes of pupils rushing out of schools. About 350 schools and 216 mosques were ruined, and about 50000 people were left homeless. It was considered as one of the largest earthquakes in Egypt during the last century (El-Sayed *et al.*, 1994; Abou Elenean *et al.*, 2000).
- **November 22, 1995 Gulf of Aqaba earthquake (M_W 7.2):** It was a strong earthquake located in the southern part of the Gulf of Aqaba, 350 km southeast of Cairo. Most of the reported damage was concentrated in Sinai Peninsula, where a certain number of hotels were damaged leading to loss of three lives and the injury of ten people (Al Ahram newspaper, 23/11/1995) in Nuweiba, on the Gulf of Aqaba. Damage was also reported in the platforms of the port facilities in Nuweiba (Fat-Helbary, 1999, and Riad and Yousef, 1999).
- **May 28, 1998 Ras El-Hikma earthquake (m_b 5.5):** It was located offshore, on the northwestern part of Egypt, and it was widely felt in Northern Egypt. The maximum intensity of VII was reported at Ras El-Hikma village (~300 km west of Alexandria) and intensity of V-VI at Alexandria. Ground fissures were observed along the beach, and some cracks also in the concrete buildings (Hassoup and Tealeb, 2000).

In Egypt, mostly population settlements are concentrated along the Nile Valley and Nile Delta, so, the seismic risk is generally related to the occurrence of moderate size earthquakes at short distances (e.g., 1992, M_S 5.9 Cairo earthquake), rather than bigger earthquakes that are known to occur at far distances along the Northern Red Sea, Gulf of Suez, and Gulf of Aqaba (e.g., 1969, M_S 6.9 Shedwan, and 1995, M_W 7.2 Gulf of Aqaba earthquakes), as well as the Mediterranean offshore (e.g., 1955, M_S 6.8 Alexandria earthquake) (Abou Elenean *et al.*, 2010).

3.4 SEISMIC RECORD IN EGYPT

The assessment of seismic hazard and mitigation of seismic risk in Egypt are very important tasks due to the fast growth, and the development of giant and strategic projects. The preparation of basic data for the seismic hazard assessment starts immediately after evaluating the seismic record (complete and unified earthquake catalogue). In evaluating earthquake hazards for a given region, it is necessary to know its earthquake history. For Egypt, the seismic record is mainly divided into two main periods: a) the historical or the pre-instrumental part (prior to 1900), and b) the instrumental period (from 1900 until the moment). The last period can be subdivided at the same time into: i) the early instrumental era (1900-1997), until the establishment of the ENSN, and ii) the modern instrumental era (post 1997 until present).

3.4.1 THE PRE-INSTRUMENTAL (HISTORICAL) ERA (PRE-1900)

Instrumental record of earthquakes has been started by the beginning of the twentieth century. The earthquake information up to 1900 is compiled mainly from historical documents and books. Therefore, this kind of records is known as historical earthquake information. The location of those earthquakes provides a reasonable indicator for future events, and in order to forecast earthquake activity, it is necessary to determine the ancient history of faults. The completeness and accuracy of available information on earthquakes have evolved with time. Since the large-magnitude earthquakes with large recurrence periods are rare events, it is important to extend the seismic catalogues as far as possible back in time.

The chief sources of historical earthquake data in Egypt are inscriptions, papyri and archeological evidences provided by temples and monuments in the pre-Islamic Period (before 622 A.D.). Arabic chronicles and literature are also an important and

rich source of macro-seismic data in the Islamic Period (from 622 A.D.). Other sources also include diplomatic correspondence, especially during the Ottoman Rule over Egypt, starting from 1517. Hence, it is obvious that, Egypt is rich in historical sources to furnish the mass of macro-seismic data, thanks to its prosperous culture, strategic location at the intersection of trade routes, in addition to its political importance since ancient times. Due to these reasons, Egypt is one of the few regions of the world which has long been known to have seismological records dating back to 2200 B.C.

The historical seismicity of Egypt was studied by many authors. Among the most earliest and most important of these studies are those given by Lyons (1907), Sieberg (1932 a,b), Karnik (1968), Maamoun (1979), Poirier and Taher (1980), Maamoun *et al.* (1984), Kebeasy (1990), Ambraseys *et al.* (1994), El-Sayed and Wahlström (1996), Badawy (1999), Fat-Helbary (1999), Riad and Yousef (1999), Riad *et al.* (2004), and Badawy *et al.* (2010). According to them, many earthquakes were reported to have occurred in and around Egypt causing great damage in different localities.

The following is a brief description for some important historical earthquake databases mentioned before, showing their limitations:

- As-Souty, an Egyptian polymath, collected a catalogue of about 130 earthquakes in the Islamic World (from Spain to Transoxania) in his work “Kashf El-Salsala fi Wasf El-Zalzala”, considered the first published chronology of the historical earthquakes in the Middle East region. As-Souty frequently names his information sources, and cites them accurately. This work contains an earthquake list for the period between the years 712 A.D. to 1499 A.D., which translated into English by Spenger in 1843 from Arabic manuscripts of the National Library at Paris. Thanks to the devotion of two of As-Souty's disciples, an invaluable continuation extends the list of events affecting Egypt down to 1588 (Badawy, 1999).
- The first catalogue devoted to the earthquakes in Egypt is Lyons (1907) "preliminary list", which included 27 events between 27 B.C. and 1906, some of them are duplicated, generally giving its sources of information. Lyons catalogue has a large gap between 1303 and 1698, into which Sieberg (1932 a,b) was able to insert only two events, both of them erroneous.

- Willis (1928) presented a list of earthquakes, which contains 130 shocks compiled on the authority of As-Souty. Willis's list was compiled in part by Sieberg (1932 a,b) and others, but they did not bother to convert into A.D. the Muslim Calendar which were given by As-Souty. Ambraseys (1962) correlated these calendar dates against another manuscript of the same work at British Museum, and suggested that this list is dated about six centuries too early.
- Rothé (1969) adopted Sieberg's work that is cited again by Maamoun (1979) and Maamoun and Ibrahim (1978).
- Taher (1979) presents a full corpus of texts and a French summary translation from Arabic sources. Taher's work is the starting point for the retrieval and reassessment of historical information. Summary results of Taher's research were published by Poirier and Taher (1980), whose catalogue unfortunately passes on the inaccuracies in the original work.
- Ambraseys *et al.* (1994) did an attempt to include an accurate compilation of macroseismic information for a region defined at its greatest extent from 0°-34°N and 10°-60°E. Concerning Egypt, many of the earthquake events included in the previous catalogues have been excluded by Ambraseys *et al.* (1994) and have been proven to be false.

According to the different authors (e.g., Sieberg, 1932 a,b; Karnik, 1968; Maamoun, 1979; Poirier and Taher, 1980; Savage, 1984; Maamoun *et al.*, 1984; Ambraseys *et al.*, 1994; Badawy, 1999), eighty-three historical earthquakes were reported to have occurred in the Egyptian territory, and have caused some damage in different localities. The uneven distribution of population in Egypt creates inaccuracy in the proper identification of the origin and effects of the Egyptian historical earthquakes. This yields some events that are spurious or to be due to other effects, which are not of seismic origin.

Badawy (1999) describes the time distribution of those earthquakes: a) seven earthquakes have been reported in the period before Christ (B.C.), b) three events were reported up to the end of the ninth century, c) eight earthquakes have been reported in the tenth century, d) a dramatic decline in earthquake number has been notified in the eleventh and twelfth centuries (Fatimid Period), e) in the fifteenth and sixteenth centuries (Mamluk Period), the number of earthquakes re-increased and

reaching ten events, f) when Egypt was a province of the Ottoman Empire, in the seventeenth and eighteenth centuries, another dramatic decline was present, and finally, g) the maximum number of the reported earthquakes was seventeen in the nineteenth century.

Furthermore, Badawy (1999) describes the spatial distribution of those earthquakes. Earthquake epicenters are located almost exclusively in Cairo, the Nile Valley and the Nile Delta. He referred that most of the earthquakes affected these areas originated from epicenters at the subduction zone in the north and rifting zone in the east, but the distribution of population in a narrow band along the Nile Valley and Delta creates challenging problems toward locating and assessing the origin and true effects of the historical earthquakes in Egypt.

In the present study, all the references mentioned previously are chronologically searched and all the available historical events were inserted and compiled into the new catalogue. This is to go back as far as possible into historical times, critically review and summarize the pre-instrumental seismic data in Egypt and its surroundings, and create a new unified version of the historical earthquake catalogue for Egypt.

3.4.2 THE INSTRUMENTAL PERIOD (POST-1900)

The early instrumental period of 1900 to 1997 is still poorly understood, even for basic parameters such as earthquake locations. In some cases, this is the result of inherent limitations in the distribution, response characteristics, and timing of the instruments. Therefore, locations for most of the pre-1964 earthquakes are poorly determined.

Recording of instrumental earthquakes in Egypt started as early as 1899 with the establishment of Helwan Observatory (HLW: 29.85°N, 31.33°E, 115 m elevation on a limestone bedrock). This site was selected for both geophysical and astronomical investigation. An E-W component of a Milne-Shaw seismograph was the only instrument used initially. Another N-S component of a Milne-Shaw and a vertical component of a Galitzin-Willip seismograph were added in 1922 and 1938, respectively, in the same location. In 1951, the first episode of modernization, started by adding another set of short-period Sprengnether seismographs in Helwan. Before 1960, the seismic monitoring was carried out by using an individual seismograph station consisting of a three-component sensor. The observations of each individual

seismograph station were collected in a data analysis center for location and source parameters determination of every seismic event. The time lag between the recording and processing was so long (Badawy, 2005).

In May 1962, the Helwan seismological station was chosen by the U.S. Coast and Geodetic Survey to be part of the World Wide Standardized Seismograph Network (WWSSN). All systems were then replaced by the standardized set of Benioff short-period and Sprengnether long-period seismographs. This station is still on operation nowadays. In December 1972, a Japanese seismograph system with visual recording and frequency analyzer was installed also in Helwan. In late 1975 the first seismograph was installed in Upper Egypt that was able to record small local earthquakes. This seismograph was one of three stations installed at the Egyptian territory at Aswan (ASW), Abu-Simbel (ABS), and Marsa-Matrouh (MAT). These stations were equipped with Russian standard short-period SKM-3 seismometers and GK-VII M galvanometers (Abou Elenean *et al.*, 2000).

Following the November 14, 1981, M_S 5.3 - m_b 5.1 Aswan earthquake, portable micro-earthquake recorders were installed around the northern part of Aswan reservoir area by the Egyptian Geological Survey (EGS) from December 1981 to June 1982 to study the possible induced seismicity in Nasser's Lake. In late June 1982, and after the occurrence of the Nasser's Lake earthquake on 14 November 1981, the portable seismic field stations were replaced by a telemetered network including eight stations. Those seismic stations were erected by the Helwan Observatory and Lamont-Doherty Geological Observatory (USA) around the northern part of Aswan reservoir. Furthermore, it was enlarged to eleven stations in 1984 and to thirteen stations in 1985. Complete playback and analysis systems were installed at Helwan for analysis of the digital data. An analog strong-motion accelerograph network also was installed at different levels of the High Dam and old Aswan Dam (Abou Elenean *et al.*, 2000).

On July 2, 1984, a m_b 5.1 earthquake happened in Abu Dabbab area, along the Red Sea. It was the maximum recorded magnitude of the earthquake swarm observed since 1970. During the period from June 19, 1984 to January 4, 1985, the National Research Institute of Astronomy and Geophysics (NRIAG) installed a temporary three station network (MEQ-800) including Abu Dabbab station, around Wadi Abu Dabbab, along the Red Sea coast, to study earthquake swarms activity. Four short-period (MEQ equipped with SS-1 ranger) single vertical-component seismograph

stations were added to the national network during 1986-1990 at Kottamia (KOT), Hurghada (HUR), Tell-El-Amarna (TAS), and Marsa Alam (MRS) (Badawy, 2005).

In August 1991, a very broad-band station (KEG) was erected at Kottamia, as a part of Med-Net Project. In cooperation with the International Institute of Seismology and Earthquake Engineering (IISEE), from Japan, and NRIAG, a local network including ten telemetered short period (L4C, Mark product) seismic stations was installed in August 1994, around the southern part of the Gulf of Suez (Hussein *et al.*, 2008).

After the occurrence of the October 12, 1992, M_w 5.8 earthquake in Dahshour area, 35 km to the southwest of Cairo, which caused 561 deaths, 9832 injured and left a damage of more than 35 million US\$ (Abou Elenean *et al.*, 2000), the Egyptian government financed NRIAG to construct the ENSN (Fig. 3-2), which covers the whole Egyptian territory to detect and record mostly of local and regional earthquakes, as well as teleseismic events. The institute upgraded the data communication system from telephone lines to satellite to increase the efficiency of the ENSN.

By the end of 2002, the installation of the ENSN was completed covering whole Egypt, and five sub-centers have been constructed and equipped. Moreover, a new Earthquake Disaster Reduction Data Center (EDRDC) was established and supported by Geographic Information System (GIS) technology. This network had to be a technologically-sophisticated system to meet the needs of public safety and emergency management, providing improved data for better quantification of hazard and risk associated with both natural and artificial seismic sources and related engineering applications, as well as basic research. The ENSN is a digital network with duplex communication that stands essentially on three major elements: a high-resolution digitizer (HRD series) providing a resolution of 24 bits (132-dB dynamic range) and Global Positioning System (GPS) timing, NAQS32-P acquisition and monitoring software, and monitoring of the required technical parameters of the remote and repeater stations (Abou Elenean *et al.*, 2000).

The ENSN (Fig. 3-2) consists of 60 remote stations transmitting data to the main center at Helwan and to five subcenters at Burg al Arab, Kharga, Marsa Alam, Hurghada and Aswan.

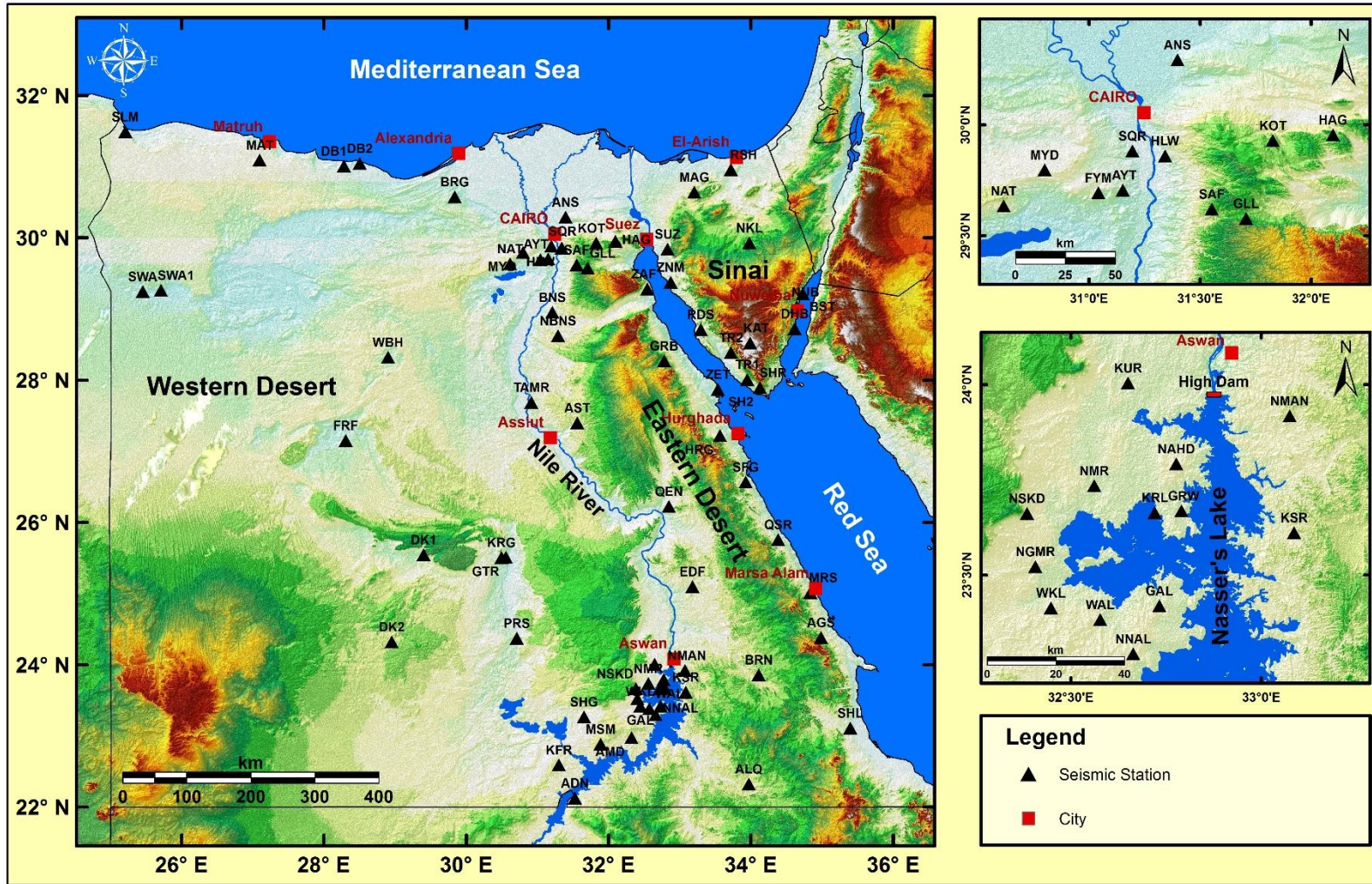


Figure (3-2): Distribution of the ENSN.

All instruments are short-period velocity sensors (43 stations have one component and 13 stations have three-component sensors) with 24-bit digital recording systems and a sampling rate of 100 Hz. It also has four broadband seismograph stations equipped with STS-1 seismometers. Most of the data are received at the main center from remote stations and subcenters via satellite communication. Data from stations close to processing centers are sent through telemetry or telephone lines. The distribution of the seismic stations and strong-motion units was chosen to cover known seismicity sources, as well as cover some regions with known historical earthquakes but little instrumental seismicity (e.g., Siwa Oasis). With this dense network of instruments it is possible to record most ongoing earthquake activity in Egypt (Badawy, 2005).

3.5 EARTHQUAKE CATALOGUE COMPILATION

In the current study, the collection, analysis and completeness of the historical and instrumental earthquake data, compiled from different local and international sources, was performed. The initial data suffered from incompleteness, duplication, and large epicentral and hypocentral location errors. Large efforts and time were required to evaluate different datasets, eliminating duplicate records after reconciling differences, and sorting out aftershocks.

As mentioned above, in developing this catalogue, the authors investigated and employed published and unpublished sources, covering different time periods with different magnitude scales, and several papers and reports on historical seismicity. The following are the different used sources arranged according to their preference:

- The regional catalogue given by Ambraseys *et al.* (1994), which cover the period from 1900 to 1992. His investigation is concerned with a large and irregular area defined at its greatest extent by the coordinates 0° - 34° N latitude and 10° - 60° E longitude. He attempts to provide a uniform account of the seismicity of the region mentioned above, based on the retrieval and assessment of original sources of macroseismic information.
- EHB (Engdahl *et al.*, 1998) catalogue, which is a revised version of the ISC bulletin, containing data from 1960 to 2008 (<http://www.isc.ac.uk/ehbulletin/>). The Engdahl *et al.* (1998) algorithm has been used to improve routine hypocenter determinations made by the International Seismological Summary (ISS), ISC and

PDE, before a new ISC location algorithm (Bondár and Storchak, 2011) was introduced. The EHB algorithm does not recalculate magnitudes. Mostly m_b and M_S values are taken from the ISC bulletin, and M_W values from the global CMT catalogue.

- The ISC online bulletin (<http://www.isc.ac.uk/>), which includes earthquake data in digital format from 1964 until 2014. It is updated periodically. It has been the basic international seismic bulletin, completed and corrected with the other sources. It includes checked and unchecked data from national and local agencies from around the world. These data, which include hypocenters, phase arrival-times, FMSs, etc., are automatically grouped into events, which form the basis of the ISC Bulletin.
- The National Earthquake Information Center (NEIC) global earthquake bulletin, also called the PDE bulletin. The PDE is an online bulletin covering the period from 1900 to 2007 (<http://earthquake.usgs.gov/earthquakes/>). The word "Preliminary" was used for the final bulletin because the bulletin of the ISC is considered to be the final global archive of parametric earthquake data (phase pick times and amplitudes).
- Global CMT catalogue provided by Harvard University, which has been the main source for the FMS data (<http://www.globalcmt.org/>). Its main database runs from January, 1976, until the present moment (Dziewonski *et al.*, 1981; and Ekström *et al.*, 2012). Furthermore, it includes the moment magnitude computed according to Kanamori (1977).
- Another important source of the FMSs data is the European-Mediterranean RCMT Catalogue (<http://www.bo.ingv.it/RCMT/>) for the European and Mediterranean area. The main product of RCMT is a routinely updated catalogue of seismic moment tensors (Pondrelli *et al.*, 2002, 2004, 2006, 2007 and 2011).
- All the available published and unpublished texts both local and international (Poirier and Taher, 1980; Maamoun *et al.*, 1984; Riad and Meyers, 1985; Kebeasy, 1990; Ambraseys *et al.*, 1994; El-Sayed and Wahlström, 1996; Badawy and Horváth, 1999; Ambraseys, 2001; and Riad *et al.*, 2004) were used to cover the pre-instrumental and the early-instrumental periods, in addition to provide macroseismic intensity for the historical events.

- The annual bulletin of the ENSN for events occurred after 1982 until the end of 2010, and the annual bulletin of the Aswan Regional Earthquake Research Centre (from 1982 until the end of 2012).

When merging different catalogues, it is necessary to avoid the duplication of events eventually reported in more than one of the source catalogues. This can be achieved by carefully checking the possible double events (i.e., records which could be associated to the same earthquake) in the obtained catalogue (Primakov and Rotwain, 2003). Accordingly, the merging procedure has been performed as follows. The possible common events, with origin time differences less than 1 minute and location differences less than 1 degree for latitude and longitude, have been first identified. All the records satisfying such conditions have been examined manually, to analyse specific cases. If the same event was listed with different coordinates and origin time, the parameters estimated from local records (i.e., national and regional catalogues) have been used. Otherwise, the parameters from the global catalogues have been considered. The depth wasn't taken into consideration, due to the large errors affecting this quantity (Hussein *et al.*, 2008).

Moreover, the straightforward merging of the data sources mentioned above would yield a heterogeneous earthquake catalogue, with different magnitude types, not always comparable. For Egypt and its surroundings, the most frequently reported size estimates are the magnitude types given by the local catalogues, that is, M_L and m_D , which comes from the annual bulletins of the ENSN and Aswan Regional Earthquake Research Centre. In addition to these magnitudes, m_b and M_S , as reported in USGS and ISC global catalogues, are also listed for moderate to large events. Furthermore, M_W values for the biggest events, from CMT and EHB bulletins, were obtained.

In order to unify magnitudes, the different magnitude scales were selected according to the following preference: moment magnitude (M_W), surface-wave magnitude (M_S), body-wave magnitude (m_b) and local magnitude (M_L and m_D), respectively. The initial compilation spanning a spatial region from 21° to 38° N and from 22° to 38° E, and includes all the events having an assigned magnitude of 3.0 and above for international sources, and any magnitude for local sources, on any magnitude scale. The initially compiled catalogue comprised more than 64000

earthquakes (historical and instrumental events), covering the time period from 2200 B.C. to the beginning of 2014.

3.6 CATALOGUE ANALYSIS

In order to produce an earthquake catalogue with a unified magnitude scale, it is necessary to follow and perform the following two important steps, upon the declustered earthquake data (Peresan and Rotwain, 1998): a) study the relationships between the different kinds of magnitude reported in the catalogue, in order to have a formal rule for the choice of any relation that can be applied for magnitude conversion, resulting into an acceptable unity of the catalogue, and b) study the completeness of the catalogue to find the magnitude thresholds above which the different data sets, as well as of the resulting catalogue over the investigated time period 2200 B.C. - 2013, are complete. The completeness analysis can be checked using the following: i) drawing plots of the cumulative number of earthquakes against time, and ii) drawing plots of the frequency of earthquakes versus magnitude, in accordance with the magnitude-frequency relationship by Gutenberg and Richter (1942):

$$\log N = a - bM \quad (3-1)$$

3.6.1 CONVERTING INTENSITIES AND REPORTED MAGNITUDES TO MOMENT MAGNITUDE

One of the main goals of this work was to obtain a unified earthquake catalogue. Moment magnitude was used as the unifying magnitude scale, because it is the most commonly used in recent seismic hazard studies. The reason is that this type of magnitude does not saturate when increase earthquake size or seismic moment. Several empirical regression relationships between the different reported magnitudes, maximum intensity (I_{max}) and M_W have been employed. These relationships are those considered after establish specific relations from our database or to use the most reliable ones after studying the available magnitude relationships in the scientific literature. In the final catalogue, in addition to the unified moment magnitude (M_W^*), the initially reported magnitude has been included. This will allow users to use other type of magnitude to unify the catalogue or to use other relationships to calculate unified magnitude if they wish.

The equivalent moment magnitude (M_W^*), i.e., the final unified moment magnitude, was computed for each set of reported magnitude data. For earthquakes with reported moment magnitude, this value was the equivalent magnitude. Events which have reported M_S or m_b magnitudes, a conversion of the reported magnitude to moment magnitude was performed using empirical relationships (Eqs. 3-2 and 3-3, respectively) developed directly from the current catalogue. The first relationship is a second-degree polynomial fit between reported M_S and M_W magnitudes, using to it 355 events ($4.0 \leq M_S \leq 7.3$). The second one is a linear fit between m_b and M_W , using 816 events ($3.5 \leq m_b \leq 6.7$). Both of them show a general agreement with widely used relationships as developed by Johnston (1996a) (Fig. 3-3 a,b).

$$M_W^* = 3.97(\pm 0.61) - 0.13(\pm 0.24)M_S + 0.080(\pm 0.023)M_S^2 \quad (3-2)$$

$$M_W^* = -1.314(\pm 0.097) + 1.262(\pm 0.020)m_b \quad (3-3)$$

For events in the catalogue with reported m_D or M_L magnitudes (Fig. 3-3 c), the relationships of Hussein *et al.* (2008) for the local magnitude scales were used here to convert m_D and M_L values to M_W (Eqs. 3-4 and 3-5, respectively). We preferred to use the Hussein *et al.* (2008) relationships rather than developing our own relations, because the current data have some gaps in the magnitudes distribution that make an obstacle to construct a good fit.

$$M_W^* = \frac{2}{3} [1.35(\pm 0.11)M_L + 16.3(\pm 0.53)] - 10.7 \quad (3-4)$$

$$M_W^* = \frac{2}{3} [1.45(\pm 0.07)m_D + 16.3(\pm 0.30)] - 10.7 \quad (3-5)$$

Finally, when I_{max} was the reported earthquake size, M_W^* was computed from the empirical polynomial second-degree relationship between maximum intensity and seismic moment developed by Johnston (1996b) (Eq. 3-6 and Fig. 3-3 d).

$$M_W^* = \frac{2}{3} (19.36 + 0.48 \cdot I_{max} + 0.0244 \cdot I_{max}^2) - 10.7 \quad \sigma = 0.77 \quad (3-6)$$

In the compiled database, there are few earthquakes with assigned I_{max} and reported magnitude. Mostly large earthquakes having these two values have a M_S macroseismic magnitude computed by Ambraseys *et al.* (1994), that does not allow to establish a robust regression analysis (Fig. 3-3 d). Furthermore, the relationships developed by Ambraseys (1985) and D'Amico *et al.* (1999) appear to be unsuitable for the current study because of its behaviour at high intensity values.

In the final catalogue, a code is employed to inform users about the method used to obtain the M_W^* for each event.

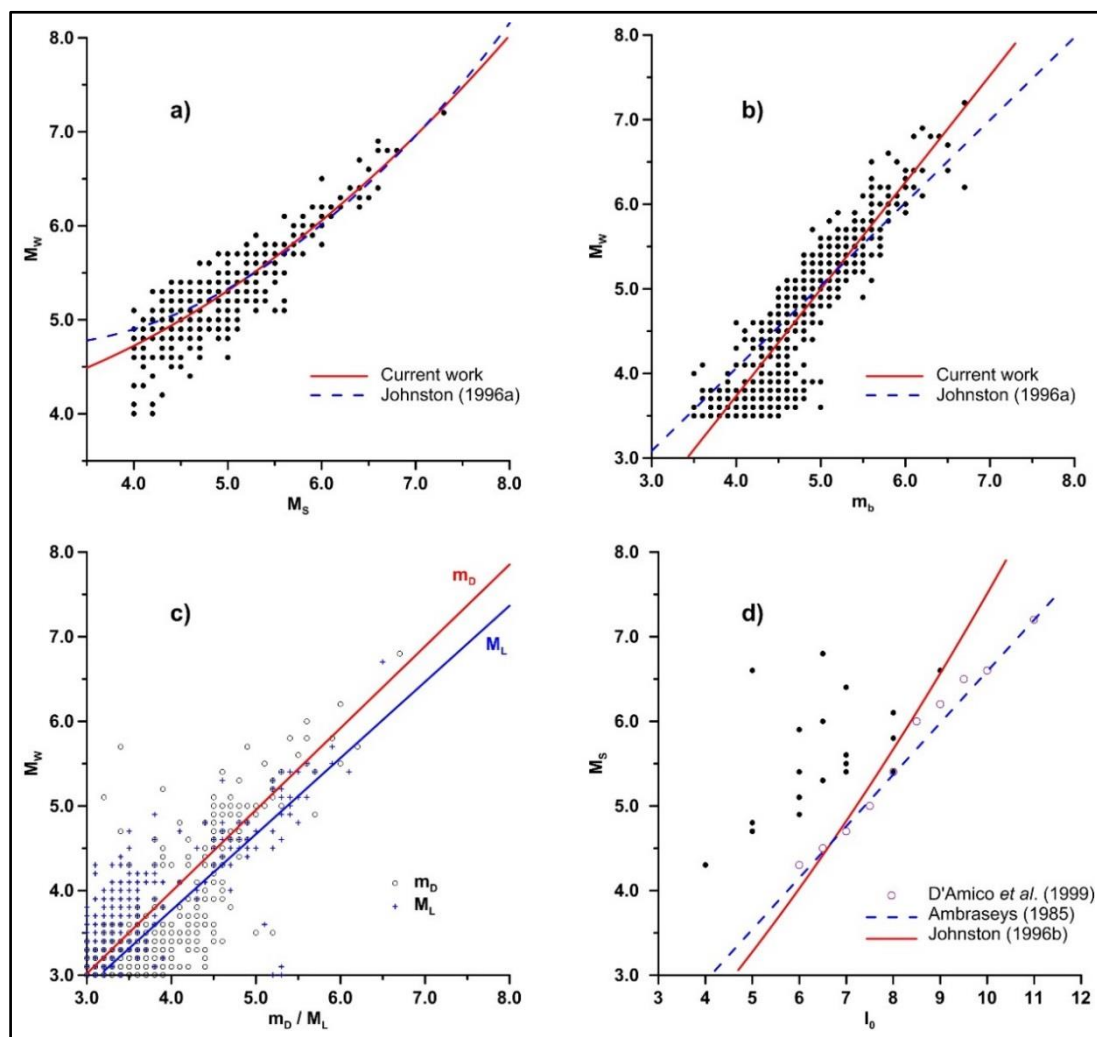


Figure (3-3): Different magnitude relationships which have been used in the current study.

3.6.2 CATALOGUE DECLUSTERING

Declustering process attempts to identify time and space-dependent earthquakes (aftershocks, foreshocks and swarm-type activity). After compiling the unified catalogue, dependent (non-Poissonian) earthquakes were removed. This is a necessary step in any time-independent seismic hazard assessment. For most hazard-related studies, it is assumed that the seismicity behaves in a time-independent fashion (e.g., Reiter, 1990; Giardini *et al.*, 1999; Frankel, 1995).

Two main declustering algorithms are normally in use: a) the approach proposed by Gardner and Knopoff (1974), which identify dependant events when they are included in the same space and time window, and b) the approach provided by Reasenberg (1985), who defines the interaction windows in space-time in a somewhat

more sophisticated way attempting to introduce physical properties behind triggering. The spatial and temporal extent of a cluster is not fixed, as it is in the windowing method, but it depends on the development of an individual sequence.

In the current work, we followed the same procedure as the Moroccan and Algerian main earthquake catalogues prepared by Peláez *et al.* (2007) and Hamadche *et al.* (2010), respectively. All dependent earthquakes were identified using the classic routine, and essentially using the same parameters, proposed by Gardner and Knopoff (1974). Given an earthquake with a certain M_W magnitude, a scan within a characteristic distance $L(M_W)$ and time $T(M_W)$ was performed for the entire catalogue. The largest earthquake in this search is considered to be the mainshock. In the current study, window sizes of 900 days and 100 km were used for a given M_W 8.0 event, and 10 days and 20 km for a M_W 3.0 event. For in-between magnitudes, proportional values for L and T were used. After this process, the catalogue was cut off below magnitude M_W 3.0. These magnitudes are not significant for seismic hazard studies and its period of completeness is very low. For example, Table (3-1) shows earthquakes above M_W 6.0 in the Egyptian territory and surroundings, that is, the most energetic ones in the final catalogue. Furthermore, maps showing the distribution of earthquakes of the declustered catalogue, for events $M_W \geq 3.0$, are depicted in Figures (3-4) and (3-5).

3.6.3 CATALOGUE COMPLETENESS

Modelling the seismicity in each seismic zone needs knowledge on the magnitude of completeness below which only a fraction of all events that have been taken place are documented (e.g., Kijko and Graham, 1999; Rydelek and Sacks, 2003; Wiemer and Wyss, 2000, 2003). The authors estimated the degree of completeness firstly for the whole set of data in the entire catalogue, and then for the Egyptian territory and surroundings (area between latitudes 22° - 33.5° N and longitudes 22° - 36° E), without data from the Mediterranean region. The procedure used to identify the completeness levels of the catalogue is the usual one, to plot the cumulative number of events above a certain magnitude versus time. This permits to identify the epochs in which the rates of events are constant.

The results of the completeness analysis, for both the whole catalogue and the Egyptian territory and its surroundings are shown on Table (3-2), and Figures (3-6) and (3-7). Those figures depict the cumulative number of earthquakes above

magnitudes M_W 3.0 to M_W 7.0 at intervals of 0.5. For example, we obtained that the earthquake catalogue of the Egyptian territory and surroundings (Fig. 3-7) is complete for earthquakes above M_W 3.0, 4.0, and 5.0 since 1993, 1983 and 1950, approximately, with seismicity rates of 67.0, 5.74, and 0.646 events/year, respectively. However, the whole catalogue appears to be complete, for the previous magnitude values, since 2003, 1993 and 1980, approximately, with rates of 1071, 69.0, and 9.76 events/year, respectively.

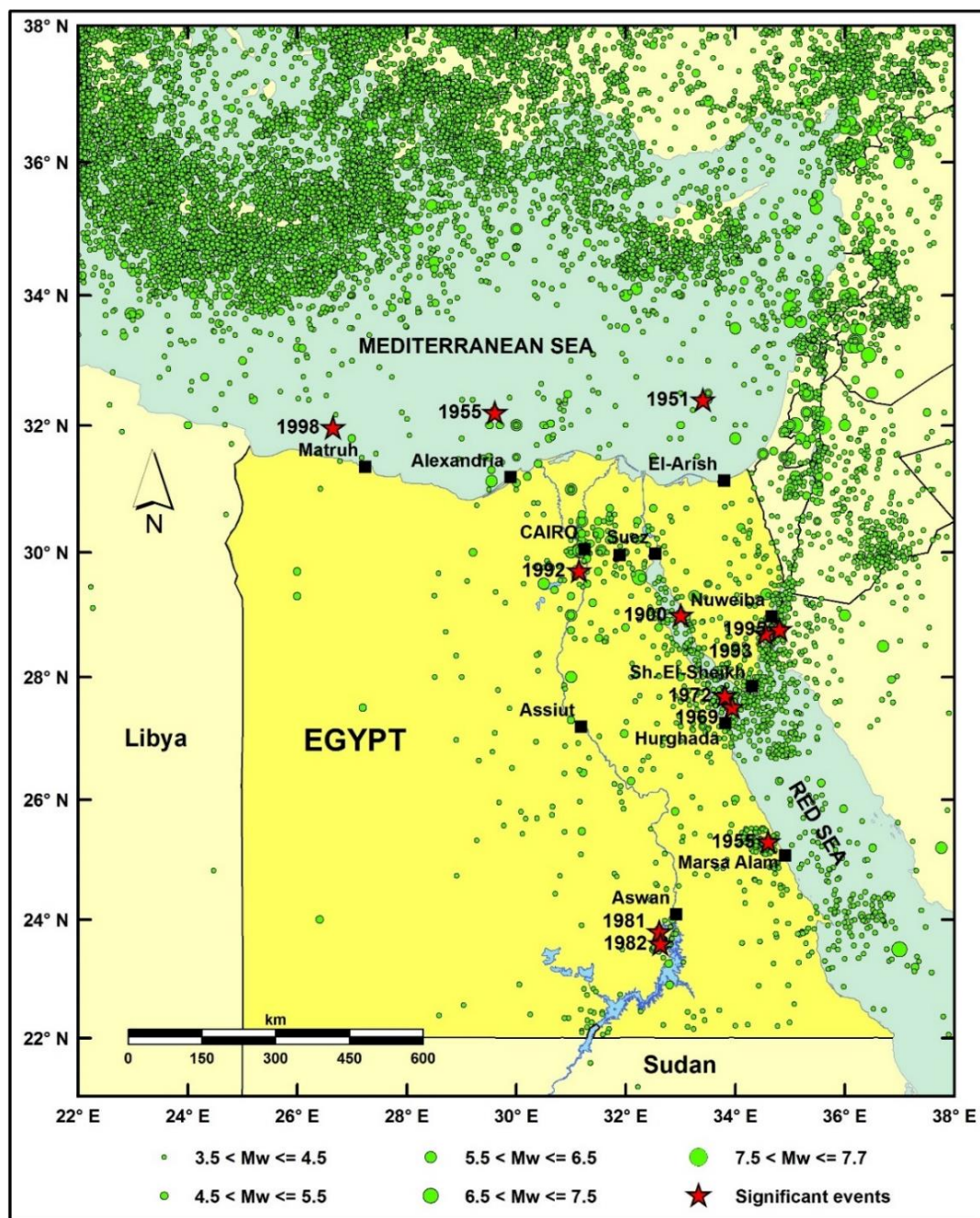


Figure (3-4): Declustered shallow seismicity ($h \leq 35$ km) and significant earthquakes for the time period (2200 B.C. – 2013).

Some of the observed completeness periods are clearly related to the establishment and improving of the local and international networks: a) 1900 is the appropriate date in which is established the Helwan Observatory, b) 1960 coincides approximately with the deployment of the WWSSN, c) 1983 is the year related to the installation of the Aswan Seismological Network after November 14, 1981, M_S 5.6 Kalabsha earthquake, d) 1993 coincides with the installation of a large number of seismic stations in Egypt after October 12, 1992, M_W 5.8 Cairo earthquake, and finally, e) 2003 reflects the final improvement and development of the ENSN.

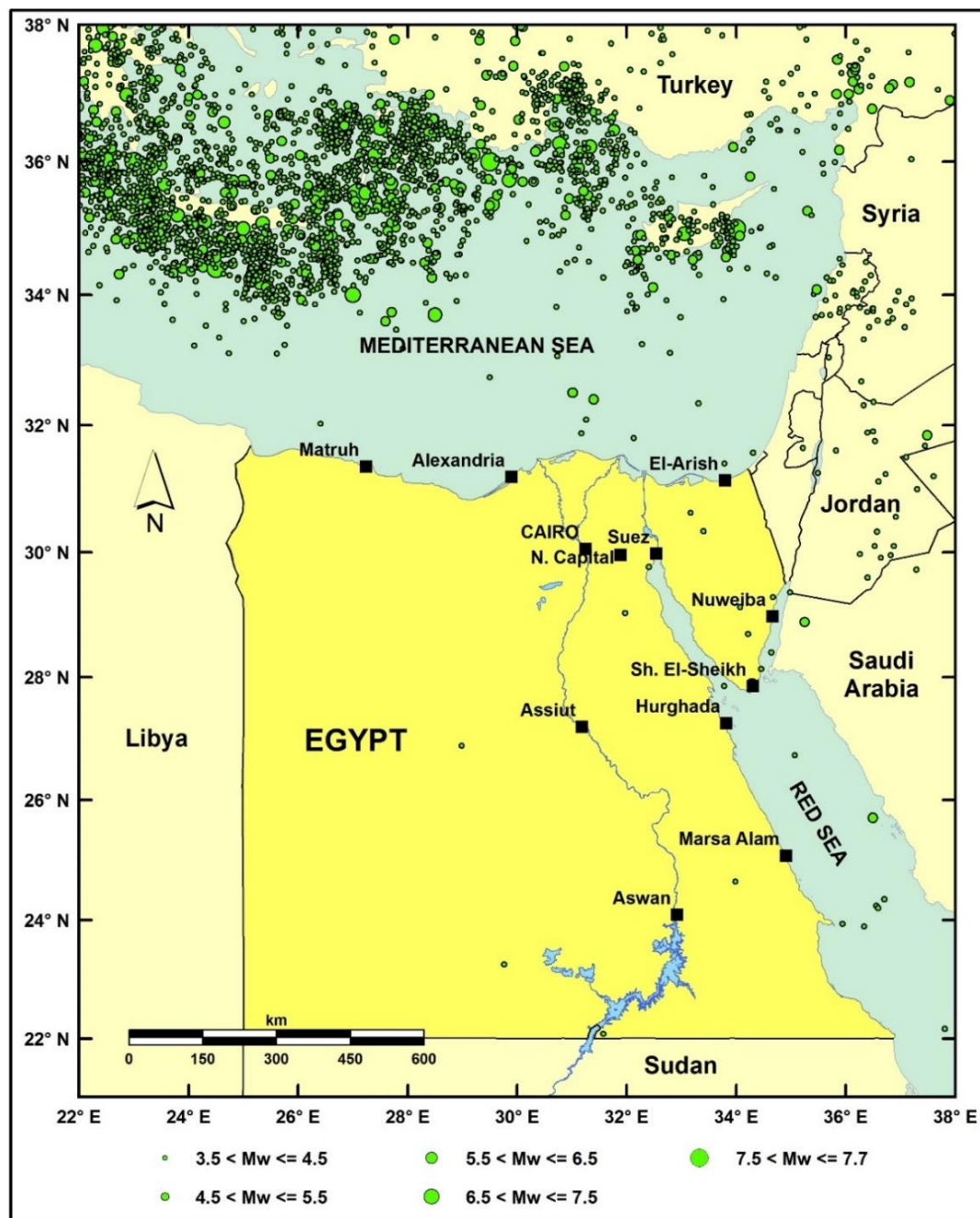


Figure (3-5): Declustered seismicity ($h \geq 35$ km).

Table (3-1): Catalogued earthquakes with magnitudes equal to or greater than M_w 6.0 (see Appendix A for events equal to or greater than M_w 5.0).

Date mm/dd/yyyy	Time hh:mm:ss	Longitude (°)	Latitude (°)	Depth (km)	Reported magnitude	Maximum intensity	Location	Final M_w	Reference
590 B.C.	-	35.200	33.300	-	-	IX	Sidon District, Syria	6.4 ¹	Maamoun <i>et al.</i> (1984)
12 B.C.	-	35.000	32.000	-	-	IX	Northern Jerusalem, Palestine	6.4 ¹	Maamoun <i>et al.</i> (1984)
---/---/0019	-	35.500	33.000	-	-	X	Southern Lebanon	7.0 ¹	Riad <i>et al.</i> (2004)
---/---/0030	-	35.200	31.800	-	-	VIII-IX	Jerusalem, Palestine	6.1 ¹	Maamoun <i>et al.</i> (1984)
---/---/0332	-	34.000	33.500	-	-	IX	Coastal Lebanon	6.4 ¹	Riad <i>et al.</i> (2004)
---/---/0419	-	35.500	33.000	-	-	IX	Southern Lebanon	6.4 ¹	Riad <i>et al.</i> (2004)
---/---/0746	-	35.600	32.000	-	-	XI	Balqa, Jordan	7.7 ¹	Riad <i>et al.</i> (2004)
---/---/0854	-	35.320	32.480	-	-	IX	Jenin, Palestine	6.4 ¹	Badawy and Horváth (1999b)
---/---/0857	-	31.000	28.000	-	M_S 6.1 ^a	VIII	SE El-Minya, Egypt	6.1 ²	Ambraseys <i>et al.</i> (1994)
10/04/0935	-	31.200	30.500	-	M_S 6.1 ^a	VIII	Banha, Nile Delta, Egypt	6.1 ²	Ambraseys <i>et al.</i> (1994)
09/15/0951	18:00:00	29.550	31.130	-	M_S 6.1 ^a	VIII	Near Alexandria, Egypt	6.1 ²	Ambraseys <i>et al.</i> (1994)
01/04/1034	-	35.320	32.480	-	-	X-XI	Jenin, Palestine	7.4 ¹	Badawy and Horváth (1999b)
08/31/1111	-	31.000	31.000	-	M_S 6.1 ^a	VIII	Gharbia, Nile Delta, Egypt	6.1 ²	Badawy and Horváth (1999b)
05/02/1212	-	34.570	29.330	-	-	VIII-IX	Eastern Sinai, Egypt	6.1 ¹	Badawy and Horváth (1999b)
---/---/1262	-	31.150	30.030	-	-	IX-X	Northern Cairo, Egypt	6.7 ¹	Badawy and Horváth (1999b)
02/20/1264	-	31.000	29.000	-	M_S 6.1 ^a	VIII	Beni Suef, Egypt	6.1 ²	Ambraseys <i>et al.</i> (1994)

^aAmbraseys *et al.* (1994), using macroseismic data.

¹From I_{\max} , using the Johnston (1996b) relationship between I_{\max} and M_w .

²From M_S , using the relationship established in this work (Eq. 3-2).

Table (3-1): Continued.

Date mm/dd/yyyy	Time hh:mm:ss	Longitude (°)	Latitude (°)	Depth (km)	Reported magnitude	Maximum intensity	Location	Final M_w	Reference
---/---/1269	-	35.000	32.000	-	-	IX	NW Jerusalem, Palestine	6.4 ¹	Riad <i>et al.</i> (2004)
---/---/1287	-	35.270	32.570	-	-	VIII-IX	Northern Jerusalem, Palestine	6.1 ¹	Badawy and Horváth (1999b)
07/30/1303	-	31.150	30.030	-	-	IX	Cairo, Egypt	6.4 ¹	Badawy and Horváth (1999b)
05/---/1341	-	29.550	31.130	-	-	VIII-IX	Near Alexandria, Egypt	6.1 ¹	Badawy and Horváth (1999b)
01/14/1546	16:00:00	35.100	32.000	-	-	X	Northern Jerusalem, Palestine	7.0 ¹	Ambraseys <i>et al.</i> (1994)
04/09/1588	-	31.550	30.030	-	-	IX	Near Cairo, Egypt	6.4 ¹	Badawy and Horváth (1999b)
10/---/1754	-	32.250	29.600	-	M_S 6.6 ^a	V	SW Suez, Egypt	6.6 ²	Ambraseys <i>et al.</i> (1994)
07/11/1879	18:00:00	33.000	29.000	-	M_S 5.9 ^a	VI	Gulf of Suez, Egypt	6.0 ²	Ambraseys <i>et al.</i> (1994)
03/06/1900	17:58:00	33.000	29.000	-	M_S 6.2 ^a	-	Gulf of Suez, Egypt	6.2 ²	Ambraseys <i>et al.</i> (1994)
07/11/1927	13:04:00	35.300	32.200	15	M_S 6.1, m_b 5.4	-	Northern Jerusalem, Palestine	6.1 ²	Ambraseys (2001)
09/12/1955	06:09:24	29.610	32.200	20	M_S 6.4, m_b 6.5	VII	Mediterranean Sea, NW Alexandria	6.4 ²	Ambraseys (2001)
03/31/1969	07:15:51	33.938	27.513	6	M_W 6.8, M_S 6.6	IX	Shedwan Island, Red Sea	6.8	ISC / EHB
08/03/1993	12:43:08	34.548	28.708	18	M_W 6.1, M_S 5.8	-	Eastern Sinai, Egypt	6.1	ISC / EHB
11/22/1995	04:15:15	34.809	28.769	19	M_W 7.2, M_S 7.3	-	Gulf of Aqaba, Egypt	7.2	ISC / EHB

^aAmbraseys *et al.* (1994), using macroseismic data.

¹From I_{max} , using the Johnston (1996b) relationship between I_{max} and M_w .

²From M_S , using the relationship established in this work (Eq. 3-2).

Table (3-2): Completeness period and seismicity rate for different magnitude values.

M_w	The whole catalogue		The Egyptian territory	
	Time	Rate (events/year)	Time	Rate (events/year)
≥ 3.0	2003	1071	1993	67.0
≥ 3.5	1993	206	1983	16.9
≥ 4.0	1993	69.0	1983	5.74
≥ 4.5	1980	30.4	1977	1.86
≥ 5.0	1980	9.76	1950	0.646
≥ 5.5	1960	2.46	1950	0.187
≥ 6.0	1920	0.591	700	0.0166
≥ 6.5	1900	0.186	700	0.00446
≥ 7.0	200 B.C.	0.00911	0	0.00207

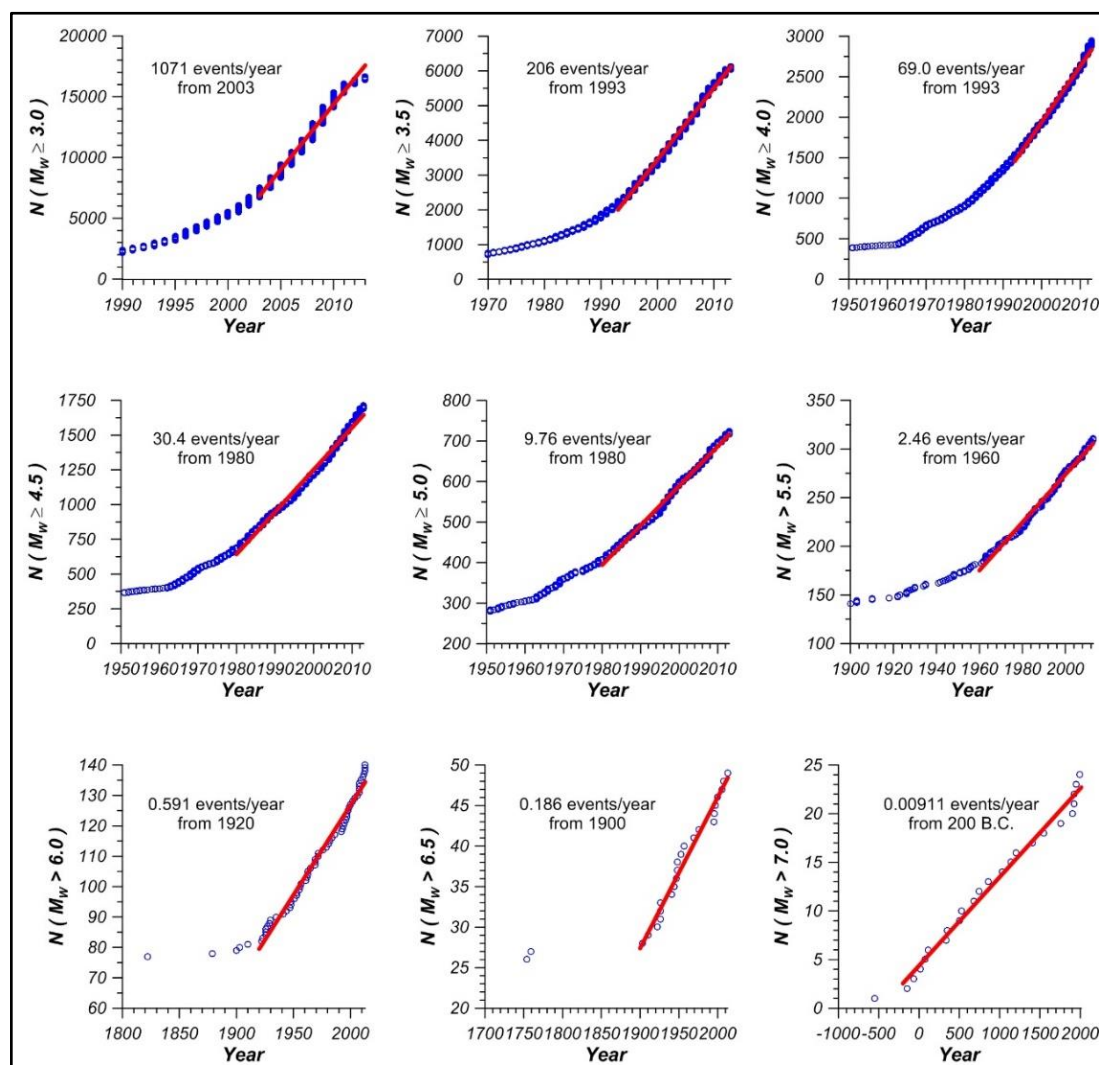


Figure (3-6): Cumulative number of earthquakes above different magnitude values for the whole catalogue.

3.6.4 MAGNITUDE-FREQUENCY RELATIONSHIPS

As it was mentioned before, Gutenberg and Richter (1942) noted that the magnitude frequency relationship obeys a power law given by Equation (3-1), where N is the number of earthquakes of magnitude M or larger, and a and b are parameters.

The a -value depends on the period of observation, the size of the investigated area, and the level of seismicity. The b -value is generally assumed to be related to the degree of the fracturing and the heterogeneity of the materials and stress regime, among other factors, depicting the relation among large and small earthquakes. A b -value equals to 1.0 means that the number of earthquakes in the area decreases by tenfold when magnitude increases in a unit.

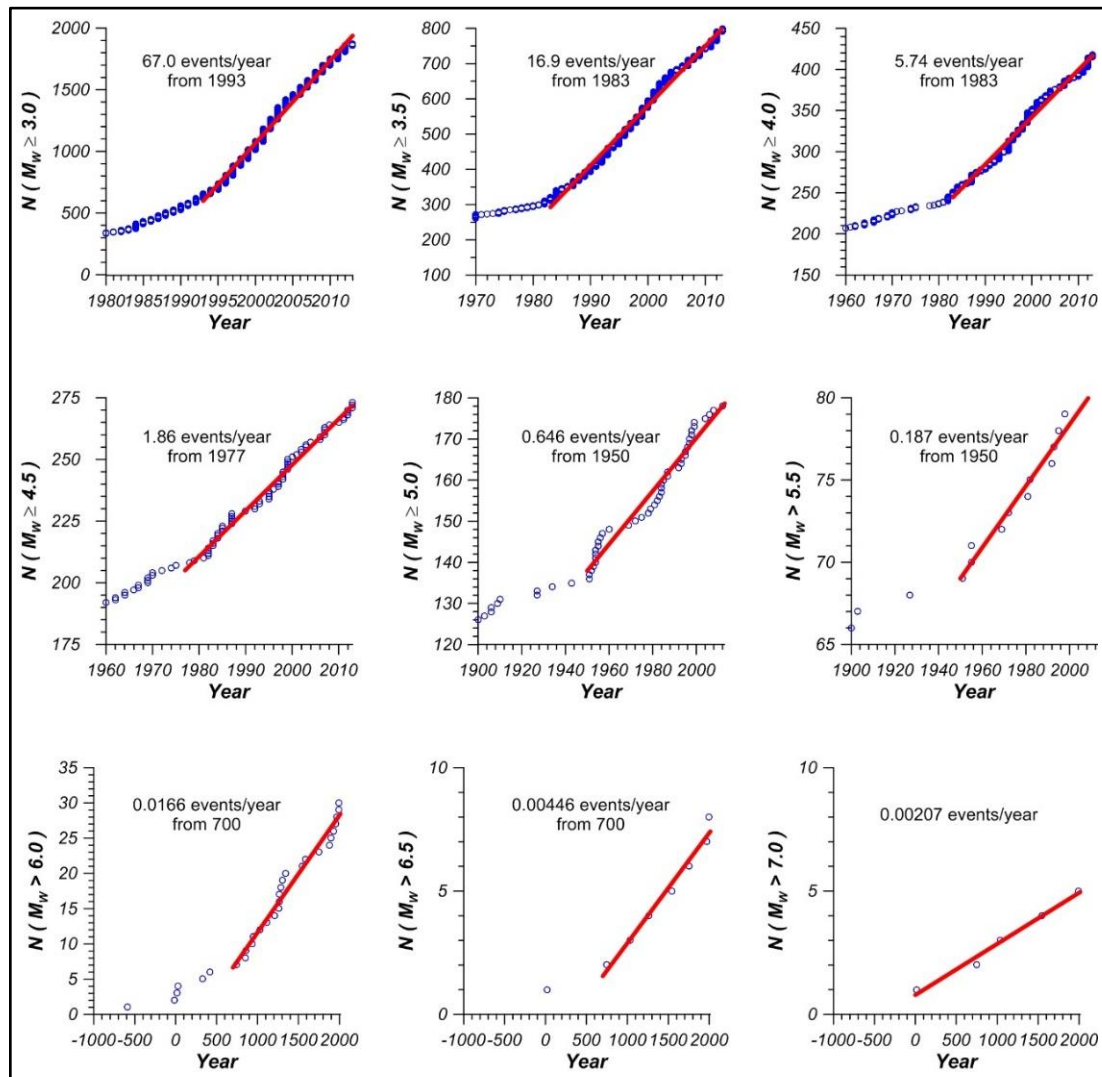


Figure (3-7): Cumulative number of earthquakes above different magnitude values for the Egyptian territory and its surroundings.

Figure (3-8) displays the recurrence (magnitude-frequency) relationship for earthquakes in both the whole catalogue and the Egyptian territory, in the time period likely complete for magnitudes above M_w 3.5, from 1993 and 1983, respectively. There is a good fit in both plots, with a typical b -value equal to 0.94 and 1.08, respectively. These values emphasize the fact that, for those time intervals, the catalogue is likely complete and Poissonian, for the quoted magnitudes. In the recurrence relationship for Egypt and its surroundings (Fig. 3-8), the November 22,

1995, M_w 7.2 Gulf of Aqaba earthquake does not follow the magnitude-frequency relationship. It must be investigated if it could be considered a characteristic earthquake (Youngs and Coppersmith, 1985).

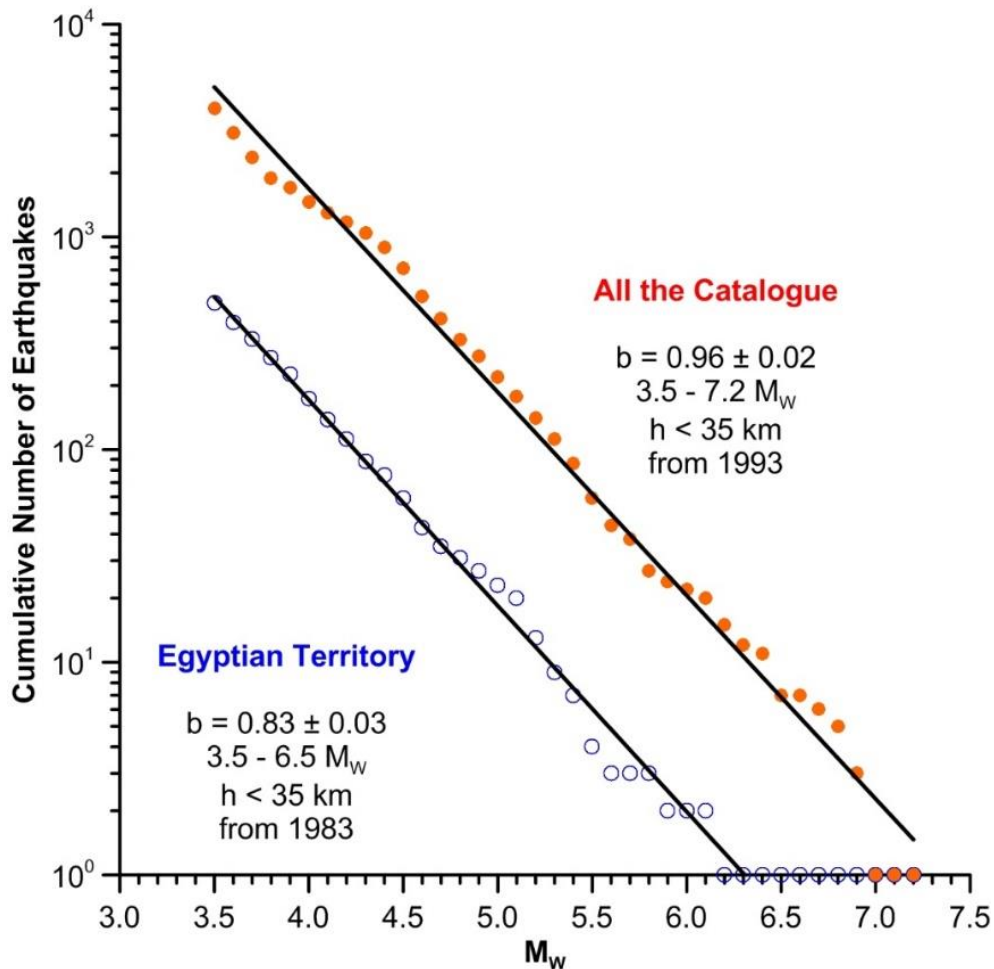


Figure (3-8): Cumulative number of shallow earthquakes vs. magnitude for the entire catalogue for Egypt and its surroundings.

3.7 FOCAL MECHANISM SOLUTION DATABASE (1940 - 2013)

Earthquake source mechanisms or fault-plane solutions are of prime importance in monitoring local, regional and global seismicity and seismotectonics. They have proven to be of great importance in defining the nature of earthquake faulting and its causative stresses in many regions of the world. They reflect the stress pattern acting in the area under study and may help to map its tectonic structure, which causes the earthquakes. Instrumental recordings provide an ever-expanding source of data for understanding earthquakes and their locations, source properties, and radiated seismic waves. FMSs help us to identify the fault plane (with the aid of geological information and/or aftershocks distribution), the type of faulting, the direction of slip and the compatibility of our solution with the general sense of ground motion in the area.

Furthermore, the use of earthquake focal mechanisms or seismic stress tensors for analysis of seismotectonic deformation is a fundamental goal of the modern geodynamics. As such, it has been widely used to evaluate, in a more or less independent manner, the nature of recent crustal deformations on scales ranging from global to regional and local scale.

The insufficient coverage of seismic stations until the 1980's limited the number of fault-plane solutions that have been computed in the Egyptian territory (Badawy, 2005). In the current study, different local and international sources were examined, and FMSs data were compiled into a single database. Those sources are the following: Constantinescu *et al.* (1966), Huang and Solomon (1987), Hussein (1989), Eck and Hofstetter (1990), Riad and Hosney (1992), Abou Elenean (1993, 1997, and 2007), Abdel Fattah *et al.* (1997), El-Sayed *et al.* (2001), Badawy (2001), Badawy and Abdel Fattah (2001, 2002), Salamon *et al.* (2003), Hofstetter (2003), Hofstetter *et al.* (2003), Fat-Helbary and Mohamed (2003), Abou Elenean *et al.* (2004), El-Sayed *et al.* (2004), Korrat *et al.* (2005), Badawy (2005), Badawy *et al.* (2006), Hussein *et al.* (2006), Marzouk (2007), Abdel-Rahman *et al.* (2009), Badawy *et al.* (2008), Abou Elenean and Hussein (2007, 2008), ENSN (1998-2010), Morsy *et al.* (2011, 2012), Abu El-Nader (2013) and Hussein *et al.* (2013).

In addition, the solutions of the CMT Harvard catalogue, the ISC, the NEIC, the RCMT in the Mediterranean region, as well as ZUR-RMT catalogue of the Institute of Technology (ETH) of Zurich, were also included in the final catalogue. Hence, a total number of 688 FMSs were collected covering different active seismogenic zones (Figs. 3-9 to 3-12) in Egypt and surroundings, including Eastern Mediterranean Sea, spanning the spatial area from 21° to 38° N, and from 22° to 38° E. Most of them have a magnitude greater than or equal to M_W 3.0, occurring in the time period 1940 to 2013. Table (3-3) shows the focal mechanism parameters for some selected biggest events which took place in and around Egypt, and their related M_W values.

3.8 DISCUSSION

The seismicity distribution of the compiled catalogue is depicted in Figures (3-4) and (3-5). Most of the crustal seismicity (Fig. 3-4) is concentrated and released within specific seismogenic belts that are mainly related to the different plate boundaries surrounding Egypt. These seismic belts are: The DST, the Cyprian and the Hellenic Arcs, and the Gulf of Suez-Red Sea rift.

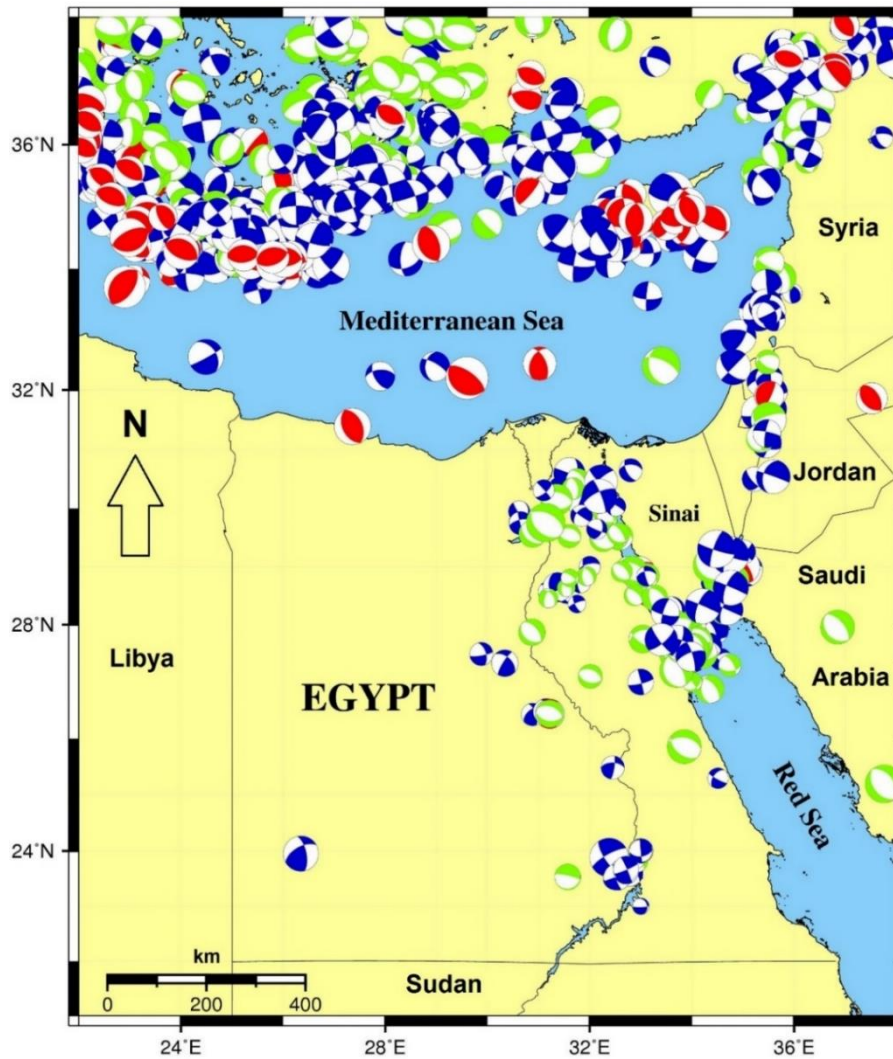


Figure (3-9): Distribution of the catalogued FMSs in and around Egypt for earthquake events included in the current database. Sphere sizes are in proportion to the M_w . Different colours refer to different fault types (Blue: strike-slip faulting mechanism, Green: normal-faulting mechanism, Red: reverse-faulting mechanism).

Thus, Egypt is characterized by a unique tectonic situation including the convergence of the African and Eurasian Plates across a wide zone of deformation in the Eastern Mediterranean to the north, strike-slip movement along the DST to the east and the Gulf of Suez-Red Sea rift. In addition, there is a moderate seismic activity inside the Egyptian territory and away from the surrounding plate boundaries. This seismicity is mainly due to different fault systems: a) around Nasser's Lake, b) Red Sea Coast, especially in Abu Dabbab area, c) Cairo-Suez region, and d) Mediterranean Sea Coastal zone.

However, there is a significant difference between the distribution of the deep ($h > 35$ km) seismicity (Fig. 3-5) and the crustal one (Fig. 3-4). Deeper earthquake events are concentrated along the Hellenic and the Cyprian Arcs, in the EMR. This is due to the convergence and subduction which take place between the African and the

European Plates. In addition, a few deep earthquakes are also observed along the DST, and in the triple junction point, at the northern part of the Red Sea, which represents the intersection between the Gulf of Suez and Gulf of Aqaba. Furthermore, there are few activities along the Pelusium and Qattara lines, which extend in the direction NE-SW to the northern part of Egypt.

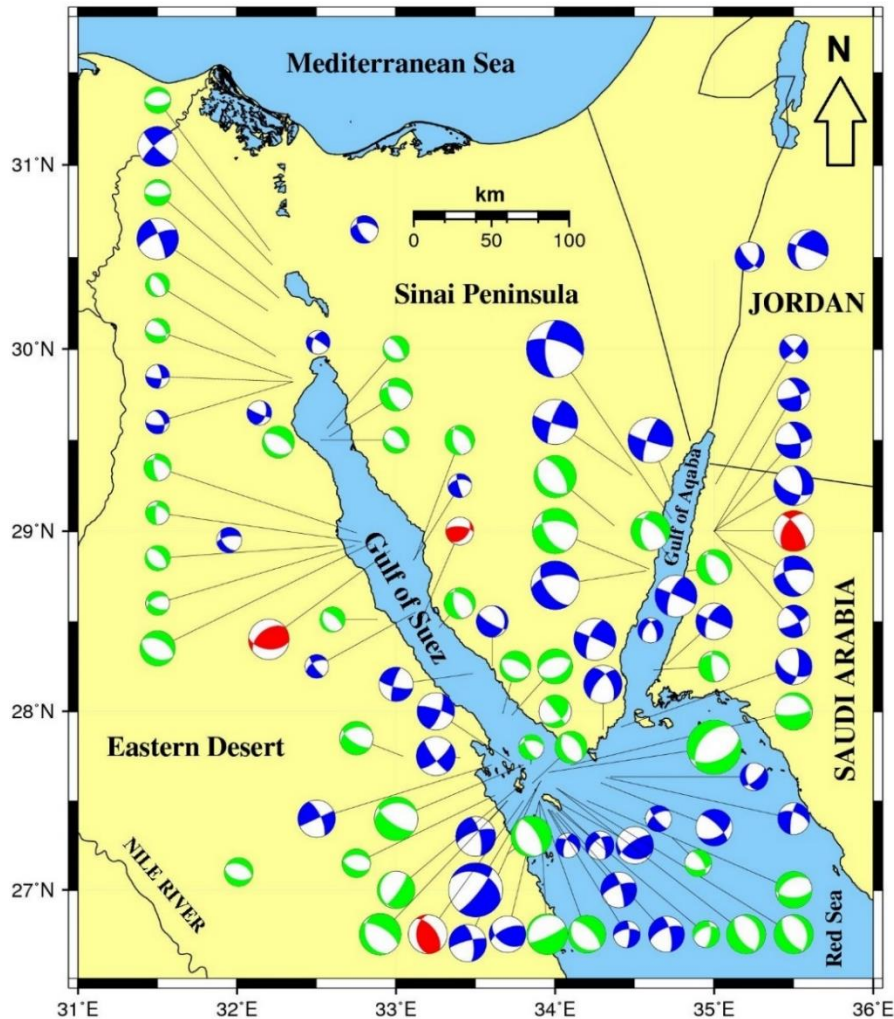


Figure (3-10): Distribution of the catalogued FMSs in Sinai Peninsula. Sphere sizes are in proportion to the M_w . Different colours refer to different fault types.

On the other hand, regarding the FMSs plots (Figs. 3-9 to 3-12), it can be concluded that:

- The focal mechanisms of the events occurred in the southern side of the Hellenic Arc (Fig. 3-9) show a behavior either pure reverse faults or reverse faults with strike-slip components. However, the dominant mechanisms of the northern side of the arc are normal focal mechanisms which are related to the extensional stress field, due to the back-arc activity. Some events, which occur either in the southern

side or in the northern side, show normal faulting or normal faulting with strike-slip component behavior.

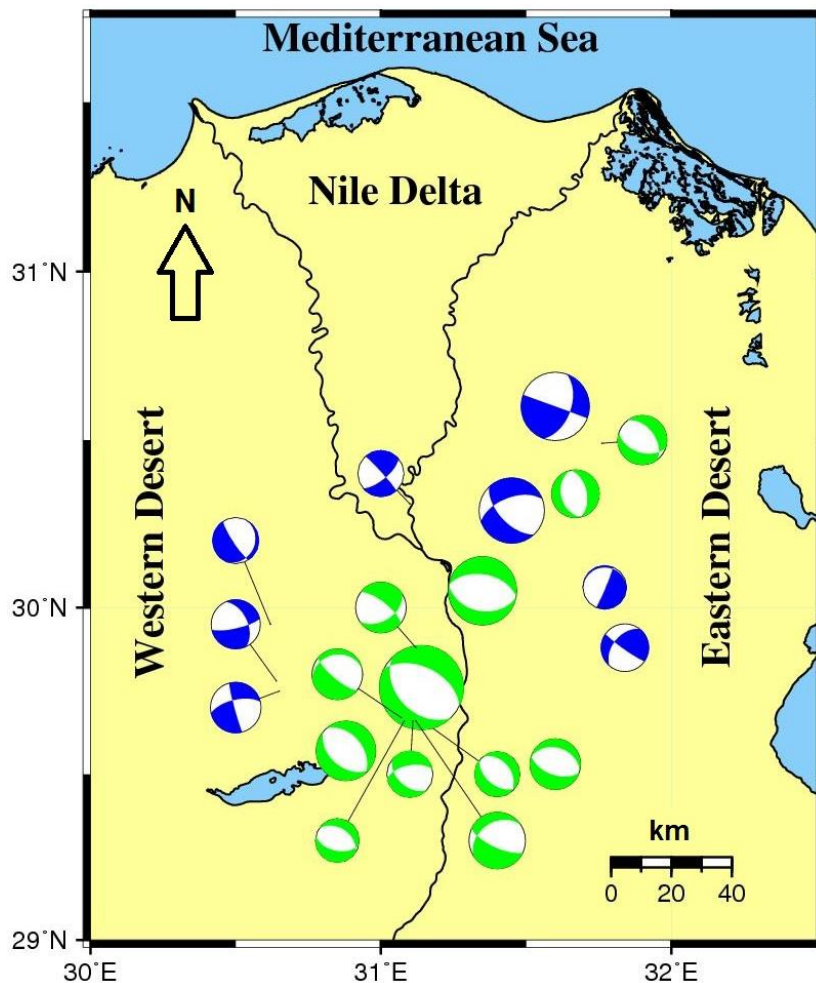


Figure (3-11): Distribution of the catalogued FMSs around Cairo area. Sphere sizes are in proportion to the M_w . Different colours refer to different fault types.

- The Cyprian Arc (Fig. 3-9) is generally characterized by thrusting and shear mechanisms. Reverse faults or reverse faults with small strike-slip components are also obtained for some events in Southern Cyprus. Strike-slip mechanisms with small reverse or normal components are located to the west of the Cyprian Arc.
- Earthquakes along the DST (Figs. 3-9 and 3-10) have left-lateral to normal mechanisms, in general agreement with the tectonic model given by Mart and Hall (1984).
- Earthquake focal mechanisms in Northern Egypt (Fig. 3-11) indicate normal-faulting mechanisms with strike-slip component, suggesting a probable extension of the stress field of the Gulf of Suez and Red Sea rifts beneath the Nile Delta (Meshref, 1990; Badawy, 1998, 2001; Badawy and Horváth, 1999; El-Sayed *et al.*, 2001).

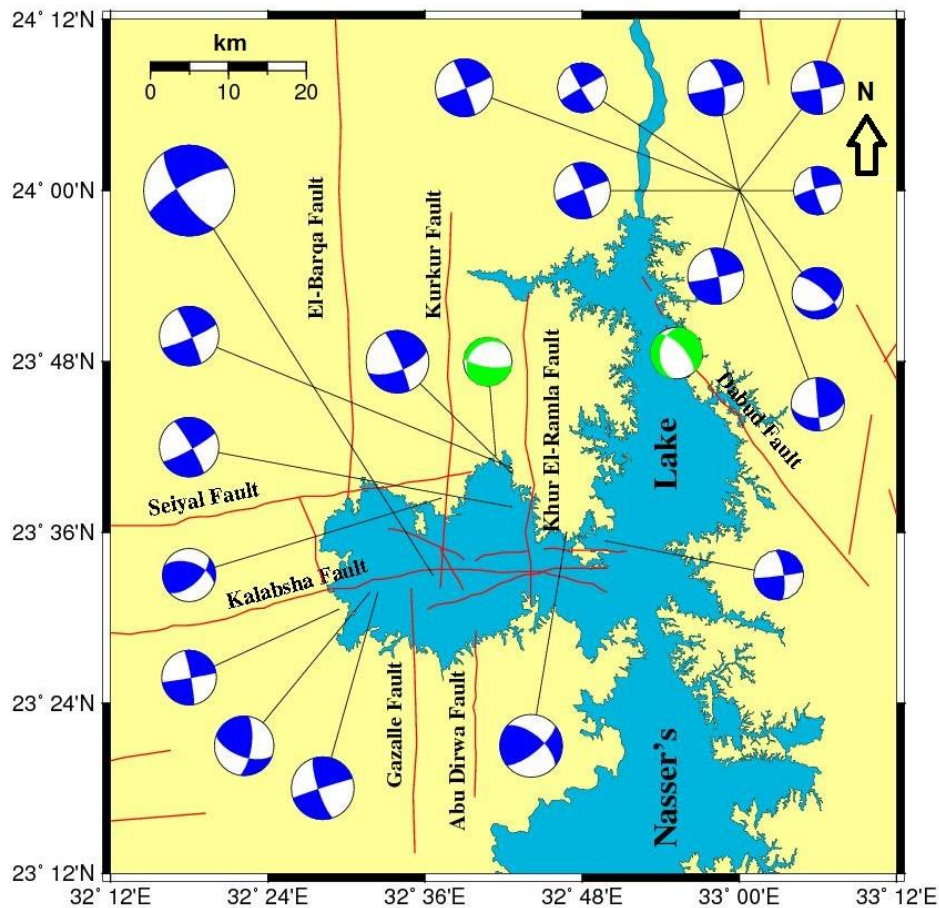


Figure (3-12): Distribution of the catalogued FMSs in Aswan region. Sphere sizes are in proportion to the M_w . Different colours refer to different fault types.

- In southern Egypt (Fig. 3-12), focal mechanisms show relatively pure right-lateral with a few normal-faulting mechanisms, perhaps suggesting a relatively homogeneous stress field. This is in good agreement with recent GPS analyses (Badawy *et al.*, 2003; Mahmoud, 2003).

3.9 CONCLUSIONS

In the current study, a Poissonian earthquake catalogue of 16642 main shocks, with a magnitude above or equal to M_w 3.0 was obtained after compiling all the available national and international sources. The catalogue spans the years from 2200 B.C. to the end of 2013, within a region bounded by 21°- 38°N and 22°-38°E. This study represents an extension and upgrading of different databases on Egyptian seismicity. Tabulated data contain origin time, coordinates, depth, reported magnitudes and/or maximum intensity, and unified moment magnitude. The reported size is also included in the database in reference to those scientists who might prefer to use relationships other than those employed in the current work.

Table (3-3): Focal mechanism solution parameters for the most energetic earthquakes ($M_w \geq 5.5$) that have taken place in Egypt and its surroundings.

Date mm/dd/yyyy	Time hh:mm:ss	Longitude (°)	Latitude (°)	Depth (km)	M_w	Strike (°)	Dip (°)	Rake (°)	Reference
01/30/1951	23:07:24	33.400	32.400	10.0	5.7	295	65	-116	Constantinescu <i>et al.</i> (1966)
09/12/1955	06:09:24	29.600	32.200	33.0	6.4	125	25	90	Salamon <i>et al.</i> (2003)
03/16/1956	19:32:00	35.300	33.300	33.0	5.9	280	90	-15	Salamon <i>et al.</i> (2003)
03/16/1956	19:43:28	35.500	33.300	0.0	5.1	288	50	12	Salamon <i>et al.</i> (2003)
18/12/1956	17:53:00	35.500	31.500	10.0	5.3	251	71	-113	Salamon <i>et al.</i> (2003)
03/31/1969	07:15:51	33.960	27.660	6.2	6.8	220	45	-110	Salamon <i>et al.</i> (2003)
31/03/1969	07:15:54	33.910	27.610	6.2	6.8	294	37	-18	Huang and Solomon (1987)
08/04/1969	10:31:52	33.700	27.500	8.2	5.0	250	70	-20	Salamon <i>et al.</i> (2003)
19/12/1970	22:44:27	33.900	27.500	25.1	5.1	65	80	-86	Salamon <i>et al.</i> (2003)
08/07/1971	23:40:56	33.700	27.200	35.6	5.1	160	25	-80	Salamon <i>et al.</i> (2003)
12/01/1972	08:15:44	33.700	27.500	36.0	5.2	155	30	-60	Salamon <i>et al.</i> (2003)
28/06/1972	09:49:35	33.800	27.700	6.1	5.5	260	30	-130	Huang and Solomon (1987)
09/12/1978	07:12:52	26.350	23.950	7.2	5.3	241	58	150	Abou Elenean (1993)
23/04/1979	13:01:56	35.590	30.540	15.0	5.1	197	40	-4	CMT
14/11/1981	09:05:35	32.380	23.880	15.0	5.8	146	72	-15	CMT
12/06/1983	12:00:09	32.960	28.890	25.1	5.1	95	50	120	Salamon <i>et al.</i> (2003)
29/03/1984	21:36:07	32.190	30.210	8.0	5.2	245	70	-10	Salamon <i>et al.</i> (2003)
02/07/1984	01:47:10	33.850	25.860	10.0	5.1	281	45	-110	CMT
24/08/1984	06:02:25	34.910	32.880	39.0	5.3	28	65	38	Salamon <i>et al.</i> (2003)
24/08/1984	06:02:29	34.810	32.380	28.0	5.3	134	56	0	CMT
31/12/1985	19:42:41	35.050	28.950	9.0	5.1	261	64	-146	Salamon <i>et al.</i> (2003)
02/01/1987	10:14:46	32.220	30.460	20.0	5.0	136	80	-13	Abou Elenean (1993)
28/06/1987	00:50:20	24.490	32.550	15.0	5.3	326	40	-7	CMT

Table (3-3): Continued.

Date mm/dd/yyyy	Time hh:mm:ss	Longitude (°)	Latitude (°)	Depth (km)	M_w	Strike (°)	Dip (°)	Rake (°)	Reference
12/10/1992	13:09:55	31.140	29.760	22.0	5.8	136	42	-75	CMT
03/08/1993	12:43:06	34.570	28.780	15.0	6.1	145	57	-43	Abdel-Fattah <i>et al.</i> (1997)
03/08/1993	16:33:24	34.590	28.790	15.0	5.7	149	55	-47	Abdel-Fattah <i>et al.</i> (1997)
03/11/1993	18:39:32	35.000	29.000	10.0	5.1	324	69	47	Abou Elenean (1997)
04/12/1993	23:34:14	35.000	29.000	19.2	5.0	359	55	-38	Abou Elenean (1997)
22/11/1995	04:15:26	34.730	29.070	18.4	7.2	181	61	-27	Abdel-Fattah <i>et al.</i> (1997)
22/11/1995	18:07:15	34.740	29.200	10.0	5.7	199	77	7	CMT
22/11/1995	22:16:55	34.760	28.640	15.0	5.3	202	67	-3	CMT
22/11/1995	22:16:57	34.210	28.320	15.0	5.3	202	67	-3	CMT
23/11/1995	18:07:26	34.480	29.310	15.0	5.7	199	77	7	CMT
21/02/1996	04:59:57	34.370	29.030	15.0	5.3	132	30	-104	CMT
26/03/1997	04:21:51	35.450	33.390	10.0	5.1	104	35	-167	RCMT
28/05/1998	18:33:33	27.360	31.390	39.0	5.5	154	44	89	CMT
11/02/2004	08:15:06	35.310	31.620	26.1	5.3	340	50	-15	CMT
15/02/2008	10:36:22	35.320	33.270	12.1	5.1	71	69	-167	CMT
19/10/2012	03:35:14	31.020	32.440	29.0	5.0	206	44	131	CMT


From the compilation of the entire catalogue, the following conclusions can be drawn:

- a) The occurrence of both aftershocks and swarm-type activities represents a large number of events in the initial compilation of the current catalogue.
- b) It is clearly appeared that after the deployment of both WWSSN, Aswan telemetered network, and the establishment of the ENSN, the number of recorded earthquakes increased abruptly, and the magnitude threshold was reduced, which it is shown clearly in the catalogue completeness analysis in the different epochs.
- c) A general concentration of the historical earthquake activity is quite clear around the Nile Valley and Nile Delta. This is due to the settlement patterns, as well as a potential amplification of sediments.
- d) Both of historical and instrumental earthquakes show a clear concentration in northern Egypt, being distributed in relatively similar ways, showing that these areas have witnessed activity for many centuries.
- e) Egypt is suffering both interplate and intraplate earthquakes. Intraplate earthquakes are less frequent, but still represent an important component of seismic risk in Egypt. Shallow seismicity is concentrated mainly in the surrounding plate boundaries and on some active seismic zones, like Aswan, Abu Dabbab, and Cairo-Suez regions, while the deeper activity is concentrated mainly along the Cyprian and Hellenic Arcs due to the subduction process between Africa and Europe.
- f) Different FMSs are distributed in different locations in and around Egypt, and all have a general agreement with the geology and tectonics of the studied regions, and also with previous studies.

In conclusion, the authors are confident that the resulting databases cover some gaps and lack of homogeneity observed in previous catalogues for the region.

3.10 ACKNOWLEDGMENTS

The first author wants to thank the Egyptian Government for funding him in the Joint-Supervision Mission program at the University of Jaén, Spain. This research was supported by the Spanish Seismic Hazard and Active Tectonics research group and the Aswan Regional Earthquake Research Centre.



Chapter **4**

Delineation and Characterization of a New Seismic Source Model for Seismic Hazard Studies in Egypt

Sawires, R., Peláez, J.A., Ibrahim, H.A., Fat-Helbary, R.E., Henares, J., and Hamdache, M. (2016). Delineation and characterization of a new seismic source model for seismic hazard studies in Egypt. *Natural Hazards* 80, 1823-1864.

ABSTRACT


In the present study, a new seismic source model for the Egyptian territory and its surroundings is proposed. This model can be readily used for seismic hazard assessment and seismic forecasting studies. Seismicity data, focal mechanism solutions, as well as all available geological and tectonic information (e.g. active faults) were taken into account during the definition of this model, in an attempt to define zones which do not show only a rather homogeneous seismicity release, but also exhibit similar seismotectonic characteristics.

This work presents a comprehensive description of the different tectonic features and their associated seismicity to define the possible seismic sources in and around Egypt. The proposed seismic source model comprises 28 seismic sources covering the shallow seismicity ($h \leq 35$ km) for the Egyptian territory and its surroundings. In addition, for the Eastern Mediterranean region, we considered the shallow seismic source zones ($h \leq 20$ km), used in the SHARE project for estimating the seismic hazard for Europe. Furthermore, to cover the intermediate-depth seismicity ($20 \leq h$

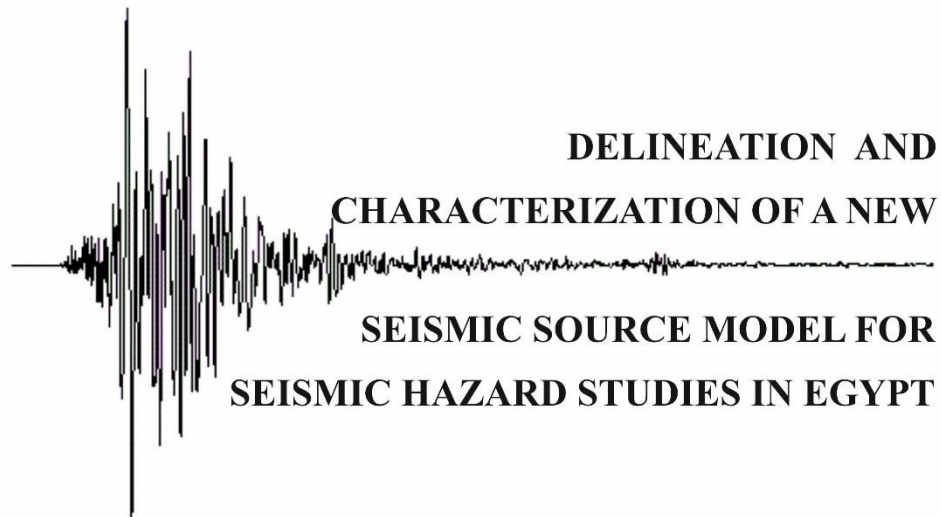
≤ 100 km), seven intermediate seismic source zones were delineated in the Eastern Mediterranean region.

Following the determination of zone boundaries, a separate earthquake and focal mechanism sub-catalogue for each seismic zone was created. Seismicity parameters (b-value, activity “a-value” and maximum expected magnitude) have been computed for each source. In addition, the predominant focal mechanism solution was assigned for each source zone using the stress field inversion approach. The proposed seismic source model and its related seismicity parameters can be employed directly in seismic hazard assessment studies for Egypt.

HEADINGS:		Page
4.1	Data Sources.....	85
4.1.1	An Updated Earthquake Catalogue.....	85
4.1.2	Focal Mechanism Solutions Data.....	86
4.1.3	Active Faults Data.....	86
4.1.4	Crustal Structure Data.....	89
4.2	Estimation of the Seismicity Parameters.....	89
4.3	Description and Characterization of the Proposed Shallow Seismic Source Model.....	91
4.3.1	Seismic Sources along the Gulf of Aqaba–Dead Sea Transform Fault.....	91
4.3.2	Seismic Sources along the Red Sea Rift.....	98
4.3.3	Seismic Sources along the Gulf of Suez Rift.....	102
4.3.4	Seismic Sources of the Egyptian Eastern Desert.....	105
4.3.5	Seismic Sources along Nasser’s Lake, Nile Valley and Cairo–Suez District.....	107
4.3.6	Seismic Sources along the Mediterranean Coastal Line.....	112
4.3.7	Seismic Sources of the Western Desert.....	114
4.4	Eastern Mediterranean Region Seismic Sources.....	115
4.4.1	SHARE Shallow Seismic Sources.....	116
4.4.2	Intermediate-depth Seismic Sources	118



4.5	Stress Pattern from the Inversion of Focal Mechanism Solutions	
	Data.....	119
4.6	Conclusions.....	124
4.7	Acknowledgments.....	126



DELINEATION AND CHARACTERIZATION OF A NEW SEISMIC SOURCE MODEL FOR SEISMIC HAZARD STUDIES IN EGYPT

Since the pioneering work of Cornell (1968), it was obvious that the delimitation and characterization of the seismic sources, in a particular region, is a very important input for seismic hazard assessment studies. Although, it has been common practice in seismic hazard to use seismically homogeneous areal source zones (e.g., Abrahamson, 2006), in the present study, the seismic source zones are defined including all the available data, i.e., seismicity, geological, geophysical (gravity and aeromagnetic) and tectonic information.

Egypt is situated in the northeastern corner of the African Plate, along the southeastern edge of the EMR. It is interacting with the Arabian and Eurasian Plates through divergent and convergent plate boundaries, respectively. Hence, it is bounded by three active tectonic plate margins: the African-Eurasian plate margin, the Gulf of Suez-Red Sea plate margin, and the DST (Fig. 4-1). Mostly seismic activity of Egypt results from the interaction and the relative motion between the plates of Eurasia, Africa and Arabia. Within the last decades, some events resulting from this interaction struck different regions in Egypt, causing considerable damage (e.g., M_w 7.2, November 22, 1995 Gulf of Aqaba earthquake).

Numerous seismic hazard assessments for specific regions in Egypt, based on the seismic zoning approach, has been carried out by many researchers in the last decades. Among these studies, those carried out by the following authors: Albert (1986, 1987), Kebeasy *et al.* (1981), Sobaih *et al.* (1992), Fat-Helbary and Ohta (1996), El-Sayed and Wahlstörn (1996), Abou Elenean (1997, 2010), Deif (1998), Riad *et al.* (2000), El-Sayed *et al.* (2001), El-Hefnawy *et al.* (2006), Fat-Helbary *et al.* (2008), Deif *et al.* (2009, 2011), and Mohamed *et al.* (2012). In these assessments, the

studied region was divided into different seismic zones depending mainly on the distribution of the instrumental earthquakes and the prevailing tectonic setting.

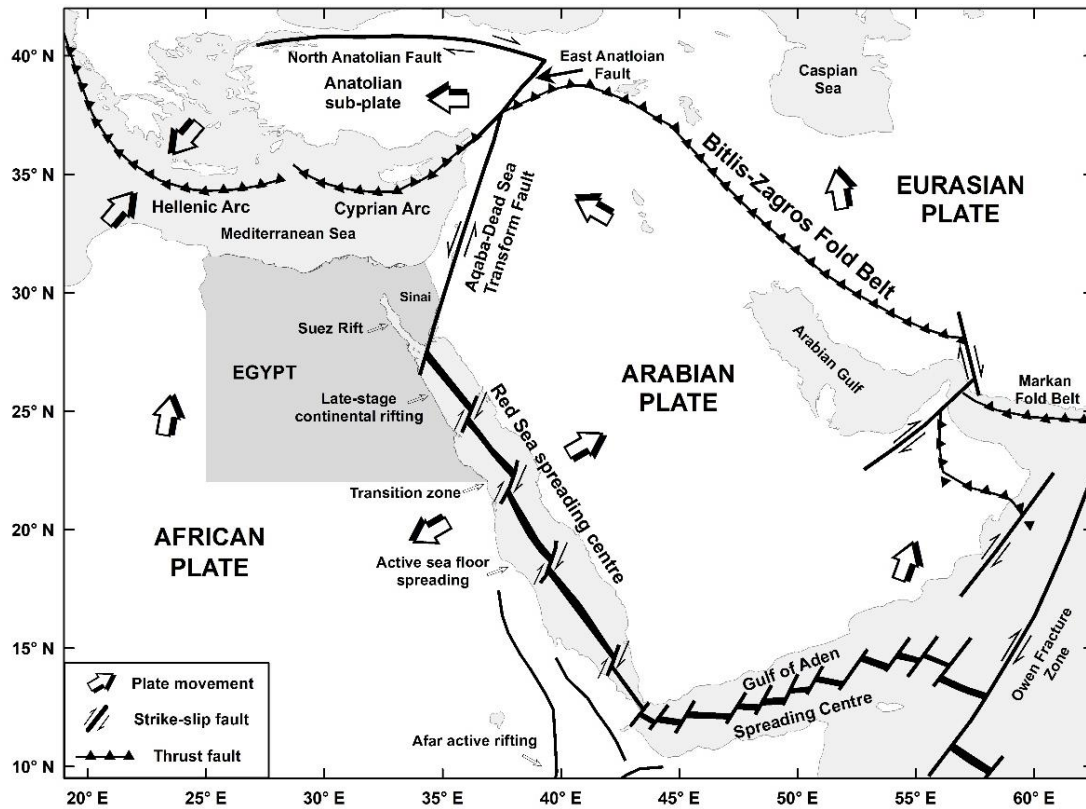


Figure (4-1): Global tectonic sketch for Egypt and its vicinity (compiled and replotted after Ghebreab, 1998; Ziegler, 2001 and Pollastro, 2003). The study area is from 21° to 38°N and from 22° to 38°E.

In the present chapter, we identified and characterized regional seismic source zones for Egypt and its surroundings. We compiled an updated earthquake catalogue (including FMSs) from various sources and prepared a complete database of the Egyptian earthquakes from 2200 B.C. until 2013. Different earthquake magnitude relationships, correlating different magnitude scales, were used during the development of the catalogue. Using the Gardner and Knopoff (1974) procedure, all dependent events were removed from the unified earthquake catalogue to ensure the Poissonian distribution of earthquakes. The delineation of the proposed seismic source model is based on the seismic activity distribution, geology, and fault orientations. Separate sub-catalogues for each zone were created, and the seismicity parameters for all the source zones were computed. In addition, the predominant focal mechanism stress pattern was identified for each seismic source using the stress inversion approach by Delvaux and Sperner (2003) and Delvaux and Barth (2010).

In the current work, all previous attempts to delineate seismic sources in Egypt were taken into our consideration. In addition, applying a new and updated earthquake catalogue (for historical and instrumental data) and taking into our consideration the published FMSs and their related geologic interpretations, it represents an advantage in the characterization of the proposed model.

4.1 DATA SOURCES

4.1.1 AN UPDATED EARTHQUAKE CATALOGUE

A complete and consistent earthquake catalogue in a region is the keystone for any seismotectonic and seismic hazard studies. In the present study, the definition and characterization of the seismic source model is based on an updated earthquake catalogue. The historical and instrumental earthquake data from different sources, agencies and bulletins (national and international) have been compiled. The initial compiled data suffered from incompleteness, duplication, and large epicentral and hypocentral location errors. Evaluating the different datasets, eliminating duplicate events, and sorting out the dependent events were taken place.

The initial compilation of the earthquake catalogue spanning a spatial region from 21° to 38°N and from 22° to 38°E, covering the time period from 2200 B.C. to 2013, and included all the events having an assigned magnitude of 3.0 and above (for international sources) and any magnitude (for local sources) on any magnitude scale. Different sources were used in the compilation such as: the regional catalogue by Ambraseys *et al.* (1994), the EHB (Engdahl *et al.*, 1998) catalogue, ISC (2011), and the ENSN bulletins (1998-2010). All of the compiled earthquake data, from different sources, were merged together and the duplicate entries were removed.

In the compilation, the earthquake events were reported in different magnitude scales: m_b , M_S , m_D , M_L , and M_W magnitudes, as well as I_{max} , which were derived and reported by different analytical methods. For seismic hazard analyses, the catalogue has to be consistent in magnitudes. Preference for using the M_W scale, which is the most widely used and reliable magnitude for describing the size of an earthquake as it does not saturate.

Several empirical regression relationships between the different reported magnitudes, I_{max} and M_W have been employed. These relationships are those considered after establishing specific relationships from their database or to use the

most reliable ones after studying the available magnitude relationships in the scientific literature. The equivalent M_W^* was computed for each set of reported magnitude data.

Finally, the dependent events were removed using the Gardner and Knopoff (1974) methodology. Given an earthquake with a certain M_W , a scan within a characteristic distance and time was performed for the entire catalogue. The largest earthquake in this search is considered to be the mainshock. Window sizes of 900 days and 100 km were used for a given M_W 8.0 event, and 10 days and 20 km for a M_W 3.0 event. For in-between magnitudes, proportional values for distance and time were used. The resultant declustered data consists of a 16642 events, which represent a final Poissonian catalogue including main shocks with magnitude above or equal to M_W 3.0.

4.1.2 FOCAL MECHANISM SOLUTIONS DATA

FMSs are essential for the study of the seismotectonics of a region. It illustrates the relationship between earthquakes and known faults, the local and global stress field, as well as their relation with other possible faults not already known. In the current study, the characterization of the seismic source model is also based on the FMSs data compiled by the authors. In their studies, different local and international sources were searched and examined, to compile the FMSs data into one database. For example, the solutions of the Global CMT catalogue, the ISC, the NEIC, the RCMT in the Mediterranean region, as well as ZUR-RMT catalogue of the ETH of Zurich, are included in the catalogue .

More than 600 FMSs (including earthquake events in the EMR) were collected in their studies, covering different active seismic zones (Fig. 4-2) in and around Egypt, spanning the same study area. Most of these solutions have a magnitude greater than or equal to M_W 3.0, occurring in the time period from 1940 to 2013. In the current work, the compiled FMSs database was classified depending on the rake angle provided for each solution (Stein and Wysession, 2003). Three types of faulting mechanism were chosen, for simplicity, to discriminate between the different faulting mechanisms (normal, reverse and strike-slip).

4.1.3 ACTIVE-FAULTS DATA

Several geological, geophysical (gravity and aeromagnetic) and tectonic maps were inspected for the purpose of getting more information about the present active

faults and also for the identification of the prevailed tectonic and structural trends in the study region (Fig. 4-3). Among the most important studies are those of Said (1990), Youssef (1968), Neev (1975), El-Shazly (1977), Riad (1977), Issawi (1981), EGSM (1981), Sestini (1984), Schlumberger (1984), WCC (1985), Meshref (1990), Guiraud and Bosworth (1999), Abdel Aal *et al.* (2000), Philobos *et al.* (2000), and Hussein and Abd-Allah (2001).

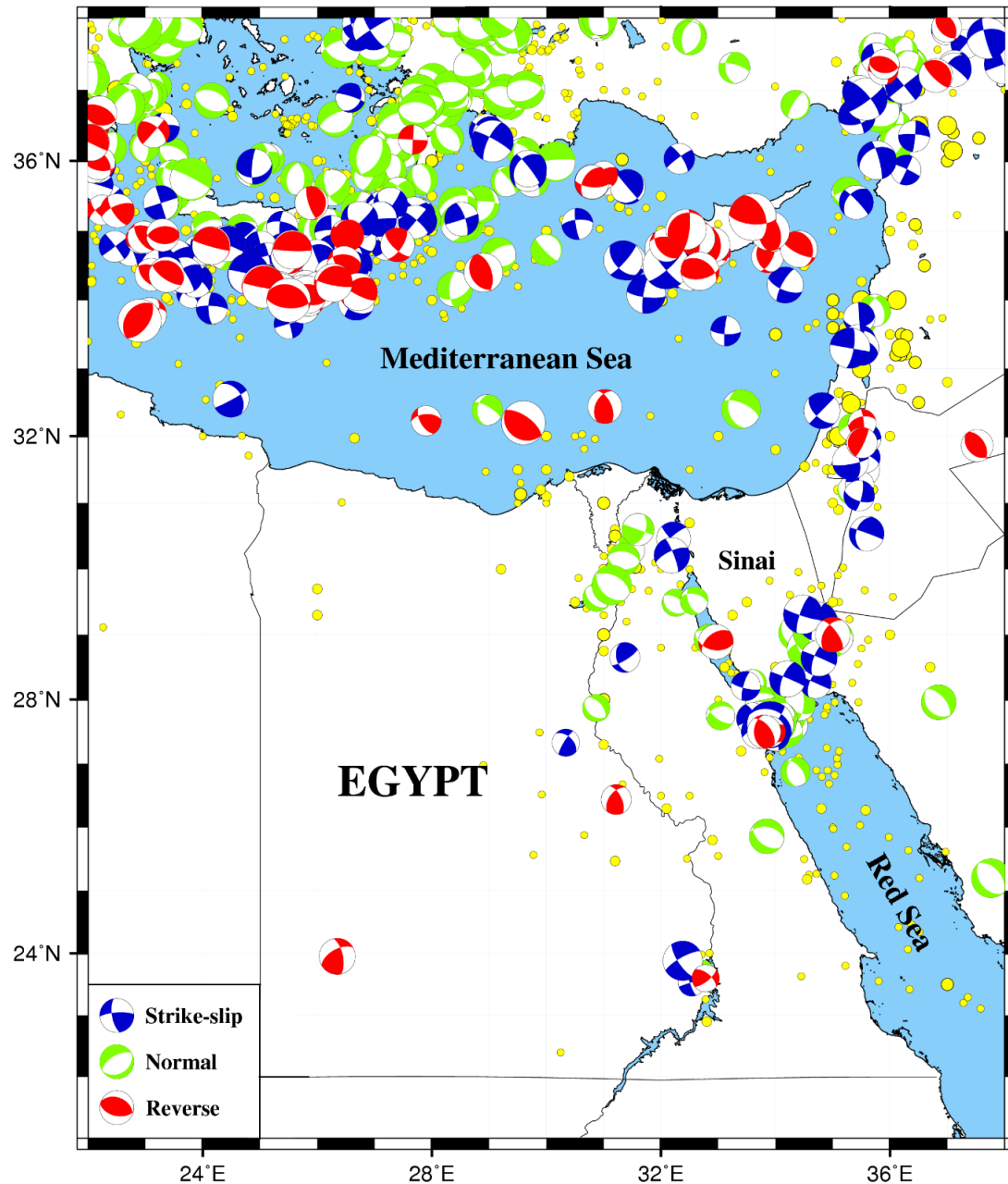


Figure (4-2): Distribution of the seismicity and FMSs (over M_w 4.0) in and around Egypt. Symbols and focal sphere sizes are in proportion to the M_w . FMSs follow Stein and Wyession (2003) classification.

Based on the structural studies in the territory of Egypt, Youssef (1968) classified the main structural elements of Egypt (Fig. 4-3) into the following fault

trends: a) Gulf of Suez-Red Sea, b) Gulf of Aqaba, c) east-west, d) north-south, and e) N45°W trends. However, Meshref (1990), from the aeromagnetic tectonic trend analysis, showed the main tectonic trends which influenced Egypt throughout its geologic history as: a) NW (Gulf of Suez-Red Sea), b) NNE (Gulf of Aqaba), c) east-west (Tethyan or Mediterranean Sea), d) north-south (Nubian or East African), e) WNW (Drag), f) ENE (Syrian Arc), and g) NE (Aualitic or Tibesti) trends.

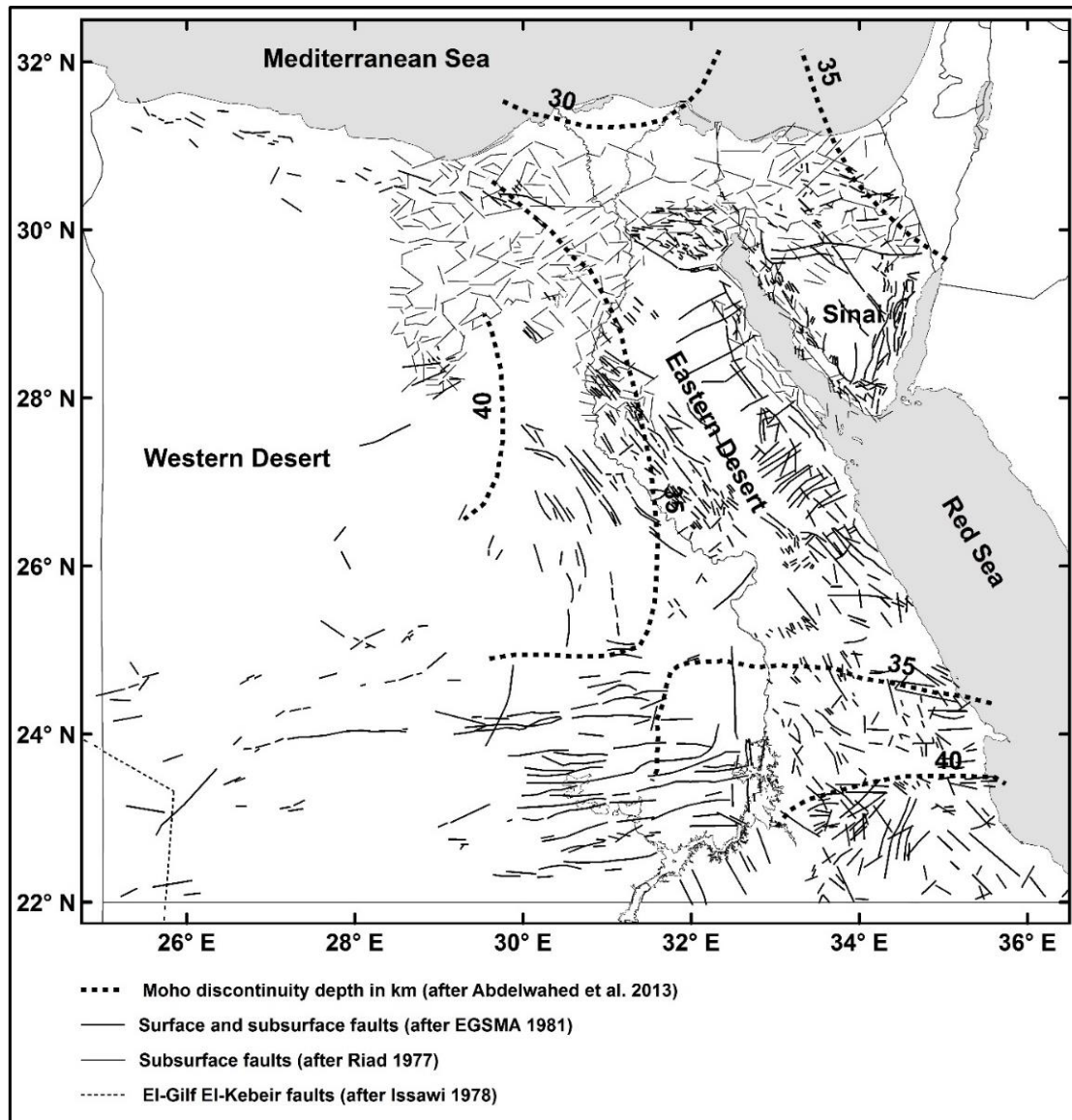


Figure (4-3): Distribution of major surface and subsurface faults and depth distribution of Moho discontinuity in Egypt. Compiled from Riad (1977), Issawi (1978), EGSMA (1981) and Abdelwahed *et al.* (2013).

However, active fault data from the seismological point of view is very scarce in Egypt. Only five active faults defined by WCC (1985) in the Nasser's Lake region, in Southern Egypt, are considered to be active. They are Kalabsha, Seiyal, Gebel El-Barqa, Khur El-Ramla, and Kurkur faults. More recently, Deif *et al.* (2011)

considered two more faults in the same region to be active, they are the Abu Dirwa and Dabud faults. See Section 4.3.5 for more details about these faults.

4.1.4 CRUSTAL STRUCTURE DATA

The crustal structure plays an important role in Seismology. It can be used, as in the current study, for the discrimination between the crustal (shallow-depth) seismicity, the intermediate-depth, and the deeper one. Several studies have been carried out to evaluate the crustal structure and thickness in Egypt by using different types of datasets coming from seismic reflection surveys, deep seismic sounding, shallow seismic refraction, and gravity data (e.g., Marzouk, 1988; El-Hadidy, 1995; Makris *et al.*, 1988; Dorre *et al.*, 1997).

In the present delimitation of the different seismic sources, the most recent study (Abdelwahed *et al.*, 2013) was taken into our consideration. Their results (Fig. 4-3) show that the Moho discontinuity is getting shallower toward the northern and eastern coasts of Egypt, and deeper toward the Egyptian Western Desert and Northeastern Sinai Peninsula. This discontinuity is located at depth of 31-33 km in the surrounding of Greater Cairo, 32-35 km in Sinai Peninsula, 33–35 km along the Nile River, 30 km near the Red Sea coast, and 39 km towards the Egyptian Western Desert. Thus, we used a mean value of 35 km, for the Moho discontinuity, to discriminate between the shallow- and intermediate-depth earthquake events.

4.2 ESTIMATION OF THE SEISMICITY PARAMETERS

Seismic sources define areas that share common seismological, tectonic, and geologic attributes, and that can be described by a unique magnitude-frequency relationship. For PSHAs, a seismic source represents a region in which future seismicity is assumed to follow specified probability distributions for occurrences in time, earthquake sizes, and locations (Araya and Der Kiureghian, 1988).

Once a seismic source is identified and its corresponding zone boundaries are characterized, the seismic hazard analyst's attention is turned towards the evaluation of the size of earthquakes that the source zone can be expected to produce. In the current work, following the determination of each zone boundaries, separate earthquake catalogue for each seismic zone were created. The estimation/adoption of a statistical model for the magnitude distribution of the earthquakes within each source, which is parameterized by a Gutenberg–Richter type frequency-magnitude

relationship (Gutenberg and Richter, 1944) is done. The total rate of earthquakes in a given source zone is estimated by first calculating the cumulative rate of earthquakes in each magnitude interval using that portion of the catalogue that is considered complete. Finally, values of the slope (b -value) and intercept (a -value) are determined from a linear, least-squares regression on the logarithm of the cumulative rate of earthquakes versus magnitude.

On the other hand, the knowledge of the largest magnitude which may occur within a potential seismic source is of practical importance. The estimation of maximum magnitudes is usually based on the features of seismic activity and geological analogy. No widely-accepted method exists for estimating the M_{max} that can be occurred in each seismic source. In the current study, the procedure of Robson–Whitlock–Cooke (Cooke, 1979; Robson and Whitlock, 1964; Kijko and Singh, 2011) for determining the M_{max} , was followed for some delineated seismic sources. This procedure showed that, when the earthquake data are arranged in ascending order of magnitude, namely $M_1 \leq M_2 \leq \dots \leq M_{n-1} \leq M_{max}^{obs}$, then the estimation of the M_{max} and its variance is as follows:

$$M_{max} = M_{max}^{obs} + 0.5(M_{max}^{obs} - M_{n-1}) \quad (4-1)$$

$$\sigma(M_{max}) = 0.5 \left[3\sigma_M^2 + 0.5(M_{max}^{obs} - M_{n-1})^2 \right] \quad (4-2)$$

where σ_M denotes standard error in the determination of the two largest observed magnitudes, i.e., M_{max}^{obs}, M_{n-1} .

Finally, the computed maximum expected magnitudes, for the delineated seismic sources, are crosschecked against the paleo-seismic data provided by Deif *et al.* (2009 and 2011). We found that, three seismic sources (EG-05, EG-09 and EG-22) have maximum magnitudes, based on the paleo-seismic data, higher than the computed ones in our appraisals. So, we preferred to consider them, since they are more conservative and more reliable one.

The maximum observed magnitude, seismicity parameters (b -value, activity rate and M_{max}), as well as the completeness period, for each delineated seismic source zone will be tabulated in the following section, after discussing the prevailed tectonic environment and its possible related seismicity.

4.3 DESCRIPTION AND CHARACTERIZATION OF THE PROPOSED SHALLOW SEISMIC SOURCE MODEL

Araya and Der Kiureghian (1988) discriminate between four types of seismic sources. The first type is the seismotectonic zone, i.e., seismic sources in which a causal relationship has been established between a geologic structure (e.g., faults) and earthquakes. The second one is the paleoseismic zone, which has an important Quaternary-Holocene structural history that may indicate the possibility of the seismic activity in the future. The third type is the seismogenic zone, which lacks the development of a clear history relating the seismic activity to a geologic structure. For such zones, critical gaps in the Quaternary geologic structure history preclude direct evidence of active faulting. They are the most common type of seismic sources employed in PSHA. The last one is the seismicity zone, which defined with no consideration of their relation to geologic structures, but they are defined based on the spatial distribution of the seismic history.

In the current study, due to the lack of active faults and paleoseismic data in the Egyptian territory, the only possible types to consider in this work are the seismogenic and seismicity sources, and this will be the terminology used in this work. Accordingly, Egypt and the neighbor regions were divided into 28 area sources (Fig. 4-4). Many of these zones are related to the tectonic activity of the previously defined local active belts. Mostly of the proposed source zones are seismogenic ones, with the exception of nine sources which have been considered seismicity sources. The delineation of these last sources was based only upon the earthquake distribution.

In the following, we are dividing the proposed seismic sources into different groups, depending on the prevailing geologic and tectonic features. The details of the selection of these seismic sources, together with the estimation of its seismicity parameters and M_{max} , are given for each seismic source.

4.3.1 SEISMIC SOURCES ALONG THE GULF OF AQABA-DEAD SEA TRANSFORM FAULT

The DST is a 1100 km long left-lateral strike-slip fault (Fig. 4-5) that accommodates the relative motion between Africa and Arabia (Salamon *et al.*, 1996, 2003). It is a seismically active transform boundary, connecting the Red Sea spreading center in the south to the Northern Mediterranean Triple Junction to the north. Its

main left-lateral sense of motion is recognized by minor pull-aparts in young sediments (Garfunkel *et al.*, 1981), cut and offset of drainage lines and man-made structures (e.g., Reches and Hoexter, 1981; Marco *et al.*, 1997, 2000).

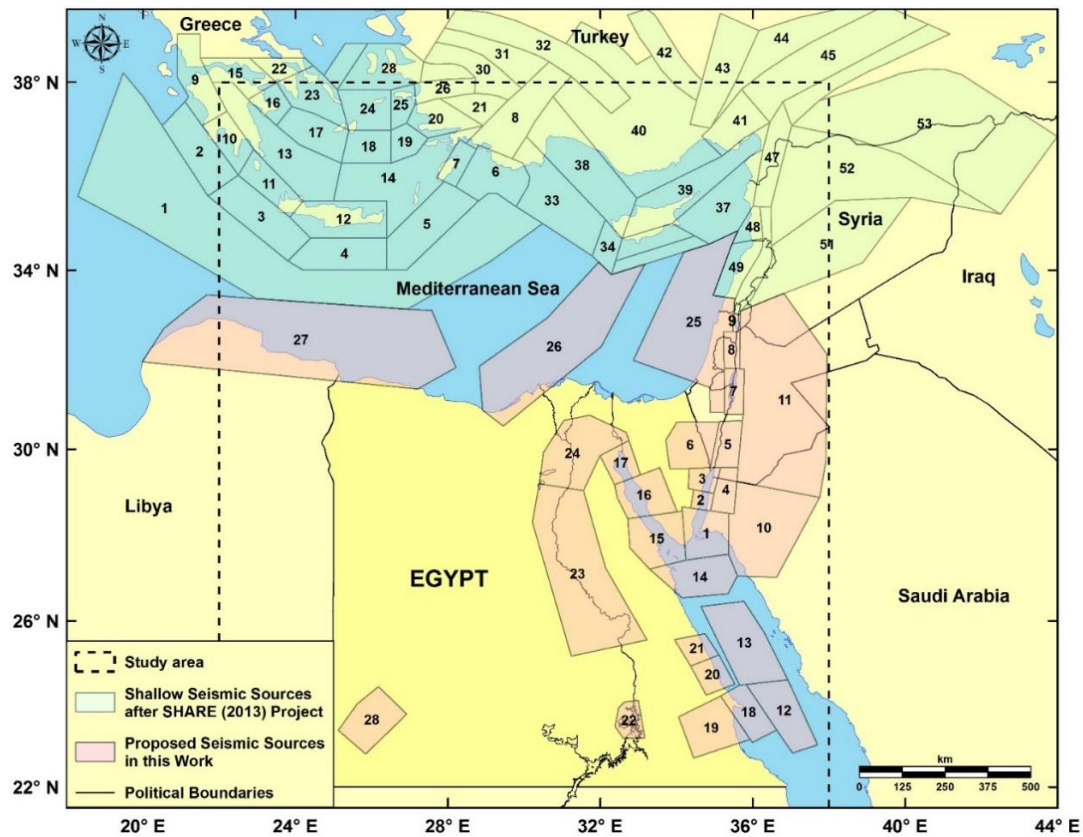


Figure (4-4): Proposed shallow seismic source zones in Egypt and its surroundings.

The DST (Fig. 4-5) is generally subdivided into three main sections (Garfunkel, 1981). The southern section, extending from the Gulf of Aqaba (Red Sea) through the Dead Sea and the Jordan Valley, is characterized by the presence of predominantly left-lateral strike-slip faults, striking between N12°E and N20°E. The central section of the DST is characterized by the presence of approximately 200 km long NNE–SSW striking restraining bend, running through Lebanon and SW Syria, where the DST splays into distinct fault branches. The major branch, called the Yammouneh Fault, connects the southern and northern parts of the DST, while the other branches connect at about 45° the DST with the Palmyride Fold Belt (Girdler, 1990). The northern section of the DST is characterized by the presence of two distinct N–S striking faults bounding the 70 km long Ghab Valley and intersecting through a complex braided fault system with the East Anatolian Fault and the Cyprian Arc (e.g., Gomez *et al.*, 2003). This intersection corresponds to the Hatay “fault–fault–trench” triple junction that forms the plate boundaries between Arabia, Africa and Anatolia (Mahmoud *et al.*, 2013).

4.3.1.1 Gulf of Aqaba Seismic Sources (EG-01 – EG-04)

The Gulf of Aqaba experienced the largest Egyptian earthquake (M_W 7.2, November 22, 1995). The length of the aftershocks area reaches about 110 km, and its strike running N 30° E, parallel to the strike of the Gulf of Aqaba (Dziewonski *et al.*, 1997). Heavy damage was occurred at Nuweiba city, along the western coast of the gulf.

The Gulf of Aqaba has been considered to be the most active seismic area over the last few decades, characterized by swarm activity (e.g., Shapira and Jarradat, 1995). Until 1983, there was no instrumental information on the seismicity along the Gulf of Aqaba, while from January up to April 1983, more than 500 earthquakes, reaching a magnitude of M_L 4.8, were recorded. These earthquakes were felt at towns and villages along the gulf, as well as at the Arava Valley, causing a widespread concern (Heidbach and Ben-Avraham, 2007). From August 1993 up to February 1994, a large earthquake swarm was associated with relatively high magnitudes, reaching a M_L 5.8 value. This swarm included about 1200 events occurred south to the 1983 swarm. On November 2002, another earthquake sequence occurred at the middle of the Gulf of Aqaba. More than 10 earthquakes with magnitude above M_L 4.0 were recorded. Some of these earthquakes were felt, but without damage for buildings at the epicentral area.

The Gulf of Aqaba is occupied by three elongated en-echelon basins transected by longitudinal faults (Eyal *et al.*, 1981). This en-echelon system produces several tectonic basins, which are forming rhombic-shaped grabens. Thus, three basins in the Gulf of Aqaba are present. They are, from south to north, Tiran “Arnona”-Dakar, Aragonese and Elat “Aqaba” Basins.

According to the seismic activity, the epicentral distribution and the local tectonics, different seismogenic sources were delineated in the gulf area (Figs. 4-5 and 4-6).

- a) The EG-01 (Tiran – Dakar Basin) seismogenic source lies at the southern part of the Gulf of Aqaba. It includes the M_S 4.4, February 2, 2006 earthquake. There is no historical earthquakes included in this source zone. The majority of the available FMSs inside this area source reflects normal-faulting mechanism.

- b) The EG-02 (Aragonese Basin) seismogenic source lies to the north of the previous EG-01 zone, and it includes the M_W 7.2, November 22, 1995 earthquake, which is considered the largest event to occur along the DST in the last century. No historical events were reported in this area source.
- c) The EG-03 (Elat Basin) seismogenic source located to the north of the EG-02 seismic zone and considered as the extension area of the M_W 7.2, November 22, 1995 Aqaba earthquake rupture. It is characterized by a low seismicity level, if compared with the other previously mentioned zones of the Gulf of Aqaba. Two historical events have been included in this area source, the I_{max} VIII, March 18, 1068, and the I_{max} VIII-IX, May 2, 1212 earthquakes.
- d) In addition to the previous seismogenic sources, the delineation of a separate and fourth zone is considered. This source lies to the east of the gulf, characterized by dispersed moderate seismicity. It is the EG-04 (Eastern Gulf of Aqaba) seismogenic source. The major earthquake included in this source is the m_b 4.5, December 26, 1995 earthquake. This seismic source does not include any historical events.

The variety of the FMSs reflects the complexity of the geologic structure within the gulf. Previous FMS studies for moderate to large earthquakes located in the Gulf of Aqaba region (e.g., Hofstetter *et al.*, 2003; Abdel Fattah *et al.*, 2006) assert the dominance of a ENE-WSW extension (N60°- 80°E). Furthermore, field studies (Bayer *et al.*, 1988) observed two conjugate faults along the Gulf of Aqaba: NNE left-lateral strike-slip faults parallel to the gulf that release the majority of stress, and a nearly ESE-WNW normal faults along the margins of pull-apart basins. On the other hand, body waveform inversion of the M_W 6.1, August 3, 1993, and the M_W 7.2, November 22, 1995 events, support the occurrence that normal faulting taken place along the transverse NNW-SSE and ESE-WNW faults, while left-lateral strike-slip movement occurs along NNE major Aqaba trend (Pinar and Türkelli, 1997). Abou Elenan (1997) studied the focal mechanism of the M_W 7.2, November 22, 1995 Gulf of Aqaba earthquake, as well as some aftershocks. He concluded that mostly of these solutions show a strike-slip movement with normal component, with the exception of one event on the eastern side of the Gulf of Aqaba that shows strike-slip movement with reverse component in the NNW-SSE and ENE-WNW trending planes. Thus, Salamon *et al.* (2003) quoted that normal-faulting mechanisms are attributed to the faults that form

the boundaries of the major basins in the gulf, while others indicate the left-lateral motion of the transform.

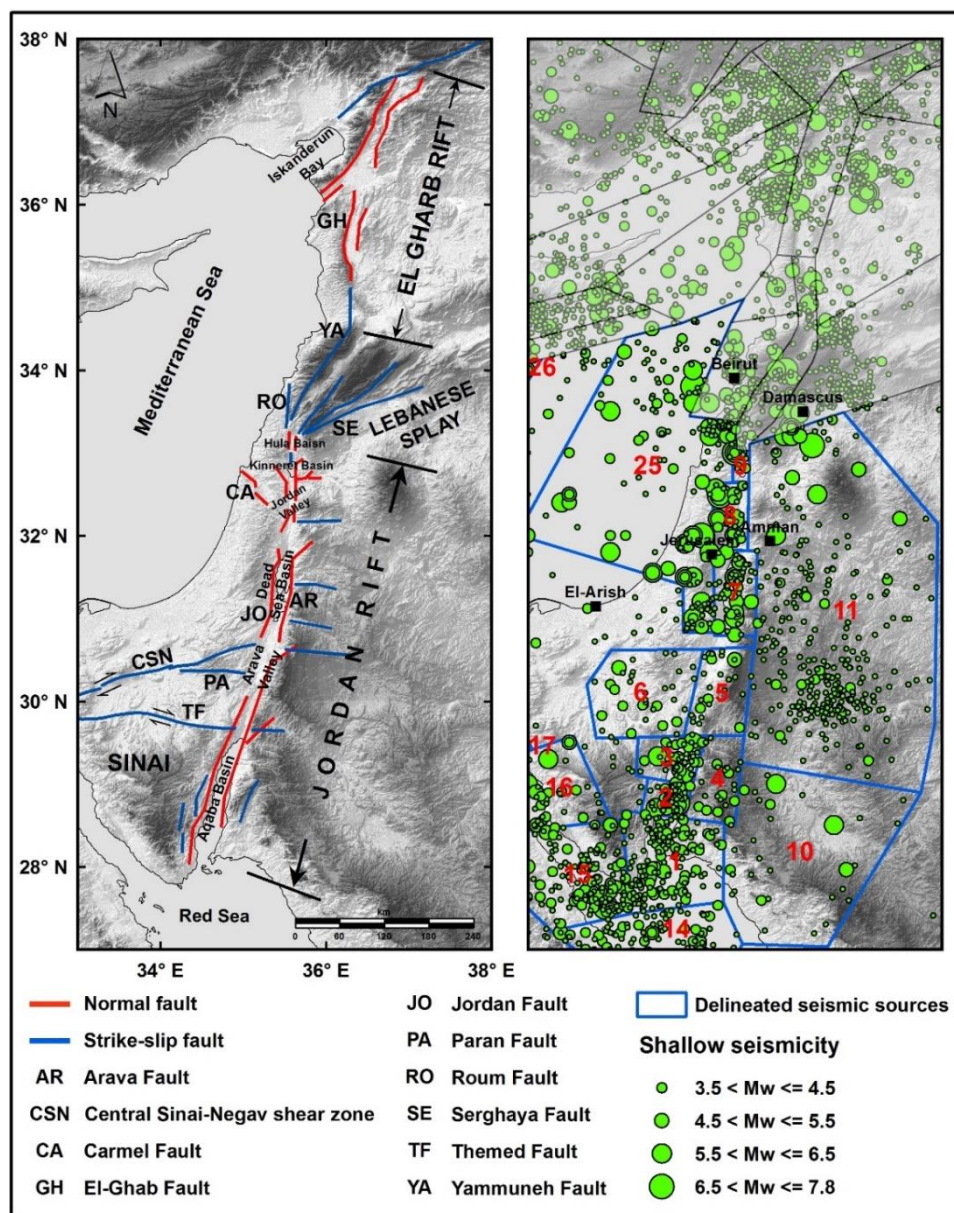


Figure (4-5): The main structural elements (compiled and replotted after Heidbach and Ben-Avraham, 2007), delineated seismic sources and shallow seismicity ($h \leq 35$ km) along the DST.

4.3.1.2 Arava Valley (EG-05) Seismogenic Source

The Arava Valley is located to the north of the Gulf of Aqaba. It is an inter-basin zone trending NE-SW. Its faults extend over 160 km from the Gulf of Aqaba to the Dead Sea, and provide morphological evidence of essentially strike-slip motion (Klinger *et al.*, 2000). It is characterized by a low seismicity level compared with the surrounding area, despite clear indications of recent faulting (Gerson *et al.*, 1993). Klinger *et al.* (2000) emphasized the limited earthquake activity in the Arava Valley

in the instrumental period. Shapira and Jarradat (1995) stated that, from preliminary paleoseismicity studies, the border-faults of Arava Valley can generate earthquakes bigger than magnitude 6.0 with an average return period of 1000-3000 years.

There is no historical earthquakes included in this seismogenic source zone. The biggest recorded event was the m_b 5.2, December 18, 1956 earthquake. Two FMSs are known in the northern part of this source, both of them exhibiting strike-slip faulting with normal component.

4.3.1.3 Eastern Central Sinai (EG-06) Seismogenic Source

An E-W trending dextral strike-slip faults with up to 2.5 km of displacement has been recognized in Central Sinai by Steintz *et al.* (1978). It is called the Themed Fault (Figs. 4-5 and 4-7). The Tih Plateau (in Central Sinai) is traversed by the Themed Fault, which extends for about 200 km from the vicinity of eastern margin of the Suez Rift to the DST (Said, 1990). Themed Fault has been rejuvenated along a pre-existing fault, marking the southernmost edge of the Early Mesozoic passive continental margin of the Eastern Mediterranean Basin in Central Sinai (Moustafa and Khalil, 1995).

To the north of the previous fault, a narrow belt of E to ENE oriented faults separates the Northern Sinai Fold Belt from the Tih Plateau. This narrow fault corresponds to Shata's (1959) hinge belt and Bartov's (1974) Central Sinai-Negev shear zone. This belt separates a tectonically unstable crustal block in Northern Sinai from a tectonically stable crustal block in Central and Southern Sinai (Moustafa and Khalil, 1994).

The EG-06 seismogenic source lies to the west of the previous EG-05 source and to the east of the Sinai Sub-plate. This seismogenic source includes the low seismic activity related to the Themed Fault, Central Sinai-Negav shear zone, Paran Fault and Baraq/Paran Fault junction (Figs. 4-5 and 4-7). This source has a great tectonic effect on Sinai Peninsula and its surrounding areas. There is no historical earthquakes included in this source, being the biggest earthquake located in this zone the m_b 4.8, September 24, 1927 event.

4.3.1.4 Dead Sea Basin (EG-07) Seismogenic Source

The Dead Sea Basin is characterized by a double fault system that is bounded by the Arava Fault from the east, and by the Jordan (Jericho) Fault from the west (Fig. 4-

5), hence it occupies a rhomb-shaped graben between two left-lateral slip faults. The average slip rate on the Dead Sea portion of the transform fault is estimated to be 0.7 cm/yr. (Reches and Hoexter, 1981), which is consistent with the average slip of the overall plate boundary of 0.7-1.0 cm/yr.

Earthquake swarms and a mainshock-aftershock activity characterize this seismogenic source. Trenching studies across the Jordan Fault indicate that two large earthquake swarms occurred since about 2000 years ago. One of them is between 200 B.C.- 200 A.D., while the other one is between 700 A.D.- 900 A.D. (Reches and Hoexter, 1981). El-Isa *et al.* (1984) attributes these swarms to subsurface magmatic activity and/or to the isostatic adjustments along the Gulf of Aqaba.

Several historical earthquakes are included inside this source. They are the 745 B.C., 33 A.D., 1048, 1212, 1293, and 1458 earthquakes. Their assigned intensities are ranging from VII to VIII. Ben-Menahem *et al.* (1976) obtained FMSs for some recent events (e.g., the M_S 4.9, October 8, 1970 earthquake) which took place in the Dead Sea area. All solutions indicate a left-lateral strike-slip movement on a sub-vertical fault striking with an average trend of $N8^\circ-10^\circ E$. However, Salamon *et al.* (2003) also obtained normal FMSs for some relatively recent events. These solutions seem to reflect the activity of the longitudinal N-S striking normal faults that extend along the margins of the Dead Sea Basin that cannot be related to the expected lateral motion along the transform fault. Field observations confirmed this type of activity (Garfunkel *et al.*, 1981; Gardosh *et al.*, 1990).

4.3.1.5 Jordan Valley (EG-08) Seismogenic Source

The Jordan Valley trends in the N-S direction, linking between the Hula Basin to the north and the Dead Sea Basin to the south. The details about its end in the Sea of Galilee are not clear from the surface features (Ben-Menahem *et al.*, 1976). Garfunkel *et al.* (1981) noticed a small amount of compression along the valley and near the Jordan Fault trace. Recent earthquake activity along the Jordan Valley is low compared to the Southern Dead Sea Basin. Ten historical events (before 1900) are included in this area source. They are the 1020 B.C., 578 A.D., 580, 746, 854, 1034, 1105, 1160, 1260, and 1287 events. Their assigned intensities are ranging between IV and XI. The most important earthquake included in this source zone is the I_{max} XI, 746 event.

4.3.1.6 Kineret-Hula Basin (EG-09) Seismogenic Source

To the north of the previous Jordan Valley source are located the Hula (Shamir-Almagor Fault) and Kineret (Kineret-Sheikh Ali Fault) Basins (Heimann, 1990). Seismic activity in these two basins has been recorded up to the NE-bend of the transform at the Yammuneh Fault. Shamir *et al.* (2001) consider this area as a seismogenic step zone lying between the Roum Fault in the west and the Jordan Fault in the east. Three historical events are included in this zone. They are the 19 A.D., 419, and 756 earthquakes. The biggest felt earthquake was the I_{max} X, 19 A.D. event.

4.3.1.7 Northwestern Saudi Arabia (EG-10) Seismicity Source

To the east of the EG-01 and EG-02 seismogenic sources, the Northwestern Saudi Arabia EG-10 source has been considered. This source zone covers disperse and low-magnitude seismicity in the northwestern part of Saudi Arabia. This source zone has been delimited in such way in order to consider its contribution to the seismic hazard in Egypt. Two historical events are reported to occur inside this area source. They are the March 18, 1068, and January 4, 1588 earthquakes, both of them were felt with intensity VIII.

4.3.1.8 Lebanon (EG-11) Seismicity Source

To the north of the previous seismic source and along the eastern boundaries of the EG-04, EG-05, EG-07, EG-08, and EG-09 sources, the Lebanon EG-11 seismicity source has been considered. This area source covers a disperse low-magnitude seismicity in Lebanon and South Syria. Nine historical earthquakes are located inside this area source. The most important among them are the 972, 1159, and 1182 events. Their assigned I_{max} are IX, IX-X, and IX, respectively.

The computed b -value, the annual rate of earthquakes, the approximate completeness periods, the observed recorded maximum magnitude, as well as the computed M_{max} , for the delineated seismic sources along the DST are displayed in Table (4-1).

4.3.2 SEISMIC SOURCES ALONG THE RED SEA RIFT

The Arabian Plate is continuing to rotate away from the African Plate along the Red Sea Rift spreading center. The Red Sea occupies a long and slightly sinuous NW-trending escarpment-bound basin, 250-450 km wide and 1900 km long, between the

uplifted shoulders of the African and Arabian Shields. It is part of a rift system extending from the Gulf of Aden to the northern end of the Gulf of Suez (Fig. 4-1). The overall trend of the rift is N30°W, although a few kinks occur at around 15°N, 18°N, and 22°N.

Table (4-1): *b*-value, annual rate of earthquakes, approximate completeness period, maximum observed and expected magnitude for the delineated seismic source zones along the DST.

Source Zone	<i>b</i> -value	Yearly Number of Earthquakes		Completeness Period (years)		Observed M_{max}/ I_{max}	Expected M_{Wmax}
		Above M_W 4.0	Above M_W 5.0	M_W 4.0	M_W 5.0		
EG-01	1.13 ± 0.05	0.980 ± 0.083		31		m_b 4.4 on 2006/02/02	4.8 ± 0.2 ^A
EG-02	0.98 ± 0.06	0.495 ± 0.064	0.052 ± 0.007	30	63	M_W 7.2 on 1995/11/22	7.2 ± 0.3 ^B
EG-03	0.97 ± 0.07	0.276 ± 0.044	0.030 ± 0.005	31	63	I_{max} 8.5 on 1212/05/02	6.2 ± 0.8 ^A
EG-04	1.01 ± 0.12	0.196 ± 0.039	0.019 ± 0.004	31	36	m_b 4.5 on 1995/12/26	4.6 ± 0.4 ^A
EG-05	0.88 ± 0.06	0.188 ± 0.039	0.025 ± 0.005	30	63	m_b 5.2 on 1956/12/18	7.5 ± 0.5 ^C
EG-06	1.12 ± 0.10	0.185 ± 0.032	0.014 ± 0.002	55	87	m_b 4.8 on 1927/09/24	4.8 ± 0.6 ^A
EG-07	0.87 ± 0.08	0.323 ± 0.047	0.044 ± 0.006	30	100	I_{max} 8.0 on 1458/11/12*	5.8 ± 0.7 ^A
EG-08	0.71 ± 0.02	0.187 ± 0.037	0.037 ± 0.007	30	84	I_{max} 9.0 on 746 A.D.	7.8 ± 0.8 ^A
EG-09	0.91 ± 0.15	0.065 ± 0.027	0.008 ± 0.003	30	67	I_{max} 10.0 on 19 A.D.	6.8 ± 0.6 ^C
EG-10	1.03 ± 0.09	0.193 ± 0.035	0.018 ± 0.003	31	63	I_{max} 8.0 on 1588/01/04*	5.8 ± 0.7 ^A
EG-11	0.97 ± 0.10	0.365 ± 0.063	0.039 ± 0.007	30	90	I_{max} 9.5 on 1159/06/06	6.9 ± 0.8 ^A

(*) The most recent event.

^A Calculated using Robson-Whitlock-Cooke procedure (Kijko and Singh, 2011).

^B Equal to maximum recorded magnitude.

^C Taken from Deif *et al.* (2009, 2011).

The Red Sea can be divided into four distinct zones (Fig. 4-1), each one characterized by different morphology and structure, which appear to represent different stages in the development of a continental margin and the establishment of a mid-ocean ridge spreading system (Cochran, 1983; Cochran *et al.*, 1986). These zones are:

- i. **Active Sea-floor Spreading (Southern Red Sea):** It is located between 15°N and 20°N and characterized by a well-developed axial trough which has developed through normal sea-floor spreading during the last 5 Ma (e.g., Girdler and Styles, 1974; Roeser, 1975) or even older, at about 9–12 Ma (Makris and Rihm, 1991).
- ii. **Transition Zone (Central Red Sea):** It is located between 20° N to about 23° 20' N, where the axial trough becomes discontinuous, in which the Central Red Sea consists of a series of 'deeps' alternating with shallow 'inter-trough zones' (Searle and Ross, 1975). A similar transitional zone may flank the deep axial

trough between the flanking walls of a shallow main trough on both sides of other zones.

- iii. **Late Stage Continental Rifting (Northern Red Sea):** The Northern Red Sea consists of a broad trough without a recognizable spreading center, although there are a number of small isolated “deeps” (Cochran *et al.*, 1986).
- iv. **Active Rifting:** the future line along which the Southern Red Sea is now due to propagate through the Danakil Depression Afar, may either be added to the first zone or considered separately.

Based on the morphological and structural features of the Red Sea, the Egyptian part (to the north of latitude 22°N) can be divided into three distinct seismogenic source zones (EG-12, EG-13, and EG-14) (Fig. 4-6). Each zone represents different stage of development (Cochran and Martinez, 1988). The delineation is made, based upon the occurrence of the transverse structures, change of the fault trend along the axial rift and the variety of the seismic activity along the rift axis.

4.3.2.1 Southern Red Sea (EG-12) Seismogenic Source

The EG-12 Southern Egyptian Red Sea seismogenic source represents the northern part of the transition zone. It is characterized by NW-SE trending faults. The boundary proposed by Bonati (1985), north of latitude 25°N, is found herein to coincide with the NE-trending transform faults and the associated seismicity. Only one historical event, which represents the biggest reported event, is included in this seismic source, the I_{max} VI-VII, 1121 earthquake.

4.3.2.2 Central Red Sea (EG-13) Seismogenic Source

The EG-13 Central Egyptian Red Sea seismogenic source has been delineated to the northwest of the previous zone. It corresponds to the region north of latitude 23°20'N, which consists of a broad main trough without a recognizable spreading center (Cochran *et al.*, 1986). Recent recorded seismicity could indicate the expected location of the axial rift. This is a low and scattered seismicity area, compared to the previous zone. Like the previous zone, there is only one historical event included here. It is the I_{max} V, 1899 earthquake. The maximum observed magnitude along this source corresponds to the m_b 4.7 (M_S 5.1), July 30, 2006 earthquake.

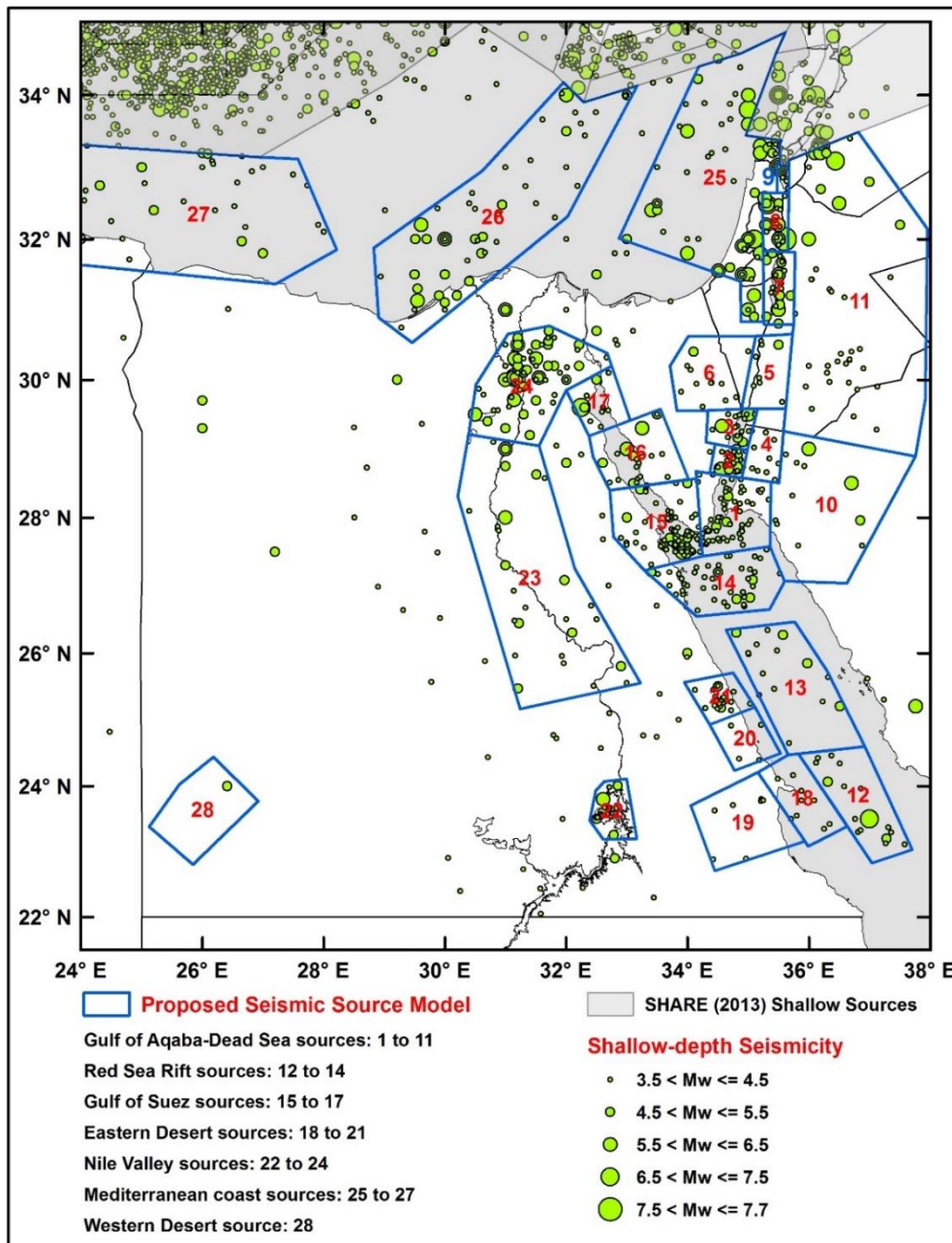


Figure (4-6): Shallow seismicity ($h \leq 35$ km) and delineated seismic sources for the whole Egyptian territory.

4.3.2.3 Northern Red Sea (EG-14) Seismogenic Source

The EG-14 Northern Egyptian Red Sea seismogenic source is characterized by higher seismic activity than the previous two sources. This activity is due to the juncture between the two gulfs. Daggett *et al.* (1986) shows that, the high seismic activity of the Northern Red Sea is different from the activity at the southern part of the Gulf of Suez. For this seismic source, there is no related earthquakes before the year 1900. In addition, the m_b 5.0 (M_S 5.0) March 22, 1952 event represents the biggest recorded earthquake until now.

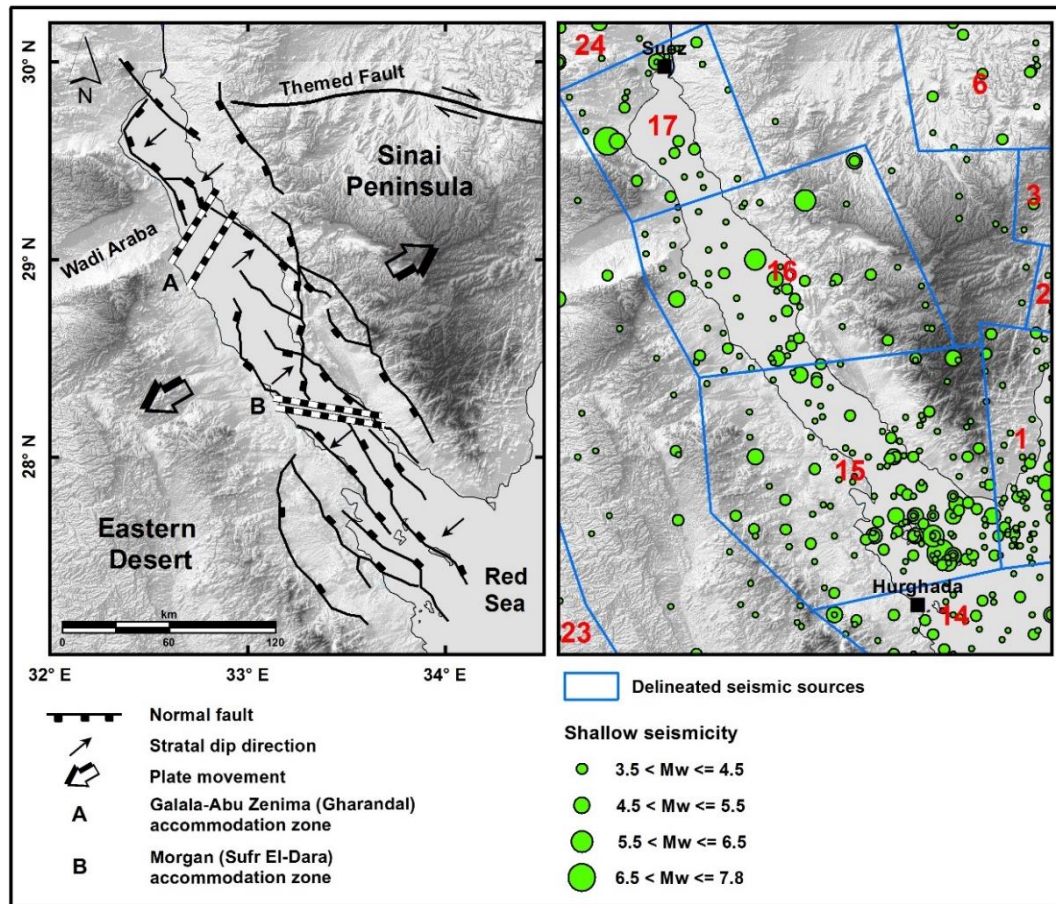


Figure (4-7): Tectonic setting (compiled and modified after Meshref, 1990, and Younes and McClay, 2002), delineated seismic sources and seismicity of the Gulf of Suez.

4.3.3 SEISMIC SOURCES ALONG THE GULF OF SUEZ RIFT

The Gulf of Suez is considered to be the plate boundary between the African Plate and Sinai Sub-plate (McKenzie *et al.*, 1970). It extends along a NW trend from latitude 27°30' N to 30°N. It represents the northern termination of the Red Sea Rift System, which evolved as an arm of the Sinai Triple Junction, together with the Gulf of Aqaba and the Red Sea (e.g., Robson, 1971; Garfunkel and Bartov, 1977; Schlumberger, 1984; Said, 1990; Bosworth and Taviani, 1996).

The Gulf of Suez has been interpreted as being a complex half-graben system (Lyberis, 1988), or an asymmetric graben (Moustafa, 1996). It is composed of three half-grabens with opposite tilt directions which were attributed by Moustafa (1976) to the three transverse dip provinces, including northern, central, and southern parts of the rift. These dip provinces include several rift blocks of consistent dip direction. The dip direction of fault blocks along the direction of the Gulf of Suez Rift, from north to south, changes as: SW to NE and again to SW defining the three half-grabens, respectively.

Two-accommodation zones coexist among these half-grabens (Bosworth, 1985), which extend transversely across the rift (Fig. 4-7). These zones are the Galala-Zenima (Moustafa, 1976) or Gharandal (Moustafa, 1996) accommodation zone, of broad extension (about 60 km wide) in the north, and the Morgan (Moustafa, 1976) or Sufr El Dara (Moustafa and Fouda, 1988) accommodation zone, a relatively narrow zone (20 km wide) in the south. These accommodation zones show a wide range of deformation, including either discrete faults affected by normal-slip, oblique-slip, or strike-slip (Chorowicz and Sorlien, 1992), or wide complex zones of normal faulting, trans-tension or broad warping (Colletta *et al.*, 1988).

The Gulf of Suez was considered to be an aseismic area during the first half of the last century, and this consideration let some researchers (e.g., Mart, 1991) to conclude that all the present motion taking place in the Red Sea Rift is transferred into shearing along the DST. Ben-Menahem (1979) and Salamon *et al.* (1996) studied the seismic activity of the Gulf of Suez Rift. FMSs of the m_b 6.1, March 31, 1969 earthquake, and other low-magnitude earthquakes show that the Gulf of Suez Rift is active, which agree with Ben-Menahem and Aboodi (1971) results.

Considering the tectonic setting, seismicity and earthquake faulting mechanisms, the Gulf of Suez has been divided into three seismogenic sources (Figs. 4-6 and 4-7) as follow.

4.3.3.1 Southern Gulf of Suez (EG-15) Seismogenic Source

The EG-15 Southern Gulf of Suez seismogenic source is distinguished by intensive structural deformation. It is characterized by its relatively high seismic activity. The high rate of seismicity at the southern end of the Gulf of Suez is attributed to the crustal movements among the Arabian Plate, African Plate, and the Sinai Sub-plate. Six historical events are included in this zone. Those are 28 B.C., 955, 1091, 1195, 1778, and 1839 events. Their assigned intensities are ranging from VI-VII to VIII. The most important event occurred inside this area source was the M_W 6.8, March 31, 1969 Shedwan earthquake (Fairhead and Girdler, 1970; Maamoun *et al.*, 1984). This event was preceded by three foreshocks and followed by 17 aftershocks (m_b 4.5-5.2) in the neighborhood of Shedwan Island. Maamoun and El-Khashab (1978) reported 35 foreshocks during the last half of March 1969, preceding the main earthquake. The FMSs of the largest two earthquakes in this source (M_W 6.8, March 31, 1969 and M_W 5.5, June 28, 1972 earthquakes) show normal-faulting

mechanisms with negligible shear component along the NW-trending fault plane, which is in agreement with the main axis of the Gulf of Suez (Jackson and McKenzie, 1984). This is also consistent with the results obtained using waveform inversion techniques (Huang and Solomon, 1987).

4.3.3.2 Central Gulf of Suez (EG-16) Seismogenic Source

The seismic activity in the EG-16 Central Gulf of Suez seismogenic source is relatively low when compared with the previous source. Five historical events are included in this source zone: the 1220 B.C., 1425, 1710, 1814, and 1879 earthquakes. Their assigned intensities are ranging between IV and VII. The most important earthquake located inside this source was the M_S 6.2, March 6, 1900 event.

Abou Elenean (2007) computed some FMSs for earthquakes located in the central part of the gulf, showing generally normal faulting, following the main gulf trend. A few of these events show slight strike-slip component, especially for those events closer to the transfer zones of the three gulf dip provinces (Meshref, 1990). This variation, from a purely normal faulting in the southern part to a mixed (strike-slip and normal) movement, supports the distinction between the southern and middle seismogenic zones in the Gulf of Suez.

4.3.3.3 Northern Gulf of Suez (EG-17) Seismogenic Source

Finally, the EG-17 Northern Gulf of Suez seismogenic source is characterized by its low seismic activity. Two earthquakes have been catalogued, in the current study, before the year 1900. They are the I_{max} VI, 742, and I_{max} V, 1754 earthquakes. Focal mechanism analyses for this seismogenic zone indicate a normal-faulting mechanism. Fault plane solutions computed by Abou Elenean (2007) showed that the events located at the gulf apex show normal faults, generally trending NW-SE to WNW-ESE, and reflect a good agreement with the surface faults crossing the Eastern Desert from the gulf apex towards Cairo.

Abou Elenean (2007) concluded that the FMSs of small to moderate size earthquakes computed by Badawy and Horváth (1999), Badawy (2001) and Salamon *et al.* (2003), show the existence of few thrust-faulting mechanisms along the Gulf of Suez trend. The author argues that these unexpected mechanisms could be due to the lack of local stations, with clear polarities, at that time. On the other hand, borehole

breakouts analyses performed by Badawy (2001) show a different stress direction, inconsistent with the NE-SW tension direction estimated from earthquake FMSs.

The computed b -value, the annual rate of earthquakes, the approximate completeness periods, the observed maximum magnitude, as well as the computed M_{max} for the delineated seismic sources along the Gulf of Suez-Red Sea Rift are displayed in Table (4-2).

Table (4-2): b -value, annual rate of earthquakes, approximate completeness period, maximum observed and expected magnitude for the delineated seismic source zones along the Gulf of Suez-Red Sea Rift.

Source Zone	b -value	Yearly Number of Earthquakes		Completeness Period (years)		Observed M_{max}/ I_{max}	Expected M_{Wmax}
		Above M_w 4.0	Above M_w 5.0	M_w 4.0	M_w 5.0		
EG-12	1.00 ± 0.05	0.436 ± 0.059	0.043 ± 0.006	40	63	I_{max} 6.5 on 1121 A.D.	6.8 ± 0.6^B
EG-13	0.91 ± 0.06	0.303 ± 0.044	0.038 ± 0.005	30	105	m_b 4.7 on 2006/07/30	5.6 ± 0.3^A
EG-14	1.13 ± 0.07	0.643 ± 0.061	0.047 ± 0.005	40	108	m_b 5.0 on 1952/03/22	5.4 ± 0.6^A
EG-15	1.06 ± 0.04	0.835 ± 0.079	0.072 ± 0.007	40	63	M_w 6.8 on 1969/03/31	6.8 ± 0.3^B
EG-16	0.80 ± 0.06	0.309 ± 0.040	0.049 ± 0.006	30	67	M_S 6.2 on 1900/03/06	6.3 ± 0.6^A
EG-17	0.86 ± 0.08	0.138 ± 0.029	0.019 ± 0.004	40	62	M_S 6.6 on 1754 A.D.*	6.6 ± 0.6^B

(*) Macroseismic M_S magnitude (after Ambraseys *et al.*, 1994).

^A Calculated using Robson-Whitlock-Cooke procedure (Kijko and Singh, 2011).

^B Equal to maximum recorded magnitude.

4.3.4 SEISMIC SOURCES IN THE EGYPTIAN EASTERN DESERT

The Eastern Desert of Egypt, structurally, is part of the Arabian-Nubian Shield. It lies within the fold and thrust belt of the Pan-African continental margin (El-Gaby, 1983). Stern and Hedge (1985) divided the Eastern Desert Belt into three structural domains (Figs. 4-3 and 4-8): northern, central and southern. These domains are separated by two major faults: i) the Safaga-Qena zone, extending from Safaga to Qena, and ii) the Marsa Alam-Aswan fault zone. The Eastern Desert is characterized by E-W trending faults in its southern part, which changes to ENE-WSW in the middle one, near to the Hurghada city. Further to the north, towards the Cairo-Suez District, the main fault trend becomes in the E-W direction (Fig. 4-3).

However, Youssef (1968) classified the main tectonic structures developed in the Eastern Desert into three main groups: i) a set of normal faults trending NW-SE, nearly parallel the Gulf of Suez-Red Sea trend, ii) a set of fault systems trending NE-SW, nearly parallel to the Gulf of Aqaba trend (these two trends of faulting are assumed to be two complementary sets of shear fractures produced by a $N10^\circ W - S10^\circ E$ oriented stress (Said, 1990), and iii) a set of fault system trending nearly in the

E-W direction. In addition, there are many simple and open folds with a NW-SE trend and low plunges.

Deif *et al.* (2011) quote that the relationship between the earthquake activity in the Eastern Desert and the causal structures is not fully understood, due to the lack of geological and geophysical studies in this region. Furthermore, Kebeasy (1990) and Badawy (1999) mentioned that there is no historical earthquakes have been reported in this region, which coincides with the current study. The following seismogenic sources have been identified (Figs. 4-3 and 4-8).

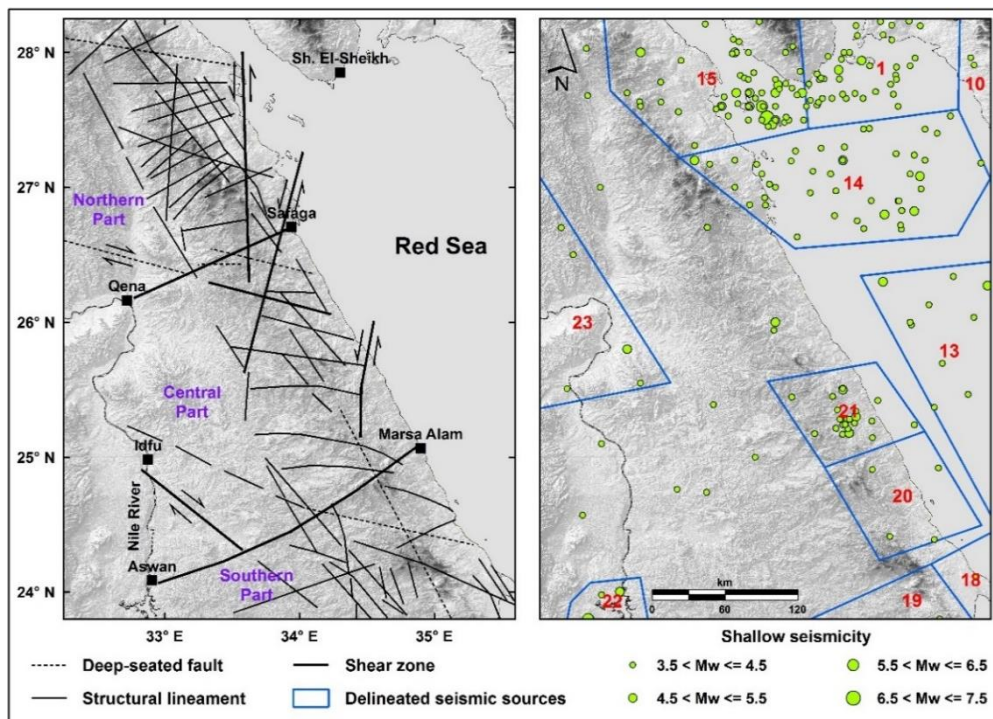


Figure (4-8): Tectonic setting (modified after El-Rakaiby, 1989), delineated seismic sources and seismicity of the Egyptian Eastern Desert.

4.3.4.1 Western Red Sea Coast (EG-18) Seismicity Source

In addition to the Red Sea seismogenic sources mentioned above, there are some earthquakes located in the region which extends to the west, from the EG-12 Southern Egyptian Red Sea source till the western coast of the Red Sea. This activity may be related to the block adjustment in this region or to some ocean floor spreading. This source is characterized by a low seismic activity. The biggest recorded earthquake was the M_L 4.5, May 23, 1990 earthquake.

4.3.4.2 Southern Eastern Desert (EG-19) Seismicity Source

This seismicity source exhibit a low seismic activity rate in comparison to the adjacent Red Sea seismic sources. There are no FMSs for earthquake events inside

this area source. The M_L 4.4, July 15, 1991 earthquake was the biggest recorded event in this zone.

4.3.4.3 Southern Abu Dabbab (EG-20) Seismicity Source

Considering the observed changes both in the seismicity rate and distribution, another seismicity source (EG-20) has been considered to the north of the previous one. The same as the previous, there is no FMSs in this source. The biggest recorded event was the M_L 4.7, January 21, 1982 earthquake.

4.3.4.4 Abu Dabbab (EG-21) Seismicity Source

The Abu Dabbab region is located in the central part of the Eastern Desert of Egypt. The moderate seismic activity and extremely tight clustering of low-magnitude earthquakes at Abu Dabbab suggests that the seismicity in this area is not directly related to regional tectonics. One possible explanation is that it could be related to magmatic intrusions into the Pre-Cambrian crust, but there is no direct evidence to support this hypothesis (Daggett *et al.*, 1986).

The most important event included inside this area source is the M_S 5.3, November 12, 1955 earthquake. This event was felt in Upper Egypt in Aswan and Qena cities, and as far as Cairo, but no damage was reported. Its FMS is normal and strike-slip faulting components produced by a NNW minimum compressive stress and a NE maximum compressive stress. Fault planes strike roughly E-W or N-S to NE-SW. Another important event related to this area is the M_W 5.1, July 2, 1984 earthquake, which was felt strongly in Aswan, Qena and Quseir. A large number of foreshocks and a huge sequence of aftershocks were recorded.

4.3.5 SEISMIC SOURCES AROUND NASSER'S LAKE, NILE VALLEY AND CAIRO-SUEZ DISTRICT

Considering the seismicity, and the structural and tectonic setting of the Nile Valley, the following seismic sources have been delineated in the current study taking into account the distribution of the historical and instrumental earthquakes.

4.3.5.1 Southern Aswan (EG-22) Seismogenic Source

Faults around the Aswan region, according to their behavior, were grouped into three categories (WCC, 1985):

- i. E-W trending faults (Fig. 4-9), as the Kalabsha and Seiyal Faults, which lay to the west of Nasser's Lake. The Kalabsha Fault is a right-lateral strike-slip fault with closely related traces extending 185 km. The slip rate of the Kalabsha Fault is estimated to be 0.028 mm/yr, and the Seiyal Fault has a similar behavior like the previous one (WCC, 1985).
- ii. N-S trending faults (Fig. 4-9), which can be subdivided into two main sets. The first set lies to the NW of Nasser's Lake and consists of three faults: the Gebel El-Barqa, the Kurkur and the Khur El-Ramla Faults. Both of the Gebel El-Barqa and the Kurkur Faults are left-lateral strike-slip faults, the first one has a total length of 110 km. The Khur El-Ramla Fault is 36 km length, without direct evidence of its sense of motion. The second set of faults lies to the SW of Nasser's Lake, consisting mainly of two faults: the Abu Dirwa and the Ghazala Faults. The Abu Dirwa Fault is a 20 km long left-lateral strike-slip fault. In addition, for the Ghazala Fault, the analysis of its geomorphic expression shows no active features.
- iii. The third category comprises a fault system trending NNE-SSW (Fig. 4-9) lying to the east of Nasser's Lake. The Dabud Fault, which represents the main fault of this group, is about 36 km length. Geological evidences indicate reverse-slip, opposed to the tectonic setting of the area.

In addition to the previous fault systems, three faults are identified at the High Dam site (the Powerhouse, the Spillway and the Channel Faults). Mostly evidence of the presence of these faults is hidden under the concrete and the water of the Aswan High Dam and Nasser's Lake. These three faults show no evidence of being active in the Quaternary, and are considered as inactive with no significant hazard to the Aswan area (WCC, 1985).

Ambraseys *et al.* (1994) showed no historical earthquakes in this source, while Maamoun *et al.* (1984) showed two historical earthquakes with epicentral intensity VII, almost at the same location of the M_w 5.8, November 14, 1981 earthquake. These two events occurred in 1210 B.C. and in 1854.

After the occurrence of the M_w 5.8, November 14, 1981 earthquake, WCC (1985) studied the aerial photographs of the surrounding area, its tectonic and geological setting, and the seismicity from December 1981 to July 1982. They excavated many trenches at different sites, and found much evidence for successive paleo-earthquakes on some of the previously mentioned faults. They concluded that

the area, at present, has a low seismic activity. Deif *et al.* (2011) mentioned that seismicity around the Aswan area shows a close association with the present faults, with noticeable increase at the intersection of the N-S and E-W faults or at their tips. Also, this activity is limited primarily to the upper 25 km of the earth's crust.

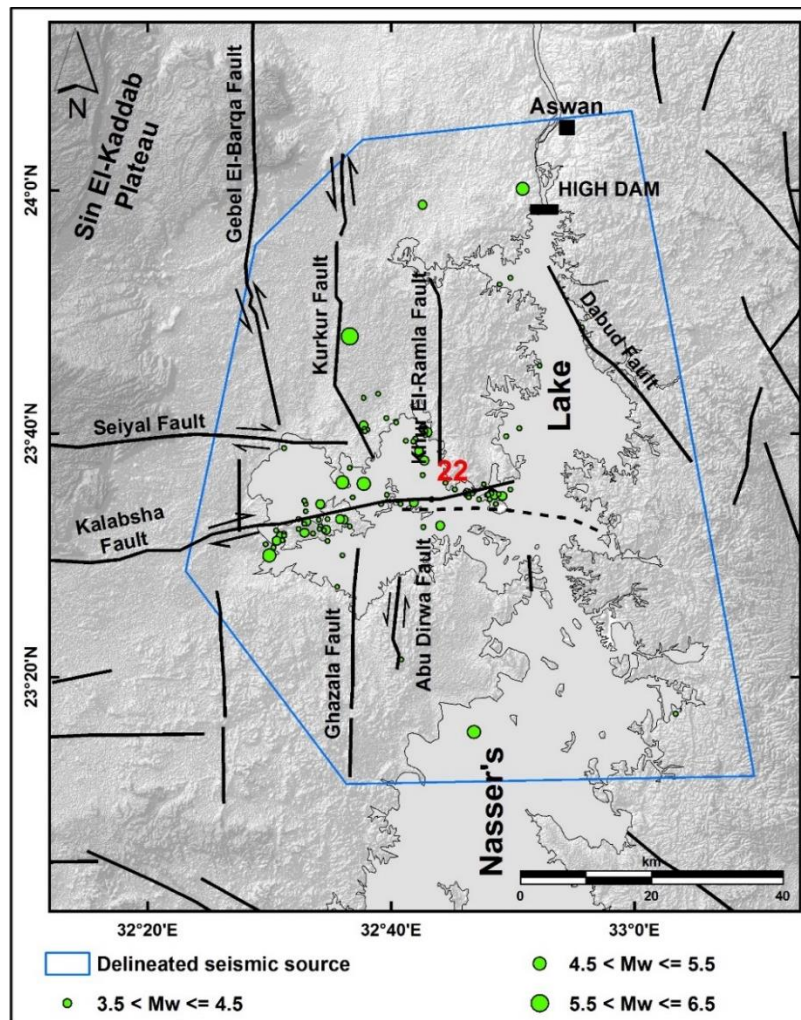


Figure (4-9): Geological and tectonic features (replotted after WCC, 1985), delineated seismic source and seismicity around Nasser's Lake.

Many seismic hazard studies have been carried out in the Aswan area and its surroundings due to its importance and neighborhood to the High Dam (e.g., Fat-Helbary and Ohta, 1996; Deif *et al.*, 2011). Three alternative seismotectonic models for Aswan area have been considered in these studies. The first model consider the Aswan area as one seismotectonic model, while the second one is subdividing the region into six seismotectonic provinces. The third one is based on the defined active faults and its associated seismic activities.

However, in the current work, the Aswan region and its surroundings is considered as only one seismic source zone (Figs. 4-6 and 4-8). The main earthquake

that took place inside this area was the M_W 5.8, November 14, 1981 event. This earthquake occurred in the Nubian Desert of Aswan. Its effects were strongly felt up to Assiut city, as well as to Khartoum. Several cracks on the western bank of the Nasser's Lake, and several rock-falls and minor cracks on the eastern bank, were reported. The largest one of these cracks was about one meter in width and 20 km in length. This earthquake was preceded by three foreshocks and followed by a large number of aftershocks. The focal depth of this earthquake was estimated to be 25 km. The composite FMS of this event indicates a nearly pure strike-slip faulting with a normal-fault component (Fat-Helbary *et al.*, 2008).

4.3.5.2 Luxor- Southern Beni Suef (EG-23) Seismogenic Source

The Nile Valley is a large elongated Oligo-Miocene rift, trending N-S as an echo of the Red Sea rifting. The origin of the Nile Valley has been a subject of controversy. Beadnell (1901) and Sandford (1934) advocated that the Nile Valley has an erosional origin. On the other hand, many authors (e.g., Said, 1990; Meshref, 1990) considered a tectonic origin. This is supported by the fault scarps bordering the cliffs of the Nile Valley, the numerous faults recognized on its sides (Said, 1990) and the focal mechanisms of the most recent earthquakes.

From the structural point of view, the faults and joints are the most deformational features observed at the cliffs bordering the Nile stream (Said, 1990). These faults have different directions (Fig. 4-3). The most abundant are the NW-SE and NNW-SSE trends, while others (less abundant) exhibit the WNW-ESE, ENE-WSW and NE-SW directions. Most of the major valleys, at the east of the Nile River, are generated and controlled in a more or less degree by these faults.

To the north of Aswan area, in the region between Luxor and Southern Beni Suef, along the Nile River, there is a low seismicity level, which nearly coincides with the main trend of the Nile River. This active area has been considered as a separate seismogenic source. Several historical earthquakes are reported to occur along the Nile River in this area source that may be due to the high population density along it in the ancient times. These earthquakes are the 600 B.C., 27 B.C., 857, 967, 997, 1264, 1299, 1694, 1778, and 1850 events. Their intensities are ranging from V to VIII. FMSs exhibit reverse-faulting mechanism to the west of the Nile River, in the area between Luxor and Assiut. However, normal-faulting mechanism with strike-slip component appears to the north of Assiut till Beni Suef city.

4.3.5.3 Beni Suef – Cairo – Suez District (EG-24) Seismogenic Source

To the north of the previous zone, and to the west of the Gulf of Suez, there is a moderate seismic activity between Beni Suef and Cairo, on the River Nile, till Suez, on the apex of the Gulf of Suez (Fig. 4-6). The Cairo-Suez district is affected by three fault trends (Fig. 4-3): one of them is the E-W trend, mostly pronounced and almost aligned by latitude 30°N , and where the other two trends (ENE and NW) are spatially more dispersed. The faults are predominantly normal, and have produced a series of fault blocks with a large strike-slip component (Abdel-Rahman and El-Etr, 1978).

Field observations, satellite images, aerial photographs and seismic profiles confirm that the region between Cairo and Suez is active from a tectonic point of view (Abdel-Rahman *et al.*, 2009). Active spots on this belt lie at Wadi Hagul and Abu Hammad. The epicentral distribution along this area is very diffuse, and cannot be attributed specifically to any of the known faults. This disperse seismicity yields a difficulty in delineating seismic zones. It is assumed that the seismic potential is uniform throughout the zone, although this is not entirely clear.

Sixty-one historical earthquakes are included in this area source. The most important among them are the 935, 1111, 1259, 1262, 1303, and 1588 events. Moreover, the most important instrumental earthquake recorded in this source was the M_s 5.9, October 12, 1992 event. Its epicenter was located about 40 km southwest of Cairo, in Dahshour. It caused a disproportional damage (estimated at more than L.E. 500 million), and the loss of many lives. The shock was strongly felt, and caused sporadic damage and life loss in the Nile Delta, around Zagazig. Damage extended throughout Fayoum and as far as Southern Beni Suef and Minia. The area mostly affected was Cairo, in particular the old sections of Cairo, Bulaq and the region to the south, along the western bank of the Nile to Gerza (Jirza) and El-Rouda. In all, 350 buildings collapsed completely and 9000 were irreparably damaged, killing 545 persons and injuring 6512. Many of the casualties in Cairo were victims of panic-stricken stampedes of pupils rushing out of schools. About 350 schools and 216 mosques were ruined and there was about 50000 homeless (El-Sayed *et al.*, 1994; Abou Elenean *et al.*, 2000).

Abdel Tawab *et al.* (1993) studied the surface tectonic features of the area around Dahshour and Kom El-Hawa, and found a major $\text{N}55^{\circ}\text{E}$ trending normal fault at Kom El-Hawa (800 m length of surface trace with a vertical displacement of 40 cm)

and a major E-W trending open fracture at Dahshour area (1200 m in length). Maamoun *et al.* (1993) concluded that, most of the surface lineaments recorded after the occurrence of the main shocks are trending E-W to NW-SE. Abou Elenean (1997) studied the FMSs for some earthquakes in Dahshour area, and found normal faulting with a large strike-slip component. The first nodal plane is trending nearly E-W, showing coincidence with the surface lineaments that appeared directly after the occurrence of the M_S 5.9, October 12, 1992 earthquake.

In addition to the previous earthquake, there were three important earthquakes located inside this source zone. One of them located to the southwest of Suez. It was the m_b 4.9 (M_S 4.8), March 29, 1984 Wadi Hagul earthquake. It is strongly felt in Suez, Ismailia and Cairo. A large number of aftershocks were recorded by nearby temporary stations. The second earthquake was located to northeast of Cairo. It was the m_b 4.8, April 29, 1974 Abu Hammad earthquake. It was strongly felt in Lower Egypt (Nile Delta) and Southwest Israel. The last important earthquake was the m_b 5.0, January 2, 1987 Ismailia earthquake.

Mousa (1989) and Hassib (1990) computed two nodal planes trending ENE-WSW and NNW-SSE, with left-lateral strike-slip motion along the second plane, for the Abu Hammad event. They computed the same strike-slip with reverse component for the Wadi-Hagul earthquake. In addition, the mechanism of the Ismailia earthquake shows also strike-slip movement with two nodal planes trending $N68^\circ E$ and $S24^\circ E$, with steep dip angles (each of them is 80°) (Megahed and Dessoky, 1988).

4.3.6 SEISMIC SOURCES ALONG THE MEDITERRANEAN COASTAL LINE

The Mediterranean coastal area is characterized by small to moderate seismicity. This area is located at the southeastern part of the Mediterranean Sea. It separates between the high seismic activity along the DST and the seismicity of the Mediterranean Sea (Hellenic and Cyprian Arcs). Moreover, it separates the Southern Cyprus seismic activity from the Northern Egypt activity. Hence, this area has been divided into three seismogenic sources (Fig. 4-6), based mainly on the available FMS data and the seismic activity.

4.3.6.1 Eastern Mediterranean Coast (EG-25) Seismicity Source

This area source is parallel to the eastern coastal line of the Mediterranean Sea. It is located to the west of the previous quoted sources EG-07, EG-08, and EG-09, and to the southeast of Cyprus. It includes all the seismicity located to the west of the DST, and those earthquakes are not related with the Cyprian Arc. Twenty-nine historical events are included inside this area source. The most important event among them are the 590 B.C., 525 B.C., 12 B.C., 306, 332, 551, 1269, and 1546 earthquakes.

4.3.6.2 Northern Delta (EG-26) Seismicity Source

This source is located to the northwest of the Nile Delta region. It extends from Alexandria towards the Mediterranean Sea in NE direction. Twenty-three historical events are included inside this large area source, among them the 796, 951, 955, 956, 1303, 1341, and 1375 earthquakes. Moreover, the m_b 6.5 (M_S 6.8), September 12, 1955 Alexandria earthquake, represents the most important recorded event inside this source. This earthquake was felt in the entire Eastern Mediterranean Basin. In Egypt, it was strongly felt, and led to the loss of 22 lives and few damage in the Nile Delta, between Alexandria and Cairo (Kebeasy, 1990). The destruction of more than 300 buildings of old brick construction was reported in Rosetta, Idku, Damanhour, Mohmoudya and Abu-Hommos. A maximum intensity of VII was assigned to a limited area in the Behira province.

Mostly of the FMSs data inside this area source reflects reverse-faulting mechanism with, sometimes, strike-slip component, with the exception of one earthquake, showing a strike-slip motion with a notable normal component (the M_W 4.5, April 9, 1987 event).

4.3.6.3 Western Mediterranean Coast (EG-27) Seismicity Source

The Western Egyptian Mediterranean Coastal zone is located to the north of the Egyptian-Libyan boundary. Only two historical events were reported inside this source: the I_{max} VIII, 262, and I_{max} VI, 1537 earthquakes. However, the most important recorded one was the M_W 5.5, May 28, 1998 Ras El-Hekma event. This earthquake was widely felt in Northern Egypt. A felt intensity equals to VII was assigned at Ras El- Hekma village (~300 km west of Alexandria), and V–VI at Alexandria. Ground fissures trending NW–SE were observed along the beach. Some cracks were also observed in concrete buildings (Hassoup and Tealeb, 2000).

Recent studies concerning the crustal structure and FMS of the M_W 5.5, May 28, 1998 Ras El-Hekma earthquake suggest that this source is an extension of the compressional stress from the Southeastern Hellenic Arc. This compressional stress reactivated old Triassic normal faults as reverse faults, or reverse faults with strike-slip component. This activity coincides with the hinge zone geometry proposed by Kebeasy (1990). Mostly of the FMS data indicate reverse faulting with some strike-slip component.

4.3.7 SEISMIC SOURCES OF THE WESTERN DESERT

4.3.7.1 El-Gilf El-Kebeir (EG-28) Seismogenic Source

Issawi (1978) studied the geology of El-Gilf El-Kebeir region, and concluded that the area is affected by three main faults (Fig. 4-3). The first one is the Gilf Fault, which strikes N-S for a distance of 150 km inside Egypt. Its extension in Sudan is unknown and its northward extension is not traced. The second one is the Kemal Fault, which limits the northwestern side of the Gilf Plateau. It is striking NW-SE and intersects the Gilf Fault at its northern end. The third one is the Tarfawi Fault, which has the same trend, similar to the Gilf Fault. Its length, in Egypt, is 220 km, but it also extends inside Sudan. The author interpreted the first and the third faults as normal ones.

The only recorded earthquake in this area source (above M_W 4.0) was the m_b 5.3 (M_L 5.7), December 9, 1978 El-Gilf El-Kebeir earthquake. It has a reverse-faulting mechanism. Riad and Hosney (1992) studied its FMS and concluded that, a shear direction did exist in the basement rocks of the southern part of the Western Desert, and it is explained as due to a compressional stress resulting from the spreading of the Red Sea. Its focal planes show that the P-axis is almost perpendicular to the Red Sea spreading axis. The authors concluded that the Gilf Plateau is probably divided into two parts by a fault striking nearly E-W. Other authors (e.g., Talwani and Rajendrank, 1991) pointed out that this activity is linked to the pre-existing weak zones, while, Abou Elenean (1997) linked such an intraplate activity to the intersection of more than one local fault.

In our present study, the El-Gilf El-Kebeir (EG-28) seismogenic source is an area source which includes the above mentioned recorded earthquake as well as the previously quoted faults in this region. While some historical earthquakes are ignored (e.g., events located in the Western Desert) during the delimitation of the nearby

seismic sources, due to the significant uncertainty in their locations, it was necessary considering this recent recorded event (M_L 5.7, December 9, 1978 El-Gilf El-Kebeir earthquake) together with the possible causative faults (Issawi, 1978) in a separate seismic source.

The computed b -value, the annual rate of earthquakes, the approximate completeness periods, the observed recorded maximum magnitude, as well as the computed M_{max} , for the delineated seismic sources of the Eastern Desert, along the Nile Valley, along the Mediterranean coastal line, and for the Western Desert are displayed in Table (4-3).

Table (4-3): b -value, annual rate of earthquakes, approximate completeness period, maximum observed and expected magnitude for the delineated seismic source zones of the Eastern Desert of Egypt, along the Nile Valley, and along the Mediterranean coastal line.

Source Zone	b -value	Yearly Number of Earthquakes		Completeness Period (years)		Observed M_{max}/I_{max}	Expected M_{Wmax}
		Above M_W 4.0	Above M_W 5.0	M_W 4.0	M_W 5.0		
EG-18	1.29 ± 0.01	0.157 ± 0.025	0.008 ± 0.001	27		M_L 4.5 on 1990/05/23	4.2 ± 0.4^A
EG-19	1.15 ± 0.03	0.118 ± 0.022		32		M_L 3.9 on 1991/07/15	4.2 ± 0.4^B
EG-20	1.20 ± 0.00	0.063 ± 0.016	0.004 ± 0.001	32		M_L 4.7 on 1982/01/21	4.4 ± 0.3^A
EG-21	0.87 ± 0.09	0.371 ± 0.042	0.050 ± 0.006	32	63	m_b 6.2 on 1955/11/12	5.7 ± 0.6^A
EG-22	0.79 ± 0.07	0.586 ± 0.060	0.095 ± 0.010	31	63	M_W 5.8 on 1981/11/14	7.0 ± 0.4^C
EG-23	0.73 ± 0.05	0.295 ± 0.051	0.055 ± 0.009	40	63	I_{max} 8.0 on 857 A.D.	6.1 ± 0.7^A
EG-24	0.99 ± 0.06	0.596 ± 0.076	0.061 ± 0.008	30	63	I_{max} 9.5 on 1262 A.D.	6.8 ± 0.8^A
EG-25	0.97 ± 0.08	0.520 ± 0.044	0.055 ± 0.005	35	65	I_{max} 10.0 on 1546/01/14	7.2 ± 0.8^A
EG-26	0.94 ± 0.07	0.598 ± 0.085	0.069 ± 0.010	25	63	m_b 6.5 on 1955/09/12	6.6 ± 0.6^A
EG-27	0.60 ± 0.03	0.713 ± 0.102	0.179 ± 0.026	33	63	I_{max} 8.0 on 262 A.D.	6.0 ± 0.8^A
EG-28	1.00 ± 0.06	0.150 ± 0.050				M_S 5.3 on 1978/12/09	5.3 ± 0.3^B

^A Calculated using Robson-Whitlock-Cooke procedure (Kijko and Singh, 2011).

^B Equal to maximum recorded magnitude.

^C Taken from Deif *et al.* (2009, 2011).

4.4 EASTERN MEDITERRANEAN REGION SEISMIC SOURCES

The Mediterranean region is characterized by a very complex tectonics that can be generally described in the context of the collision between the Eurasian and African Plates (e.g., McKenzie, 1972; Jackson and McKenzie, 1984; Westaway, 1994; Ambraseys and Jackson, 1998; McClusky *et al.*, 2000). It can be divided into western, central, and eastern basins.

The EMR, which defines the region lying between the Caspian Sea and the Adriatic Sea through Caucasus, Anatolia, Aegean Sea and Greece, is one of the world's most seismically active regions. Recent tectonics has been studied intensely in

the last four decades. These studies reflect a highly complicated tectonic setting of the EMR.

It is characterized by two main seismic regions: the Hellenic and Cyprian Arcs (Fig. 4-10). The Cyprian Arc has a similar geometry to the Hellenic Arc and the two are often compared (e.g., Papazachos and Papaioannou, 1999). However, the well-determined plate motion in the EMR and the observed seismicity, suggest that the two arcs are subjected to a very different tectonic activity. The convergence across the Hellenic Arc is 20–40 mm/yr., about two to three times faster than across the Cyprian Arc. This higher displacement rate yields a significantly higher level of seismicity and at much deeper levels (up to 300 km).

In the following, a brief description of both considered shallow-depth and delineated intermediate-depth seismic sources which proposed in the current seismic source model to cover the seismicity in the EMR.

4.4.1 SHARE (2013) SHALLOW SEISMIC SOURCES ($h \leq 20$ km)

From 2009 to 2013, the Seismic Hazard Harmonization in Europe project (SHARE, 2013) worked to provide an updated state-of-the-art time-independent seismic hazard model covering Europe and Turkey, envisioned to serve as a reference model for the revision of the European seismic regulations for building design, EC (Eurocode 8: 2004), which came into force in 2010. The EU-FP7 European Commission Project (SHARE), in addition, sharing its results to the Global Earthquake Model (GEM, www.globalquakemodel.org), a public/private partnership initiated and approved by the Global Science Forum of the OECD- GSF, aiming at provide a uniform hazard and risk model around the globe.

The Euro-Mediterranean area is complex, from a seismotectonic point of view. The plate boundary between Africa and Europe runs roughly west to east from the Mid-Atlantic ridge to Eastern Turkey with different mechanisms including continental collision, subduction, and transcurrent movement. Moving away from the plate boundary, the stable continental regions are also locally rather active.

SHARE inherits knowledge from national, regional and site-specific PSHAs, assessed new data, assembled the data in a homogeneous fashion, and built comprehensive relevant hazard databases. In the framework of this project, the establishment of a seismic source model for Europe and the surrounding areas was

considered. This model is built upon the available local and regional models as well as newly defined source zones. It has been developed during eight separate workshops by the SHARE consortium. Almost 80 experts from 28 countries from the informed European-Mediterranean seismological community have participated in establish the zonation model.

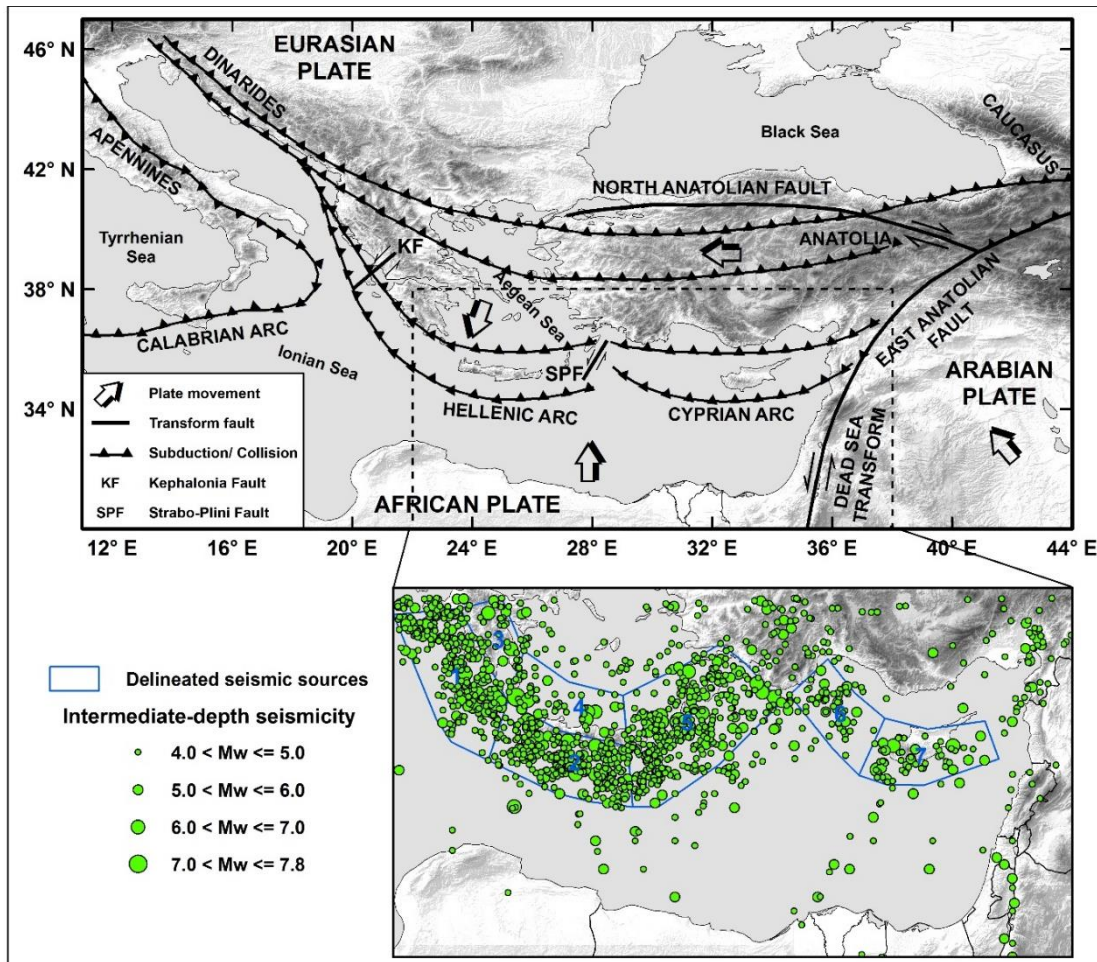


Figure (4-10): Tectonic map (after Ziegler, 2001; Meulenkamp *et al.*, 1988; Dewey *et al.*, 1989), intermediate-depth seismicity ($20 \leq h \leq 100$ km) and delineated seismic source zones for the EMR.

The principle for seismic source zones is that they represent enclosed areas within which, a uniform seismicity distribution and M_{max} are expected. Background sources have been avoided in the sense that all areas have been covered by seismic sources, even very low seismicity areas. The principles along which seismic source zones in the current model have been constructed are based on information from geological structures on different scales, tectonics and seismicity.

Seismicity also follows these structures well, e.g., as can be seen along the North Anatolian Fault, the Gulf of Corinth and the Hellenic Arc. The use of fault source information has also been done in the delineation of the source zones,

especially in the case of the foundation of the sources for Balkans, Greece and Turkey, Italy and Portugal. b -values, annual activity rates, and M_{max} were computed using different approaches and included in the SHARE project database (www.share-eu.org) (Woessner *et al.*, 2012).

In the current study, 53 shallow seismogenic sources ($h \leq 20$ km) from the SHARE source model (Fig. 4-4), were considered to the north of Egypt, until latitude 38°N , and covering Greece and Turkey regions. Some of the events located at this region were felt and caused few damages in the northern part of Egypt (e.g., the I_{max} VIII, August 8, 1303 offshore Mediterranean earthquake, the I_{max} VI, February 13, 1756 and the M_S 7.4, June 26, 1926 Hellenic Arc earthquakes, the M_W 6.8, October 9, 1996 Cyprus earthquake, and the M_S 6.4, October 12, 2013 Crete earthquake). Thus, these source zones are expected to contribute to the seismic hazard in Northern Egypt.

The model in the Greek and Cyprian area build to a large extent upon the previous works of Papiouannou and Papazachos (2000) and Papiouannou (2001). The Turkish model (Demircioglu *et al.*, 2007; Demircioglu, 2010) is provided as a cooperation between the EMME (2013) project and SHARE. The Turkish model is further a hybrid model, in the sense that the area sources have been delineated with respect to the main faults, like the North and East Anatolian Faults.

4.4.2 INTERMEDIATE-DEPTH SEISMIC SOURCES ($20 \leq h \leq 100$ km)

Intermediate-focal depth earthquakes also occur in the EMR (Southern Greece and Turkey) and their foci define a Benioff zone of stair shape which dips from the convex side of the Cyprian and the Hellenic Arcs to its concave side, that is, from the EMR to the Greek and Turkish lands (Papazachos and Comninakis 1971; Comninakis and Papazachos 1980). Some of these earthquakes are moderate to large earthquakes, and constitute a seismic threat for the whole Mediterranean area, including Northern Egypt. Since, because of their magnitudes and focal depths, these earthquakes produce seismic waves of large amplitude and period which travel with low attenuation (Papazachos *et al.* 1985). Therefore, these earthquakes can contribute to the seismic hazard of Northern Egypt.

As mentioned before, the SHARE (2013) project considered a seismogenic depth of 20 km for the shallow seismicity in the EMR. So, it was very important to define intermediate-depth seismic sources to include the seismicity below this depth. Thus, in our work, intermediate-depth sources for earthquakes having focal depths

ranging from 20 km to 100 km have been delineated. Below this depth (100 km) and considering the large distance of the subducting plate from Egypt, earthquake events have no contribution to the Egyptian seismic hazard. Seven intermediate-depth source zones have been considered in the Hellenic and Cyprian subduction zones to cover the intermediate seismicity ($20 \leq h \leq 100$ km) (Fig. 4-10). The zoning was based on the seismicity distribution and the tectonic setting of the region.

The computed b -value, the annual rate of earthquakes, the approximate completeness periods, the observed recorded maximum magnitude, as well as the computed M_{max} , for the delineated intermediate-depth seismic sources are displayed in Table (4-4).

Table (4-4): b -value, annual rate of earthquakes, approximate completeness period, maximum observed and expected magnitude for the intermediate-depth seismic source zones of the Eastern Mediterranean region.

Source Zone	b -value	Yearly Number of Earthquakes		Completeness Period (years)		Observed M_{max}/I_{max}	Expected M_{Wmax}
		Above M_w 4.0	Above M_w 5.0	M_w 4.0	M_w 5.0		
MD-01	0.88 ± 0.07	12.209 ± 0.477	1.621 ± 0.063	20	33	M_w 6.9 on 2008/02/14	7.0 ± 0.3^A
MD-02	0.97 ± 0.04	14.140 ± 0.482	1.528 ± 0.052	30	33	m_b 6.4 on 2013/10/12	6.9 ± 0.3^A
MD-03	0.78 ± 0.07	1.989 ± 0.153	0.332 ± 0.026	20	33	m_b 6.9 on 1962/08/28	6.5 ± 0.4^A
MD-04	0.83 ± 0.06	2.891 ± 0.155	0.432 ± 0.023	20	33	m_b 7.2 on 1903/08/11	7.3 ± 0.5^B
MD-05	0.88 ± 0.03	14.878 ± 0.451	1.943 ± 0.059	20	33	m_b 7.1 on 1984/02/09	7.7 ± 0.5^B
MD-06	0.93 ± 0.03	2.299 ± 0.174	0.273 ± 0.021	20	33	M_s 5.8 on 1984/04/30	6.0 ± 0.6^A
MD-07	0.82 ± 0.08	2.908 ± 0.167	0.441 ± 0.025	20	55	m_b 6.5 on 1941/01/20	7.1 ± 0.6^A

^A Calculated using Robson-Whitlock-Cooke procedure (Kijko and Singh, 2011).

^B Equal to maximum recorded magnitude.

4.5 STRESS PATTERN FROM THE INVERSION OF FOCAL MECHANISM SOLUTIONS DATA

The stress field existing in various sectors in Egypt has been described in numerous studies (e.g., Abou Elenean, 1997; Badawy, 2001, 2005; Salamon *et al.*, 2003; Hussein *et al.*, 2013). In the current study, the prevailed stress regime for the delineated shallow seismic sources (EG-01 until EG-28) is estimated using the available FMS data and by applying the inversion method and WIN-TENSOR software (Delvaux and Sperner, 2003; Delvaux and Barth, 2010). Among the twenty-eight shallow seismic sources covering the Egyptian territory, only twenty-one zones contain FMS data, some of them having only one or two FMSs (Table 4-5).

Table (4-5): Stress inversion results for the delineated seismic sources.

Seismic Source	EQ	n/n _t	σ_1		σ_2		σ_3		R	α Aver.	α Max	F5	R'	SH		Q	Stress Regime
			Az.	Pl.	Az.	Pl.	Az.	Pl.						Max	Min		
EG-01	8	8/16	305	03	207	70	036	19	0.29	4.9	169.8	5.0	1.71	125	035	B	SS
EG-02	5	5/10	122	50	314	40	219	06	0.24	3.9	18.8	1.1	0.24	125	035	C	NS
EG-03	8	4/8	157	31	314	57	061	11	0.89	0.7	32.2	0.0	1.11	151	061	C	SS
EG-04	6	6/12	123	41	344	41	234	21	0.70	18.7	29.8	13.1	0.70	139	049	C	UF
EG-05	2	4/4	347	39	164	51	256	01	0.98	4.0	50.0		1.03	166	070	D	SS
EG-07	6	6/12	120	76	290	14	020	02	0.11	20.9	116.5	27.7	0.11	113	023	C	NF
EG-08	5	5/10	112	50	265	37	005	14	0.18	11.9	53.2	10.8	0.18	106	016	C	NS
EG-10	1	2/2	233	75	138	01	048	15	0.50	0.0	0.0		0.50	138	048	D	NF
EG-11	1	2/2	049	04	140	06	285	83	0.50	0.0	0.0		2.50	049	139	D	TF
EG-14	4	4/8	299	53	145	34	046	12	0.48	1.8	9.3	1.2	0.48	131	041	C	NF
EG-15	31	37/62	039	64	242	25	148	09	0.70	4.1	144.1	7.2	0.70	057	147	A	NF
EG-16	11	13/22	315	34	161	53	054	13	0.52	8.3	131.1	11.9	1.48	140	050	B	SS
EG-17	11	11/22	309	58	124	32	216	02	0.79	4.4	44.5	2.6	0.79	126	036	B	NF
EG-21	1	2/2	070	34	339	01	247	56	0.00	0.0	0.0		2.00	070	160	D	TF
EG-22	12	12/24	322	16	119	73	230	06	0.75	27.5	155.4	49.7	1.25	141	051	C	SS
EG-23	14	13/28	124	34	333	52	224	14	0.59	14.3	54.9	17.2	1.41	130	040	B	SS
EG-24	27	27/54	113	78	244	08	335	09	0.12	17.3	147.9	24.9	0.12	074	164	B	NF
EG-25	6	4/12	167	76	067	02	336	14	0.66	3.3	6.7	3.8	0.66	066	156	C	NF
EG-26	2	4/4	056	17	322	11	200	69	1.00	2.0	26.0		2.41	110	157	D	TF
EG-27	2	4/4	292	37	031	12	137	51	0.11	10.4	46.6		1.99	110	168	D	UF
EG-28	1	2/2	313	07	047	27	209	62	0.50	0.0	0.0		2.50	131	041	D	TF

EQ: total number of earthquakes; n: the number of data explained by the stress tensor; n_t: the total population of fault plane solutions; σ_1 , σ_2 and σ_3 : the principal stress axes where azimuth is Az. and plunge is Pl.; R: stress ratio; α Aver.: average misfit angle; α Max: maximum misfit angle; F5: misfit function of Delvaux and Barth (2010); R': stress regime index; SH (Max, Min): maximum and minimum horizontal stress axes; Q: quality rank (A is the best, D is the worst), and for stress regime (NF: normal-faulting regime, NS: normal faulting with strike-slip component regime, SS: strike-slip regime, TF: thrust-faulting regime, and UF: unknown or oblique-slip faulting regime).

It is not necessary to choose between the two nodal planes, available for each FMS, before the inversion process. The improved Right Dihedron method (Delvaux and Sperner, 2003) which was proposed originally by Angelier and Mechler (1977) was applied in the current study, in combination with the iterative Rotational Dihedron method for estimating the different parameters of the reduced stress tensor.

First, the improved Right Dihedron method (Delvaux and Sperner, 2003) have been used to compute the four parameters of the reduced stress tensor: the principal stress axes σ_1 (maximum compression), σ_2 (intermediate compression), σ_3 (minimum compression) and the stress ratio $R = (\sigma_2 - \sigma_3) / (\sigma_1 - \sigma_3)$. This method allows, not only giving the first computations of the four reduced stress tensor parameters, but also obtaining the first filtered FMSs data. In this method, nodal planes which are incompatible with the average stress regime are removed. The results obtained from this step, the compatible FMSs and the calculated stress tensor, are used directly as the starting point in the tensor Rotational Optimization method (Fig. 4-11).

Secondly, the iterative grid-search “Rotational Optimization” procedure is based on a controlled grid search of stress tensors with the aim of minimizing what is called “the misfit function” F5 in the WIN-TENSOR software code (Delvaux and Barth, 2010). This function minimizes the angle deviation between the observed and modeled slip lines on the planes (respectively the slip vector and the calculated shear) using the stress tensor that is being tested, but also favors a higher shear stress magnitude and lower normal stress magnitude (Delvaux and Barth, 2010). In this procedure, both nodal planes for each FMS were inverted to a stress tensor at the beginning, and the plane that is best explained by the stress tensor is selected among them and considered as the actual fault plane (Hussein *et al.*, 2013). It considers the movement plane best fit to the general tensor (has the lowest misfit value) and the auxiliary plan has the highest value of the misfit function. Therefore, the final inversion will includes the focal planes that are best fitted by a uniform stress field (Gephart and Forsyth, 1984). This category of focal planes that fit a single stress tensor contains the correct choices, and hence the inferred stress tensor represents the final one.

Finally, it was necessary to re-check the excluded focal planes without changing the stress tensor for testing, after the last optimization, when some of the focal planes can become compatible with the computed stress tensor. If so, we had to re-

incorporate it to the database, re-optimize the stress tensor and check the rejected data again. This method was repeated as often as necessary. In the seismic sources which includes only two earthquakes (Fig. 4-11), only the improved Right Dihedron method (Delvaux and Sperner, 2003) has been used.

The above-mentioned inversion methodology was applied to the FMS data included in the twenty-one-defined shallow seismic sources in Egypt. The stress inversion results (Table 4-5, Fig. 4-11) show the number of the FMS data used in this study, principal stress axes, stress ratio, average misfit angle, misfit function F_5 , stress regime index, minimum and maximum horizontal stress axes, quality rank and stress regime for each considered seismic source.

In general, the obtained results agree well with the tectonic framework of Egypt (Fig. 4-12). The results indicate that there is a different tectonic stress regimes, including extensional tectonic, transtensional and strike-slip. For those seismic sources delineated along the DST (from EG-01 till EG-10), the stress field is in agreement with the preferentially strike-slip and normal faulting which coincides with directions of the faults forming the pull-apart basins in this region. The EG-11 seismic source shows a reverse-fault regime, which coinciding with the Palmyride Fold Belt. The seismic sources located along and to the west from the Red Sea and Gulf of Suez (from EG-14 till EG-17) are predominantly influenced by the extensional stress field, which reflects a clear normal-faulting regime with dominant extension trending N–NNE (with the exception of the EG-15, in which the extension trending N–NNW). The seismic sources delineated for the Egyptian Eastern Desert and along the Nile Valley (from EG-21 till EG-24), reflect different regimes. For example, the results shows that the seismic sources EG-22 and EG-23 reflect strike-slip regime, while solutions in the EG-24 zone reflect normal-faulting regime. Finally, the stress inversion results for those seismic sources delineated along the Mediterranean coastal area reflects, thrust-faulting mechanism which may be related to the subduction zones in the Mediterranean region (with the exception of the EG-25 that exhibits normal faulting, which may be due to the change from DST strike-slip faulting, from the eastern part, to thrusting mechanism along the Cyprian Arc, from the northwestern part).

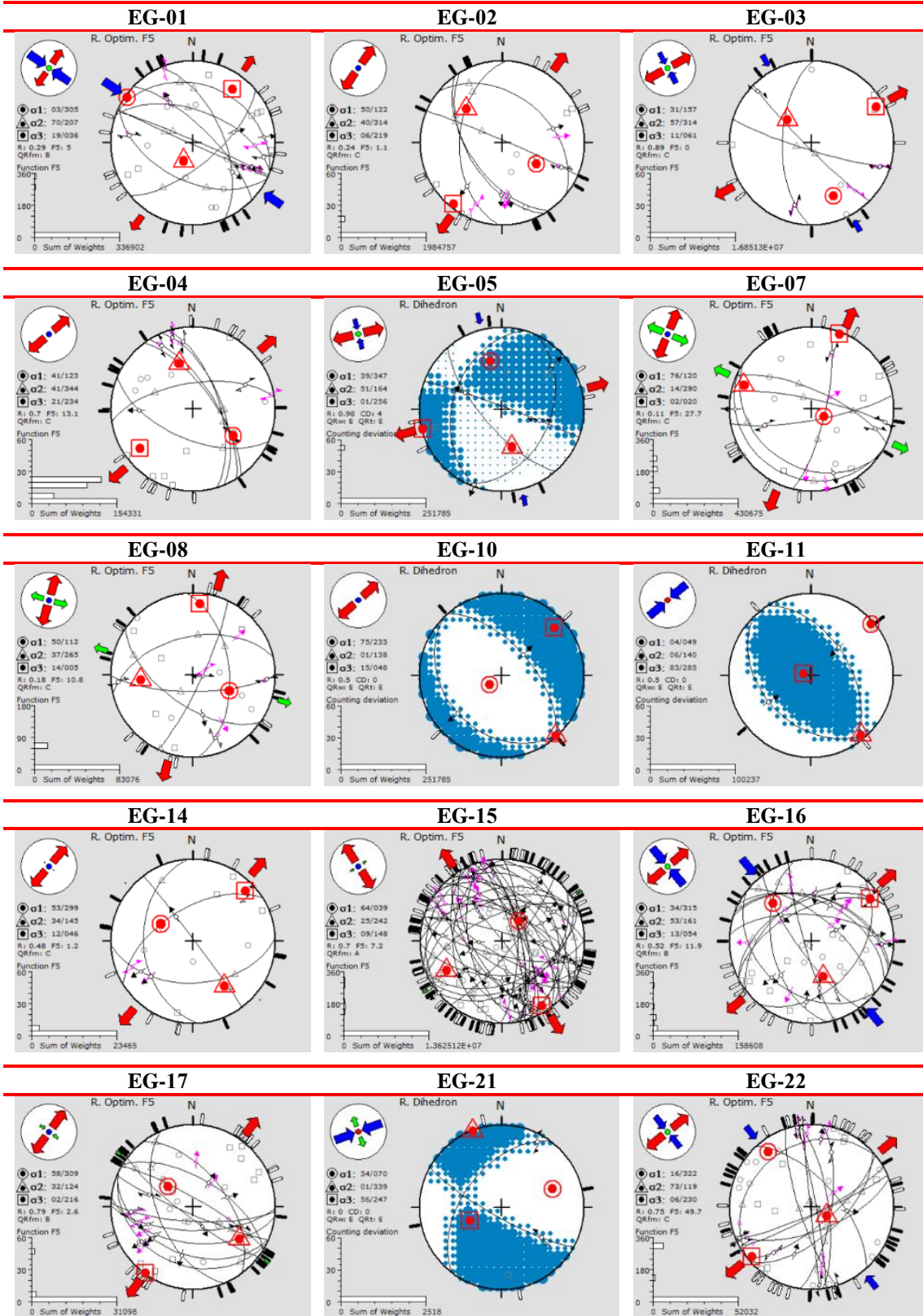


Figure (4-11): Lower-hemisphere equal-area stereoplots of the selected focal planes for the proposed seismic sources and associated slip lines. Results are represented by the orientation of the three principal stress axes (a black dot surrounded by a circle for σ_1 , a triangle for σ_2 and a square for σ_3). The related SH_{max} and SH_{min} orientations are represented by large arrows outside the stereogram. The histogram represents the distribution of the misfit angle F5 weighted arithmetically according to the magnitude.

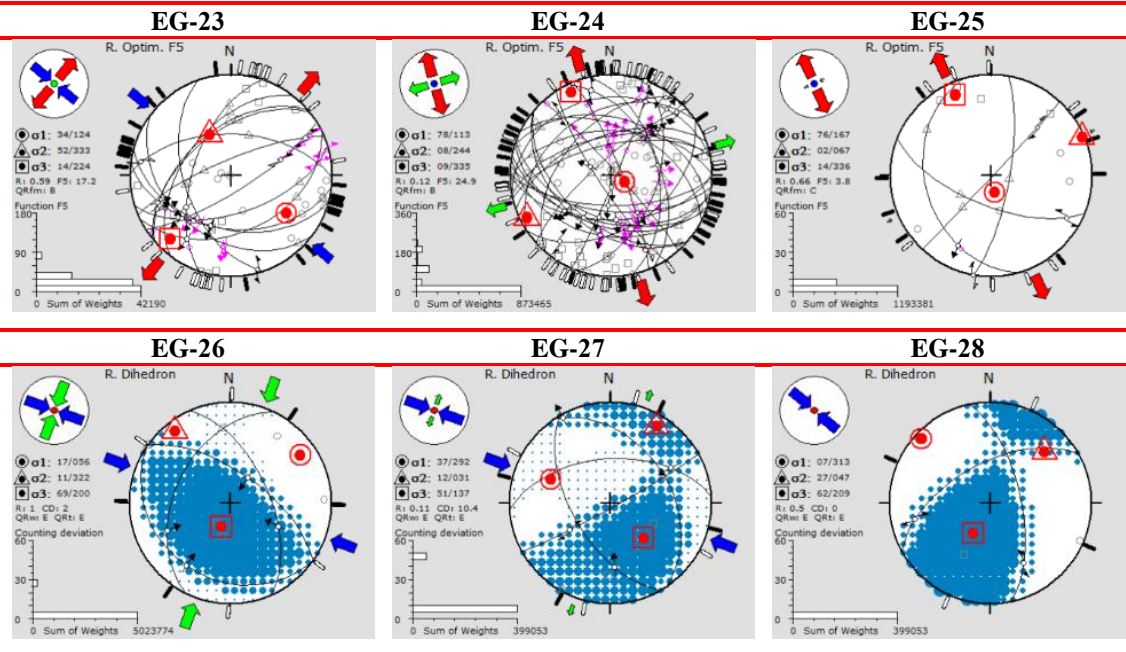


Figure (4-11): Continued.

4.6 CONCLUSIONS

To perform a realistic quantification and spatial distribution of the seismic hazard in Egypt, it is crucial, at first step, to define a seismic source zone model, including all the seismicity that can affect the country and the well-constrained seismotectonic information. The current work is an attempt to develop and propose a new seismic source model for Egypt and its surroundings, using available geological, geophysical, tectonic and earthquake data, aimed at carrying out seismic hazard and forecasting studies.

This work presents a detailed review on major tectonic features and the correlation of seismicity with them, to demarcate seismic sources in Egypt and neighborhood. The DST, the Gulf of Suez-Red Sea Rift, and the Cyprian and Hellenic Arcs are the three most active seismotectonic belts in the region, which have produced several large earthquakes in the recent past. On the basis of a comprehensive and critical analysis of the seismotectonic characteristics, different seismic sources are defined to model the seismicity.

FMSs data, active-faults data, as well as an updated earthquake catalogue for the period 2200 B.C.–2013 were taken into account. Potential seismic sources are modeled as area sources, in which the configuration of each seismic source is controlled, mainly, by the fault extension and seismicity distribution.

The proposed seismic source model consists of 28 shallow seismic zones ($h \leq 35$ km) for the Egyptian territory and its surroundings, specified on the basis of mainly seismotectonic and seismicity criteria. In addition, we have considered 53 shallow seismic sources ($h \leq 20$ km) for the EMR after SHARE (2013). Furthermore, the current model involves 7 delineated intermediate-depth seismic sources ($20 \leq h \leq 100$ km) covering the intermediate-depth seismicity in the EMR.

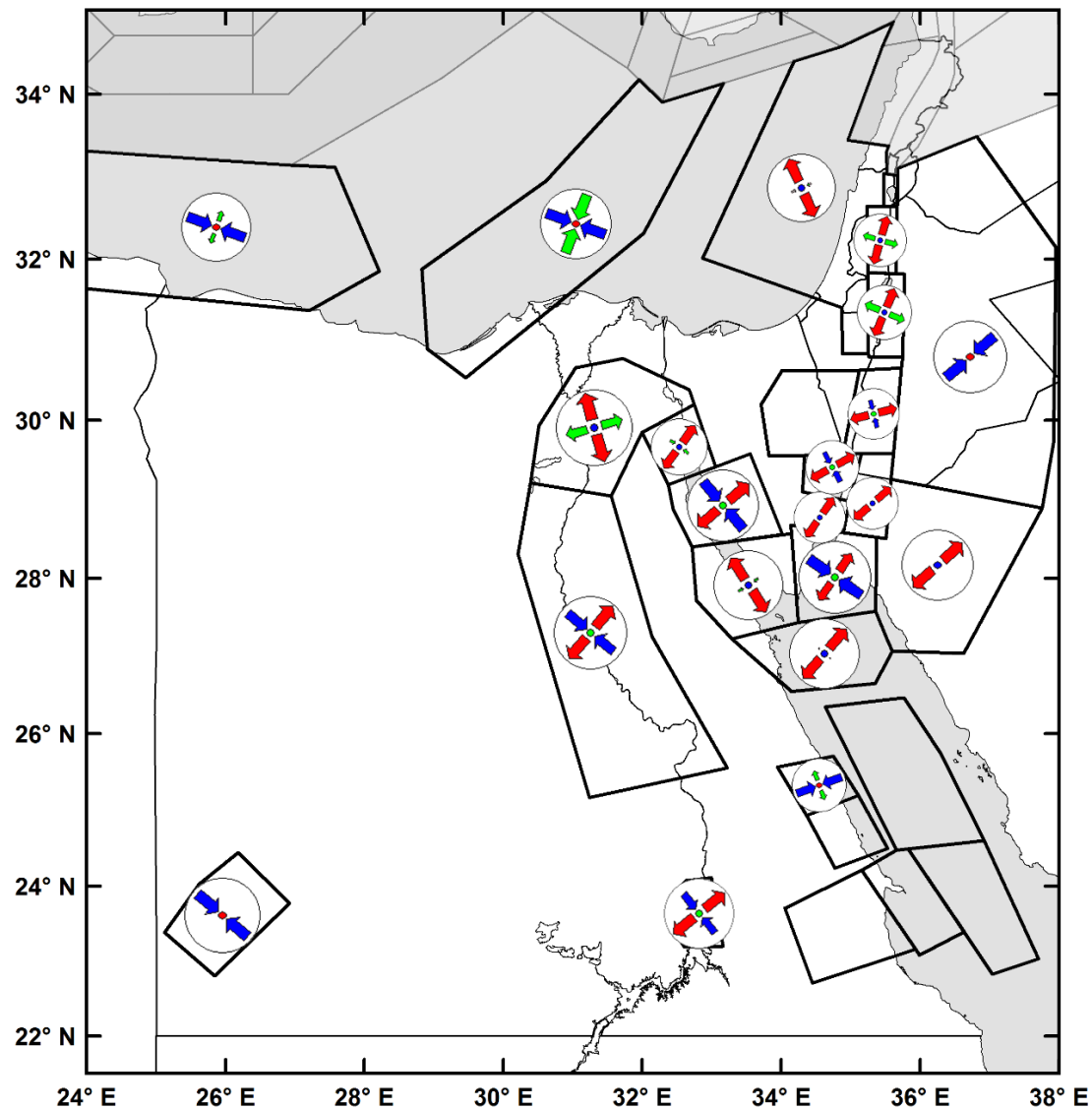


Figure (4-12): Geographic representation of the SH_{max} and SH_{min} results for the different studied seismic sources in Egypt.

Seismicity parameters (b -values and activity rates) of the Gutenberg–Richter magnitude–frequency relationship have been estimated for each one of the seismic sources. In addition, the M_{max} for each seismic source zone was reported. Moreover, the predominant stress pattern was estimated for each seismic source by using the

stress inversion approach and the compiled FMSs data. The inversion results are in agreement with the tectonic framework in and around Egypt.

4.7 ACKNOWLEDGMENTS

We would like to thank the Dr. L. Matias, and an anonymous reviewer for their valuable comments and suggestions. This research work is supported by the Egyptian Ministry of the Higher Education (Cultural Affairs and Missions Sector, Cairo), the Aswan Regional Earthquake Research Center and the Spanish Seismic Hazard and Active Tectonics research group.



Chapter 5

Updated Probabilistic Seismic Hazard Values for Egypt

Sawires, R., Peláez, J.A., Fat-Helbary, R.E., and Ibrahim, H.A. (2016). Updated probabilistic seismic hazard values for Egypt. *Bulletin of the Seismological Society of America* 106, 1788–1801.

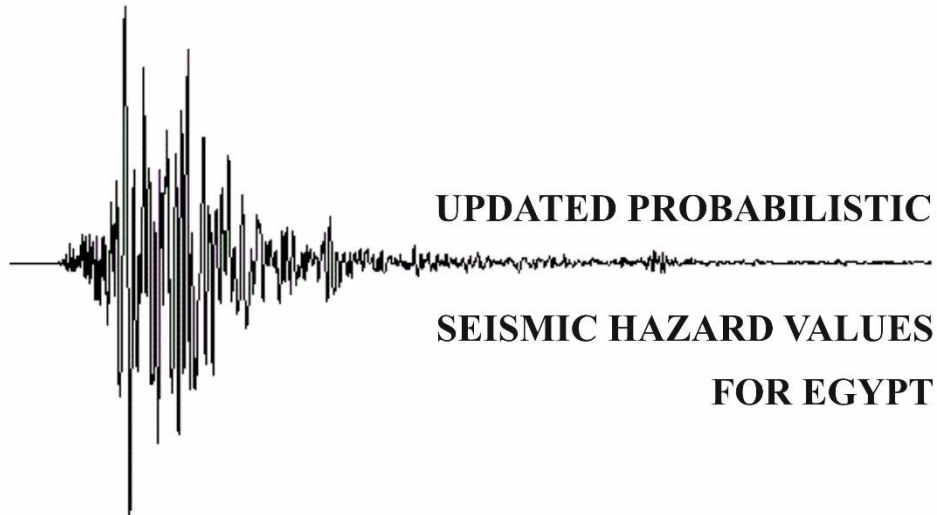
ABSTRACT

Seismic hazard in terms of mean peak ground acceleration (PGA) and spectral acceleration (SA) values has been computed for Egypt using both historical and instrumental earthquake data. For this purpose, an updated earthquake catalogue, spanning the time period from 2200 B.C. to 2013, has been compiled for Egypt and its surrounding regions, and prepared to be used in a new probabilistic seismic hazard assessment of Egypt. The earthquake sizes were unified in terms of the moment magnitude scale. A new seismic source model, for the seismic activity in and around Egypt, consisting of a total of 88 seismic zones (for shallow- and intermediate-depth seismicity) was considered in this new assessment. The seismicity parameters have been specifically computed for 35 seismic sources covering the Egyptian territory and the Eastern Mediterranean region. A logic-tree design was setup in order to consider the epistemic uncertainty in the Gutenberg-Richter b-value, maximum possible magnitude (M_{max}) and the selected ground-motion prediction equations (GMPEs).

Seismic hazard computations, for rock-site conditions, with 10% and 5% probability of exceedance in 50 years were carried out. In addition, uniform hazard spectra for twelve, among the most important and populated cities in Egypt, are computed and compared with the most recent Egyptian building code values. It is interesting to

highlight that the maximum hazard values are observed at the Gulf of Aqaba region, specifically around the epicentral location of the biggest Egyptian recorded earthquake of 22 November 1995 (M_w 7.2) Aqaba earthquake. The obtained seismic hazard values for Nuweiba city (located in this region), for mean PGA and SA (0.1 - s) are 0.29 g and 0.74 g, respectively, for a return period of 475 years.

HEADINGS:		Page
5.1	Introduction.....	127
5.2	Previous Assessments.....	130
5.3	Data and Methodology.....	133
	5.3.1 Earthquake Catalogue.....	133
	5.3.2 Seismic Source Model.....	134
	5.3.3 Ground-Motion Prediction Equations.....	138
	5.3.4 Logic-Tree Approach and PSHA Calculations.....	140
5.4	Results and Discussion.....	143
5.5	Conclusions.....	148
5.6	Data and Resources.....	149
5.7	Acknowledgments.....	149



Earthquakes damage and vulnerability are increasing steadily as the urbanization and development occupy more areas prone to moderate or strong earthquakes. Moreover, the uncontrolled growth and spreading of cities is usually associated with the construction of seismically unsafe buildings and infrastructure, mostly due to the insufficient knowledge of seismic hazard in the area under construction. Sometimes, moderate or even small earthquakes may turn catastrophic in areas with poor building and construction practice. The most suitable and effective way to reduce disasters and fatalities caused by earthquakes is to estimate the seismic hazard that should serve to improve the seismic building and design codes for a particular region.

5.1 INTRODUCTION

Egypt is located in the northeastern corner of the African Plate, along the southeastern corner of the EMR. The seismotectonic framework of the Egyptian territory (Fig. 5-1), covering an area of one million square kilometers, is spatially varied. It can be described in the context of the surrounding three plate boundaries: a) the convergent African-Eurasian, b) the divergent Gulf of Suez-Red Sea, and c) the DST plate boundaries. Clearly, the seismicity of Egypt is mainly related to the tectonic deformation and the relative movement between the African Plate and the surrounding plates (Eurasian and Arabian Plates).

Egypt is affected by moderate seismic activity compared to other countries, nevertheless it is exposed to a high seismic risk. This is due to several factors: a) the population in Egypt, as well as all important and archaeological sites, are concentrated within a narrow belt along the Nile Valley and Delta, b) most of the densely-populated cities and villages are located near moderate to high active seismic foci, c) the methods

of construction vary between old and new buildings with poor construction practice and, d) the soil characteristics in different localities in Egypt have a clear influence on seismic amplification (Riad *et al.*, 2000), among others.

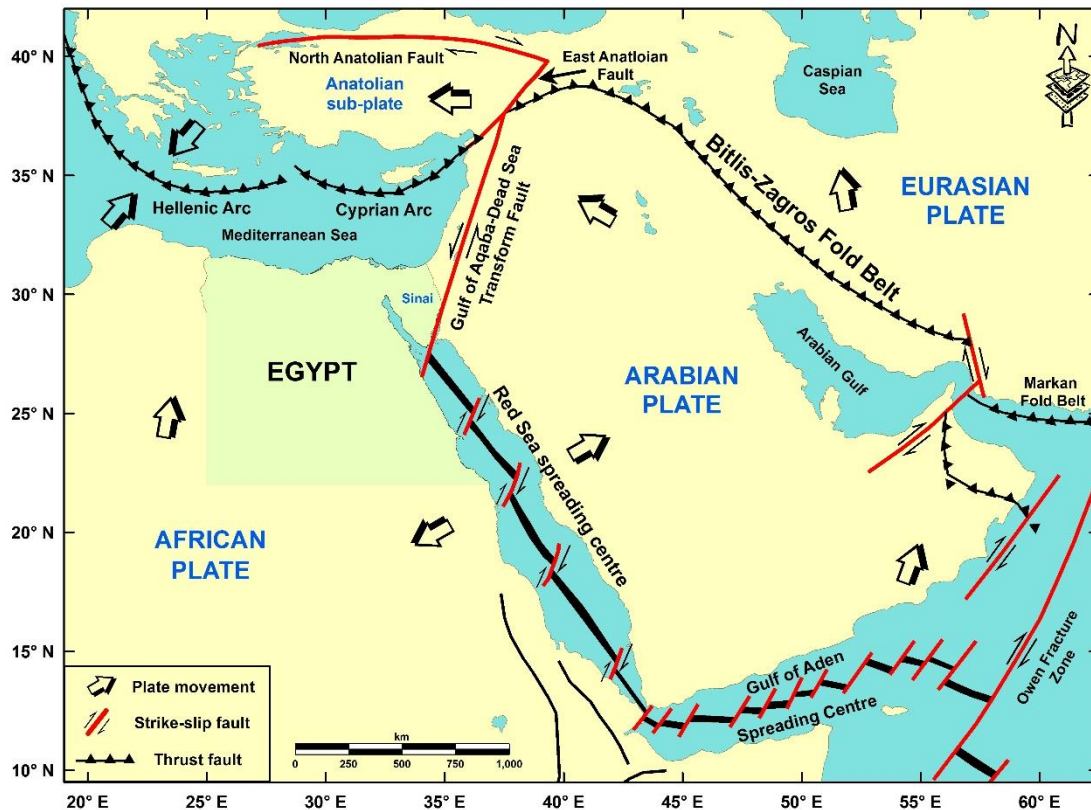


Figure (5-1): Global tectonic sketch for Egypt and its vicinity (compiled and replotted after Ziegler, 1988; Meulenkamp *et al.*, 1988; Dewey *et al.*, 1989; Guiraud and Bosworth, 1999).

Several moderate to strong earthquakes (e.g., M_S 6.9, 31 March 1969 Shedwan, M_S 5.9, 12 October 1992 Cairo, and M_W 7.2, 22 November 1995 Gulf of Aqaba earthquakes) in the last 50 years (Table 5-1), have been taken place in Egypt causing a considerable damage. In addition, many historical events happened and were reported to be located inside the Egyptian territory (Table 5-2). Although the M_W 7.2, 22 November 1995 Gulf of Aqaba earthquake was the strongest one among the instrumental events, it was the M_S 5.9, 12 October 1992 event that left the deepest imprints on everyone, not only because it resulted in hundreds killed and injured people, but also because it incurred a huge economic loss in damages, making it one of the costliest natural disasters in Egypt (Abou Elenean *et al.*, 2010). As a result, a damaging earthquake is a real, as well as a current threat to the society, and economic wellbeing of the population in Egypt.

Table (5-1): Largest instrumental events (magnitudes above M_w 5.0) in Egypt in the last 50 years.

Date	Time (hh:mm:ss)	Longitude (°E)	Latitude (°N)	Depth (km)	Reported Magnitude	Unified M_w	Epicentral Region
9 February 1964	06:07:30	36.500	25.700	40	m_b 4.8, M_S 4.9	5.2	Red Sea
31 March 1969	07:15:51	33.938	27.513	06	m_b 6.1, M_S 6.6, M_W 6.8	6.8	Shedwan Island, Red Sea
28 June 1972	09:49:35	33.810	27.700	07	m_b 5.7, M_S 5.5, M_W 5.5	5.5	Shedwan Island, Red Sea
9 December 1978	07:12:52	26.410	24.000	07	m_b 5.3, M_S 5.0, M_L 5.7	5.3	Gilf El-Kebeir, Southern Egypt
14 November 1981	09:05:23	32.610	23.800	19	m_b 5.5, M_S 5.8, M_L 5.6	5.8	Aswan, Southern Egypt
23 April 1982	14:42:57	32.629	23.598	11	m_D 5.6, M_L 5.6	5.5	Aswan, Southern Egypt
12 June 1983	12:00:09	33.110	28.500	25	m_b 5.0, M_S 4.7, M_L 4.8	5.1	Gulf of Suez
2 July 1984	01:47:01	34.549	25.179	10	m_b 5.1, M_S 3.8, M_L 5.2, M_W 5.1	5.1	Abu Dabbab, Eastern Desert
31 December 1985	19:42:41	34.910	29.100	10	m_b 4.8, M_S 4.6	5.1	Gulf of Aqaba
2 January 1987	10:14:00	32.210	30.500	21	m_b 5.0	5.0	Northern Eastern Desert
12 October 1992	13:09:57	31.142	29.712	22	m_b 5.8, M_S 5.4, M_L 5.9, M_W 5.8	5.8	Dahshour, Southwest Cairo
3 August 1993	12:43:08	34.548	28.708	18	m_b 5.8, M_S 5.8, M_W 6.1	6.1	Gulf of Aqaba
3 November 1993	18:39:34	34.680	28.706	10	m_b 4.8, M_S 4.6, M_L 4.6	5.1	Gulf of Aqaba
22 November 1995	04:15:15	34.809	28.769	19	m_b 6.7, M_S 7.3, M_W 7.2	7.2	Gulf of Aqaba
11 December 1995	01:32:09	34.829	28.913	16	m_b 4.9, M_S 4.8, m_D 5.2	5.2	Gulf of Aqaba
21 February 1996	04:59:55	34.802	28.878	20	m_b 5.1, M_S 4.7, M_W 5.3	5.3	Gulf of Aqaba
8 March 1997	06:00:05	34.200	27.700	-	m_D 5.5	5.4	Northern Red Sea
28 May 1998	18:33:32	26.650	31.970	10	m_b 5.5, M_S 5.0, M_W 5.5	5.5	Offshore, Northwestern Egypt
14 December 1998	20:48:00	31.220	26.440	18	M_L 5.4	5.0	Sohag, Southern Egypt
30 April 1999	23:27:00	31.200	25.470	10	M_L 5.5	5.1	SW Qena, Southern Egypt
30 July 2006	01:54:56	35.574	26.272	14	m_b 4.7, M_S 5.1, M_L 4.5	5.4	Red Sea
19 October 2012	03:35:11	30.940	32.480	10	m_b 5.1, M_L 4.8, M_W 5.0	5.0	Offshore, Northern Nile Delta

Table (5-2): Largest historical events (macroseismic magnitudes above M_w 6.0) in Egypt.

Date	Time (hh)	Long. (°E)	Lat. (°N)	Felt Intensity	Unified M_w	Epicentral Region
April 857	--	31.000	28.000	VIII	6.1	SE Minia
4 October 935	--	31.200	30.500	VIII	6.1	Banha, Nile Delta
15 September 951	18	29.550	31.130	VIII	6.1	Near Alexandria
31 August 1111	--	31.000	31.000	VIII	6.1	Gharbia, Nile Delta
1121	--	37.000	23.500	VI-VII	6.8	Red Sea
2 May 1212	--	34.570	29.330	VIII-IX	6.1	Eastern Sinai
1262	--	31.150	30.030	IX-X	6.7	Northern Cairo
20 February 1264	--	31.000	29.000	VIII	6.1	Beni Suef
30 July 1303	--	31.150	30.030	IX	6.4	Cairo
May 1341	--	29.550	31.130	VIII-IX	6.1	Near Alexandria
9 April 1588	--	31.550	30.030	IX	6.4	Near Cairo
October 1754	--	32.250	29.600	V	6.6	SW Suez
11 July 1879	18	33.000	29.000	VI	6.0	Gulf of Suez

Moreover, the Egyptian government is proposing a national plan aiming at construction of a number of new cities and strategic projects covering different areas all over the country (e.g., the recently announced New Capital city, and the New Suez Canal project), in addition to the development of established old projects (e.g., Tushka and Nasser's Lake, Sinai development, and Port Said projects). These national programs, in turn, could solve the problem of a high population density along the Nile Valley and Delta regions, creating new communities in these arid regions. On the other hand, the consideration of the seismic action in the current Egyptian building code (ECP-201, 2011) is still depending on a seismic hazard assessment that does not consider neither the historical earthquake events nor an up-to-date earthquake catalogue and seismic source model for the Egyptian territory. Thus, there is an urgent need to estimate up-to-date seismic hazard values and to supply this information for application and use in improving seismic zoning maps and building design and construction.

In the current study, we developed a new PSHA of the Egyptian territory mainly in terms of the mean horizontal PGA and SA values. To carry out this assessment, a typical zoning approach was used. Here we show the main results of this assessment, specifically for twelve significant cities, for two different return periods (475 and 975 years) and for rock-site conditions.

5.2 PREVIOUS ASSESSMENTS

In the last three decades, initial attempts to estimate the seismic hazard have been done, for the whole territory of Egypt as a general, and for specific cities in particular,

which mainly based on deterministic approaches (e.g., Kebeasy *et al.*, 1981; Albert, 1987; Sobaih *et al.*, 1992; El-Sayed and Wahlström, 1996; Fat-Helbary and Ohta, 1996; and Badawy, 1998). Some of these authors evaluated the seismic hazard regardless to seismic source zones, while in other studies, authors estimated the seismic hazard upon the delineation of seismic sources depending on the major prevailing tectonic trends in Egypt.

More recently, new deterministic and probabilistic hazard studies have been carried out (e.g., Riad *et al.*, 2000; El-Sayed *et al.*, 2001; El-Hefnawy *et al.*, 2006; Fat-Helbary *et al.*, 2008; Deif *et al.*, 2009 and 2011; and Mohamed *et al.*, 2012). Among these assessments, the study carried out by Riad *et al.* (2000) estimated the PGA values for the whole Egyptian territory, that was considered in the GSHAP (1999) and later in the current Egyptian building code (ECP-201, 2011). This study used a compiled earthquake catalogue covering the seismicity of Egypt and its surroundings until the year 1996. In addition, authors used a seismic source model based upon the work done by Papazachos (1990) and Shapira and Shamir (1994), and the GMPEs by Campbell (1981) and Crouse (1991). From the obtained results in this study, Egypt was divided, in the current building code, into five broad seismic zones (I, II, III, IV, Va and Vb). Zone I (PGA = 0.01 g) is identified with the lowest hazard, and zone Vb (PGA = 0.30 g) with the highest hazard. Some of the obtained results for specific cities are shown in Table (5-3).

Nowadays, the scientific interest regarding seismology as a general, and seismic hazard assessment in particular, has greatly increased in Egypt. It is well-known that seismic hazard analysis represents the most significant way to provide useful information on the earthquake-prone areas to help engineers improving the seismic design codes. Moreover, most of the previous mentioned studies used former databases and did not consider appropriately the uncertainty in the seismic hazard calculations. Furthermore, other question is the fact that the current building code (ECP-201, 2011) does not give a certain PGA value for each city in Egypt, instead it just divides the whole territory of Egypt into five broad zones, assigning to each one a single seismic hazard value.

Table (5-3): Seismic hazard values for selected cities (return periods of 475 and 975 years) in comparison with mean PGA values considered for both GSHAP (1999) and the current Egyptian building code (ECP-201, 2011) for a return period of 475 years. [SA_{max} : maximum spectral acceleration, T_{max} : spectral period related to SA_{max}].

City	PGA (g) after GSHAP (1999) & ECP-201 (2011)	475 years					975 years				
		PGA (g)	SA_{max} (g)	T_{max} (s)	SA (0.2-s) (g)	SA (1.0-s) (g)	PGA (g)	SA_{max} (g)	T_{max} (s)	SA (0.2-s) (g)	SA (1.0-s) (g)
Nuweiba	0.20	0.29	0.74	0.1	0.64	0.15	0.38	0.98	0.1	0.85	0.20
Aswan	0.13	0.19	0.46	0.1	0.42	0.11	0.25	0.62	0.1	0.56	0.15
Sharm El-Sheikh	0.20	0.15	0.39	0.1	0.30	0.06	0.18	0.51	0.1	0.39	0.07
NEW Capital	0.15	0.14	0.35	0.1	0.30	0.07	0.20	0.49	0.1	0.41	0.09
Suez	0.15	0.13	0.32	0.1	0.29	0.07	0.18	0.44	0.1	0.39	0.09
CAIRO	0.15	0.13	0.32	0.1	0.28	0.06	0.18	0.44	0.1	0.38	0.09
Hurghada	0.25	0.13	0.35	0.1	0.29	0.05	0.17	0.46	0.1	0.37	0.07
Marsa Alam	0.13	0.11	0.28	0.1	0.23	0.04	0.14	0.37	0.1	0.30	0.06
Alexandria	0.13	0.09	0.22	0.1	0.19	0.05	0.13	0.32	0.1	0.27	0.07
Assiut	0.10	0.07	0.16	0.1	0.14	0.03	0.09	0.23	0.1	0.20	0.05
Matruh	0.13	0.05	0.11	0.1/0.2	0.11	0.05	0.07	0.16	0.1	0.15	0.06
El-Arish	0.13	0.03	0.07	0.3	0.07	0.05	0.04	0.09	0.3	0.09	0.06

5.3 DATA AND METHODOLOGY

5.3.1 EARTHQUAKE CATALOGUE

Earthquake catalogues, along with a good understanding of the geology and seismotectonic environment, are the fundamental bases to define a seismic source model, which is a key element needed to carry out any PSHA. In the absence of a reliable, updated and unified earthquake catalogue for the study region, based on the original data, it was necessary to compile previously a new one from the available sources.

Thus, an updated and unified catalogue for earthquakes located in Egypt and its vicinity in the period 2200 B.C. - 2013 has been compiled. Data were obtained from different local (e.g., Maamoun *et al.*, 1984; Riad and Meyers, 1985; Kebeasy, 1990; Badawy and Horváth, 1999; and Riad *et al.*, 2004), regional and international sources (e.g., Ambraseys *et al.*, 1994; Engdahl *et al.*, 1998; ISC bulletin (2011), as well as the ENSN bulletins (1998-2010).

The compilation covers an area from 21° to 38°N and from 22° to 38°E, and initially included all the events having an assigned magnitude equal to 3.0 and above for international sources, and any magnitude for local sources, on any magnitude scale. Earthquake magnitudes were reported in different sizes (I_{max} , and m_b , M_S , M_W , m_D and M_L magnitudes), and come from a variety of sources. For establishing a unified magnitude scale, some relationships were specifically developed and considered to convert the reported sizes to the M_W scale.

All non-Poissonian (dependent) events were identified and removed using the Gardner and Knopoff (1974) procedure. Following this approach, and in case of a particular earthquake with a certain M_W value, a full scanning for the entire catalogue within a distance $L(M_W)$ and time $T(M_W)$ windows was performed. During the scanning, the biggest earthquake event is considered to be the mainshock. In the current study, we applied window sizes of 10 days and 20 km for a M_W 3.0 event, and 900 days and 100 km for a given M_W 8.0 event. For in-between magnitudes, proportional values for both distance and time windows were used according to the Gardner and Knopoff (1974) approach. More than 16000 events above M_W 3.0 are representing the final catalogue of main earthquakes.

Concerning the completeness of the unified catalogue, from Figure (5-2) it can be seen some characteristics of its Poissonian behavior. In this appraisal, the fact that

earthquakes follow a Poisson distribution in time has been considered in order to minimize any spatial bias of the earthquake occurrence process, as it is usual in mostly seismic hazard assessments, both in zoning and non-zoning methods. Some recent papers (*e.g.*, Boyd, 2012; Marzocchi and Taroni, 2014) advise the use of aftershocks in the seismic hazard computation, noticing the underestimation of the seismic hazard when declustering process is carried out, and proposing different initial approaches to correct it. Taking into account the characteristics of the used catalogue in this work, especially its spatial completeness, as well as the different behavior of different observed seismic sequences, among other issues, finally led us to follow a typical zoning method.

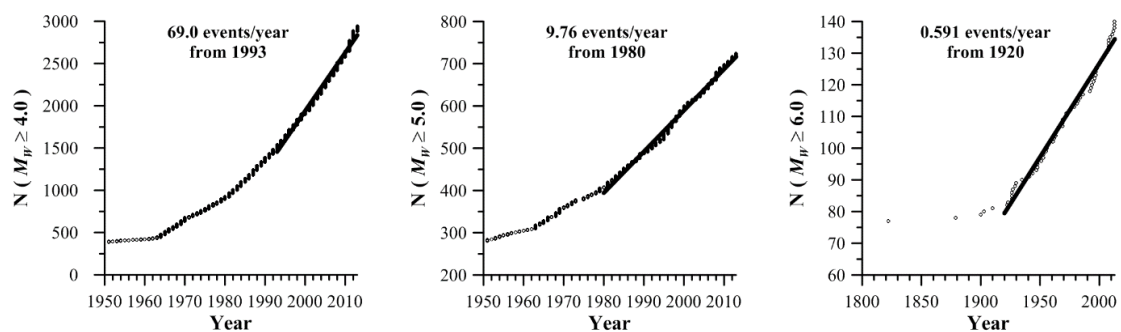


Figure (5-2): Cumulative number of earthquakes above M_w 4.0, 5.0 and 6.0 for the used catalogue.

5.3.2 SEISMIC SOURCE MODEL

The identification and characterization of the seismic source zones in any region, as it was quoted above, is another important and critical input for any seismic hazard analysis. In our assessment, the seismic sources were defined including all available information, *i.e.*, seismicity (historical and instrumental), and geological, seismotectonic (faults and FMSs) and geophysical data (crustal thickness). Active fault data are very scarce in Egypt. In spite of the definition of some faults (Kalabsha, Seiyal, Gebel El-Barqa, Khur El-Ramla, Kurkur, Abu Dirwa and Dabud faults) in Southern Egypt (around Nasser's Lake) by WCC (1985) and Deif *et al.* (2011), we haven't included them in the final seismic hazard computation. This is because there are no available data about the slip rate nor the paleoseismological history of these faults, thus it has been preferred to use only an area source model.

The considered seismic source model consists of 28 shallow ($h \leq 35$ km) seismic zones (Fig. 5-3) for the Egyptian territory and its surroundings, specified on the basis of mainly seismotectonic and seismicity criteria. Many of the defined seismic zones are related to the earthquake distribution along the well-known active belts (*e.g.*, the DST

and the Gulf of Suez-Red Sea Rift). On the other hand, a mean value of 35 km has been used in the discrimination between shallow- and intermediate-depth earthquakes. This rule is based on the study performed by Abdelwahed *et al.* (2013), which gives a range of 30-39 km to the Moho discontinuity in Egypt. Depths for the 28 defined seismic sources have been estimated separately for each delineated seismic source.

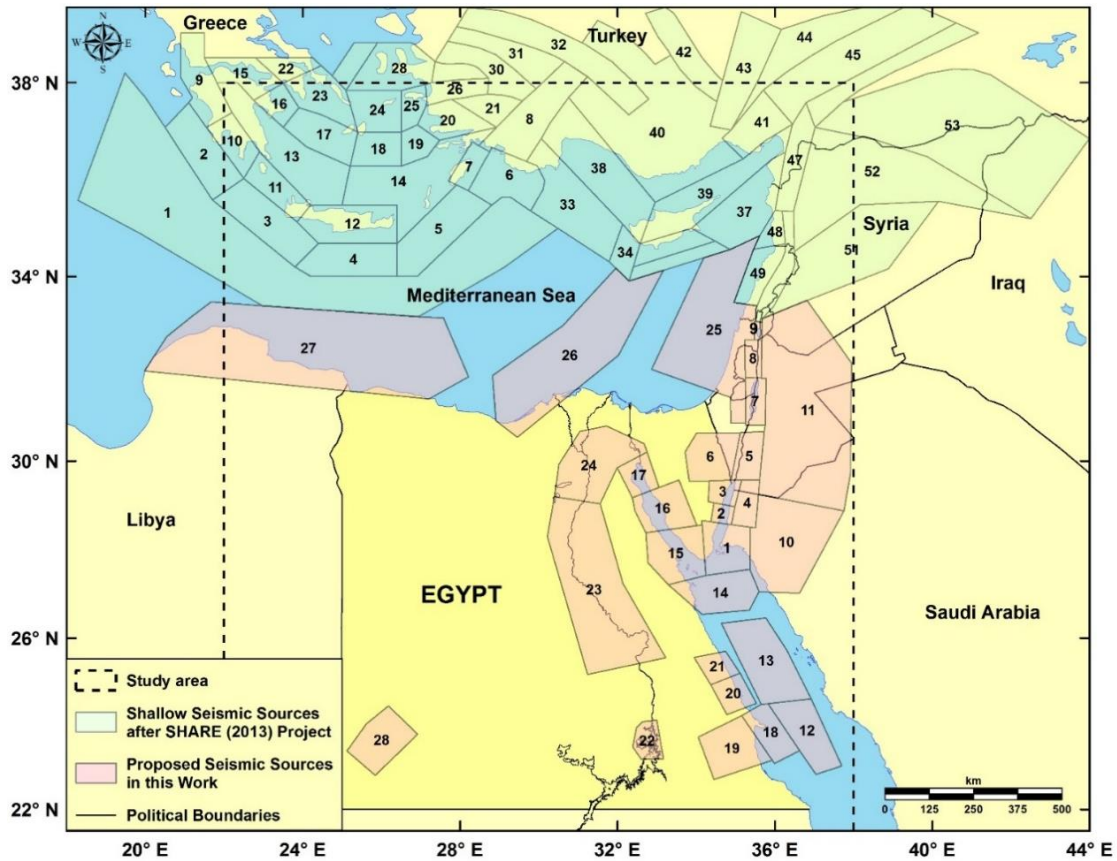


Figure (5-3): Proposed shallow seismic source zones in Egypt and its surroundings.

In addition, 53 shallow ($h \leq 20$ km) seismic sources (Fig. 5-3) for the EMR after SHARE (2013) have been considered. Furthermore, the current model involves 7 specifically delineated intermediate-depth ($20 \leq h \leq 100$ km) seismic sources (Fig. 5-4) covering the intermediate-depth seismicity in the EMR.

The prevailing stress field, seismicity parameters and M_{\max} for those specifically delineated seismic sources (shallow seismic zones for the Egyptian territory and intermediate-depth seismic sources for the EMR) have been estimated. However, the used seismicity parameters and M_{\max} values for the shallow seismic sources in the EMR have been considered the same as those values in the SHARE (2013) project.

The prevailed stress field for each delineated seismic source was estimated using FMSs data. This information was not used directly in the seismic hazard computation but in the delineation of the seismic source model in a feedback process. Seismic

sources should be characterized not only by a single recurrence relationship, but among other features, for a homogeneous stress regime. The inversion method by Delvaux and Sperner (2003) and Delvaux and Barth (2010) was used to compute the stress regime of the delineated shallow seismic sources. By fitting the seismicity included in each seismic source to a Gutenberg-Richter recurrence relationship (Gutenberg and Richter, 1944), the a - and b -values were estimated. The M_{\max} was also estimated for mostly seismic sources using the Robson-Whitlock-Cooke procedure (Cooke, 1979; Robson and Whitlock, 1964; Kijko and Singh, 2011). The procedure considers that if the magnitudes of the earthquakes in a specific seismic source are arranged in ascending order, namely $M_1 \leq M_2 \leq \dots \leq M_{n-1} \leq M_{\max}^{obs}$, then, the estimation of the M_{\max} together with its variance can be computed from the following equations:

$$M_{\max} = M_{\max}^{obs} + 0.5(M_{\max}^{obs} - M_{n-1}) \quad (5-1)$$

$$\sigma(M_{\max}) = 0.5[3\sigma_M^2 + 0.5(M_{\max}^{obs} - M_{n-1})^2] \quad (5-2)$$

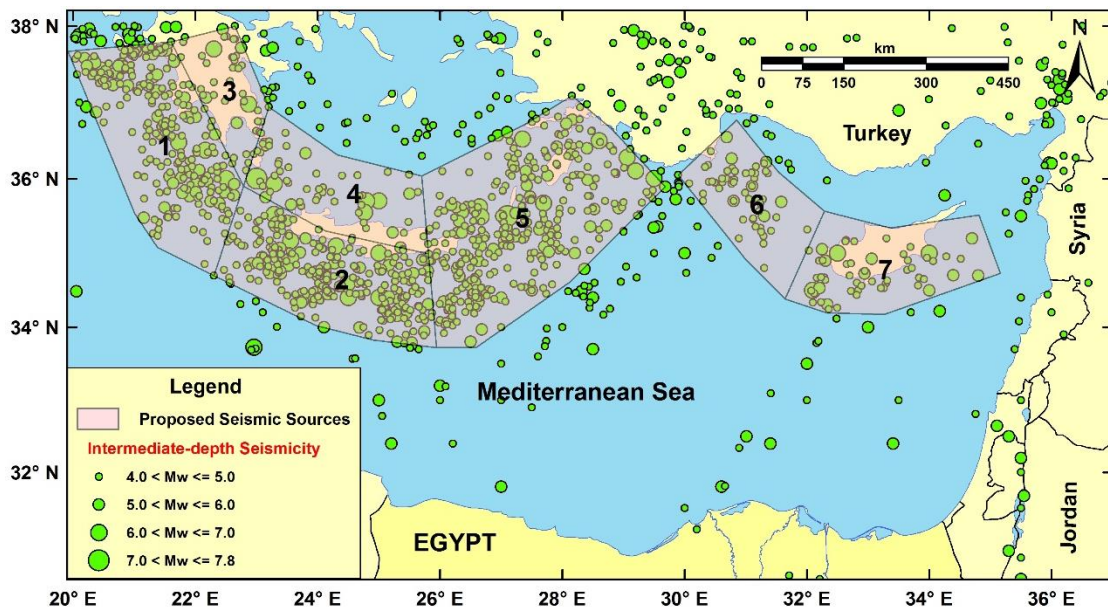


Figure (5-4): Intermediate-depth seismicity ($20 \leq h \leq 100$ km) and delineated intermediate-depth seismogenic source zones for the EMR.

This computed parameter (considering both the historical and instrumental earthquakes) was crosschecked against the available paleo-seismic data (for seismic sources along the DST) addressed in Deif *et al.* (2009, 2011). Table (5-4) shows for each defined shallow seismic source the main seismicity parameters and its uncertainties to be used in the seismic hazard, taking into account that the considered M_{\min} in the final computations was equal to M_w 4.0 for the whole Egyptian territory. In our study, events of magnitude below M_w 4.0 are not believed to be capable of

damaging engineered structures, especially, taking into account the used GMPEs. Moreover, given the low-magnitude earthquakes located outside the defined source zones, independently of some isolated historical events with a great uncertainty both in their location and size, they were not considered neither in the zoning nor in the final assessment. We considered that they are not reliable data in order to help to define the source zones, neither in order to establish a reliable earthquake rate outside these source zones.

Table (5-4): b -value, annual rate of earthquakes above M_W 4.0, observed M_{max}/I_{max} and expected maximum magnitude for the delineated shallow (Fig. 5-3) seismic sources.

Source zone	$b \pm \sigma$	$\lambda \pm \sigma$	Observed M_{max}/I_{max}	Expected M_{Wmax}
01	1.13 ± 0.05	0.980 ± 0.083	m_b 4.4 on 2006/02/02	4.8 ± 0.2^A
02	0.98 ± 0.06	0.495 ± 0.064	M_W 7.2 on 1995/11/22	7.2 ± 0.3^B
03	0.97 ± 0.07	0.276 ± 0.044	I_{max} VIII-IX on 1212/05/02	6.2 ± 0.8^A
04	1.01 ± 0.05	0.196 ± 0.039	m_b 4.5 on 1995/12/26	4.6 ± 0.4^A
05	0.88 ± 0.06	0.188 ± 0.039	m_b 5.2 on 1956/12/18	7.5 ± 0.5^C
06	1.12 ± 0.10	0.185 ± 0.032	m_b 4.8 on 1927/09/24	4.8 ± 0.6^A
07	0.87 ± 0.08	0.323 ± 0.047	I_{max} VIII on 1458/11/12	5.8 ± 0.7^A
08	0.71 ± 0.02	0.187 ± 0.037	I_{max} IX on 746 A.D.	7.8 ± 0.8^A
09	0.91 ± 0.15	0.065 ± 0.027	I_{max} X on 19 A.D.	6.8 ± 0.6^C
10	1.03 ± 0.09	0.193 ± 0.035	I_{max} VIII on 1588/01/04	5.8 ± 0.7^A
11	0.97 ± 0.10	0.365 ± 0.063	I_{max} IX-X on 1159/06/06	6.9 ± 0.8^A
12	1.00 ± 0.05	0.436 ± 0.059	I_{max} VI-VII on 1121 A.D.	6.8 ± 0.6^B
13	0.91 ± 0.06	0.303 ± 0.044	m_b 4.7 on 2006/07/30	5.6 ± 0.3^A
14	1.13 ± 0.07	0.643 ± 0.061	m_b 5.0 on 1952/03/22	5.4 ± 0.6^A
15	1.06 ± 0.04	0.835 ± 0.079	M_W 6.8 on 1969/03/31	6.8 ± 0.3^B
16	0.80 ± 0.06	0.309 ± 0.040	M_S 6.2 on 1900/03/06	6.3 ± 0.6^A
17	0.86 ± 0.08	0.138 ± 0.029	M_S 6.6 on 1754 A.D.*	6.6 ± 0.6^B
18	1.29 ± 0.01	0.157 ± 0.025	M_L 4.5 on 1990/05/23	4.2 ± 0.4^A
19	1.15 ± 0.03	0.118 ± 0.022	M_L 3.9 on 1991/07/15	4.2 ± 0.4^B
20	1.20 ± 0.01	0.063 ± 0.016	M_L 4.7 on 1982/01/21	4.4 ± 0.3^A
21	0.87 ± 0.09	0.371 ± 0.042	m_b 6.2 on 1955/11/12	5.7 ± 0.6^A
22	0.79 ± 0.07	0.586 ± 0.060	M_W 5.8 on 1981/11/14	7.0 ± 0.4^C
23	0.73 ± 0.05	0.295 ± 0.051	I_{max} VIII on 857 A.D.	6.1 ± 0.7^A
24	0.99 ± 0.06	0.596 ± 0.076	I_{max} 9.5 on 1262 A.D.	6.8 ± 0.8^A
25	0.97 ± 0.08	0.520 ± 0.044	I_{max} X on 1546/01/14	7.2 ± 0.8^A
26	0.94 ± 0.07	0.598 ± 0.085	m_b 6.5 on 1955/09/12	6.6 ± 0.6^A
27	0.60 ± 0.03	0.713 ± 0.102	I_{max} VIII on 262 A.D.	6.0 ± 0.8^A
28	1.00 ± 0.06	0.150 ± 0.050	M_S 5.3 on 1978/12/09	5.3 ± 0.3^B

* Macroseismic M_S magnitude (after Ambraseys *et al.*, 1994). ^AComputed using the Robson-Whitlock-Cooke procedure (Kijko and Singh, 2011). ^BEqual to maximum recorded magnitude. ^CTaken from Deif *et al.* (2009, 2011).

In our case, the small number of earthquakes in certain seismic sources, the quality of our data, and the observed behavior of the seismicity in the defined seismic sources, advised the use of a widely-used recurrence relationship, the truncated Gutenberg-

Richter model, because of its simplicity and because it fits our data reasonably well over mostly range of magnitudes. Moreover, given the quality of our data and the return periods for which the seismic hazard is computed, no minimum seismicity rates for defined seismic sources were set.

5.3.3 GROUND-MOTION PREDICTION EQUATIONS

In spite of several strong-motion stations were installed in Egypt by the NRIAG since 2008 (Marzouk *et al.*, 2011), there are no specific GMPEs developed for Egypt, because there is a scarcity of ground-motion acceleration records. Consequently, it has been necessary to adopt worldwide accepted and well-known GMPEs to implement this assessment. Moreover, the acceleration records available for Egyptian earthquakes are not enough even to check, given the magnitudes and distances of the earthquakes, the validity and compatibility of the selected GMPEs.

Following the guidelines proposed by Cotton *et al.* (2006) and modified later by Boomer *et al.* (2010), certain well-known GMPEs were selected in the current study, to account for the epistemic uncertainty associated with not knowing the true attenuation characteristics of the region.

The GMPEs of Ambraseys *et al.* (1996), Abrahamson and Silva (1997), Zhao *et al.* (2006) and Boore and Atkinson (2008) were used together, in a logic-tree design, to model the ground-motion attenuation for earthquakes located within the specifically-defined Egyptian active shallow crustal seismic zones (Fig. 5-3). These GMPEs appear to be the most suitable ones to be considered in a logic tree for the Egyptian seismic sources, after checking the range of distances and magnitudes for which they are defined, as well as the definition of soil conditions and spectral periods for which it is possible to obtain ground-motion values.

On the other hand, the GMPE of Tavakoli and Pezeshk (2005) was chosen to model the ground-motion attenuation for earthquakes occurring within the considered SHARE (2013) seismic sources, covering the EMR. We preferred to apply this model over other GMPEs (e.g., Zhao *et al.*, 2006; Bindi *et al.*, 2014) considered in the SHARE project itself, because of the large distance between the SHARE seismic sources and the northern Egyptian coasts. It is the only GMPE that provides some contribution in the seismic hazard in the northern part of Egypt.

Furthermore, the GMPE of Youngs *et al.* (1997) was selected in order to estimate the ground motion for earthquakes located in the intermediate-depth subduction

seismic sources in the EMR (Fig. 5-4). This model was preferred over the most recent one by Atkinson and Boore (2003), because the Youngs *et al.* (1997) relationship gives more conservative results and agrees well with the known felt effects of these earthquakes in Northern Egypt.

Compatibility among all chosen GMPEs was also considered in their selection for the seismic hazard computations. All the considered GMPEs are expressed in terms of the M_W scale, with the exception of the GMPE by Ambraseys *et al.* (1996), expressed in terms of the M_S magnitude. In the current assessment, no conversion has been applied upon the M_S magnitudes when applying the GMPE by Ambraseys *et al.* (1996). Thereby, it has been checked that when use this relationship in terms of M_W does not include any additional error. Taking into account the developed relationship between M_S and M_W magnitudes in order to unify the magnitudes of the earthquake catalogue, the differences among these two magnitude values, in the range M_S 5.5-8.5, do not exceed 0.1.

Despite the fact that the different GMPEs use different types of distance (Joyner-Boore, rupture and hypocentral distance), the CRISIS 2014 (Ordaz *et al.*, 2014) software code, which is used to perform the current assessment, allows the use of different distance definitions for different models. Thus, distance conversions are not required. Moreover, the software takes into account the focal depth, making it possible to use GMPEs (e.g., Youngs *et al.*, 1997) in which the focal depth is considered as an independent variable.

In this assessment, we have considered rock-site conditions ($V_s^{30} = 760$ m/s), which is corresponding to the boundary between National Earthquake Hazards Reduction Program NEHRP-A and NEHRP-B site classifications. The exception to this, being the GMPEs of Abrahamson and Silva (1997) and Zhao *et al.* (2006), in which they consider a lower boundary ($V_s^{30} > 600$ m/s) for rock sites. Thus, it is considered as a relatively small difference in which all the considered GMPEs can be considered compatible. Corrections for site conditions have not been performed, and the value of $V_s^{30} > 600$ m/s was selected and considered in the final computations.

Finally, all chosen GMPEs consider different types of the faulting mechanism. However, in this assessment, the “unspecified” faulting-mechanism class has been used

for all seismic sources. Thus, nor adjustments or corrections were needed for this component of the GMPEs.

5.3.4 LOGIC-TREE APPROACH AND PSHA CALCULATIONS

As it is well-known, due to the incomplete understanding of the earthquake phenomena, various inherent uncertainties are associated to any PSHA procedure and computation. So, it is important to treat and handle these uncertainties in the seismic hazard computation in a logical way so that the hazard results can be considered appropriately. The usual way to deal with uncertainties is to design a logic-tree formulation.

In the current work, a logic-tree framework (Fig. 5-5) is considered only for the delineated Egyptian shallow seismic sources. After a detailed sensitivity analysis, only the two most crucial parameters (the b -value and M_{max}), together with the GMPEs, are included and considered in its design. A total of 36 branches were set up for each seismic source, representing each one an alternative seismic hazard scenario. The selection of the GMPE is much more critical in the final hazard results than uncertainties in any seismic source parameter. Concerning the three main seismic parameters to be considered for each seismic source, that is, b , rate of earthquakes above magnitude 4.0, and M_{max} , the sensitivity analysis was carried out as follows. In more than 30 cities included in the different seismic sources, seismic hazard was computed using a fixed GMPE and two of the three quoted parameters, and using for the third one the mean, mean+sigma and mean-sigma values for all the considered sources. The M_{max} parameter was the most critical one in the assessment, followed by the b -value. No noticeable influence was observed when varying the rate of earthquakes above magnitude 4.0 in the quoted range (mean \pm sigma).

The input parameters, for the b -value and M_{max} , are defined by three values, consisting of a preferred mean value (higher weight) and higher (+ σ) and lower (- σ) values. In the weighting process, we tried to consider subjective weights reflecting as possible our confidence in the different values for the two parameters, and following some published works (e.g., Cheng *et al.*, 2007; Aldama-Bustos *et al.*, 2009). Weights of 0.2 ($b-\sigma$), 0.6 (mean b -value) and 0.2 ($b+\sigma$) were used for the Gutenberg-Richter b -value, while weights of 0.3 ($M_{max}-\sigma$), 0.4 (mean M_{max}) and 0.3 ($M_{max}+\sigma$) were assigned to the M_{max} value, for each seismic source (Fig. 5-5). However, regarding the selected GMPEs, it is common to use uniform weights for different branches (e.g., Petersen *et*

al., 2008; Sutiwanich *et al.*, 2012; Kolathayar and Sitharam, 2012), representing equal levels of the analyst’s confidence. From our side, an equal weight to the four considered GMPEs for the Egyptian shallow seismic sources (Fig. 5-3) has been proposed, because it was difficult, without acceleration records, to decide what the most suitable one for the region is.

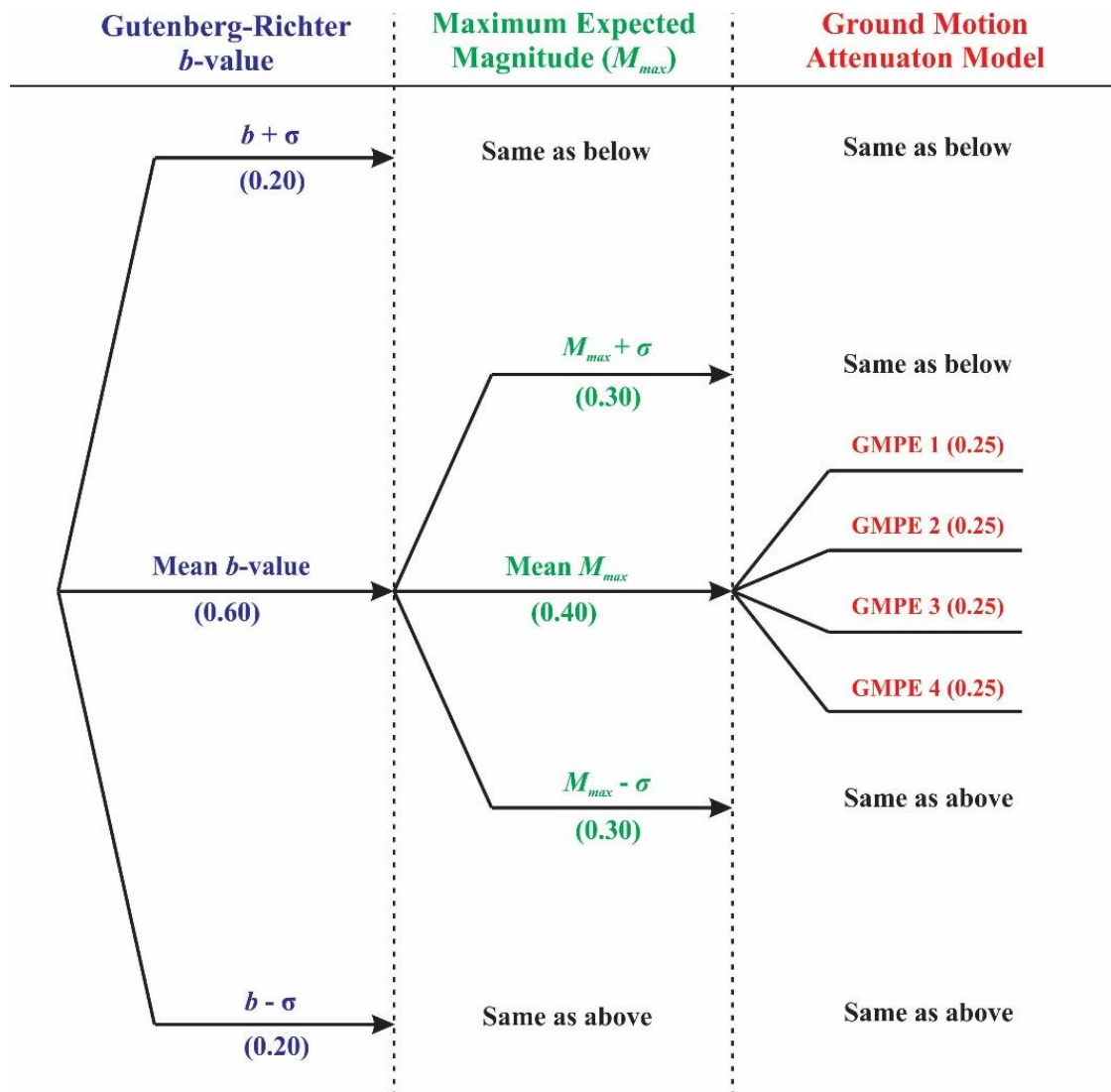


Figure (5-5): Logic-tree design applied in the current study.

The PSHA procedure applied in the current work is the standard one, which based on the Cornell (1968) methodology. The seismic hazard has been computed using the well-known total probability theorem, expressed in terms of the rate of exceedance of a certain level of ground motion for rock-site conditions. Rock is characterized by a V_s^{30} value equals to 760 m/s, corresponding to the soil type A in the current Egyptian building code (ECP-201, 2011) and the Eurocode 8 (EC-8, 2004) classifications. The computations were performed using the CRISIS 2014 software code, for grid points covering the Egyptian territory at a spacing of $0.1^\circ \times 0.1^\circ$ (about 10 km x 10 km). This

software requires the following parameters, for each seismic source zone, in order to specify the Poisson model: i) the M_{\min} to be used in the integration process, which considered in our case to be equal to M_W 4.0 for all seismic sources, ii) the rate of occurrence for earthquakes of magnitude equal or greater than M_{\min} , iii) the Gutenberg-Richter beta value $\beta = b \cdot \ln(10) \approx 2.3 \cdot b$, and iv) the M_{\max} for each seismic source. In addition, to account for epistemic uncertainties, the coefficients of variation for β and M_{\max} are considered.

Regarding the GMPEs, the CRISIS 2014 software code admits three families of GMPEs: attenuation tables furnished by the user, built-in parametric models, and generalized attenuation models. For this assessment, attenuation tables for the previously mentioned GMPEs were built following the same structure defined in and compatible with the CRISIS 2014 software. Finally, the seismic hazard results are given for each computation site, in terms of probabilities of exceeding a given ground-motion intensity value in different return periods.

Among all the seismic hazard results computed for Egypt, contour maps for rock-site conditions (Fig. 5-6) for mean PGA and SA (for a 5% damping ratio) at 0.2- and 1.0-s natural periods, with a 10% and 5% probability of exceedance in 50 years are shown. The reason for selecting these two natural periods is that seismic hazard values for spectral periods of 0.2 and 1.0 s are representative, to some extent, of the overall UHS shape. Moreover, these two values permit the application of the Malhorta (2005) procedure, which based on the Newmark-Hall approach (Newmark and Hall, 1982), to establish a design spectrum for specific places. Moreover, including only seismicity data does not seem reliable to compute seismic hazard values for return periods above 975 years (5% probability of exceedance in 50 years).

In addition to these results, specific hazard curves (Fig. 5-7) as well as specific UHS (Fig. 5-8), for rock-site conditions, for twelve selected cities, are depicted. The choice of the selected cities is mainly based on their population density, geographic distribution and their socio-economic importance. The selected cities are also representative of the regions with different tectonic and seismic environments in the Egyptian territory. As a result, from the computed UHS, different characteristic values (mean PGA, SA_{\max} , SA (0.2-s) and SA (1.0-s)) for the selected cities were derived for the two considered return periods (Table 5-3).

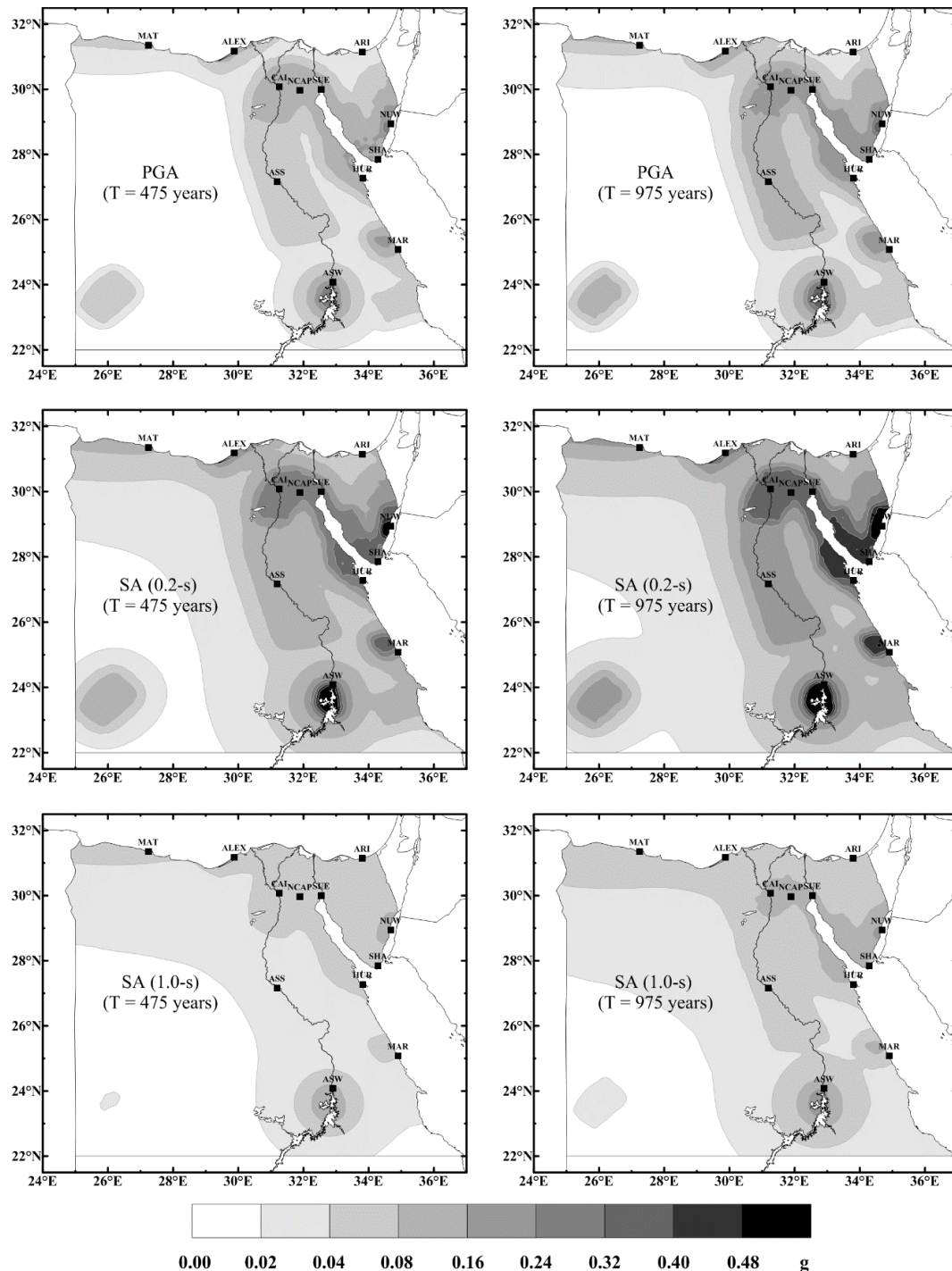


Figure (5-6): Seismic hazard maps (for rock-site conditions) depicting mean PGA, SA (0.2-s) and SA (1.0-s) for return periods of 475 and 975 years. [ALEX: Alexandria, ARI: El-Arish, ASS: Assiut, ASW: Aswan, CAI: Cairo, HUR: Hurghada, MAR: Marsa Alam, MAT: Matruh, NCAP: New Capital, NUW: Nuweiba, SHA: Sharm El-Sheikh, SUE: Suez].

5.4 RESULTS AND DISCUSSION

The iso-acceleration maps (Fig. 5-6) delineate the Gulf of Aqaba region with relatively higher seismic hazard from the rest of the country, which is characterized by its relatively moderate seismic hazard levels. For a return period of 475 years, in this region values up to 0.36, 0.89 and 0.76 g for mean PGA, SA (0.1-s) and SA (0.2-s), are

reached, respectively, for rock-site conditions. This region coincides with the location of the m_b 5.8, 3 August 1993 and M_W 7.2, 22 November 1995 Gulf of Aqaba earthquakes, which the last one considered as the biggest earthquake event shocked Egypt since 1900 until now. This area appears to be the region, including Nuweiba city, which generating the higher seismic hazard level, independently of the considered return period. For Nuweiba, they have been obtained values of 0.29 and 0.64 g for the mean PGA and SA (0.2-s), respectively, for the same return period.

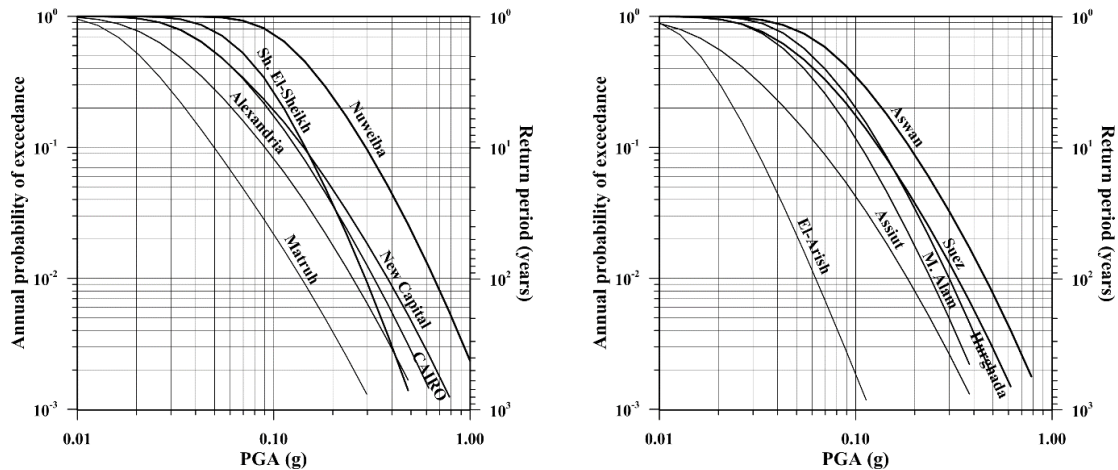


Figure (5-7): Seismic hazard curves for the selected cities depicted in Figure (5-6).

In a decreasing order of seismic hazard values, a second higher hazard area appears at the southern part of Egypt, to the south of Aswan city. For a return period of 475 years, it is characterized by maximum hazard values of 0.30, 0.71 and 0.64 g for mean PGA, SA (0.1-s) and SA (0.2-s), respectively, for rock-site conditions (Fig. 5-6). It also coincides with some well-known earthquakes in this region (e.g., M_S 5.6, 14 November 1981 and M_L 5.6, 23 April 1982 Kalabsha earthquakes), related mainly to the seismic activity along Kalabsha Fault and the surrounding faults. For Aswan, for a return period of 475 years, the obtained mean PGA and SA (0.2-s) values are 0.19 and 0.42 g, respectively.

A third important seismic hazard area occurred at the southern part of the Gulf of Suez (in the surroundings of Sharm El-Sheikh and Hurghada cities). The biggest mean PGA, SA (0.1-s) and SA (0.2-s) values, for a return period of 475 years and rock-site conditions are 0.19, 0.50 and 0.40 g, respectively (Fig. 5-6). This area coincides with the reported locations of some well-known earthquakes (e.g., M_S 6.9, 31 March 1969 and m_b 5.7, 28 June 1972 Shedwan Island earthquakes). The computed mean PGA and SA (0.2-s) values are 0.15 and 0.30 g, for Sharm El-Sheikh city, and 0.13 and 0.29 g, for Hurghada city.

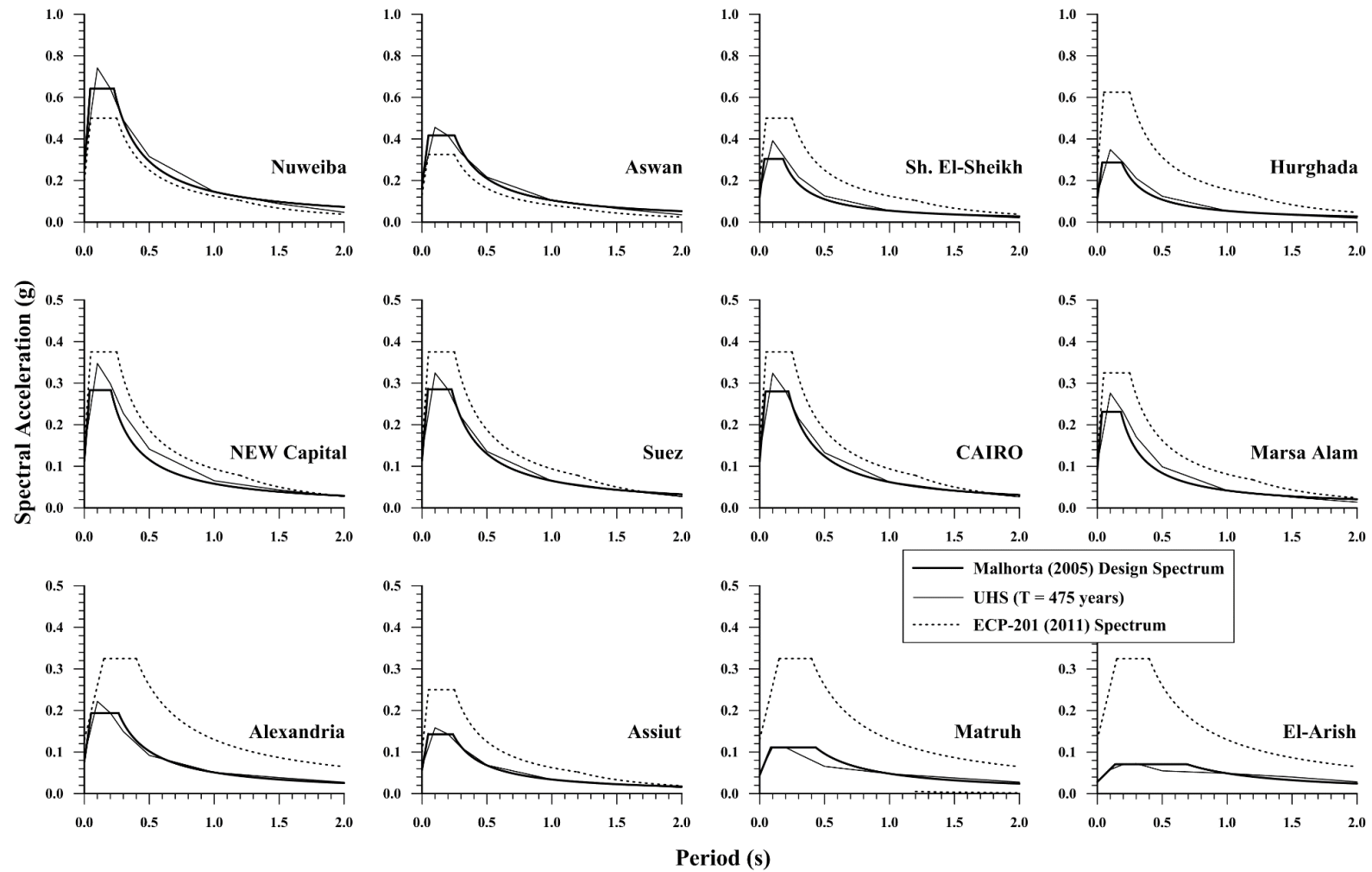


Figure (5-8): UHS, ECP-201 (2011) elastic design spectra, and Malhorta (2005) proposed design spectra, all damped at 5%, for rock-site conditions and for a return period of 475 years, for the considered cities.

A fourth area lies at the western coast of the Red Sea, near the city of Marsa Alam. For a return period of 475 years, biggest computed mean PGA, SA (0.1-s) and SA (0.2-s) values equal to 0.19, 0.48 and 0.39 g, are reached, respectively, for rock-site conditions (Fig. 5-6). This area passed with some low- to moderate-size earthquakes (e.g., M_S 5.3, 12 November 1955 and m_b 5.1, 2 July 1984 Abu Dabbab events), which in turn represent the main reason of such values of seismic hazard. The mean PGA and SA (0.2-s) values for Marsa Alam are 0.11 and 0.23 g, respectively.

A fifth area lies in the surrounding region of Cairo, including the proposed New Capital city and the most important archeological sites, which is related to several historical and instrumental events (e.g., M_S 5.9, 12 October 1992 Dahshour earthquake). For a 475 years return period and for rock-site conditions (Fig. 5-6), this area reaches biggest mean PGA, SA (0.1-s) and SA (0.2-s) values of 0.14, 0.35 and 0.31 g, respectively. The mean PGA and SA (0.2-s) values for Cairo are 0.13 g and 0.28 g, respectively. Approximately the same values are obtained for the New Capital city as it can be seen from Table (5-3).

Finally, a last area appears in the surroundings of Alexandria, along the Mediterranean Sea coast, from the seismic hazard point of view. For a return period of 475 years and for rock-site conditions (Fig. 5-6), values of 0.09, 0.23 and 0.20 g have been obtained for the biggest mean PGA, SA (0.1-s) and SA (0.2-s) values, respectively. This seismic hazard is mainly related to some moderate-size far earthquakes such as the m_b 6.5 (M_S 6.4), 12 September 1955 offshore Alexandria event. For Alexandria, the mean obtained PGA and SA (0.2-s) values are 0.09 and 0.19 g, respectively.

In addition to the described seismic hazard maps, Figure (5-7) shows the computed hazard curves, and Figure (5-8) displays the UHS, for a return period of 475 years, in relation to both of the current Egyptian building code (ECP-201, 2011) elastic response spectra and the Malhorta (2005) proposed design spectra, at the selected cities. Moreover, Table (5-3) shows the computed SA values (for return periods of 475 and 975 years) for the same cities, in comparison with PGA values (for a return period of 475 years) considered in the GSHAP (1999) and later in the current Egyptian building code (ECP-201, 2011). The displayed SA values, in the current study, are the PGA (SA (0.0-s)), maximum spectral acceleration (SA_{max}) and its related natural period (T_{max}), and SA (0.2-s) and SA (1.0-s) values.

From the UHS (Fig. 5-8), it is more noticeable that the greatest computed seismic hazard value among the selected cities was obtained at Nuweiba, as mentioned before, reaching a mean PGA value of 0.29 g, and a SA_{\max} value of 0.74 g for a return period of 475 years. In addition, it is clear that SA_{\max} values for all cities were noticed at natural periods of about 0.1-s (one-story buildings), which characterize the Egyptian territory. Furthermore, it is clear that there are some clear differences between the computed UHS for some cities, and the elastic response spectra considered in the Egyptian building code. Higher seismic hazard values were obtained for Nuweiba and Aswan cities than those included in the Egyptian building code. These two cities exhibit the higher seismic hazard values among all main Egyptian cities. For other cities, the computed mean PGA gives nearly the same values (Cairo, Suez and Assiut) or lower ones (e.g., Matruh and Alexandria) than those considered in the Egyptian code.

The differences between the current computed seismic hazard values and those included in the Egyptian building code, for the same cities, can be attributed to several factors: i) the unified earthquake catalogue, in our assessment, is more updated (until 2013) and complete than the catalogue used in the assessment by Riad *et al.* (2000) (until 1996) considered by the GSHAP (1999), ii) the delineated and considered seismic sources in the current study is different than those considered in the previous assessments, especially for the EMR and the southern and northeastern parts of Egypt, which mainly control the contribution of the seismic hazard in the region, iii) in this assessment, a different combination of GMPEs has been used, than that considered in the current Egyptian building code, so it is expected to get different results, and iv) the current seismic hazard computations incorporates the variability in different parameters through a logic-tree approach (b -value, M_{\max} and GMPEs) which in turn represents one of the major reasons for such differences.

Finally, an attempt has been done to shed more light on some relationships between the different computed ground-motion parameters obtained in the current seismic hazard assessment, in particular, mean PGA and SA_{\max} values, for the computed return periods. Two relationships have been tried in the same way as those obtained for Northern Algeria by Peláez *et al.* (2006) and Hamdache *et al.* (2012). The comparison between seismic hazard values obtained for the same ground-motion parameter for return periods of 475 and 975 years provides a clear linear relationship (Fig. 5-9). These relationships imply that mean PGA and SA_{\max} values of the UHS damped at 5% for a return period of 975 years (5% probability of exceedance in 50

years) in any location, are approximately 1.3 times those values for the same parameter for a return period of 475 years (10% probability of exceedance in 50 years), which coincides with Peláez *et al.* (2006) and Hamdache *et al.* (2012) results for Northern Algeria. It appears as an important and interesting result independently of the used seismic hazard approach and the considered GMPE. Hence, from the above mentioned relationships, from mean PGA and SA_{\max} values for a specific return period, it is possible to infer in a reliable way the values of the two parameters for the other return period.

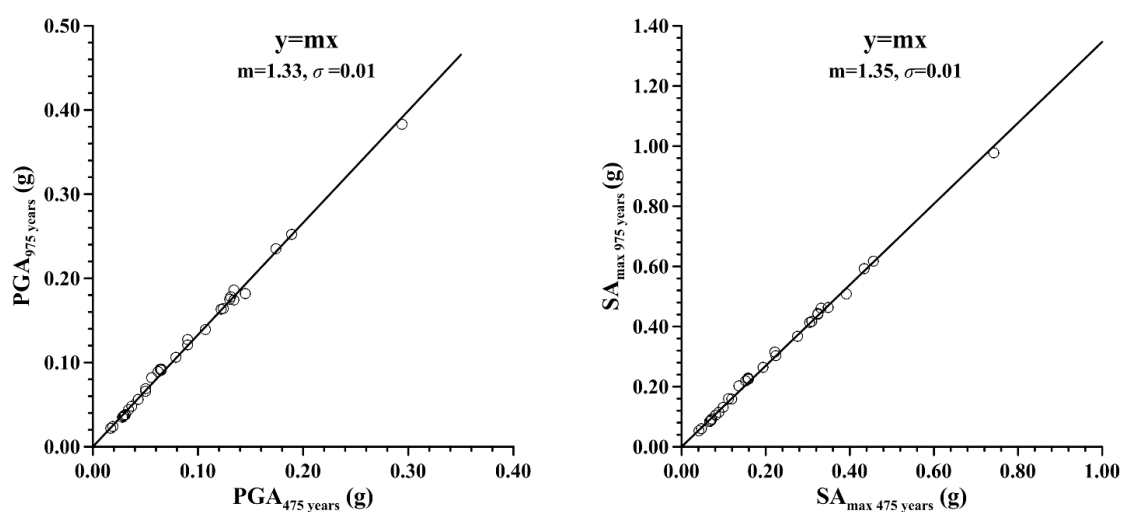


Figure (5-9): Relationships between mean PGA and SA_{\max} values for the two computed return periods.

5.5 CONCLUSIONS

The current study presents a new and up-to-date PSHA for Egypt. In this work, an attempt has been made to reach a significant improvement in the seismic hazard with the aid of a new updated and unified earthquake catalogue, and a new seismic source model. Moreover, well-known worldwide GMPEs were selected and incorporated into a logic-tree design to treat the uncertainties.

We presented here the results as PGA and SA maps, for rock-site conditions at different natural periods, with 10% and 5% probability of exceedance in 50 years. Moreover, seismic hazard curves and UHS for twelve Egyptian cities have been specifically derived in comparison to the elastic response spectra in the current Egyptian building code. According to this assessment, the highest seismic hazard values occur at the Gulf of Aqaba region which experienced the biggest recorded Egyptian earthquake (M_W 7.2, 22 November 1995 event). At Nuweiba, and for a return period of 475 years, computed values of 0.29 and 0.64 g for mean PGA and SA (0.2-

s), respectively, were obtained. Away from Nuweiba, other important seismic hazard areas are observed at Nasser's Lake (Southern Egypt), along the southern part of the Gulf of Suez and near Shedwan Island, at the surrounding region of Cairo, and near Abu Dabbab area (Eastern Desert of Egypt). All those regions exhibit moderate to high earthquake activity, both in the historical and recent times, which in turn contributes to the seismic hazard.

Finally, when comparing the computed UHS for the selected cities with mean PGA values (for a return period of 475 years) included in the most recent Egyptian building code, significant differences were noticed among the UHS and elastic design spectra, especially for some important cities (e.g., Aswan). It is concluded that a change in the seismic hazard representation of the current Egyptian building code is required in terms of the definition of the seismic hazard values, as well as a new definition of the elastic response spectra for each city.

5.6 DATA AND RESOURCES

All data used in this work came from published sources listed in the References section. The CRISIS 2014 (Ordaz *et al.*, 2014) code was provided directly by the authors.

5.7 ACKNOWLEDGMENTS

This research work was supported by the Egyptian Ministry of Higher Education (Cultural Affairs and Missions Sector, Cairo) and the Spanish Seismic Hazard and Active Tectonics research group. We thank Associate Editor Matt Gerstenberger and two anonymous reviewers for thoughtful comments.



Chapter 6

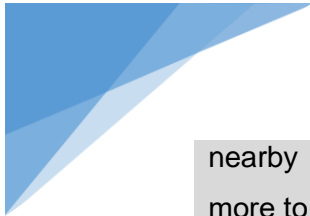
Probabilistic Seismic Hazard Deaggregation for Selected Egyptian Cities

Sawires, R., Peláez, J.A., Fat-Helbary, R.E., Panzera, F., Ibrahim, H.A., and Hamdache, M. (2017). Probabilistic seismic hazard deaggregation for selected Egyptian cities. *Pure and Applied Geophysics* 174, 1,581-1,600.

ABSTRACT

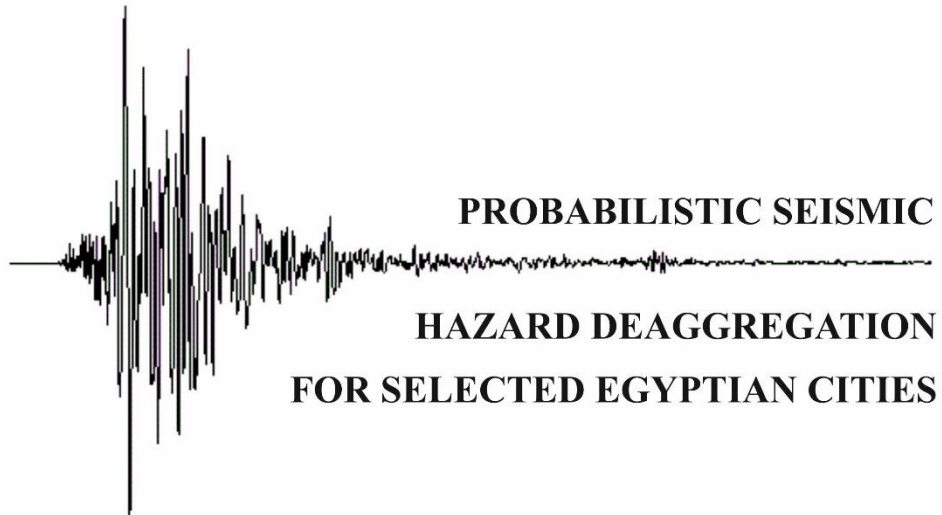
A probabilistic seismic hazard analysis in terms of peak ground acceleration (PGA) and spectral acceleration (SA) values has been performed for the Egyptian territory. Eighty-eight potential seismic sources (for shallow- and intermediate-depth seismicity) in and around Egypt were identified and characterized based on an updated and unified earthquake catalogue spanning the time period from 2200 B.C. until 2013 A.D. A logic-tree approach was followed, after a sensitivity analysis, to consider the epistemic uncertainty in the different input parameters, including the selected ground-motion attenuation models in order to predict the ground motion for the different tectonic environments. Then the seismic hazard deaggregation results, in terms of distance and magnitude, for the most important cities in Egypt has been computed to help understanding the relative contributions of the different seismic sources. Seismic hazard deaggregation, in particular, was computed for PGA and SA at periods of 0.2, 1.0 and 2.0 s for rock-site conditions, and for 10% probability of exceedance in 50 years.

In general, the results at most of the cities indicate that the distance to the seismic sources which mostly contributes to the seismic hazard is mainly controlled by the



nearby seismic sources (especially for PGA). However, distant events contribute more to the hazard for larger spectral periods (for 1.0 and 2.0 s). A significant result of this type of work is that seismic hazard deaggregation provides useful data on the distance and magnitude of the contributing seismic sources to the hazard in a certain place, which can be applied to generate scenario earthquakes and select acceleration records for seismic design.

HEADINGS:		Page
6.1	Introduction.....	150
6.2	Methodology.....	152
6.2.1	Seismic Source Model.....	153
6.2.2	Recurrence Model for Seismic Sources.....	154
6.2.3	Ground-Motion Attenuation Model.....	155
6.2.4	Logic-Tree Framework.....	156
6.2.5	Seismic Hazard Computations.....	158
6.2.6	Seismic Hazard Deaggregation.....	159
6.3	Deaggregation Results.....	160
6.4	Summary and Conclusions.....	166
6.5	Acknowledgments.....	169



PROBABILISTIC SEISMIC HAZARD DEAGGREGATION FOR SELECTED EGYPTIAN CITIES

The amount of damage and the number of victims caused by an earthquake, in a particular region, depend on several factors such as magnitude, epicentral distance, population density, soil conditions and structural design of the buildings. Low- or moderate-magnitude earthquakes may be turned catastrophic in regions having poor building and construction practice. The most effective way to prevent or even reduce the earthquake damage is the seismic design of buildings and structures.

6.1 INTRODUCTION

The hazard curves and the UHS, which represent the main output from PSHA, represent the overall effect of all pair earthquakes (magnitudes and distances) on the probability of exceeding a specific ground-motion level. In this case, all applied seismic sources, magnitudes and distances are mixed together, so that it is difficult to understand which seismic foci are controlling the seismic hazard in a particular site.

The seismic hazard values can be processed and exploited in order to define the predominant seismic sources of hazard and to provide design magnitudes and distances throughout the so-called *deaggregation* process (e.g., Harmsen and Frankel, 2001). Seismic hazard deaggregation was performed for the first time by Bernreuter (1992). Since this time, deaggregation studies were extensively applied, discussed and improved by many authors (e.g., Frankel, 1995; McGuire, 1995; Bazzurro and Cornell, 1999; Harmsen *et al.*, 1999; Harmsen and Frankel, 2001; Peláez *et al.*, 2002; Tselentis and Danciu, 2010; Abdi *et al.*, 2013).

Deaggregation analysis represents an important tool in understanding the seismic hazard (e.g., Bazzurro and Cornell, 1999). It enables dividing the total seismic hazard, at a certain specific site, into magnitude and distance contributions, as well as it

recommends suitable solutions for the design earthquakes required by engineers for the building purposes (McGuire, 1995). Thus, it becomes an important tool in interpreting and understanding the contribution of the different sources used to the seismic hazard values. Moreover, it enables the engineers and the decision-makers to identify the predominant hazardous earthquakes for each studied place, and provides guidance in the selection of scenario earthquakes for their design.

Egypt is situated in the northeastern corner of the African Continent, along the southeastern corner of the EMR (Fig. 6-1). Its seismotectonic framework can be described in the context of the surrounding plate boundaries: the African-Eurasian convergent plate margin, the Gulf of Suez-Red Sea divergent plate margin, and the DST. The seismicity of Egypt (Fig. 6-2) is mainly due to the tectonic deformation and the relative movement between the African Plate and the surrounding ones (Eurasian and Arabian Plates).

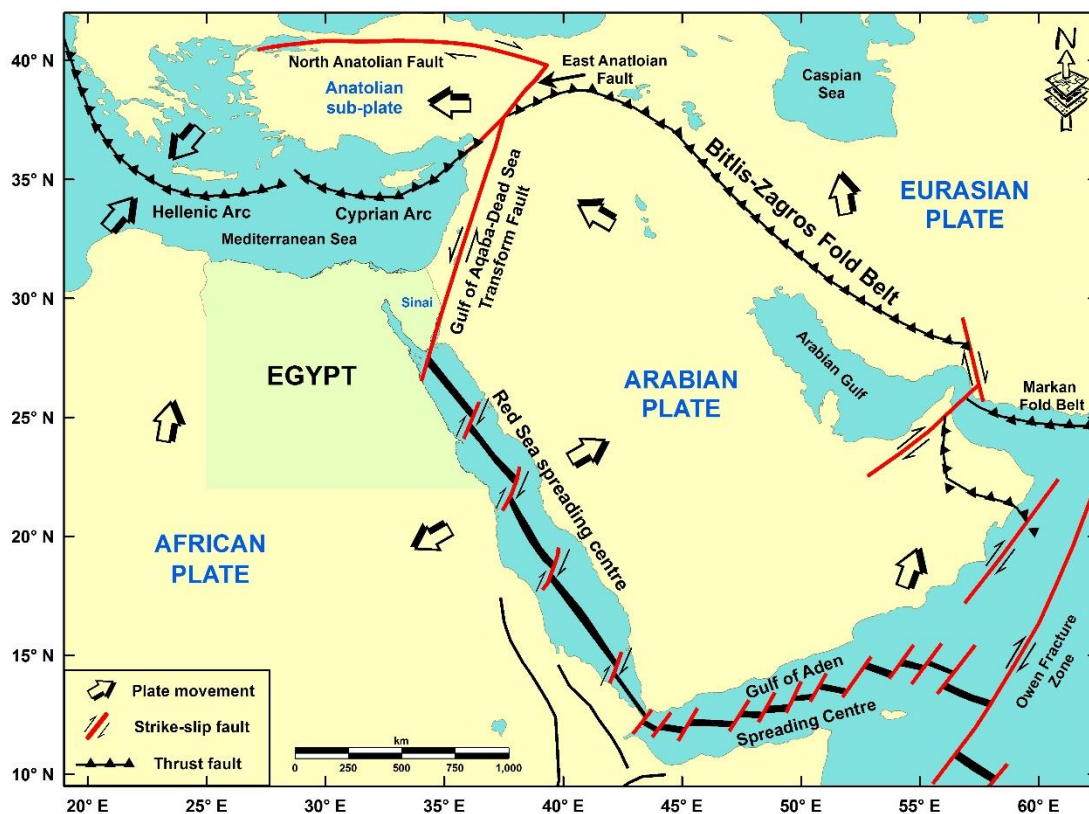


Figure (6-1): Global tectonic sketch for Egypt and its vicinity (compiled and replotted after Ziegler, 2001, and Pollastro, 2003).

Although Egypt is characterized by low to moderate seismic activity (Abou Elenean and Hussein, 2007), it has experienced local damaging earthquakes (e.g., M_s 5.9 October 12, 1992 Cairo earthquake), as well as significant earthquakes from the EMR, Southern Palestine and the Northern Red Sea regions (Ambraseys *et al.*, 1994).

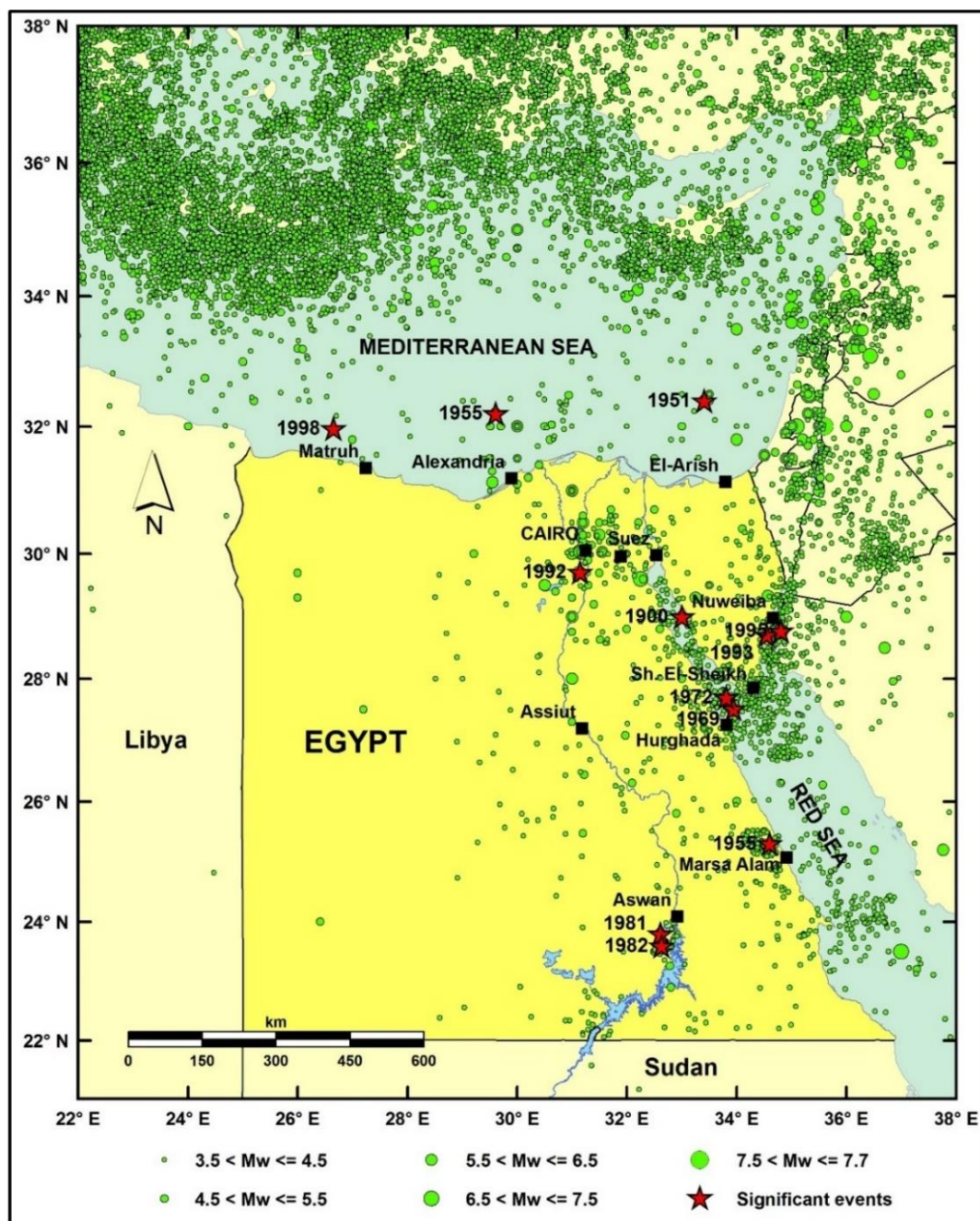


Figure (6-2): Distribution of the shallow seismicity ($h \leq 35$ km) in and around Egypt.

In the present chapter, the seismic hazard values for the most important and geographically distributed cities in Egypt were deaggregated to determine the seismic sources that mostly contribute at hazard levels of 10% probability of exceedance in 50 years (return period of 475 years). This is, in turn, will help bridging the gaps between the seismic hazard assessment and the engineering applications.

6.2 METHODOLOGY

Following the standard PSHA methodology (Cornell, 1968; Esteva, 1970), a new updated PSHA of the Egyptian territory has been performed in terms of PGA and SA

values. This assessment consisted of the following steps: i) defining the potential seismic sources in and around the studied region, ii) characterizing the seismicity for each considered seismic source, iii) selecting suitable GMPEs, iv) computing the ground-motion values, by applying a logic-tree approach, and following the standard PSHA approach, and finally, v) computing seismic hazard deaggregation in terms of magnitudes and distances. In the following, a brief discussion about each mentioned step is given.

6.2.1 SEISMIC SOURCE MODEL

The definition and delineation of the seismic sources in a region, represent one of the main steps in any seismic hazard assessment (e.g., Peláez and López Casado, 2002; Peláez *et al.*, 2005; Panzera *et al.*, 2011). A new seismic source model for Egypt and its vicinity has been delineated and characterized. This was based on an updated earthquake catalogue spanning the time period from 2200 B.C. until 2013, and covering the region between 21°-38° latitudes and 22°-38° longitudes.

Earthquake data was obtained from different local (e.g., Maamoun *et al.*, 1984; Riad and Meyers, 1985; Kebeasy, 1990; Badawy and Horváth, 1999; and Riad *et al.*, 2004), regional and international sources (e.g., Ambraseys *et al.*, 1994; Engdahl *et al.*, 1998; ISC bulletin, 2011), as well as the ENSN bulletins (1998-2010). Earthquake magnitudes were reported in different scales (I_{max} , and m_b , M_S , M_W , m_D and M_L magnitudes), and came from a variety of sources. For establishing a unified magnitude scale, some relationships were specifically developed and considered to convert the reported sizes to the M_W scale. All non-Poissonian (dependent) events were identified and removed using the Gardner and Knopoff (1974) procedure. More than 16000 events above M_W 3.0 are representing the final catalogue of main earthquakes. Moreover, all available information, *i.e.*, seismicity (historical and instrumental), geological (active faults), seismotectonic (FMSs) and geophysical data (crustal thickness) were considered in the delimitation of the seismic sources.

The used model consisted of 88 seismic sources (shallow and intermediate-depth) covering different tectonic regimes in and around Egypt (Fig. 6-3). Many of the defined seismic zones are related to the earthquake distribution along the well-known active belts (e.g., the DST and the Gulf of Suez-Red Sea Rift). Twenty-eight shallow ($h \leq 35$ km) seismic sources were used to cover the seismic activity within the Egyptian territory. Moreover, 53 shallow ($h \leq 20$ km) seismic sources were considered after

SHARE (2013) project to take into account the shallow earthquakes in the EMR. Furthermore, 7 intermediate-depth ($20 \leq h \leq 100$ km) seismic sources were proposed to consider the intermediate-depth seismicity in the EMR.

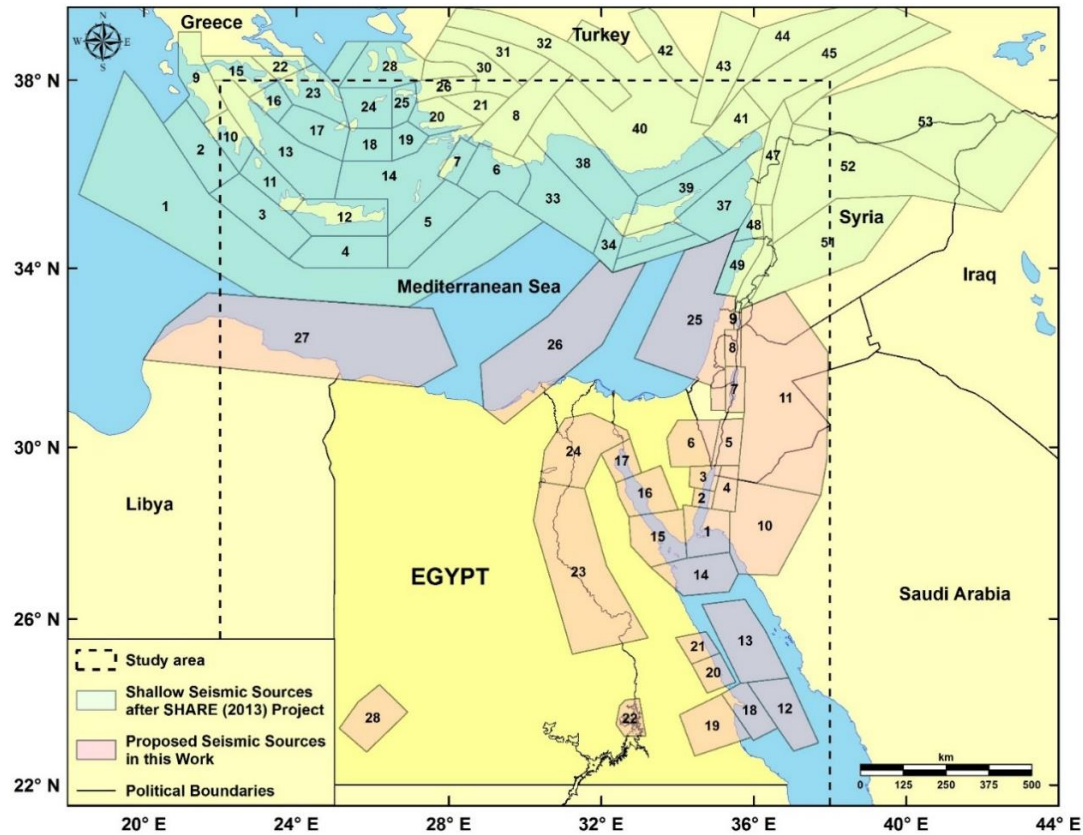


Figure (6-3): Considered shallow seismic sources in and around Egypt.

6.2.2 RECURRENCE MODEL FOR SEISMIC SOURCES

After the definition of the source boundaries, it was necessary to compute the seismicity parameters and the maximum magnitudes for each seismic source. Seismicity parameters for each considered zone were characterized in terms of the Gutenberg-Richter (1944) frequency-magnitude relationship. The total rate of earthquakes in a given source zone was estimated by calculating the cumulative rate of earthquakes in each magnitude interval using the complete portion of the catalogue. Finally, values of the slope (b -value) and intercept (a -value) were determined from a linear, least-squares regression on the logarithm of the cumulative rate of earthquakes versus magnitude.

Moreover, the M_{max} was computed using the Robson-Whitlock-Cooke procedure (Cooke, 1979; Robson and Whitlock, 1964; Kijko and Singh, 2011) and crosschecked against the paleoseismic data included in Deif *et al.* (2009, 2011). Table (6-1) shows the main seismicity parameters and their uncertainties for each defined shallow seismic

source that have been applied in the seismic hazard, taking into account that the considered M_{min} in the final computations was equal to M_W 4.0 for the whole Egyptian territory. For the shallow seismic sources in the EMR, the seismicity parameters and M_{max} values have been considered the same values as those published by SHARE (2013).

Table (6-1): b -values, annual rate of earthquakes above M_W 4.0, recorded M_{max}/I_{max} and expected maximum magnitude for the specifically characterized seismic sources.

Source zone	$b \pm \sigma$	$\lambda \pm \sigma$	Recorded M_{max}/I_{max}	Expected M_{Wmax}
01	1.13 ± 0.05	0.980 ± 0.083	m_b 4.4 on 2006/02/02	4.8 ± 0.2^A
02	0.98 ± 0.06	0.495 ± 0.064	M_W 7.2 on 1995/11/22	7.2 ± 0.3^B
03	0.97 ± 0.07	0.276 ± 0.044	I_{max} VIII-IX on 1212/05/02	6.2 ± 0.8^A
04	1.01 ± 0.05	0.196 ± 0.039	m_b 4.5 on 1995/12/26	4.6 ± 0.4^A
05	0.88 ± 0.06	0.188 ± 0.039	m_b 5.2 on 1956/12/18	7.5 ± 0.5^C
06	1.12 ± 0.10	0.185 ± 0.032	m_b 4.8 on 1927/09/24	4.8 ± 0.6^A
07	0.87 ± 0.08	0.323 ± 0.047	I_{max} VIII on 1458/11/12	5.8 ± 0.7^A
08	0.71 ± 0.02	0.187 ± 0.037	I_{max} IX on 746 A.D.	7.8 ± 0.8^A
09	0.91 ± 0.15	0.065 ± 0.027	I_{max} X on 19 A.D.	6.8 ± 0.6^C
10	1.03 ± 0.09	0.193 ± 0.035	I_{max} VIII on 1588/01/04	5.8 ± 0.7^A
11	0.97 ± 0.10	0.365 ± 0.063	I_{max} IX-X on 1159/06/06	6.9 ± 0.8^A
12	1.00 ± 0.05	0.436 ± 0.059	I_{max} VI-VII on 1121 A.D.	6.8 ± 0.6^B
13	0.91 ± 0.06	0.303 ± 0.044	m_b 4.7 on 2006/07/30	5.6 ± 0.3^A
14	1.13 ± 0.07	0.643 ± 0.061	m_b 5.0 on 1952/03/22	5.4 ± 0.6^A
15	1.06 ± 0.04	0.835 ± 0.079	M_W 6.8 on 1969/03/31	6.8 ± 0.3^B
16	0.80 ± 0.06	0.309 ± 0.040	M_S 6.2 on 1900/03/06	6.3 ± 0.6^A
17	0.86 ± 0.08	0.138 ± 0.029	M_S 6.6 on 1754 A.D.*	6.6 ± 0.6^B
18	1.29 ± 0.01	0.157 ± 0.025	M_L 4.5 on 1990/05/23	4.2 ± 0.4^A
19	1.15 ± 0.03	0.118 ± 0.022	M_L 3.9 on 1991/07/15	4.2 ± 0.4^B
20	1.20 ± 0.01	0.063 ± 0.016	M_L 4.7 on 1982/01/21	4.4 ± 0.3^A
21	0.87 ± 0.09	0.371 ± 0.042	m_b 6.2 on 1955/11/12	5.7 ± 0.6^A
22	0.79 ± 0.07	0.586 ± 0.060	M_W 5.8 on 1981/11/14	7.0 ± 0.4^C
23	0.73 ± 0.05	0.295 ± 0.051	I_{max} VIII on 857 A.D.	6.1 ± 0.7^A
24	0.99 ± 0.06	0.596 ± 0.076	I_{max} 9.5 on 1262 A.D.	6.8 ± 0.8^A
25	0.97 ± 0.08	0.520 ± 0.044	I_{max} X on 1546/01/14	7.2 ± 0.8^A
26	0.94 ± 0.07	0.598 ± 0.085	m_b 6.5 on 1955/09/12	6.6 ± 0.6^A
27	0.60 ± 0.03	0.713 ± 0.102	I_{max} VIII on 262 A.D.	6.0 ± 0.8^A
28	1.00 ± 0.06	0.150 ± 0.050	M_S 5.3 on 1978/12/09	5.3 ± 0.3^B

^A Computed using the Robson-Whitlock-Cooke procedure (Kijko and Singh, 2011). ^B Equal to maximum recorded magnitude. ^C Taken from Deif *et al.* (2009, 2011).

6.2.3 GROUND-MOTION ATTENUATION MODEL

GMPEs are derived for specific geologic setting, tectonic environment and style of faulting, as well as soil conditions. Currently, due to the lack of ground-motion acceleration records in Egypt, there is no a specific GMPE for the country. Moreover,

the acceleration records available for Egyptian earthquakes are not enough even to check, given the magnitudes and distances of the earthquakes, the validity and compatibility of the selected GMPEs. Consequently, it was necessary to select well-known worldwide GMPEs to consider them in our assessment. Therefore, in the present study, following Cotton *et al.* (2006) and Boomer *et al.* (2010) guidelines, a total of six attenuation models have been selected. Two of them are kept fixed while the other four are considered in a logic-tree scheme.

The GMPEs of Ambraseys *et al.* (1996), Abrahamson and Silva (1997), Zhao *et al.* (2006) and Boore and Atkinson (2008), were used together, in a logic-tree approach, to model the ground motion for earthquakes within the shallow seismic sources covering Egypt. However, considering the large distance between the shallow seismic sources located in the EMR and the Egyptian northern coasts, other specific GMPEs were selected, in particular, the Tavakoli and Pezeshk (2005) ground-motion model for earthquakes occurring within the considered SHARE (2013) seismic sources, and Youngs *et al.* (1997) model for the intermediate-depth seismicity in the EMR.

Compatibility among the considered GMPEs was checked. Despite the fact that the different GMPEs use different types of distance (Joyner-Boore, rupture and hypocentral distance), the CRISIS 2014 (Ordaz *et al.*, 2014) software code, which was used to perform the current assessment, allows the use of different distance definitions for different models. Thus, distance conversions are not required. Moreover, the software takes into account the focal depth, making it possible to use GMPEs (e.g., Youngs *et al.*, 1997) in which the focal depth is considered as an independent variable.

In the current assessment, rock-site conditions ($V_{30}^S = 760$ m/s), which is corresponding to the boundary between NEHRP-A and NEHRP-B site classifications has been considered. The exception to this, being the GMPEs of Abrahamson and Silva (1997) and Zhao *et al.* (2006), in which they consider a lower boundary ($V_S^{30} > 600$ m/s) for rock sites. Finally, all chosen GMPEs consider different types of the faulting mechanism. However, in this assessment, the “unspecified” faulting-mechanism class has been applied for all seismic sources.

6.2.4 LOGIC-TREE FRAMEWORK

It is critical to handle the uncertainties related to different input parameters of the PSHA in a region, throughout the application of a logic-tree framework. In our

assessment, a logic-tree approach was considered only for the 28 shallow seismic sources covering Egypt (Fig. 6-4). After a detailed sensitivity analysis, the Gutenberg-Richter b -value, and the M_{max} , as well as the GMPEs were included in the final logic-tree design. Thirty-six branches are the total number of the seismic hazard scenarios represented by the considered logic-tree design. The corresponding weights assigned to each branch for b -values and M_{max} , as well as to the different GMPEs are shown in the logic tree (Fig. 6-4).

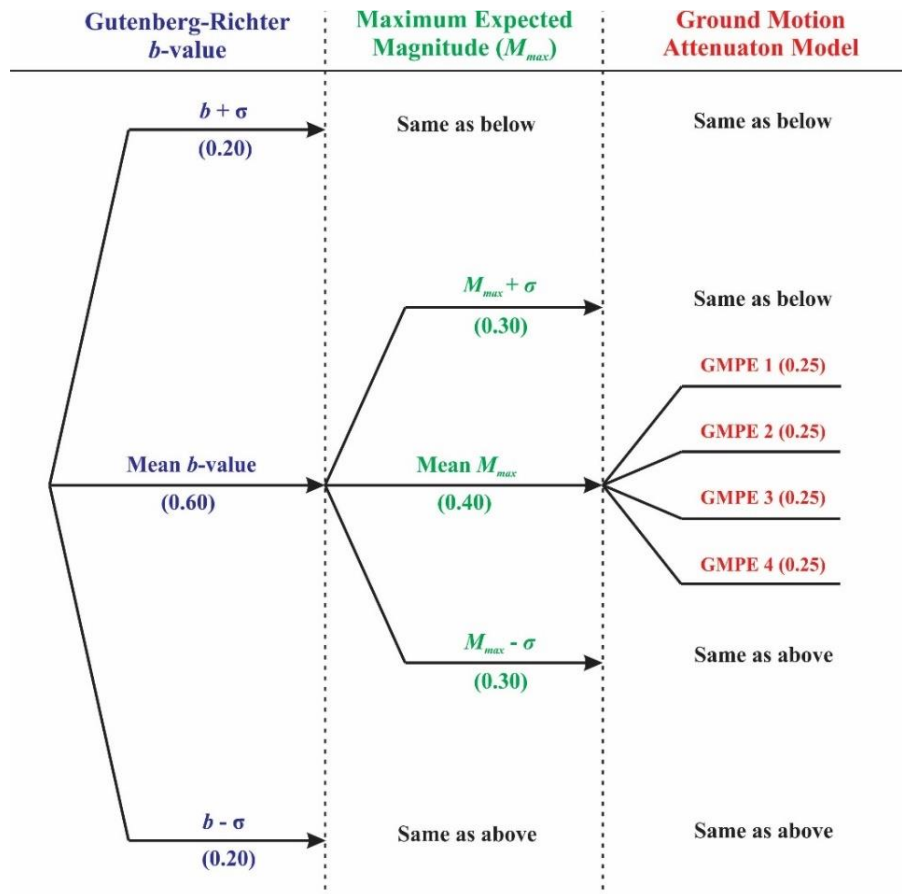


Figure (6-4): Logic-tree design applied in the current study.

The input parameters, for the b -value and M_{max} , are defined by three values, consisting of a preferred mean value (higher weight) and higher ($+\sigma$) and lower ($-\sigma$) values. Weights of 0.2 ($b-\sigma$), 0.6 (mean b -value) and 0.2 ($b+\sigma$) were used for the Gutenberg-Richter b -value, while weights of 0.3 ($M_{max}-\sigma$), 0.4 (mean M_{max}) and 0.3 ($M_{max}+\sigma$) were assigned to the M_{max} value, for each seismic source. However, regarding the selected GMPEs, an equal weight to the four considered GMPEs for the Egyptian shallow seismic sources has been used, because it was difficult, without acceleration records, deciding what the most suitable one for the region is. Those subjective weights are reflecting as possible our confidence in the different inputs for the mentioned parameters.

6.2.5 SEISMIC HAZARD COMPUTATIONS

The seismic hazard has been computed for rock-site conditions using the well-known probability theorem, in terms of the rate of exceedance of a specific level of ground motion. Computations have been done using a grid spacing of $0.1^\circ \times 0.1^\circ$ for the whole Egyptian territory, using CRISIS 2014 (Ordaz *et al.*, 2014) software code. The ground-motion results in this assessment were exported to ArcGIS© for the production of different seismic hazard maps. The final hazard results for Egypt have been presented for mean PGA and SA at a number of spectral periods (0.1, 0.2, 0.3, 0.5, 1.0, 1.5, and 2.0 s), with a 39.3%, 10%, and 5% probability of exceedance in 50 years (return periods of 100, 475, and 975 years, respectively). Here we show only the PGA and SA (0.2 s) maps for a return period of 475 years (Fig. 6-5).

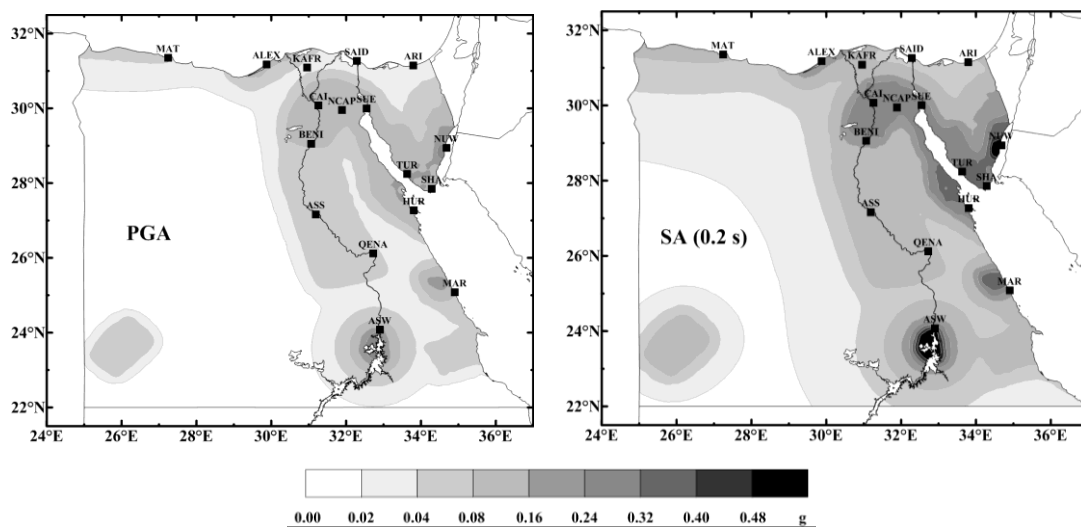


Figure (6-5): Mean seismic hazard values (PGA and SA (0.2 s)) for a 10% probability of exceedance in 50 years (return period of 475 years), for rock-site conditions. [ALEX: Alexandria, ARI: El-Arish, ASS: Assiut, ASW: Aswan, BENI: Beni Suef, CAI: Cairo, NCAP: New Capital, HUR: Hurghada, KAFR: Kafr El-Sheikh, MAR: Marsa Alam, MAT: Matruh, NUW: Nuweiba, QENA: Qena, SAID: Port Said, SHA: Sharm El-Sheikh, SUE: Suez, TUR: El-Tur]

PGA results (Fig. 6-5) show that the maximum PGA value (0.29 g) for a return period of 475 years, is occurred at Nuweiba, along the Gulf of Aqaba, very close to the epicentre location of the M_W 7.2, November 22, 1995 Aqaba earthquake. A second nucleus appears to the south of Aswan in Southern Egypt (PGA = 0.19 g), which coincides with the location of the M_S 5.6, November 14, 1981 Kalabsha earthquake. The third one is located in the southern triangle of the Sinai Peninsula (PGA at Sharm El-Sheikh and Hurghada cities are 0.15 g and 0.13 g, respectively), which in turn coincides with some reported earthquakes (e.g., M_S 6.9, March 31, 1969 Shedwan Island

earthquake). A fourth nucleus is observed at the surrounding of Cairo (PGA = 0.13 g), which also is related to several historical and instrumental events (e.g., M_S 5.9, October 12, 1992 Dahshour earthquake). Finally, another nucleus occurred near the city of Marsa Alam (Red Sea coast) (PGA = 0.11 g). This area hosted some low to moderate earthquakes (e.g., M_S 5.3, November 12, 1955 and m_b 5.1, July 2, 1984 Abu Dabbab earthquakes).

6.2.6 SEISMIC HAZARD DEAGGREGATION

In the present study, the seismic hazard values were deaggregated in terms of magnitude and distance (focal distance), following the methodology provided by Bazzurro (1998) and Bazzurro and Cornell (1999). In order to shed more light on the PSHA results, the deaggregation of the ground-motion values for 17 selected Egyptian sites has been assessed in terms of the magnitude and distance. The deaggregation was performed for four spectral periods (PGA, SA (0.2 s), SA (1.0 s) and SA (2.0 s)) at 10% probability of exceedance in 50 years (return period of 475 years), which are very significant in the seismic design of buildings.

The deaggregation was computed using CRISIS 2014 software, following the same procedure of the USGS (e.g., Harmsen *et al.*, 1999), defining magnitude bins equal to 0.5 and distance intervals equal to 25 km. In the current study, due to the application of the logic-tree methodology, which consists of 36 branches, it is not possible to get the final deaggregation results directly from the CRISIS 2014 software code. Thus, it was necessary to generate the deaggregation for each branch separately, then using its assigned weight we combined the 36 deaggregation files together for each studied location.

In the current work, each contribution of the different earthquake scenarios to the total value of the hazard was computed. Thus, it allows the identification of the so-called control (Bernreuter, 1992), design (McGuire, 1995), modal (Chapman, 1995) or dominant earthquake (Bazzurro and Cornell, 1999) for each studied location. The control earthquake can be defined using either the mean or the modal value of magnitude and source-to-site distance. The mean values are not always representing a realistic scenario. On the contrary, the modal values are corresponding to the magnitude-distance group that gives the largest contribution to the hazard and, consequently correspond to a more realistic source (Barani *et al.*, 2009). The expressions proposed

by Bernreuter (1992) were used here for the computation of the modal values for distances (\bar{D}) and magnitudes (\bar{M}):

$$\log \bar{D} = \frac{\sum_{bins} H_{md} \cdot \log d}{\sum_{bins} H_{md}} \quad (6-1)$$

$$\bar{M} = \frac{\sum_{bins} H_{md} \cdot m}{\sum_{bins} H_{md}} \quad (6-2)$$

where m is the magnitude, d is the distance, and H_{md} is the contribution to the seismic hazard of the magnitude m at a distance d from the studied site.

Then, by computing and comparing these two values, it is possible to determine whether the sources generating the hazard in a particular site are many or there is only one (Peláez *et al.*, 2002). Table (6-2) presents the deaggregation results in terms of both the modal and mean values.

6.3 DEAGGREGATION RESULTS

The deaggregation results were represented by bar charts for the magnitude, distance, and the contribution percentage to the seismic hazard values. Each bar represents a scenario earthquake whose magnitude and distance can be identified from the horizontal axes. The height of the bar indicates the relative contribution of a particular seismic event to the total seismic hazard in the studied location. These bar charts were plotted for all studied sites for all considered ground-motion spectral periods (PGA, SA (0.2 s), SA (1.0 s), and SA (2.0 s)).

The careful inspection of the deaggregation results (Fig. 6-6) suggests the possibility of the classification of the studied cities into three main groups based on the deaggregation shapes. The first typical simple deaggregation shape which has a unimodal distribution (single lobe), usually with the modal peak very close to the studied location and a tail which includes larger and more distant earthquakes. This shape of deaggregation is noticed for PGA for thirteen of the studied sites (Alexandria, Cairo, Suez, New Capital, El-Tur, Nuweiba, Sharm El-Sheikh, Assiut, Beni Suf, Hurghada, Marsa Alam, Qena and Aswan), where hazard is mainly due to a single seismic zone, more or less extensive, surrounding the city.

Table (6-2): Seismic hazard deaggregation results (mean and model values for both magnitude and distance) for the selected cities having 10% probability of exceedance in 50 years (return period of 475 years) for PGA, SA (0.2 s), SA (1.0 s) and SA (2.0 s).

City	PGA				SA (0.2 s)				SA (1.0 s)				SA (2.0 s)			
	Modal		Mean		Modal		Mean		Modal		Mean		Modal		Mean	
	M_w	D (km)	M_w	D (km)	M_w	D (km)	M_w	D (km)	M_w	D (km)	M_w	D (km)	M_w	D (km)	M_w	D (km)
Matruh	4.5-5.0	0-25	5.5	69.5	4.5-5.0	0-25	5.6	69.0	7.0-7.5	375-400	6.8	232.9	7.0-7.5	375-400	7.0	288.1
Alexandria	4.0-4.5	0-25	5.1	18.6	4.0-4.5	0-25	5.2	21.0	5.0-5.5	0-25	5.9	51.5	5.5-6.0	0-25	6.2	79.5
Port Said	7.0-7.5	375-400	6.6	223.6	7.0-7.5	375-400	6.5	195.0	7.0-7.5	375-400	7.0	297.9	7.0-7.5	375-400	7.1	331.8
El-Arish	7.0-7.5	375-400	6.7	211.1	6.5-7.0	175-200	6.6	185.7	7.0-7.5	375-400	7.1	269.2	7.0-7.5	375-400	7.2	308.2
Kafr El-Sheikh	5.5-6.0	50-100	6.0	90.2	5.5-6.0	50-100	6.0	90.5	6.5-7.0	75-100	6.7	148.6	7.0-7.5	375-400	6.9	185.9
CAIRO	5.0-5.5	0-25	5.3	17.6	5.0-5.5	0-25	5.4	19.3	5.0-5.5	0-25	6.0	35.2	6.0-6.5	0-25	6.3	42.5
Suez	5.0-5.5	0-25	5.3	17.1	5.0-5.5	0-25	5.4	18.8	5.5-6.0	0-25	6.0	37.8	5.5-6.0	0-25	6.3	49.9
El-Tur	4.0-4.5	0-25	5.1	16.1	4.0-4.5	0-25	5.2	18.6	6.0-6.5	25-50	5.9	34.9	6.0-6.5	25-50	6.1	46.6
Nuweiba	5.0-5.5	0-25	5.6	13.6	6.0-6.5	0-25	5.7	14.1	6.0-6.5	0-25	6.2	17.3	6.0-6.5	0-25	6.4	20.6
Sharm El-Sheikh	4.0-4.5	0-25	4.6	15.3	4.0-4.5	0-25	4.7	18.1	4.5-5.0	0-25	5.8	54.1	6.5-7.0	100-125	6.2	74.0
Assiut	4.0-4.5	0-25	5.2	21.3	4.5-5.0	0-25	5.2	23.8	5.0-5.5	0-25	5.8	64.1	5.5-6.0	0-25	6.1	84.9
Beni Suef	4.5-5.0	0-25	5.3	21.1	5.0-5.5	0-25	5.4	23.4	5.0-5.5	0-25	6.0	48.8	6.0-6.5	25-50	6.3	59.0
Hurghada	4.0-4.5	0-25	4.9	17.7	4.0-4.5	0-25	5.0	20.2	6.0-6.5	25-50	5.8	47.4	6.0-6.5	25-50	6.1	69.4
Marsa Alam	4.0-4.5	0-25	4.9	16.0	4.0-4.5	0-25	5.0	17.5	5.0-5.5	0-25	5.5	45.4	5.0-5.5	0-25	5.9	76.4
Qena	4.0-4.5	0-25	5.1	21.2	4.0-4.5	0-25	5.1	24.4	5.0-5.5	0-25	5.9	98.2	5.5-6.0	0-25	6.3	139.8
Aswan	5.5-6.0	0-25	5.8	15.5	5.5-6.0	0-25	5.9	16.4	6.0-6.5	0-25	6.3	23.2	6.0-6.5	0-25	6.5	27.2

In this case, using either the mean or the modal value to calculate the control earthquake, deaggregation provides results that nearly coincide. The mean distance values for the controlling earthquake, for this group of cities, are in the range of 14-21 km and 14-24 km, approximately, for PGA and SA (0.2 s), respectively. On the other hand, ensuring the fact that the longer the ground-motion period is, the more contributing distant earthquake are expected. For SA (1.0 s) and SA (2.0 s), the mean distance values for this group of cities are reaching values ranging from 17-98 km, and 21-140 km, respectively.

In the second group (Matruh and Kafr El-Sheikh), the deaggregation results also consists of a main lobe, as the sites mentioned in the first group. However, one or two secondary lobes begin to appear, that generate a small amount of seismic hazard. These secondary lobes, of less importance with respect to their contribution to the hazard, can nonetheless mean a noticeable difference between the control earthquakes computed using the mean or modal values in some cases. The distance mean values for Matruh are 70, 69, 233 and 288 km for PGA, SA (0.2 s), SA (1.0 s) and SA (2.0 s), respectively. However, for Kafr El-Sheikh, they are 90, 91, 149 and 308 km, for the same mentioned spectral periods.

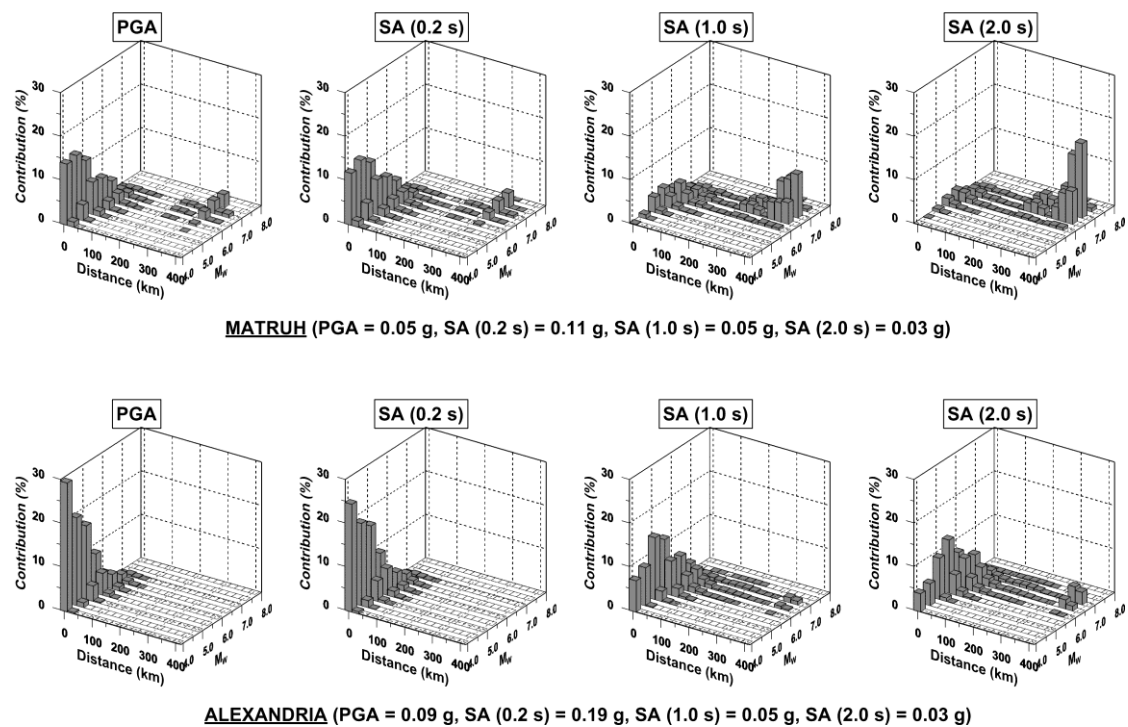


Figure (6-6): Deaggregation results showing the hazard contribution (%) in terms of magnitude and distance. It was computed for a return period of 475 years and for rock-site conditions.

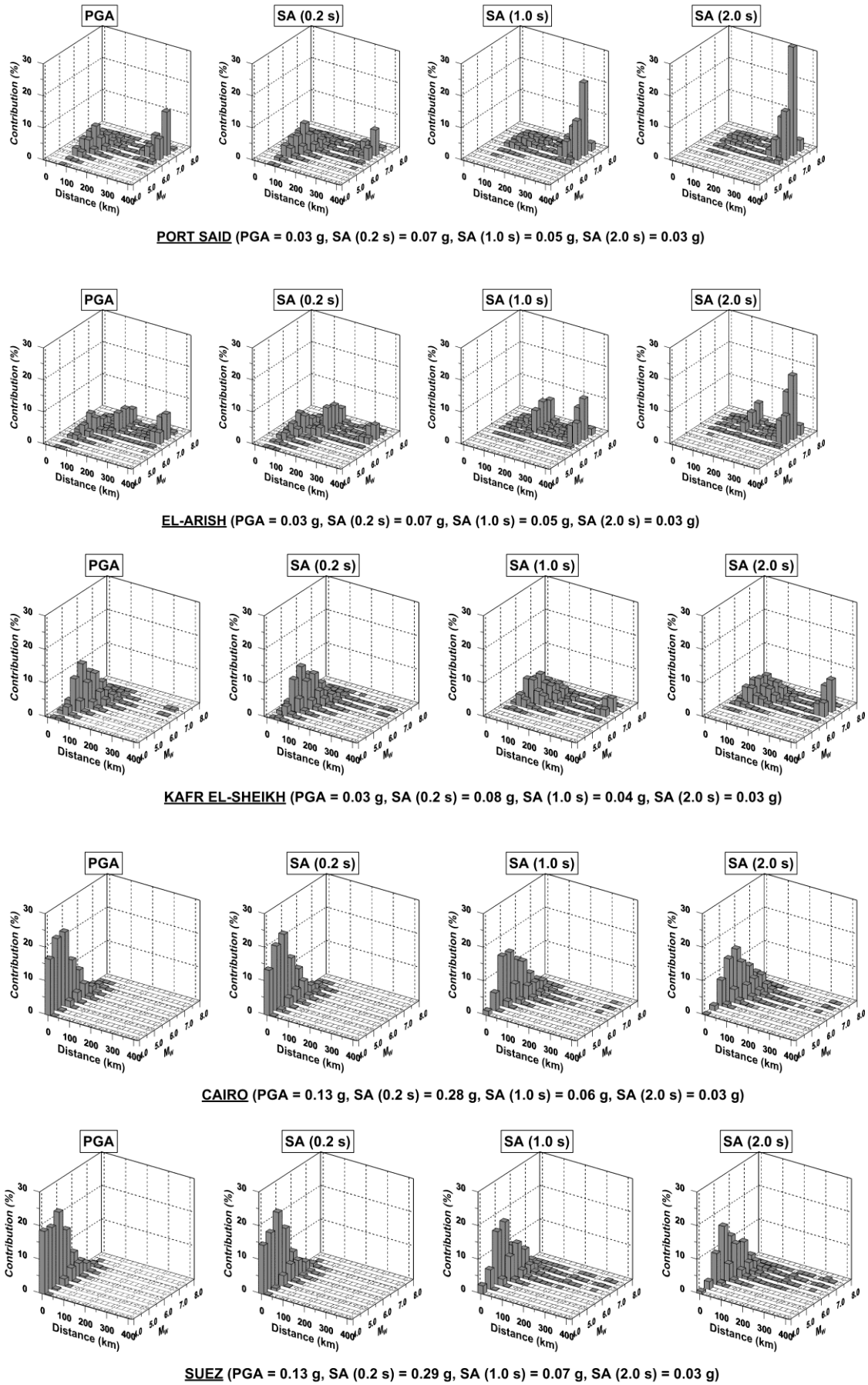
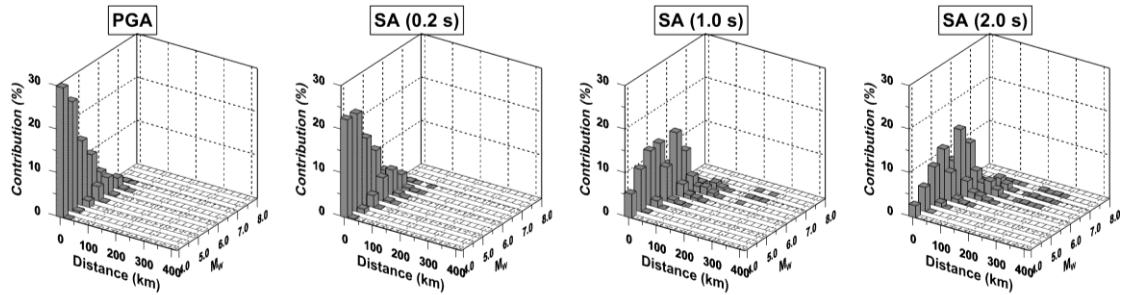
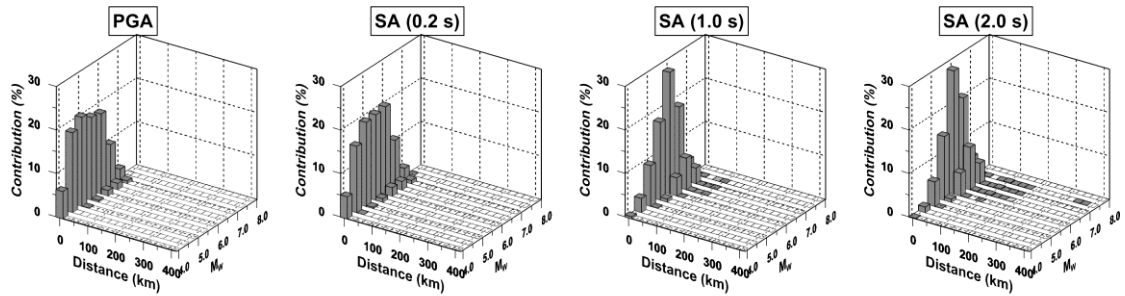


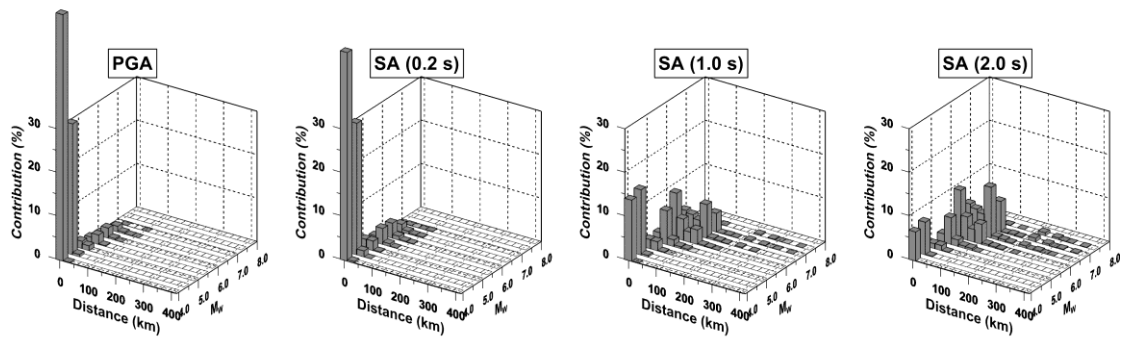
Figure (6-6): Continued.



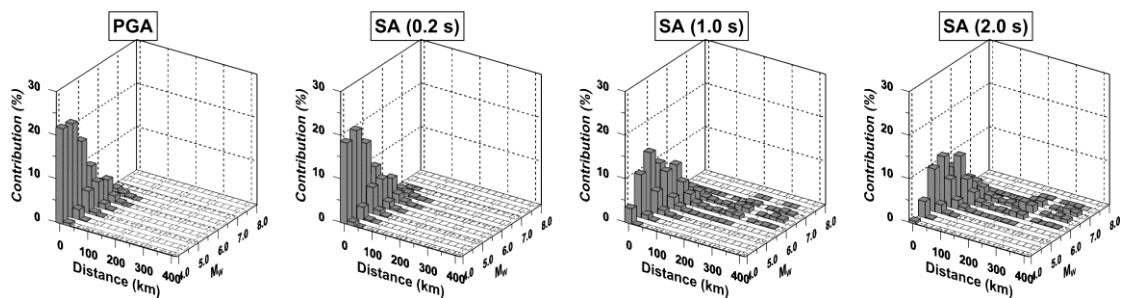
EL-TUR (PGA = 0.17 g, SA (0.2 s) = 0.37 g, SA (1.0 s) = 0.07 g, SA (2.0 s) = 0.03 g)



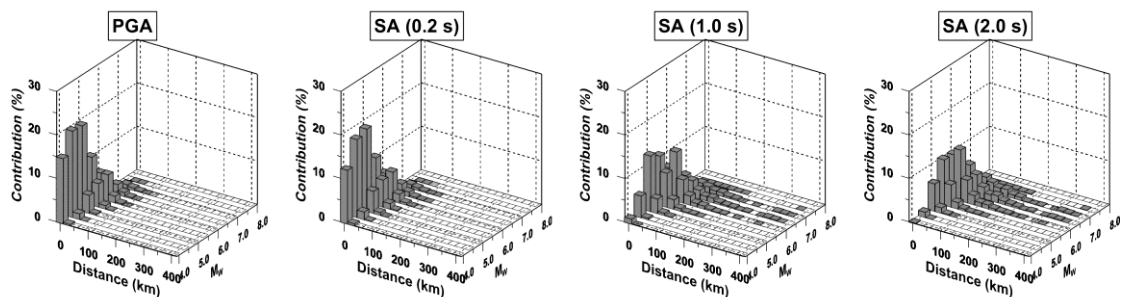
NUWEIBA (PGA = 0.29 g, SA (0.2 s) = 0.64 g, SA (1.0 s) = 0.15 g, SA (2.0 s) = 0.05 g)



SHARM EL-SHEIKH (PGA = 0.15 g, SA (0.2 s) = 0.30 g, SA (1.0 s) = 0.06 g, SA (2.0 s) = 0.02 g)

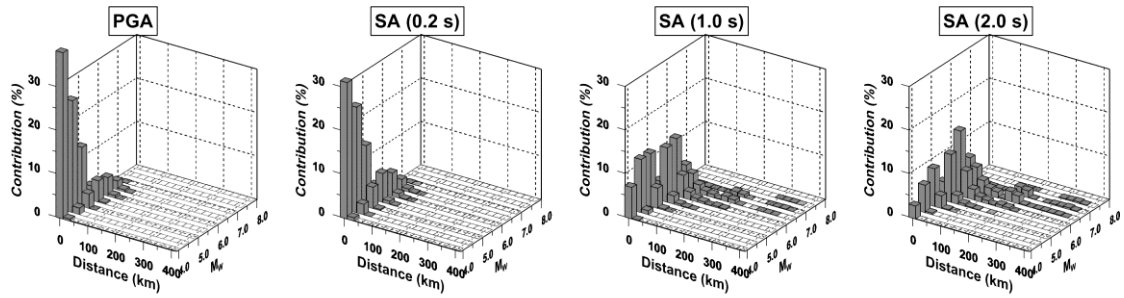


ASSIUT (PGA = 0.07 g, SA (0.2 s) = 0.14 g, SA (1.0 s) = 0.03 g, SA (2.0 s) = 0.01 g)

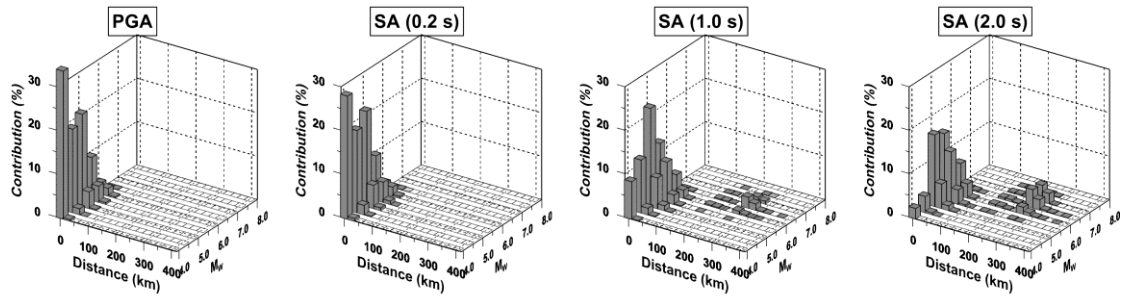


BENI SUEF (PGA = 0.09 g, SA (0.2 s) = 0.20 g, SA (1.0 s) = 0.05 g, SA (2.0 s) = 0.02 g)

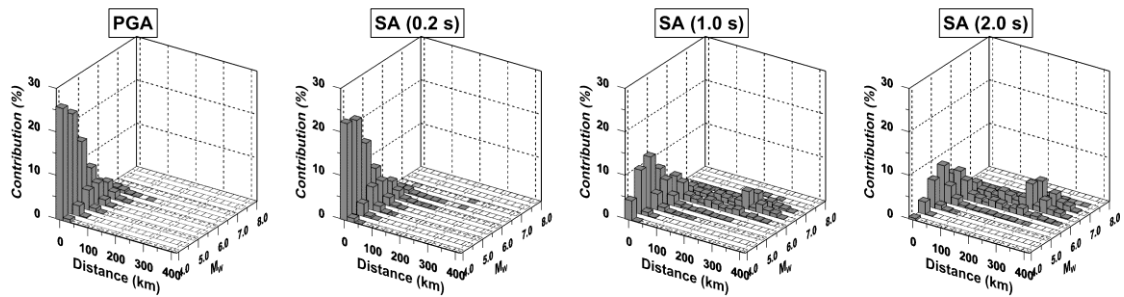
Figure (6-6): Continued.



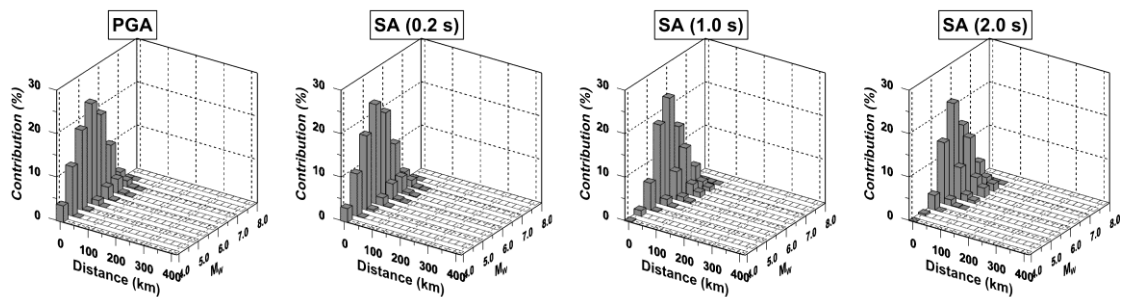
HURGHADA (PGA = 0.13 g, SA (0.2 s) = 0.29 g, SA (1.0 s) = 0.05 g, SA (2.0 s) = 0.02 g)



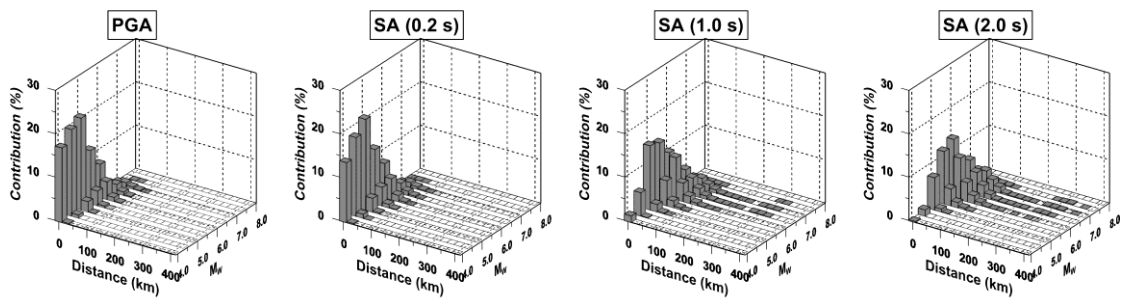
MARSA ALAM (PGA = 0.11 g, SA (0.2 s) = 0.23 g, SA (1.0 s) = 0.04 g, SA (2.0 s) = 0.01 g)



QENA (PGA = 0.06 g, SA (0.2 s) = 0.12 g, SA (1.0 s) = 0.03 g, SA (2.0 s) = 0.01 g)



ASWAN (PGA = 0.19 g, SA (0.2 s) = 0.42 g, SA (1.0 s) = 0.11 g, SA (2.0 s) = 0.04 g)



NEW CAPITAL (PGA = 0.14 g, SA (0.2 s) = 0.30 g, SA (1.0 s) = 0.07 g, SA (2.0 s) = 0.03 g)

Figure (6-6): Continued.

Finally, the last group of cities (Port Said and El-Arish) which does not lie within delineated seismic source or focus that generates the highest hazard in the location but instead lie at far distances of about 375-400 km away (the EMR). In this category, secondary lobes that have considerable importance also appear. The mean distance values for Port Said, for the studied ground motions, are 224, 195, 298 and 332 km. While for El-Arish, the mean values are 211, 186, 269 and 308 km, respectively, for the same studied ground-motion spectral periods.

On the other hand, referring to the control earthquake calculated for each location (Table 6-2), and based on the obtained modal values, we observed the following for the deaggregation of the PGA values. For 14 of the 17 studied cities (Matruh, Alexandria, Cairo, Suez, New Capital, El-Tur, Nuweiba, Sharm El-Sheikh, Assiut, Beni Suef, Hurghada, Marsa Alam, Qena and Aswan), the dominant earthquake event in these locations is at distances less than 25 km away, with a magnitude of M_W 4.0–6.0. For instance, the control earthquake for Cairo is an event with magnitude M_W 5.0-5.5 at a distance not far than 25 km for PGA, SA (0.2 s) and SA (1.0 s) whereas for SA (2.0 s) the distance remains the same but the magnitude become M_W 6.0-6.5. Therefore, the seismic hazard of such cities is mainly due to the near seismic sources, whereas the contribution of the far seismic sources is very limited (Table 6-3). On the contrary, in other cities, we did not ignore the hazard generated at distances of about 50-100 km away (Kafr El-Sheikh) or 375-400 km away (Port Said and El-Arish) from the location (Fig. 6-6). For example, for Port Said, values of M_W 7.0-7.5 and 375-400 km for the control earthquake has been obtained for PGA and for all studied spectral periods.

However, the bimodal distributions are very clear and frequent in the long-period deaggregation (for SA (1.0 s) and SA (2.0 s)), where the effect of biggest earthquakes from greater distances are more common (Table 6-3). This is very clear in many cities, for instance, Matruh, Alexandria, Port Said, El-Arish, Kafr-El-Sheikh, Hurghada, Marsa Alam and Qena.

6.4 SUMMARY AND CONCLUSIONS

The deaggregation of the seismic hazard values into relative contributions, from different seismic sources, for specific locations, achieves very important results. It gives a better representation, characterization and understanding of the seismic hazard results. These results, in turn, will improve the engineering analyses required for the design of building, as well as the development of the ground-motion time histories.

Table (6-3): Seismic foci and most contributing earthquakes to the hazard for the selected cities.

City	Main seismic focus		Secondary seismic focus	
	Most contributing source	Most contributing earthquakes	Most contributing source	Most contributing earthquakes
Matruh	Seismic focus towards the north from the city (EG-27)	m_b 5.3, M_S 4.8, M_W 5.2, May 28, 1951	Seismic foci towards the northeastern part of the city (EG-26, EG-27)	m_b 5.5, M_S 5.0, M_W 5.5, May 28, 1998 m_b 6.5, M_S 6.4, M_W 6.4, September 12, 1955 I_{max} 8.5, M_W 6.1, May, 1341
Alexandria	Seismic focus close to the city (EG-26)	M_L 5.4, M_W 5.0, July 20, 1954 I_{max} 8.0, M_W 5.8, 796 A.D. I_{max} 6.5, M_W 5.0, 1698 A.D.	–	
Port Said	Seismic foci far from the city (EG-17, EG-25, EG-26)	m_b 6.5, M_S 6.4, M_W 6.4, September 12, 1955 M_S 6.6, M_W 6.6, October 1754 I_{max} 10.0, M_W 7.0, January 14, 1546	–	
El-Arish	Seismic foci far from the city (EG-08, EG-17, EG-25) mainly along the Dead Sea Transform Fault	M_S 6.6, M_W 6.6, October 1754 I_{max} 10.0, M_W 7.0, January 14, 1546 I_{max} 11.0, M_W 7.7, 746 A.D.	–	
Kafr El-Sheikh	Seismic foci surrounding the city (EG-24, EG-26)	I_{max} 8.5, M_W 6.1, May 1341 I_{max} 8.0, M_W 5.8, May 26, 1111 I_{max} 8.0, M_W 5.8, June 6, 1259	Seismic foci far from the city (EG-17, EG-24)	m_b 5.8, M_S 5.4, M_W 5.8, October 12, 1992 M_S 6.6, M_W 6.6, October 1754
CAIRO	Seismic focus surrounding the city (EG-24)	m_b 5.8, M_S 5.4, M_W 5.8, October 12, 1992 M_S 5.6, M_W 5.7, September 20, 1385 I_{max} 8.0, M_W 5.8, June 6, 1259 I_{max} 8.0, M_W 5.8, May 26, 1111	–	
New Capital	Seismic focus towards the northwest of the city (EG-24)	I_{max} 9.0, M_W 6.4, April 9, 1588 M_S 5.5, M_W 5.7, April 21, 1576 M_S 5.1, M_W 5.4, November 12, 1529	–	
Suez	Seismic foci towards the west of the city (EG-17, EG-24)	m_b 4.9, M_S 4.8, M_W 5.2, March 29, 1984 M_S 6.6, M_W 6.6, October 1754	–	
El-Tur	Seismic focus towards the southeast of the city (EG-15)	M_S 4.3, M_W 4.9, January 26, 1911 M_S 5.3, M_W 5.5, 1839 A.D.	–	
Nuweiba	Seismic foci towards the east and the south from the city (EG-02)	m_b 5.1, M_W 5.3, February 21, 1996 M_S 7.3, M_W 7.2, November 22, 1995 m_b 5.8, M_S 5.8, M_W 6.1, August 3, 1993	–	
Sharm El-Sheikh	Seismic focus towards the southwest of the city (EG-15)	m_b 5.5, M_W 5.4, March 8, 1997 I_{max} 7.0, M_W 5.2, 1778 A.D. I_{max} 7.5, M_W 5.5, 1195 A.D.	Seismic focus towards the southwest of the city (EG-15)	m_b 5.7, M_S 5.5, M_W 5.5, June 28, 1972 m_b 6.1, M_S 6.6, M_W 6.8, March 31, 1969
Assiut	Seismic focus surrounding the city (EG-23)	M_L 5.1, M_W 4.8, June 4, 2003 M_L 5.4, M_W 5.0, December 14, 1998 M_S 5.1, M_W 5.4, October 27, 1850	–	

Table (6-3): Continued.

City	Main seismic focus		Secondary seismic focus	
	Most contributing source	Most contributing earthquakes	Most contributing source	Most contributing earthquakes
Beni Suef	Seismic focus surrounding the city (EG-23, EG-24)	M_L 5.1, M_W 4.8, October 11, 1999 M_S 5.8, M_W 5.9, August 7, 1847 M_S 4.7, M_W 5.1, December 21, 1694 M_S 5.1, M_W 5.4, January 8, 1299 M_S 6.1, M_W 6.1, February 20, 1264	–	
Hurghada	Seismic foci towards the northeast from the city (EG-14, EG-15)	m_b 5.7, M_S 5.5, M_W 5.5, June 28, 1972 m_b 6.1, M_S 6.6, M_W 6.8, March 31, 1969 I_{max} 7.0, M_W 5.2, 1778 A.D. I_{max} 7.5, M_W 5.5, 1195 A.D. m_b 5.5, M_W 5.2, December 26, 1906 I_{max} 8.0, M_W 5.8, 28 B.C.	–	
Marsa Alam	Seismic focus towards the northwest of the city (EG-21)	m_b 5.1, M_W 5.1, June 2, 1984 m_b 6.2, M_S 5.3, M_W 5.5, November 12, 1955 I_{max} 6.0, M_W 4.7, 1887	–	
Qena	Seismic focus surrounding the city (EG-23)	M_L 5.5, M_W 5.1, April 30, 1999 M_L 5.4, M_W 5.0, December 14, 1998 I_{max} 5.0, M_S 4.8, M_W 5.2, June 22, 1778	–	
Aswan	Seismic focus towards the south from the city (EG-22)	M_L 4.6, M_W 4.6, November 7, 2010 M_L 5.6, M_W 5.5, April 23, 1982 m_b 5.1, M_S 5.5, M_W 5.8, November 14, 1981	–	

In the present study, the seismic hazard for selected cities in Egypt was deaggregated for PGA, SA (0.2 s), SA (1.0 s) and SA (2.0 s) values for a return period of 475 years, to determine the magnitude and distance values that are mostly contributing to the hazard, at specific sites. This will allow civil engineers and decision-makers choosing the representative scenario earthquake in their design and planning.

Our results show that the very close seismic sources of relatively moderate magnitudes, are mostly contributing to the seismic hazard for the majority of the studied cities. However, the contribution from the more distant seismic sources (e.g., the EMR) is clearly appeared for those cities located at the Mediterranean Sea coast, especially for higher amplitudes. These results are recommended to be taken into consideration in the designing plans and the upcoming Egyptian building code.

6.5 ACKNOWLEDGMENTS

This research work was supported by the Egyptian Ministry of Higher Education (Cultural Affairs and Missions Sector), Cairo, Egypt; and the Spanish MINECO CGL2015-65602-R Project. We would like to thank Editor Andrzej Kijko and Reviewer Sebastiano D'Amico for their thoughtful comments.



SUMMARY, CONCLUSIONS AND RECOMMENDATIONS



Egypt is situated in the northeastern corner of the African Continent, along the southeastern edge of the EMR. Tectonically, it is interacting with the Arabian and Eurasian Plates through divergent and convergent plate boundaries, respectively. It is bounding by three active tectonic plate margins: the African-Eurasian plate margin, the Gulf of Suez-Red Sea plate margin and the DST.

Several moderate to strong earthquake events (e.g., M_S 6.9, March 31, 1969 Shedwan; M_S 5.9, October 12, 1992 Cairo; and M_W 7.2, November 22, 1995 Gulf of Aqaba earthquakes) in the last decades, have been taken place in Egypt causing a considerable damage. Although the M_W 7.2, November 22, 1995 Gulf of Aqaba earthquake was the strongest one among the instrumental events, it was the M_S 5.9, October 12, 1992 event that left the deepest imprints on everyone, not only because it resulted in hundreds killed and injured people, but also because it incurred a huge economic loss in damages, making it one of the costliest natural disasters in Egypt. As a result, a damaging earthquake is a real, as well as a current threat to the society, and economic well-being of the population in Egypt.

On the other hand, the Egyptian government is proposing a national plan aiming at construction of a number of new cities (e.g., the New Capital) and strategic projects (e.g., New Suez Canal) covering different areas all over the country. These national projects, in turn, could solve the problem of the high population density along the Nile Valley and Delta regions, creating new communities in these arid regions. Thus, there is an urgent need to estimate up-to-date seismic hazard values for Egypt and to supply this information for application and use in improving seismic zoning maps and building design and construction.

1. Main Objectives

The main target of the present work was to develop a new and updated PSHA for Egypt, in terms of the mean horizontal PGA, SA values and deaggregation, for different return periods and different soil conditions. This assessment was based on the compilation of a new updated earthquake catalogue, as well as on the delimitation and characterization of a new seismic source model.

2. Previous Building Codes and Seismic Hazard Assessments

In the present work, reviewing and evaluating the previous seismic hazard assessment studies and the Egyptian building codes has been done. The most important seismic hazard studies were compared and described in terms of the study region, the analysis approach, the used earthquake catalogue, the seismic source model, the considered GMPE, the software code and the obtained results. In addition, the obtained values for these studies were compared by choosing the most important cities in Egypt and studying PGA values or the PGA range in which each city is included in each study. Moreover, a detailed review for the seismic action in the successive Egyptian building codes was outlined, showing the seismic action for specific cities considered in the different codes.

It was found that each one of these assessments had used different earthquake catalogue, seismic source model, and GMPEs. Hence, it is expected to get different results among them. All the more, it is clear that successive building codes give different seismic action values for each city. Another question is the fact that the current building code (ECP-201: 2011), which based on the study proposed by Riad *et al.* (2000), does not give a certain PGA value for each specific city in Egypt, and it just divides the whole territory of Egypt into six broad zones, assigning to each zone only a value for the seismic action. Furthermore, the current building code uses two types of the elastic response spectra, one of them for the sites located along the Mediterranean Sea coast, and the other one for the other sites. Thus, the previous published studies regarding the seismic hazard in Egypt present diverse interpretations of the seismic threat with differences regarding the appropriate seismic design levels.

3. Methodology

In the present study, the standard methodology for assessing the PSHA for a particular region was followed: i) compilation of historic, macroseismic and

instrumental seismic data to create an updated earthquake catalogue, ii) delimitation of seismic sources based upon historic and instrumental seismicity, the geologic evidence, tectonic provinces, geomorphologic information, and all relevant data, iii) estimating seismicity parameters by establishing earthquake size recurrence relationships and computing the M_{\max} for each individual seismic source, and iv) selection of the appropriate GMPEs to be considered in the final seismic hazard computations.

a. *Earthquake Catalogue and Seismicity of Egypt*

A Poissonian earthquake catalogue of 16642 main shocks with magnitudes above or equal to M_w 3.0 was obtained, in the present study, after compiling all the available national and international sources. The catalogue spans the years from 2200 B.C. to the end of 2013, within a region bounded by 21°- 38°N and 22°-38°E. Tabulated earthquake data contains origin time, coordinates, depth, reported magnitudes and/or maximum intensity, and unified moment magnitude. From the completeness analysis of the current earthquake catalogue, it appears that after the deployment of both WWSSN, Aswan telemetered network, and the establishment of the ENSN, the number of recorded earthquakes increased abruptly, and the magnitude threshold decreased.

From the compilation of the entire catalogue, the following conclusions about the seismicity of Egypt (2200 B.C. - 2013), can be drawn:

- i) The occurrence of both aftershocks and swarm-type activities represents a large number of events in the initial compilation of the current catalogue,
- ii) A general concentration of the historical earthquake activity is quite clear around the Nile Valley and Nile Delta (this is due to the settlement patterns, as well as the potential amplification of sediments),
- iii) Both of historical and instrumental earthquakes show a clear concentration in Northern Egypt, being distributed in relatively similar ways, showing that these areas have witnessed activity for many centuries,
- iv) Shallow seismicity is concentrated mainly in the surrounding plate boundaries (Gulf of Suez-Red Sea, DST and African-Eurasian plate margins) on some active seismic zones like Aswan, Abu Dabbab (Central Eastern Desert) and Cairo-Suez regions,

- v) The highest density of the shallow seismicity is found at the eastern boundaries of Egypt, via the Gulf of Aqaba and the northern part of the Red Sea,
- vi) Dispersed earthquake activity is noticed in different parts of the Egyptian Eastern and Western Deserts (e.g., Southeastern and Southwestern Nasser's Lake), and
- vii) The intermediate-depth and deeper seismic activity is concentrated mainly along the Cyprian and Hellenic Arcs (EMR), due to the subduction between the African and European Plates.

b. Seismic Source Model

The delineation and characterization of the different seismic sources have been carried out in the present study to model the seismicity in and around Egypt. FMSs data, active faults data, the unified earthquake catalogue, as well as all the geological, geophysical and tectonic information, were taken into account. Potential seismic sources are modeled as area sources, in which the configuration of each of them is controlled, mainly, by the fault activity and seismicity distribution.

Eighty-eight seismic sources covering the seismic activity (shallow and intermediate-depth) in different tectonic regions have been proposed. Twenty-eight shallow seismic zones ($h \leq 35$ km) have been identified for the Egyptian territory, specified mainly on the basis of seismotectonic and seismicity criteria. In addition, fifty-three shallow seismic sources ($h \leq 20$ km) after SHARE (2013) project have been considered for the EMR. Furthermore, the current model involves seven delineated intermediate-depth seismic sources ($20 \leq h \leq 100$ km) covering the intermediate-depth seismicity in the EMR.

c. Seismicity Parameters and Stress Inversion

Seismicity parameters (b -values and activity rates) of the Gutenberg–Richter magnitude–frequency relationship have been estimated for the defined seismic sources. In addition, the M_{\max} value for each seismic source was computed. Moreover, the predominant stress pattern was estimated for each seismic source by using the stress-inversion approach and the available FMSs data. The results from this inversion for each seismic source are generally in agreement with the current tectonic framework in and around Egypt.

d. Ground-Motion Attenuation Equations

A number of well-known GMPEs were selected in the current study to account for the epistemic uncertainty associated with not knowing the true attenuation characteristics of the region. The GMPEs of Ambraseys *et al.* (1996), Abrahamson and Silva (1997), Zhao *et al.* (2006) and Boore and Atkinson (2008) were used together, in a logic-tree framework, to model the ground-motion attenuation for earthquakes located within the specifically defined Egyptian active shallow crustal seismic zones. On the other hand, the GMPE of Tavakoli and Pezeshk (2005) was chosen to model the ground-motion attenuation for earthquakes occurring within the considered SHARE (2013) shallow seismic sources, covering the EMR. Furthermore, the GMPE of Youngs *et al.* (1997) was selected in order to estimate the ground motion for earthquakes located in the intermediate-depth subduction seismic sources in the EMR.

e. Sensitivity Analysis and Logic-Tree Formulation

A sensitivity analysis is also performed in order to evaluate the effect of different input parameters on the computed seismic hazard level. Uncertainties in Gutenberg-Richter b -values, M_{\max} values and the GMPEs have been incorporated in the seismic hazard assessment, after the sensitivity analysis, using a logic-tree framework. A total of 36 branches were set up for each seismic source, representing each one an alternative seismic hazard scenario.

f. Seismic Hazard Computations and Presentations

The seismic hazard has been computed using the well-known total probability theorem, expressed in terms of the rate of exceedance of a certain level of ground motion for both rock ($V_s^{30} = 760$ m/s) and stiff-soil ($760 > V_s^{30} > 360$) site conditions. The computations were performed using the CRISIS 2014 software code (Ordaz *et al.*, 2014), for grid points covering the whole Egyptian territory at a spacing of $0.1^\circ \times 0.1^\circ$ (about 10 km x 10 km).

The final seismic hazard results for Egypt were represented as contour maps for mean PGA and SA (for a 5% damping ratio) at 0.1, 0.2, 0.3, 0.5, 1.0, 1.5 and 2.0 s, with a 39.3%, 10% and 5% probability of exceedance in 50 years, which correspond to return periods of 100, 475 and 975 years, respectively. In addition, the hazard curves as well as the UHS for thirty-one selected cities, were computed. As a result,

from the UHS, different spectral acceleration characteristic values (PGA, SA_{\max} , SA (0.2 s) and SA (1.0 s)) for the selected cities were derived for the considered return periods. Finally, seismic hazard deaggregation results (for PGA and SA at 0.2, 1.0 and 2.0 s, for 10% probability of exceedance in 50 years) in terms of distance and magnitude were computed for the most important cities.

4. *Discussion of Main Results and Conclusions*

In the current assessment, the iso-acceleration maps, hazard curves, as well as UHS delineate the Gulf of Aqaba region with relatively higher seismic hazard from the rest of the country, which is characterized by its relatively moderate hazard levels. For a return period of 475 years, it has values of 0.36 g, 0.89 g and 0.76 g for PGA, SA (0.1 s) and SA (0.2 s), respectively, for rock-site conditions, and values of 0.41 g, 0.93 g and 0.97 g for stiff-soil site conditions and for the same spectral periods. This region was experienced the biggest recorded earthquake since 1900 (M_W 7.2, November 22, 1995 Aqaba event). In spite of the M_W 5.2, June 27, 2015 and M_W 4.9, May 16, 2016 earthquakes, located near Nuweiba, were not included in the catalogue used in the current study, they coincide with the present results. Away from the Gulf of Aqaba, another seismic hazard nucleus is observed at the surroundings of Nasser's Lake in Southern Egypt. For a return period of 475 years, it is characterized by hazard values of 0.30 g, 0.71 g and 0.64 g for PGA, SA (0.1 s) and SA (0.2 s), respectively, for rock-site conditions, and values of 0.34 g, 0.75 g and 0.81 g for stiff-soil conditions and for the same spectral periods.

In a decreasing order of the seismic hazard values, other nuclei are appear in the southern part of the Gulf of Suez, at the western coast of the Red Sea near the city of Marsa Alam, in the surrounding region of Cairo, and in the surroundings of Alexandria. All those regions are exhibiting biggest to moderate earthquakes activities, both in the historical and recent times, which in turn contributes to the seismic hazard. A comparison of the computed hazard values with those considered ones in the most recent Egyptian building code (ECP-201, 2011) for a return period of 475 years, has been performed. Differences were noticed among the values of the design spectra, especially for some very important cities (e.g., Nuweiba and Aswan).

Design spectra based on Malhotra (2005) approach, for selected cities have been proposed in the present study, as well as different relationships between computed ground-motion values have been established. Finally, hazard deaggregation results

show that mostly contribution to the seismic hazard is mainly controlled by the nearby seismic sources (especially for PGA), for most of the studied cities. However, the more distant events the biggest contribution to the hazard for larger spectral periods (1.0 and 2.0 s).

It is concluded that a change in the seismic hazard representation of the current Egyptian building code is required in terms of the definition of the seismic hazard zoning maps, seismic hazard values, and new definition of the elastic response spectra for each city.

5. *Recommendations for Future Studies*

The following recommendations should be taken into account for future studies and research:

- Earthquake catalogue is one of the main components of doing a PSHA for a particular region. More studies for the historical earthquakes should be done, especially those related to their locations and intensities, as well as updating the earthquake catalogue whenever new data is available.
- Improvement of the seismic source model is another point that contributes to the enhancement of the seismic hazard results. Although some source zone boundaries are fairly well known, more geological and geophysical knowledge is required to define each single zone with a large certainty, as well as more information is required in order to define the seismicity parameters and focal depths more properly.
- Additional research (e.g., paleosismological studies) needs to be done in some regions in Egypt (e.g., Abu Dabbab and El-Gilf El-Kebeir) in order to assess the seismic potential of the geologic structures in these regions. This kind of studies may provide valuable information in the short term that might enable an improvement of the assessment of seismic hazard.
- It is strongly recommended to investigate and work on the development of a specific GMPEs for Egypt. The derivation of these GMPEs depends mainly on the availability of future ground-motion acceleration data. Therefore, installation of strong-motion stations and derivation of local attenuation characteristics should be considered in the future.

- In the present work, the given weights to alternative GMPEs and seismicity parameters in the design of the logic-tree formulation are all subjective. More research work should be done in order to have a better understanding of the implications of using multiple GMPEs in a PSHA carried out within a logic-tree formulation, and how the decision of preferring one model over another influences the final hazard results.
- In this study, two different types of soil were taken into account during the seismic hazard computations in order to consider local site conditions. Therefore, the soil properties in different regions, especially those exhibiting relatively high seismic hazard, should be identified using the microzonation studies. Microzonation of a particular region generates detailed maps that predict the hazard at much smaller scales. It is the generic name for subdividing a region into individual areas having different potentials hazardous earthquake effects, defining their specific seismic behavior for engineering design and land-use planning.
- Finally, further studies should be done using the current deaggregation results, recommending scenario earthquakes which can be used directly for the construction of critical infrastructures.



BIBLIOGRAPHY



BIBLIOGRAPHY

- Abdel Aal, A., El-Barkooky, A., Gerrites, M., Meyer, H., Schwander, M., and Zaki, H. (2000). Tectonic evolution of the Eastern Mediterranean Basin and its significance for hydrocarbon productivity in the ultra-deep water of the Nile Delta. *The Mediterranean Offshore Conference*, 2000, Alexandria, Egypt.
- Abdel-Fattah, A.K., Hussein, H.M., and El-Hady, S. (2006). Another look at the 1993 and 1995 Gulf of Aqaba earthquakes from the analysis of teleseismic waveforms. *Acta Geophysica* **54**, 260-279.
- Abdel-Fattah, A.K., Hussein, H.M., Ibrahim, E.M., and Abu El-Atta, A.S. (1997). Fault plane solutions of the 1993 and 1995 Gulf of Aqaba earthquakes and their tectonic implications. *Annali di Geofisica* **40**, 1,555-1,564.
- Abdel Raheem, Sh.E. (2013). Evaluation of Egyptian code provisions for seismic design of moment-resisting-frame multi-story buildings. *International Journal of Advanced Structural Engineering* **5**, 1-18.
- Abdel-Rahman, M.A. and El-Etr, H.A. (1978). The orientational characteristics of the structure grain of the Eastern Desert of Egypt. *Symposium of the Evolution and Mineralization of the Arabian-Nubian Shield*, February 1978, Jeddah, Saudi Arabia.
- Abdel-Rahman, K., Al-Amri, A.M.S., and Abdel-Moneim, E. (2009). Seismicity of Sinai Peninsula, Egypt. *Arabian Journal of Geosciences* **2**, 103-118.
- Abdel Rahman, M., Tealeb, A., Mohamed, A., Deif, A., Abou Elenean, K. and El-Hadidy, M.S. (2008). Seismotectonic zones at Sinai and its surrounding. *First Arab Conference on Astronomy and Geophysics*, 20-22 October 2008, Helwan, Egypt.
- Abdel Tawab, S., Helal, A., Deweidar, H. and El-Sayed, A. (1993). Surface tectonic features of 12 October 1992 earthquake, Egypt, at the epicentral area. *Ain Shams Scientific Bulletin, Special Issue*, 124-136.
- Abdelwahed, M.F., El-Khrepy, S., and Qaddah, A. (2013). Three-dimensional structure of Conrad and Moho discontinuities in Egypt. *Journal of African Earth Sciences* **85**, 87-102.
- Abdi, E., Mirzaei, N., and Shabani, E. (2013). Ground-motion scenarios consistent with PSH deaggregation for Tehran, capital city of Iran. *Natural Hazards and Earth System Sciences* **13**, 679-688.
- Abou Elenean, K.M. (1993). Seismotectonics of the Mediterranean region north of Egypt and Libya. M.Sc. thesis, Mansoura University, Egypt.
- Abou Elenean, K.M. (1997). Seismotectonics of Egypt in relation to the Mediterranean and Red Sea tectonics. Ph.D. thesis, Ain Shams University, Egypt.
- Abou Elenean, K.M. (2007). Focal mechanism of small and moderate size earthquakes recorded by the Egyptian National Seismic Network (ENSN), Egypt. *NRIAG Journal of Geophysics* **6**, 117-151.
- Abou Elenean, K.M. (2010). Seismotectonics studies of El-Dabaa and its surroundings. Submitted to the NRIAG, Cairo, Egypt.
- Abou Elenean, K.M., and Hussein, H.M. (2007). Source mechanism and source parameters of May 28, 1998 earthquake, Egypt. *Journal of Seismology* **11**, 259-274.
- Abou Elenean, K.M., and Hussein, H.M. (2008). The October 11, 1999 and November 08, 2006 Beni Suef earthquakes, Egypt. *Pure and Applied Geophysics* **165**, 1,391-1,410.
- Abou Elenean, K.M., Arvidsson, R., and Kulhanek, O. (2004). Focal mechanism of smaller earthquakes close to VBB Kottamia station, Egypt. *Annals of the Geological Survey of Egypt* **27**, 357-368.
- Abou Elenean, K.M., Hussein, H.M., Abu El-Ata, A.S., and Ibrahim, E.M. (2000). Seismological aspects of the Cairo earthquake, 12th October 1992. *Annali di Geofisica* **43**, 485-504.
- Abou Elenean, K.M., Mohamed, A.M.E., and Hussein, H.M. (2010). Source parameters and ground motion of the Suez-Cairo shear zone earthquakes, Eastern Desert, Egypt. *Natural Hazards* **52**, 431-451.

- Abrahamson, N.A. (2006). Seismic hazard assessment: problems with current practice and future developments. In: First conference on earthquake engineering and seismology, Geneva, Switzerland
- Abrahamson, N.A., and Silva, W.J. (1997). Empirical response spectra attenuation relations for shallow crustal earthquakes. *Seismological Research Letters* **68**, 94-127.
- Abu El-Nader, I. (2013). Source parameters and moment magnitude of 30 January 2012 earthquake, Northern Red Sea. *Seismological Research Letters* **84**, 805-809.
- Albert, R.N.H. (1986). Seismicity and earthquake hazard at the proposed site for a nuclear power plant in the El-Dabaa area, North Western Desert, Egypt. *Acta Geophysica Polonica* **34**, 263-281.
- Albert, R.N.H. (1987). Seismicity and earthquake hazard at the proposed site for a nuclear power plant in the Anshas area, Nile Delta, Egypt. *Acta Geophysica Polonica* **35**, 343-363.
- Aldama-Bustos, G., Bommer, J.J., Fenton, C.H., and Stafford, P.J. (2009). Probabilistic seismic hazard analysis for rock sites in the cities of Abu Dhabi, Dubai and Ra's Al Khaymah, United Arab Emirates. *Georisk* **3**, 1-29.
- Ambraseys, N.N. (1961). On the seismicity of the Southwest Asia (date from a XV century Arabic manuscript). *Revue pour L'étude calamités, Genève* **37**, 18-30.
- Ambraseys, N.N. (1962). A note on the chronology of Willis's list of earthquakes in Palestine and Syria. *Bulletin of the Seismological Society of America* **52**, 77-80.
- Ambraseys, N.N. (1978). Middle East- A reappraisal of the seismicity. *Quaternary Journal of Engineering Geology and Hydrogeology* **11**, 19-32.
- Ambraseys, N.N. (1983). A note on historical seismicity. *Bulletin of the Seismological Society of America* **73**, 1,917-1,920.
- Ambraseys, N.N. (1985). Intensity-attenuation and magnitude-intensity relationships for Northwest European earthquakes. *Earthquake Engineering and Structural Dynamics* **13**, 733-778.
- Ambraseys, N.N. (2001). Far-field effects of Eastern Mediterranean earthquakes in Lower Egypt. *Journal of Seismology* **5**, 263-268.
- Ambraseys, N.N., and Adams, R.D. (1993). Seismicity of the Cyprus region. *Terra Nova* **5**, 85-94.
- Ambraseys, N.N., and Jackson, J. (1998). Faulting associated with historical and recent earthquakes in the Eastern Mediterranean region. *Geophysical Journal International* **133**, 390-406.
- Ambraseys, N.N., Melville, C.P., and Adams, R.D. (1994). The seismicity of Egypt, Arabia and Red Sea. *Cambridge University Press*.
- Ambraseys, N.N., Simpson, K.A., and Bommer, J.J. (1996). The prediction of horizontal response spectra in Europe. *Earthquake Engineering and Structural Dynamics* **25**, 371-400.
- Angelier, J., and Mechler, P. (1977). Su rune methode graphique de recherché des contraintes principales également utilisable en tectonique et en seismologie: La methode des diedres droits. *Bulletin de la Societe Geologique de France* **19**, 651-652.
- Araya, R., and Der Kiureghian, A. (1988). Seismic hazard analysis: Improved models, uncertainties and sensitivities. Submitted to the National Science Foundation, Earthquake Engineering Research Center. No. UCB/EERC-90/11.
- Atkinson, G.M., and Boore, D.M. (1995). New ground-motion relations for Eastern North America. *Bulletin of the Seismological Society of America* **85**, 17-30.
- Atkinson, G.M., and Boore, D.M. (1997). Some comparisons between recent ground-motion relations. *Seismological Research Letters* **68**, 24-40.
- Atkinson, G.M., and Boore, D.M. (2003). Empirical ground-motion relations for subduction-zone earthquakes and their application to Cascadia and other regions. *Bulletin of the Seismological Society of America* **93**, 1,703-1,729.
- Badawy, A. (1998). Earthquake hazard analysis in Northern Egypt. *Acta Geodaetica et Geophysica Hungarica* **33**, 341-357.
- Badawy, A. (1999). Historical seismicity of Egypt. *Acta Geodaetica et Geophysica Hungarica* **34**, 119-135.

- Badawy, A. (2001). Status of the crustal stress as inferred from earthquake focal mechanisms and borehole breakouts in Egypt. *Tectonophysics* **343**, 49-61.
- Badawy, A. (2005a). Seismicity of Egypt. *Seismological Research Letters* **76**, 149-160.
- Badawy, A. (2005b). Present-day seismicity, stress field and crustal deformation of Egypt. *Journal of Seismology* **9**, 267-276.
- Badawy, A., and Abdel-Fattah, A.K. (2001). Source parameters and fault plane determinations of the 28th December, 1999 Northeastern Cairo earthquake. *Tectonophysics* **343**, 63-77.
- Badawy, A., and Abdel-Fattah, A.K. (2002). Analysis of the Southeast Beni-Suef, Northern Egypt earthquake sequence. *Journal of Geodynamics* **33**, 219-234.
- Badawy, A., and Horváth, F. (1999a). Sinai subplate and kinematic evolution of the Northern Red Sea. *Journal of Geodynamics* **27**, 433-450.
- Badawy, A., and Horváth, F. (1999b). Seismicity of the Sinai subplate region: Kinematic implications. *Journal of Geodynamics* **27**, 451-468.
- Badawy, A., and Horváth, F. (1999c). Recent stress field of the Sinai subplate region. *Tectonophysics* **304**, 385-403.
- Badawy, A., Abdel-Monem, S.M., Sakr, K., and Ali, Sh.M. (2006). Seismicity and kinematic evolution of Middle Egypt. *Journal of Geodynamics* **42**, 28-37.
- Badawy, A., Al-Gabry, M., and Girgis, M. (2010). Historical seismicity of Egypt, a study for previous catalogues producing revised weighted catalogue. *The Second Arab Conference for Astronomy and Geophysics*, 25-28 October 2010, Cairo, Egypt.
- Badawy, A., El-Hady, Sh., and Abdel-Fattah, A.K. (2008). Microearthquakes and neotectonics of Abu-Dabbab, Eastern Desert of Egypt. *Seismological Research Letters* **79**, 55-67.
- Badawy, A., Issawy, S., Hassan, G., and Tealeb, A. (2003). Kinematics engine of the ongoing deformation field around Cairo, Egypt. *Acta Geophysica Polonica* **51**, 447-458.
- Barani, S., Spallarossa, D., and Bazzurro, P. (2009). Disaggregation of probabilistic ground-motion hazard in Italy. *Bulletin of the Seismological Society of America* **99**, 2,638-2,661.
- Bartov, Y. (1974). A structural and paleogeographic study of the Central Sinai faults and domes. Ph.D. thesis, The Hebrew University of Jerusalem, Israel.
- Bayer, H., Hötzl, H., Jado, A., Bocher, B., Voggenreiter, W. (1988). Sedimentary and structural evolution of the Northwest Arabian Red Sea Margin. *Tectonophysics* **153**, 137-151.
- Bazzurro, P. (1998). Probabilistic seismic demand analysis. Ph.D. thesis, Stanford University.
- Bazzurro, P., and Cornell, C.A. (1999). Disaggregation of seismic hazard. *Bulletin of the Seismological Society of America* **89**, 501-520.
- Beadnell, H.J.L. (1901). Dakhla Oasis, its topography and geology: Egypt. *Survey Department*; 104 Pages, 9 Maps, 7 Figures.
- Ben-Avraham, Z. (1985). Structural framework of the Gulf of Elat (Aqaba). *Journal of Geophysical Research* **90**, 703-726.
- Ben-Avraham, Z., Nur, A., and Cello, G. (1987). Active transcurrent fault system along the North African passive margin. *Tectonophysics* **141**, 294 - 260.
- Bender, B., and Perkins, D. (1987). SEISRISK III, a computer program for seismic hazard estimation. *U.S. Geological Survey Bulletin* 1772:48.
- Ben-Menahem, A. (1979). Earthquake catalogue for the Middle East (92 B.C.-1980 A.D.). *Bollettino di Geofisica Teorica e Applicata* **21**, 245-310.
- Ben-Menahem, A., and Aboodi, E. (1971). Tectonic pattern in the Northern Red Sea region. *Journal of Geophysical Research* **76**, 2,674-2,689.
- Ben-Menahem, A., Nur, A., and Vered, M. (1976). Tectonics, seismicity and structure of the Afro-Eurasian junction-The breaking of an incoherent plate. *Physics of the Earth and Planetary Interiors* **12**, 1-50.

- Bernreuter, D.L. (1992). Determining the controlling earthquake from probabilistic hazards for the proposed Appendix B, *Lawrence Livermore National Laboratory Report UCRL-JC-111964*, Livermore, California.
- Bindi, D., Massa, M., Luzi, L., Ameri, G., Pacor, F., Puglia, R., and Augliera, P. (2014). Pan-European ground-motion prediction equations for the average horizontal component of PGA, PGV, and 5%-damped PSA at spectral periods up to 3.0 s using the RESORCE dataset. *Bulletin of Earthquake Engineering* **12**, 391-430.
- Bommer, J.J., Douglas, J., Scherbaum, F., Cotton, F., Bungum, H., and Fäh, D. (2010). On the selection of ground-motion prediction equations for seismic hazard analysis. *Seismological Research Letters* **81**, 783-793.
- Bonati, E. (1985). Punctiform initiation of seafloor spreading in the Red Sea during transition from a continental to an oceanic rift. *Nature* **316**, 7-33.
- Bondár, I., and Storchak, D. (2011). Improved location procedures at the International Seismological Centre. *Geophysical Journal International* **186**, 1,220-1,244.
- Boore, D.M., and Atkinson, G.M. (2008). Ground-motion prediction equations for the average horizontal component of PGA, PGV, and 5%-damped PSA at spectral periods between 0.01 s and 10.0 s. *Earthquake Spectra* **24**, 99-138.
- Boore, D.M., Joyner, W.B., and Fumal, T.E. (1997). Equations for estimating horizontal response spectra and peak acceleration from Western North American earthquakes. A summary of recent work. *Seismological Research Letters* **68**, 128-53.
- Bosworth, W. (1985). A high-strain rift model for the Southern Gulf of Suez, Egypt. In: Lambiase, L.L. (ed.) *Hydrocarbon Habitat in Rift Basins*. *Geological Society of London* **80**, 75-102.
- Bosworth, W., and Taviani, M. (1996). Late Quaternary reorientation of stress field and the extension direction in the Southern Gulf of Suez, Egypt: Evidence from uplifted coral terraces, Mesoscopic fault arrays and borehole breakouts. *Tectonics* **15**, 791-802.
- Boyd, O.S. (2012). Including foreshock and aftershocks in time-independent probabilistic seismic-hazard analyses. *Bulletin of the Seismological Society of America* **102**, 909-917
- Campbell, K.W. (1981). A ground motion model for the Central United States based on near-source acceleration data. *Earthquakes and Earthquake Engineering Conference*, 1981, Knoxville, Tennessee, the Eastern U.S.
- Campbell, K.W., and Bozorgnia, Y. (2003). Updated near-source ground motion (attenuation) relations for the horizontal and vertical components of peak ground acceleration and acceleration response spectra. *Bulletin of the Seismological Society of America* **93**, 314-331.
- Campbell, K.W., and Bozorgnia, Y. (2008). NGA ground motion model for the geometric mean horizontal component of PGA, PGV, PGD and 5% damped linear elastic response spectra for periods ranging from 0.01 to 10 s. *Earthquake Spectra* **24**, 139-171.
- Chapman, M.C. (1995). A probabilistic approach to ground-motion selection for engineering design. *Bulletin of the Seismological Society of America* **85**, 937-942.
- Cheng, Ch., Chiou, Sh., Lee, Ch., and Tsai, Y. (2007). Study on probabilistic seismic hazard maps of Taiwan after Chi-Chi earthquake. *Journal of Geo-Engineering* **2**, 19-28.
- Chorowicz, J., and Sorlien, C. (1992). Oblique extensional tectonics in the Malawi Rift, Africa. *Geological Society of America Bulletin* **104**, 1,015-1,023.
- CMT- Global Centroid Moment Tensor Catalogue: <http://www.globalcmt.org/>
- Cochran, J.R. (1983). A model for the development of the Red Sea. *American Association of Petroleum Geologists Bulletin* **67**, 41-69.
- Cochran, J.R., and Martinez, F. (1988). Evidence from the Northern Red Sea on the transition from continental to oceanic rifting. *Tectonophysics* **153**, 25-53.
- Cochran, J.R., Martinez, F., Steckler, and Hobart, M.A. (1986). Conrad deep, a new Northern Red Sea deep, origin and implications for continental rifting. *Earth and Planetary Science Letters* **78**, 18-32.

- Colletta, B., Le Quellec, P., Letouzey, J., and Moretti, I. (1988). Longitudinal evolution of the Suez Rift structure, Egypt. *Tectonophysics* **153**, 221-233.
- Comninakis, P.E., and Papazachos, B.C. (1980). Space and time distribution of the intermediate-depth earthquakes in the Hellenic Arc. *Tectonophysics* **70**, 35-47.
- Constantinescu, L., Ruprechtova, L., and Enescu D. (1966). Mediterranean-Alpine earthquake mechanisms and their seismotectonic implications. *Geophysical Journal of the Royal Astronomical Society* **10**, 347-368.
- Cooke, P. (1979). Statistical inference for bounds of random variables. *Biometrika* **66**, 367-374.
- Cornell, C.A. (1968). Engineering seismic risk analysis. *Bulletin of Seismological Society of America* **18**, 1,583-1,606.
- Cotton, F., Scherbaum, F., Mommer, J.J., and Bungum, H. (2006). Criteria for selecting and adjusting ground-motion models for specific target applications: applications to Central Europe and rock sites. *Journal of Seismology* **10**, 137-156.
- Crouse, C.B. (1991). Ground-motion attenuation equations for earthquakes on the Cascadia subduction zone. *Earthquake Spectra* **7**, 201-236.
- Daggett, P., Morgan, P., Boulous, F., Hennin, S., El-Sherif, A., El-Sayed, A., Basta, N., and Melek, Y. (1986). Seismicity and active tectonics of the Egyptian Red Sea margin and the Northern Red Sea. *Tectonophysics* **125**, 313-324.
- D'Amico, V., Albarello, D., and Mantovani, E. (1999). A distribution-free analysis of magnitude-intensity relationships: an application to the Mediterranean Region. *Physics and Chemistry of the Earth* **24**, 517-521.
- Deif, A. (1998). Seismic hazard assessment in and around Egypt in relation to plate tectonics. Ph.D. thesis, Ain Shams University, Egypt.
- Deif, A., Abou Elenean, K., El-Hadidy, M., Tealeb, A., and Mohamed, A. (2009). Probabilistic seismic hazard maps for Sinai Peninsula, Egypt. *Journal of Geophysical Engineering* **6**, 288-297.
- Deif, A., Hamed, H., Ibrahim, H.A., Abou Elenean, K., and El-Amin, E.M. (2011). Seismic hazard assessment in Aswan, Egypt. *Journal of Geophysical Engineering* **8**, 531-548.
- Delvaux, D., and Barth, A. (2010). African stress pattern from formal inversion of focal mechanism data. *Tectonophysics* **482**, 105-128.
- Delvaux, D., and Sperner, B. (2003). New aspects of tectonic stress inversion with reference to the TENSOR program. *Geological Society of London, Special Publications* **212**, 75-100.
- Demircioglu, M.B. (2010). The earthquake hazard and risk assessment for Turkey. Ph.D. thesis, Bogazici University, Turkey.
- Demircioglu, M.B., Sesetyan, K., Durukal, E., and Erdik, M. (2007). Assessment of Earthquake Hazard in Turkey. *Fourth International Conference on Earthquake Geotechnical Engineering*, 25-28 June 2007, Thessaloniki, Greece.
- Dewey, J.F., Helman, M.L., Turco, E., Hutton, D.H.W., and Knott, S.D. (1989). Kinematics of the Western Mediterranean. In: Coward, M.P., Detrich, D., and Park, R.G. (eds.) *Alpine Tectonics. Geological Society of London, Special Publication* **45**, 265-283.
- Dorre, A.S., Carrara, E., Cella, F., Grimaldi, M., Hady, Y.A., Hassan, H., Rapolla, A., and Roberti, N. (1997). Crustal thickness of Egypt determined by gravity data. *Journal of African Earth Sciences* **25**, 425-434.
- Dziewonski, A.M., Chou, T.A., and Woodhouse, J.H. (1981). Determination of earthquakes source parameters from waveform data for studies of global and regional seismicity. *Journal of Geophysical Research* **86**, 2,825-2,852.
- Eck, T.V., and Hofstetter, A. (1990). Fault geometry and spatial clustering of micro-earthquakes along the Dead Sea-Jordan Rift fault zone. *Tectonophysics* **180**, 15-27.
- ECP-Egyptian Code of Practice-201 (1993). Egyptian Code for Calculating Loads and Forces. National Research Center for Housing and Building, Ministry of Housing, Utilities and Urban Planning, Cairo.

- ECP-Egyptian Code of Practice-201 (2004). Egyptian Code of Practice No. 201 for Calculating Loads and Forces in Structural Work and Masonry. National Research Center for Housing and Building, Ministry of Housing, Utilities and Urban Planning, Cairo.
- ECP-Egyptian Code of Practice-201 (2008). Egyptian Code of Practice No. 201 for Calculating Loads and Forces in Structural Work and Masonry. National Research Center for Housing and Building, Ministry of Housing, Utilities and Urban Planning, Cairo.
- ECP-Egyptian Code of Practice-201 (2011). Egyptian Code of Practice No. 201 for Calculating Loads and Forces in Structural Work and Masonry. National Research Center for Housing and Building, Ministry of Housing, Utilities and Urban Planning, Cairo.
- EGSMA- Egyptian Geological Survey and Mining Authority (1981). Geologic Map of Egypt (Scale 1:2,000,000).
- Ekström, G., Nettles, M., and Dziewonski, A.M. (2012). The global CMT project 2004-2010: Centroid-moment tensors for 13,017 earthquakes. *Physics of the Earth and Planetary Interiors* **200-201**, 1-9.
- El-Adham, K.A. and El-Hemamy, S.T. (2006). Modelling of seismic hazard for El-Dabaa area, Egypt. *Bulletin of the Engineering Geology and the Environment* **65**, 273-279.
- El-Arab, I.E. (2011). Seismic analysis of existing school buildings using different Egyptian seismic provisions. *Twelfth East Asia-Pacific Conference on Structural Engineering and Construction*, 26-28 January 2011, Hong Kong, China.
- El-Gaby, S. (1983). Architecture of the Egyptian basement complex. *Fifth International Conference on Basement Tectonics*, 16-18 October 1983, Cairo, Egypt.
- El-Gamal, A.W., Amer, M., Adalier, K., and Abdul-Fadl, A. (1993). Engineering aspect of the October 12, 1992 Egyptian earthquake. Technical Report NCEER 91-7000B, National Center for Earthquake Engineering Research, State University of New at Buffalo, USA.
- El-Hadidy, M. (2012). Seismotectonics and seismic hazard studies in and around Egypt. Ph.D. thesis, Ain Shams University, Egypt.
- El-Hadidy, S. (1995). Crustal structure and its related causative tectonics in Northern Egypt using geophysical data. Ph.D. thesis, Ain Shams University, Egypt.
- El-Hefnawy, M., Deif, A., El-Hemamy, S.T., and Gomaa, N.M. (2006). Probabilistic assessment of earthquake hazard in Sinai in relation to the seismicity in the Eastern Mediterranean region. *Bulletin of Engineering Geology and the Environment* **65**, 309-319.
- El-Isa, Z.H., Merghelani, H., and Bazari, M. (1984). The Gulf of Aqaba earthquake swarm of 1983. *Geophysical Journal of the Royal Astronomical Society* **76**, 711-722.
- El-Rakaiby, M.L., and El-Aassy, I.E. (1989). Structural interpretation of Paleozoic-Mesozoic rocks, Southwestern Sinai, Egypt. *Annals of the Geological Survey of Egypt* **16**, 269-273.
- El-Sayed, A., and Wahlström, R. (1996). Distribution of the energy release, b-values and seismic hazard in Egypt. *Natural Hazards* **13**, 133-150.
- El-Sayed, A., Korrat, I., and Hussein, H.M. (2004). Seismicity and seismic hazard in Alexandria (Egypt) and its surroundings. *Pure and Applied Geophysics* **161**, 1,003-1,019.
- El-Sayed, A., Vaccari, V., and Panza, G.F. (2001). Deterministic seismic hazard in Egypt. *Geophysical Journal International* **144**, 555-567.
- El-Sayed, A., Wahlström, R., and Kulhánek, O. (1994). Seismic hazard of Egypt. *Natural Hazards* **10**, 247-259.
- El-Shazly, E.M. (1977). The geology of the Egyptian region. In: The Ocean Basin and Margins. Volume 4A: The Eastern Mediterranean. *Plenum Press*. New York-London.
- EMME- Earthquake Model of the Middle East region: hazard, risk assessment, economics and mitigation (2013). <http://www.emme-gem.org/>
- Engdahl, E.R., Van Der Hilst, R., and Buland, R. (1998). Global teleseismic earthquake relocation with improved travel times and procedures for depth determination. *Bulletin of the Seismological Society of America* **88**, 722-743.

- ENSN- Egyptian National Seismic Network bulletins (1998 - 2010). Earthquakes in and around Egypt. *National Research Institute of Astronomy and Geophysics (NRIAG)*, Cairo, Egypt.
- ESEE- Egyptian Society for Earthquake Engineering (1988). Regulations for earthquake resistant design of buildings in Egypt.
- Esteva, L. (1970). Seismic risk and seismic design decisions. In R. J. Hansen (Ed.), *Seismic design for nuclear power plants* (pp. 142–182). Massachusetts Institute of Technology Press, Cambridge, MA, USA.
- Eurocode 8 (2004). Design of structures for earthquake resistance. Part 1: general rules, seismic actions and rules for buildings. EN1998-1. European Committee for Standardization, Brussel.
- Eyal, M., Eyal, Y., Bartov, Y., and Steinitz, G. (1981). The tectonic development of the western margin of the Gulf of Eilat (Aqaba) Rift. *Tectonophysics* **80**, 39-66.
- Fairhead, J.D., and Girdler, R.W. (1970). The seismicity of the Red Sea, Gulf of Aden and Afar Triangle. *Philosophical Transactions of the Royal Society of London* **267**, 49-74.
- Fat-Helbary, R.E. (1994). Assessment of seismic hazard and risk in Aswan area, Egypt. Ph.D. thesis, Tokyo University, Japan.
- Fat-Helbary, R.E. (1999). Assessment of seismic hazard in Egypt. *Gerencia de Riesgos, fundación MAPFRE estudios, Spain* **67**, 31-40.
- Fat-Helbary, R.E. (2003). Probabilistic analysis of potential ground motion levels at the principal cities in Upper Egypt. *Journal of Applied Geophysics* **2**, 279-286.
- Fat-Helbary, R.E., and Mohamed, H.H. (2003). Seismicity and seismotectonics of the West Kom Ombo area, Aswan, Egypt. *Journal of Applied Geophysics* **2**, 253-260.
- Fat-Helbary, R.E., and Ohta, Y. (1996). Assessment of seismic hazard in Aswan area, Egypt. *Eleventh World Conference on Earthquake Engineering*, 23-28 June 1996, Acapulco, Mexico.
- Fat-Helbary, R.E., and Tealeb, A.A. (2002). A study of seismicity and earthquake hazard at the proposed Kalabsha Dam site, Aswan, Egypt. *Natural Hazards* **25**, 117-133.
- Fat-Helbary, R.E., El-Khashab, H.M., Dojcinovski, D., El-Faragawy, K.O., and Abdel-Motaal, A.M. (2008). Seismicity and seismic hazard analysis in and around the proposed Tushka New city site, South Egypt. *Acta Geodynamica et Geomaterialia* **5**, 389-398.
- Fouad, F.H. (1994). Egypt. In: Paz, M. (ed.) *International Handbook of Earthquake Engineering*. Chapman and Hall Inc., 195-204.
- Frankel, A. (1995). Mapping seismic hazard in the Central and Eastern United States. *Seismological Research Letters* **66**, 8-21.
- Gardner, J.K., and Knopoff, L. (1974). Is the sequence of earthquakes in Southern California, with aftershocks removed, Poissonian? *Bulletin of the Seismological Society of America* **64**, 1,363-1,367.
- Gardosh, M., Reches, Z., and Garfunkel, Z. (1990). Holocene tectonic deformation along the western margins of the Dead Sea. *Tectonophysics* **180**, 132-137.
- Garfunkel, Z. (1981). Internal structure of the Dead Sea leaky transform (rift) in relation to plate kinematics. *Tectonophysics* **80**, 81-108.
- Garfunkel, Z., and Bartov, Y. (1977). The tectonics of the Suez Rift. *Geological Survey of Israel Bulletin* **71**, 44p.
- Garfunkel, Z., Zak, I., and Freund, R. (1981). Active faulting in the Dead Sea Rift. *Tectonophysics* **80**, 1-26.
- Gephart, J.W., and Forsyth, D.W. (1984). An improved method for determining the regional stress tensor using earthquake focal mechanism data: Application to the San Fernando earthquake sequence. *Journal of Geophysical Research* **89**, 9,305-9,320.
- Gergawi, A., and El-Khashab, A. (1968). Seismicity of U.A.R. *Bulletin of Helwan Institute of Astronomy and Geophysics* No. **76**.

- Gerson, R., Grossman, S., Amit, R., and Greenbaum, N. (1993). Indicators of faulting events and periods of quiescence in desert alluvial fans. *Earth Surface Processes and Landforms* **18**, 181-202.
- Ghebreab, W. (1998). Tectonics of the Red Sea region: reassessed. *Earth-Science Reviews* **45**, 1-44.
- Giardini, D., Grünthal, G., Shedlock, K.M., and Zhang, P.Z. (1999). The GSHAP global seismic hazard map. *Annali di Geofisica* **42**, 1,225-1,230.
- Girdler, R.W. (1990). The Dead Sea Transform Fault System. *Tectonophysics* **180**, 1-13.
- Girdler, R.W., and Styles, P. (1974). Two stage sea-floor spreading. *Nature* **247**, 7-11.
- Gomez, F., Meghraoui, M., Darkal, A.N., Hijazi, F., Mouty, M., Suleiman, Y., Sbeinati, R., Darawcheh, R., Al-Ghazzi, R., and Barazangi, M. (2003). Holocene faulting and earthquake recurrence along the Serghaya branch of the Dead Sea Fault System in Syria and Lebanon. *Geophysical Journal International* **153**, 1-17.
- Grünthal, G. and GSHAP Region 3 Working Group (1999). Seismic hazard assessment for Central, North and Northwest Europe: GSHAP Region 3. *Annals of Geofisica* **42**, 999-1011.
- GSHAP- Global Seismic Hazard Assessment Project (1999). <http://www.seismo.ethz.ch/static/GSHAP/>
- Guiraud, R.A., and Bosworth, W. (1999). Phanerozoic geodynamic evolution of Northeastern Africa and the Northwestern Arabian Platform. *Tectonophysics* **315**, 73-108.
- Gutenberg, B., and Richter, C.F. (1942). Earthquake magnitude, intensity, energy and acceleration. *Bulletin of the Seismological Society of America* **32**, 163-191.
- Gutenberg, B., and Richter, C.F. (1944). Frequency of earthquakes in California. *Bulletin of the Seismological Society of America* **34**, 185-188.
- Hamdache, M., Peláez, J.A., Talbi, A., and López Casado, C. (2010). A unified catalogue of main earthquakes for Northern Algeria from A.D. 856 to 2008. *Seismological Research Letters* **81**, 732-739.
- Hamdache, M., Peláez, J.A., Talbi, A., Mobarki, M., and López Casado, C.L. (2012). Ground-motion hazard values for Northern Algeria. *Pure and Applied Geophysics* **169**, 711-723.
- Hamouda, A.Z. (2011a). Recent evaluation of the assessment seismic hazards for Nuweiba, Gulf of Aqaba. *Arabian Journal of Geosciences* **4**, 775-783.
- Hamouda, A.Z. (2011b). Assessment of seismic hazards for Hurghada, Red Sea, Egypt. *Natural Hazards* **59**, 465-479.
- Harmsen, S., and Frankel, A. (2001). Geographic deaggregation of seismic hazard in the United States. *Bulletin of the Seismological Society of America* **91**, 13-26.
- Harmsen, S., Perkins, D., and Frankel, A. (1999). Deaggregation of probabilistic ground motions in the Central and Eastern United States. *Bulletin of the Seismological Society of America* **89**, 1-13.
- Hassib, G.H. (1990). A study of focal mechanism for recent earthquakes in Egypt and their tectonic implication. M.Sc. thesis, Assiut University, Egypt.
- Hassoup, A., and Tealab, A. (2000). Attenuation of intensity in the northern part of Egypt associated with the May 28, 1998 Mediterranean earthquake. *Acta Geophysica Polonica* **48**, 79-92.
- Heidbach, O., and Ben-Avraham, Z. (2007). Stress evolution and seismic hazard of the Dead Sea Fault System. *Earth and Planetary Science Letters* **257**, 299-312.
- Heimann, A. (1990). The development of the Dead Sea Rift and its margins in Northern Israel in the Pliocene and Pleistocene. Ph.D. thesis, The Hebrew University of Jerusalem, Israel.
- Hofstetter, A. (2003). Seismic observations of the 22/11/1995 Gulf of Aqaba earthquake sequence. *Tectonophysics* **369**, 21-36.
- Hofstetter, A., Thio, H.K., and Shamir, G. (2003). Source mechanism of the 22/11/1995 Gulf of Aqaba earthquake and its aftershock sequence. *Journal of Seismology* **7**, 99-114.
- Huang, P., and Soloman, S. (1987). Centroid depth and mechanisms of mid-ocean ridge. *Journal of Geological Research* **92**, 1,361-1,383.

- Hussein, H.M. (1989). Earthquake activities in Egypt and adjacent region and its relation to geotectonic features in A.R.E. M.Sc. thesis, Mansoura University, Egypt.
- Hussein, I.M., and Abd-Allah, A.M. (2001). Tectonic evolution of the northeastern part of the African continental margin, Egypt. *Journal of African Earth Sciences* **33**, 49-68.
- Hussein, H.M., Abou Elenean, K.M., Marzouk, I.A., Korrat, I.M., Abu El-Nader, I.F., Ghazala, H., and El-Gabry, M.N. (2013). Present-day tectonic stress regime in Egypt and surrounding area based on inversion of earthquake focal mechanisms. *Journal of African Earth Sciences* **81**, 1-15.
- Hussein, H.M., Abou Elenean, K.M., Marzouk, I.A., Peresan, A., Korrat, I.M., Abu El-Nader, E., Panza, G.F., and El-Gabry, M.N. (2008). Integration and magnitude homogenization of the Egyptian earthquake catalogue. *Journal of Natural Hazards* **47**, 525-546.
- Hussein, H.M., Marzouk, I., Moustafa, A.R., and Hurukawa, N. (2006). Preliminary seismicity and focal mechanisms in the Southern Gulf of Suez: August 1994 through December 1997. *Journal of African Earth Sciences* **45**, 48-60.
- ISC- International Seismological Centre (2011) EHB Bulletin, <http://www.isc.ac.uk>, International Seismological Centre, Thatcham, United Kingdom.
- ISC- International Seismological Centre (2011). On-line Bulletin, International Seismological Centre, Thatcham, United Kingdom. <http://www.isc.ac.uk>
- Ismail, A. (1960). Near and local earthquakes at Helwan from 1903-1950. *Bulletin of Helwan Institute of Astronomy and Geophysics* No. **49**.
- Issawi, B. (1978). New findings on the geology of Uweinat, Gilf Kebir, Western Desert, Egypt. *Annals of the Geological Survey of Egypt* **8**, 275-293.
- Issawi, B. (1981). Geology of the South-Western Desert of Egypt. *Annals of the Geological Survey of Egypt* **2**, 57-66.
- Jackson, J.A., and McKenzie, D.P. (1984). Active tectonics of the Alpine Himalayan Belt between Western Turkey and Pakistan. *Geophysical Journal of the Royal Astronomical Society* **77**, 185-264.
- Johnston, A.C. (1996a). Seismic moment assessment of earthquakes in stable continental regions- I. Instrumental seismicity. *Geophysical Journal International* **124**, 381-414.
- Johnston, A.C. (1996b). Seismic moment assessment of earthquakes in stable continental regions- II. Historical seismicity. *Geophysical Journal International* **125**, 639-678.
- Joyner, W.B., and Boore, D.M. (1981). Peak horizontal acceleration and velocity from strong motion records including records from 1979 Imperial Valley, California. *Bulletin of the Seismological Society of America* **71**, 2,011-2,038.
- Kanamori, H. (1977). The energy release in great earthquakes. *Journal of Geophysical Research* **82**, 2,981-2,987.
- Karnik, V. (1968). Seismicity of the European area. *Academia, Polishing House of the Czechoslovak Academy of Science*, Praha.
- Kebeasy, R.M. (1990). Seismicity. In: Said, R. (ed.) *The Geology of Egypt*. A.A. Balkema, Rotterdam, Netherlands, 51-59.
- Kebeasy, R.M., Maamoun, M., and Albert, R.N.H. (1981). Earthquake activity and earthquake risk around the Alexandria area in Egypt. *Acta Geophysica Polonica* **29**, 37-48.
- Kijko, A., and Graham, G. (1998). Parametric-historic procedure for probabilistic seismic hazard analysis - Part I: estimation of maximum regional magnitude M(max). *Pure and Applied Geophysics* **152**, 413-442.
- Kijko, A., and Singh, N. (2011). Statistical tools for maximum possible earthquake magnitude estimation. *Acta Geophysica* **59**, 674-700.
- Klinger, Y., Avouac, J., Abou Karaki, N., Dorbath, L., Bourles, and Reyss, J. (2000). Slip rate on the Dead Sea Transform Fault in Northern Araba Valley, Jordan. *Geophysical Journal International* **142**, 755-768.

- Kolathayar, S., and Sitharam, T.G. (2012). Comprehensive probabilistic seismic hazard analysis of the Andaman-Nicobar regions. *Bulletin of the Seismological Society of America* **102**, 2,063-2,076.
- Korrat, I.M., El-Agami, N.L., Hussein, H.M., and El-Gabry, M.N. (2005). Seismotectonics of the passive continental margin of Egypt. *Journal of African Earth Sciences* **41**, 145-150.
- Lyberis, N. (1988). Tectonic evolution of the Gulf of Suez and the Gulf of Aqaba. *Tectonophysics* **153**, 209-220.
- Lyons, H.G. (1907). Earthquakes in Egypt. *Survey notes, Cairo* **1**, 277-286.
- Maamoun, M. (1979). Macroseismic observation of principal earthquakes in Egypt. *Bulletin of Helwan Institute of Astronomy and Geophysics* No. **183**.
- Maamoun, M., and El-Khashab, H.M. (1978). Seismic studies of the Shedwan (Red Sea) earthquake. *Bulletin of Helwan Institute of Astronomy and Geophysics* **171**, 22-46.
- Maamoun, M., and Ibrahim, E.M. (1978). Tectonic activity in Egypt as indicated by earthquakes. *Bulletin of Helwan Institute of Astronomy and Geophysics* No. **170**.
- Maamoun, M., Allam, A., and Megahed, A. (1984). Seismicity of Egypt. *Bulletin of Helwan Institute of Astronomy and Geophysics* **4**, 109-160.
- Maamoun, M., Allam, A., Megahed, A., and El-Ata, A. (1980). Neotectonic and seismic regionalization of Egypt. *Bulletin of International Instrumental Seismology and Earthquake Engineering (Cairo)* **18**, 27-39.
- Maamoun, M., Megahed, A., Hussein, A., and Marzouk, I. (1993). Preliminary studies on Dahshour earthquake. *National Research Institute of Astronomy and Geophysics, Cairo, Egypt*. (Abstract).
- Mahmoud, S. M. (2003). Seismicity and GPS-derived crustal deformation in Egypt. *Journal of Geodynamics* **35**, 333-352.
- Mahmoud, Y., Masson, F., Meghraoui, M., Cakir, Z., Alchalbi, A., Yavasoglu, H., Yönlü, O., Daoud, M., Ergintav, S., and Inan, S. (2013). Kinematic study at the junction of the East Anatolian Fault and the Dead Sea Fault from GPS measurements. *Journal of Geodynamics* **67**, 30-39.
- Makris, J., and Rihm, R. (1991). Shear-controlled evolution of the Red Sea: Pull-apart model. *Tectonophysics* **198**, 441-466.
- Makris, J., Rihm, R., and Allam, A. (1988). Some geophysical aspects of the evolution and structure of the crust in Egypt. In: Greiling, S.E. (ed.) *The Pan-African Belt of Northeast Africa and Adjacent Areas, Tectonic Evolution and Economic Aspects of a Late Proterozoic Orogen. Braunschweig, Friedrich. Vieweg and Sohn*, 345-369.
- Makropoulos, K.C., and Burton, P.W. (1981). A catalogue of seismicity in Greece and adjacent areas. *Geophysical Journal of the Royal Astronomical Society* **65**, 741-762.
- Makropoulos, K.C., and Burton, P.W. (1985). A Fortran program to evaluate hazard parameters using Gumbel's theory of extreme value statistics. *National Environment Research Council, Institute of Geological Sciences, Edinburgh*.
- Malhotra, P.K. (2005). Return period of design ground motions. *Seismological Research Letters* **76**, 693-699.
- Marco, S., Agnon, A., Ellenblum, R., Eidekman, A., Basson, U., and Boas, A. (1997). 817-year-old walls offset sinistrally 2.1 m by the Dead Sea Transform, Israel. *Journal of Geodynamics* **24**, 11-20.
- Marco, S., Heimann, A., Rockwell, K.T., and Agnon, A. (2000). Late Holocene earthquake deformations in the Jordan Gorge Fault, Dead Sea Transform. *Israel Geological Society Annual Meeting*, 3-4 April, Maalot, Israel.
- Mart, Y. (1991). The Dead Sea Rift: From continental rift to incipient ocean. *Tectonophysics* **197**, 155-179.
- Mart, Y., and Hall, J. K. (1984). Structural trends in the northern Red Sea. *Journal of Geophysical Research* **89**, 11,352-11,364
- Marzocchi, W., and M. Taroni (2014). Some thoughts on declustering in probabilistic seismic-hazard analysis. *Bulletin of the Seismological Society of America* **104**, 1838-1845.

- Marzouk, I.A. (1988). Study of the crustal structure of Egypt deduced from deep seismic and gravity data. Ph.D. thesis, University of Hamburg, Germany.
- Marzouk, I.A. (2007). Collecting and evaluating the focal mechanism catalogue of Egypt. *Journal of Applied Geophysics* **6**, 383-398.
- Marzouk, I.A., Mohamed, A.A., Hussein, H., Morsy, M.A., El-Rayess, M.M., and Taha, A.M. (2011). Strong motion network in the Nile Delta, Egypt. *NRIAG Journal of Geophysics, Special Issue*, 223-248.
- McClusky, S., Balassanian, S., Barka, A., Demir, C., Ergintav, S., Georgiev, I., Gurkan, O., Hamburger, M., Hurst, K., Kahle, H., Kastens, K., Kekelidze, G., King, R., Kotzev, V., Lenk, O., Mahmoud, S., Mishin, A., Nadariya, M., Ouzounis, A., Paradissis, D., Peter, Y., Prilepin, M., Reilinger, R., Sanli, I., Seeger, H., Tealeb, A., Toksoz, M.N., and Veis, G. (2000). Global Positioning System constraints on plate kinematics and dynamics in the Eastern Mediterranean and Caucasus. *Journal of Geophysical Research* **105**, 5,695-5,719.
- McGuire, R.K. (1976). FORTRAN computer programs for seismic risk analysis. *United States Geological Survey*. Open-File Report.
- McGuire, R.K. (1994). EQRISK Fortran computer program for seismic risk analysis. *United States Geological Survey*. Open-File Report.
- McGuire, R.K. (1995). Probabilistic seismic hazard analysis and design earthquakes: Closing the loop. *Bulletin of the Seismological Society of America* **85**, 1,275-1,284.
- McKenzie, D.P. (1970). Plate tectonics of the Mediterranean region. *Nature* **326**, 239-243.
- McKenzie, D.P. (1972). Active tectonics in the Mediterranean region. *Geophysical Journal of the Royal Astronomical Society* **30**, 109-185.
- McKenzie, D.P., Davies, D., and Molnar, P. (1970). Plate tectonics of the Red Sea and East Africa. *Nature* **226**, 243-248.
- Megahed, A., and Dessoky, M.M. (1988). The Ismailia (Egypt) earthquake of January 2nd, 1987 (location, macroseismic survey, radiation pattern of first motion and its tectonic implications). *First National Conference of Environmental Studies and Research*, 1988, Ain Shams University, Egypt.
- Meshref, W. (1990). Tectonic framework. In: Said, R. (ed.) *The geology of Egypt*. A.A. Balkema, Rotterdam, Netherlands, 113-155.
- Meulenkamp, J.E., Wortel, M.J.R., Van Wamel, W.A., Spakman, W., and Hoogerduyn-Strating, E. (1988). On the Hellenic subduction zone and the geodynamic evolution of Crete since the Late Middle Miocene. *Tectonophysics* **146**, 203-215.
- Mohamed, A.A., El-Hadidy, M., Deif, A., and Abou Elenean, K. (2012). Seismic hazard studies in Egypt. *National Research Institute of Astronomy and Geophysics Journal* **1**, 119-140.
- Morsy, M.A., El-Hady, Sh., and Abd El-Meneam, E. (2012). Source parameters of some recent earthquakes in the Gulf of Aqaba, Egypt. *Arabian Journal of Geosciences* **5**, 943-952.
- Morsy, M.A., Hussein, H.M., Abou Elenean, K.M., and El-Hady, Sh. (2011). Stress field in the central and northern parts of the Gulf of Suez area, Egypt from earthquake fault plane solutions. *Journal of African Earth Sciences* **60**, 293-302.
- Mousa, H.H. (1989). Earthquake activity in Egypt and adjacent regions and its relation to the geotectonic features. M.Sc. thesis, Mansoura University, Egypt.
- Moustafa, A.M. (1976). Block faulting in the Gulf of Suez. *Fifth Egyptian General Petroleum Corporation Exploration Seminar*, 1976, Cairo, Egypt.
- Moustafa, A.R. (1996). Internal structure and deformation of an accommodation zone in the northern part of the Suez Rift. *Journal of Structural Geology* **18**, 93-107.
- Moustafa, A.R., and Fouda, H.G. (1988). Gebel Sufr El-Dara accommodation zone, southwestern part of the Suez Rift. *Middle East Research Center, Ain Shams University, Earth Science Series* **2**, 227-239.

- Moustafa, A.R., and Khalil, M.H. (1994). Rejuvenation of the Eastern Mediterranean passive continental margin in Northern and Central Sinai: New data from the Themed Fault. *Geological Magazine* **131**, 435-448.
- Moustafa, A.R., and Khalil, M.H. (1995). Superposed deformation in the Northern Suez Rift, Egypt: Relevance to hydrocarbon exploration. *Journal of Petroleum Geology* **18**, 245-266.
- Neev, D. (1975). Tectonic evolution of the Middle East and the Levantine Basin (Easternmost Mediterranean). *Geology* **3**, 683-686.
- Newmark, N.M., and Hall, W.J. (1982). Earthquake spectra and design. *Earthquake Engineering Research Institute*, Oakland, California.
- Ordaz, M., Aguilar, M., and Arboleda, J. (2007). CRISIS 2007: Program for computing seismic hazard. Institute of Engineering, UNAM, Mexico.
- Ordaz, M., Faccioli, E., Martinelli, F., Aguilar, M., Arboleda, J., Meletti, C., and D'Amico, V. (2014). CRISIS 2014: Program for computing seismic hazard. Institute of Engineering, UNAM, Mexico.
- Panzer, F., Lombardo, G., and Rigano, R. (2011). Use of different approaches to estimate seismic hazard: the study cases of Catania and Siracusa, Italy. *Bollettino di Geofisica Teorica ed Applicata* **52**, 687-706.
- Papadimitriou, Ch.A., and Papazachos, B.C. (2000). Time-independent and time-dependent seismic hazard in Greece based on seismogenic sources. *Bulletin of the Seismological Society of America* **90**, 22-33.
- Papazachos, B.C. (1990). Seismicity of the Aegean and surrounding area. *Tectonophysics* **178**, 287-308.
- Papazachos, B.C., and Comninakis P.E. (1971). Geophysical and tectonic features of the Aegean Arc. *Journal of Geophysical Research* **76**, 8,517-8,533.
- Papazachos, B.C., and Papadimitriou, Ch.A. (1993). Long-term earthquake prediction in the Aegean area based on a time and magnitude predictable model. *Pure and Applied Geophysics* **140**, 595-612.
- Papazachos, B.C., and Papadimitriou, Ch.A. (1999). Lithospheric boundaries and plate motions in the Cyprus area. *Tectonophysics* **308**, 193-204.
- Papazachos, B.C., and Papazachos, C. (1997). On Greek earthquakes. *Ziti Publications*, Thessaloniki.
- Papazachos, B.C., and Papazachou, C. (2003). The earthquakes of Greece. *Ziti Publications*, Thessaloniki.
- Papazachos, B.C., Papadimitriou, E.E., Karakostas, B.G., and Karakaisis, G.F. (1985). Long-term prediction of great intermediate-depth earthquakes in Greece. *Twelfth Regional Seminar on Earthquake Engineering*, 16-25 September, Halkidiki, Greece.
- Papadimitriou, Ch.A. (2001). A model for the shallow and intermediate-depth seismic sources in the Eastern Mediterranean region. *Bollettino di Geofisica* **42**, 57-73.
- Papadimitriou, Ch.A., and Papazachos, B.C. (2000). Time-independent and time-dependent seismic hazard in Greece based on seismogenic sources. *Bulletin of the Seismological Society of America* **90**, 22-33.
- PDE- Preliminary Determination of Epicentre: USGS National Earthquake Information Center (NEIC), <http://earthquake.usgs.gov/earthquakes/>
- Peláez, J. A., and Casado, C.L. (2002). Seismic hazard estimate at the Iberian Peninsula. *Pure and Applied Geophysics* **159**, 2,699-2,713.
- Peláez, J.A., Chourak, M., Tadili, B.A., Aït Brahim, L., Hamdache, M., López Casado, C., and Martínez Solares, J.M. (2007). A catalogue of main Moroccan earthquakes from 1045 to 2005. *Seismological Research Letters* **78**, 614-621.
- Peláez, J. A., Hamdache, M., and Casado, C.L. (2005). Updating the probabilistic seismic hazard values of Northern Algeria with the 21 May 2003 M 6.8 Algiers earthquake included. *Pure and Applied Geophysics* **162**, 2,163-2,177.
- Peláez, J.A., Hamdache, M., and Casado, C.L. (2006). Seismic hazard in terms of spectral accelerations and uniform hazard spectra in Northern Algeria. *Pure and Applied Geophysics* **163**, 119-135.

- Peláez, J.A., Casado, C.L., and Henares Romero, J. (2002). Deaggregation in magnitude, distance and azimuth in the south and west of the Iberian Peninsula. *Bulletin of the Seismological Society of America* **92**, 2,177-2,185.
- Peresan, A., and Rotwain, I.M. (1998). Analysis and definition of magnitude selection criteria for NEIC (PDE) data, oriented to the compilation of a homogeneous updated catalogue for CN monitoring in Italy. *The Abdus Salam International Centre for Theoretical Physics*. ICTP, Miramare, Trieste, Italy.
- Petersen, M.D., Frankel, A.D., Harmsen, S.C., Mueller, C.S., Haller, K.M., Wheeler, R.L., Wesson, R.L., Zeng, Y., Boyd, O.S., Perkins, D.M., Luco, N., Field, E.H., Wills, C.J., and Rukstales, K.S. (2008). Documentation for the 2008 update of the United States National Seismic Hazard Maps, *U.S. Geological Survey*, Open-file report 2008-1128, 60 pp., 11 appendices.
- Petrovski, J., Mihailov, V., and Jordanovski, L.I. (1983). Trans-European North-South Motorway Project (TEM), V.I Seismic hazard maps, United Nations Development Programme-Economic Commission for Europe.
- Philobos, E.R., Riad, S., Omran, A.A., and Othman, A.B. (2000). Stages of fracture development controlling the evolution of the Nile Valley in Egypt. *Egyptian Journal of Geology* **44**, 503-532.
- Pinar, A., and Türkelli, N. (1997). Source inversion of the 1993 and 1995 Gulf of Aqaba earthquakes. *Tectonophysics* **283**, 279-288.
- Poirier, J., and Taher, M. (1980). Historical seismicity in the Near and Middle East, North Africa and Spain from Arabic documents (7th-17th century). *Bulletin of the Seismological Society of America* **70**, 2,185-2,201.
- Pollastro, R.M. (2003). Total petroleum systems of the Paleozoic and Jurassic, Greater Ghawar Uplift and adjoining provinces of Central Saudi Arabia and Northern Arabian-Persian Gulf. *U.S. Geological Survey Bulletin* 2202-H.
- Pondrelli, S., Morelli, A., and Ekström, G. (2004). European-Mediterranean Regional Centroid Moment Tensor catalog: solutions for years 2001 and 2002. *Physics of the Earth and Planetary Interiors* **145**, 1-4 and 127-147.
- Pondrelli, S., Morelli, A., Ekström, G., Mazza, S., Boschi, E., and Dziewonski, A.M. (2002). European-Mediterranean Regional Centroid Moment Tensors: 1997-2000. *Physics of the Earth and Planetary Interiors* **130**, 71-101.
- Pondrelli, S., Salimbeni, S., Ekström, G., Morelli, A., Gasperini, P., and Vannucci, G. (2006). The Italian CMT dataset from 1977 to the present. *Physics of the Earth and Planetary Interiors* **159**, 286-303.
- Pondrelli, S., Salimbeni, S., Morelli, A., Ekström, G., and Boschi, E. (2007). European-Mediterranean Regional Centroid Moment Tensor catalog: solutions for years 2003 and 2004. *Physics of the Earth and Planetary Interiors* **164**, 1-2 and 90-112.
- Pondrelli, S., Salimbeni, S., Morelli, A., Ekström, G., Postpischl, L., Vannucci, G., and Boschi, E. (2011). European-Mediterranean Regional Centroid Moment Tensor catalog: solutions for 2005-2008. *Physics of the Earth and Planetary Interiors* **185**, 74-81.
- Primakov, I., and Rotwain, I. (2003). The package for analysis of earthquake catalogues (EDCAT, CATAL and AFT). *Seventh workshop on non-linear dynamics and earthquakes prediction*, 29 September-11 October 2003, ICTP, Trieste, Italy.
- RCMT- European-Mediterranean RCMT Catalogue: <http://www.bo.ingv.it/RCMT/>
- Reasenber, P.A. (1985). Second-order moment of Central California seismicity. *Journal of Geophysical Research* **90**, 5,479-5,495.
- Reches, Z., and Hoexter, D.F. (1981). Holocene seismic activity in the Dead Sea area. *Tectonophysics* **80**, 235-254.
- Reiter, L. (1990). Earthquake hazard analysis. *Columbia University Press*.
- Riad, S. (1977). Shear zones in North Egypt interpreted from gravity data. *Geophysics* **24**, 1,207-1,214.

- Riad, S., and Hosney, H. (1992). Fault plane solution for the Gilf Kebir earthquake and the tectonics of the southern part of the Western Desert of Egypt. *Annals of the Geological Survey of Egypt* **18**, 239-248.
- Riad, S., and Meyers, H. (1985). Earthquake catalogue for the Middle East countries (1900-1983). National Geophysical Data Centre, World Data Centre A for Solid Earth Geophysics. Rep. SE-40. NOAA, U.S. Department of Commerce, Boulder, Colorado, USA.
- Riad, S., and Yousef, M. (1999). Earthquake hazards assessment in the southern part of the Western Desert of Egypt. Submitted to the NARSS, Cairo, Egypt.
- Riad, S., Ghalib, M., El-Difrawy, M.A., and Gamal, M. (2000). Probabilistic seismic hazard assessment in Egypt. *Annals of the Geological Survey of Egypt* **23**, 851-881.
- Riad, S., Taeleb, A.A., El-Hadidy, S., Basta, N.Z., Abou Elela, A.M., Mohamed, A.A., and Khalil, H.A. (2004). Ancient earthquakes from some Arabic sources and catalogue of Middle East historical earthquakes. EGSM, NARSS, UNDP, UNESCO, 71-91.
- Robson, D. (1971). The structure of the Gulf of Suez (Clysmic) Rift with special reference to the eastern side. *Geological Society of London* **115**, 247-276.
- Robson, D.S., and Whitlock, J.H. (1964). Estimation of a truncation point. *Biometrika* **51**, 33-39.
- Roeser, H.A. (1975). A detailed magnetic survey of the Southern Red Sea. *Geologie Jahrbuch* **13**, 131-153.
- Rothé, J.P. (1969). The seismicity of the earth 1953-1965. UNESCO, Paris.
- Rydelek, P.A., and Sacks, I.S. (2003). Comment on "Minimum magnitude of completeness in earthquake catalogs: examples from Alaska, the Western United States, and Japan" by Stefan Wiemer and Max Wyss. *Bulletin of Seismological Society of America* **93**, 1,862-1,867.
- Said, R. (1990). The geology of Egypt. A.A. Rotterdam, Brookfield: A.A. Balkema.
- Salamon, A., Hofstetter, A., Garfunkel, Z., and Ron, H. (1996). Seismicity of the Eastern Mediterranean region: Perspective from the Sinai Subplate. *Tectonophysics* **263**, 293-305.
- Salamon, A., Hofstetter, A., Garfunkel, Z., and Ron, H. (2003). Seismotectonics of the Sinai Subplate-the Eastern Mediterranean region. *Geophysical Journal International* **155**, 149-173.
- Sandford, K.S. (1934). Paleolithic man and the Nile Valley in Upper and Middle Egypt. *Chicago University Oriental Institute Publications* **18**, 1-131.
- Savage, W.U. (1984). Evaluation of regional seismicity. Woodward and Clyde Consultants. Submitted to Aswan High Dam Authority, Ministry of Irrigation, Egypt.
- Schlumberger (1984). Geology of Egypt. *Well Evaluation Conference*, 1984, Schlumberger, Cairo, Egypt.
- Searle, R.C., and Ross, D.A. (1975). A geophysical study of the Red Sea axial trough between 20.58° and 22.8°N. *Geophysical Journal of the Royal Astronomical Society* **43**, 555-572.
- Sestini, G. (1984). Tectonic and sedimentary history of NE African margin (Egypt/Libya). In: Dixon, J.E., and Robertson, A.H.F. (eds.) *The Geological Evolution of the Eastern Mediterranean*. Blackwell Scientific Publications, Oxford, 161-175.
- Shamir, G., Bartov, A., Fleischer, L., Arad, V., and Rosensaft, M. (2001). Preliminary seismic zonation. Geological Survey of Israel. Report No. GSI/12/2001, *Geophysical Institute of Israel* Report No. GII 550/95/01/ (1).
- Shapira, A., and Jarradat, M. (1995). Earthquake risk and loss assessment in Aqaba and Eilat regions. Submitted to the U.S. Aid-Merc Program.
- Shapira, A., and Shamir, G. (1994). Seismicity parameters of seismogenic zones in and around Israel. *The Institute of Petroleum Research and Geophysics*. Report No. Z1/567/79 (109).
- SHARE- Seismic Hazard Harmonization in Europe (2013). <http://www.share-eu.org/>
- Shata, A. (1959). Structural development of the Sinai Peninsula (Egypt). *Twentieth International Geological Congress*, 1959, Mexico City, Mexico.
- Sieberg, A. (1932a). Handbuch der Geophysik. Band IV, *Erdbeben-geographie*. Borntraeger, Berlin.

- Sieberg, A. (1932b). Erdbeben und Bruchschollenbau in Östlichen Mittelmeergebiet. Denkschriften der Medizinisch-Naturwissenschaftlichen Gesellschaft zu Jena 18, No. 2.
- Sobaih, M. (1988). Regulations for earthquake-resistant design of buildings in Egypt. Egyptian Society for Earthquake Engineering (ESEE), Cairo.
- Sobaih, M.E., Kebeasy, R.M., and Ahmed, K.A. (1992). Development of seismic hazard maps for Egypt. *International Journal of Earthquake Engineering* **2**, 33-58.
- Sofratome Group. (1984). El-Daba nuclear power plant. Unpublished Report, NPPA Ministry of Electricity, Egypt.
- Stein, S., and Wysession, M. (2003). An introduction to Seismology, earthquakes, and earth structure. *Blackwell Publishing*.
- Steinitz, G., Bartov, Y., and Hunziker, J.C. (1978). K-Ar age determinations of some Miocene-Pliocene basalts in Israel: their significance to the tectonics of the rift valley. *Geological Magazine* **115**, 329-340.
- Stern, R.J., and Hedge, C.E. (1985). Geochronologic and isotopic constraints on Late Precambrian crustal evolution in the Eastern Desert of Egypt. *American Journal of Science* **285**, 97-127.
- Sutiwanich, Ch., Hanpattanapanich, Th., Pailoplee, S., and Charusiri, P. (2012). Probability seismic hazard maps of Southern Thailand. *Songklanakarinn Journal of Science and Technology* **34**, 453-466.
- Taher, M.A. (1979). Corpus des textes arabes relatifs aux tremblements de terre et autres catastrophes naturelles, de la conquête arabe au XII H/XVIII JC. LLD thesis, University Paris I, France.
- Talwani, P., and Rajendrank (1991). Some seismological and geometric features of intraplate earthquakes. *Seismological Research Letters* **59**, 305-310.
- Tavakoli, B., and Pezeshk, Sh. (2005). Empirical-stochastic ground-motion prediction for Eastern North America. *Bulletin of the Seismological Society of America* **95**, 2,283-2,296.
- Tselentis, G. A., and Danciu, L. (2010). Probabilistic seismic hazard assessment in Greece-Part 3: Deaggregation. *Natural Hazards and Earth System Sciences* **10**, 51–59
- UBC- Uniform Building Code (1997). Volume 2: Structural engineering design provisions. *International Conference of Building Officials (ICBO)*, Whittier, California.
- WCC- Woodward Clyde Consultants (1985). Earthquake activity and stability evaluation for the Aswan High Dam. Submitted to Aswan High Dam Authority, Ministry of Irrigation, Egypt.
- Westaway, R. (1994). Present-day kinematics of the Middle East and Eastern Mediterranean. *Journal of Geophysical Research* **99**, 12,071-12,090.
- Wiemer, S., and Wyss, M. (2000). Minimum magnitude of complete reporting in earthquake catalogues: examples from Alaska, the Western United States, and Japan. *Bulletin of Seismological Society of America* **90**, 859-869.
- Wiemer, S., and Wyss, M. (2003). Reply to “Comment on ‘Minimum magnitude of completeness in earthquake catalogues: examples from Alaska, the Western United States, and Japan’ by Stefan Wiemer and Max Wyss” by Paul A. Rydelek and I.S. Sacks”. *Bulletin of Seismological Society of America* **93**, 1,868-1,871.
- Willis, B. (1928). Earthquakes in the Holy Land. *Bulletin of Seismological Society of America* **18**, 73-103.
- Younes, A.I., and McClay, K. (2002). Development of accommodation zones in the Gulf of Suez-Red Sea Rift, Egypt. *The American Association of Petroleum Geologists Bulletin* **86**, 1,003-1,026.
- Youngs, R.R., and Coppersmith, K.J. (1985). Implications of fault slip rates and earthquake recurrence models to probabilistic seismic hazard estimates. *Bulletin of the Seismological Society of America* **75**, 939-964.
- Youngs, R.R., Chiou, S.J., Silva, W.J., and Humphery, J.R. (1997). Strong ground motion attenuation relationships for subduction zone earthquakes. *Seismological Research Letters* **68**, 58-73.
- Youssef, M.I. (1968). Structural pattern of Egypt and its interpretation. *The American Association of Petroleum Geologists Bulletin* **53**, 601-614.

- Zhao, J.X., Zhang, J., Asano, A., Ohno, Y., Oouchi, T., Takahashi, T., Ogawa, H., Irikura, K., Thio, H.K., Somerville, O.G., Fukushima, Y., and Fukushima, Y. (2006). Attenuation relations of strong ground motion in Japan using site classification based on predominant period. *Bulletin of the Seismological Society of America* **96**, 898-913.
- Ziegler, M.A. (2001). Late Permian to Holocene paleofacies evolution of the Arabian Plate and its hydrocarbon occurrences. *GeoArabia* **6**, 445-504.
- Ziegler, P. A. (1988). Evolution of the Arctic-North Atlantic and Western Tethys. *American Association of Petroleum Geologists*, 43, 1–206.
- ZUR-RMT: Zurich Moment Tensor. Swiss Seismological Service.